Nuclear magnetic resonance studies in solids containing dipolar coupled spin-half species.

Thesis

NUCLEAR MAGNETIC RESONANCE STUDIES IN SOLIDS CONTAINING DIPOLAR COUPLED SPIN-$\frac{1}{2}$ SPECIES

A thesis submitted to the Open University
for the degree of Doctor of Philosophy

by

David Charles Apperley BSc

Chemistry Discipline
January, 1986

Date of submission: January 1986

Date of award: 16 April 1986

ABSTRACT

Closed analytical expressions for the NMR response to various pulse sequences for small, isolated heteronuclear spin systems containing dipolar coupled spin-$\frac{1}{2}$ nuclei are derived and discussed. In particular, the responses of single crystal and polycrystalline assemblies of two, three and four spin systems to single, strong, resonant rf pulses and $P_y(90^o)-\tau-P_\phi(\theta)$ pulse sequences are considered. The calculations are carried out using the density matrix formulism. The results of the moment expansion for the treatment of a general multi-spin system are included for comparison. The calculated response to one pulse (the FID) is compared to the experimentally observed FID for potassium hydrogen difluoride, caesium hydrogen difluoride and sodium fluoroethanoate. The calculated response to a two pulse sequence is compared to the experimentally observed response for KHF_2. It is shown that the expressions for the responses to two pulse sequences can, in general, be decomposed into three components: an FID component, an echo component and a cross-term component. The effect that these components have on observed spin echoes is discussed for model systems. It is demonstrated that the separation of homonuclear and heteronuclear interactions using spin echo techniques is not as straightforward as has previously been suggested. The predictions of the operator formulism often used in spin echo studies are shown to be of limited value.

Finally, a general treatment of nuclear spin relaxation in heteronuclear spin systems is given. Two specific motional models are included: (i) a three spin, two site model and (ii) a four spin, two site model. A generalisation of the former model is also included. These models are used to interpret the spin-lattice relaxation behaviour of both polycrystalline KHF_2 and $CsHF_2$. The results of the study of the latter compound differ in several aspects from those previously reported.

ACKNOWLEDGEMENTS

I would like to thank my supervisors Dr. E.A. Moore and Dr. M. Mortimer for their help and enthusiasm throughout this project and for their advice on the presentation of this work. I would also like to thank Professor L.J. Haynes for the use of the facilities of his department and the Open University for providing financial support.

I am indebted to Mr. G. Oates for technical assistance in the laboratory and for carrying out some of the relaxation measurements. I thank Dr. C.J. Ludman for supplying the sample of caesium hydrogen difluoride.

Finally I would like to thank Mrs. A. Earls and Mrs. S Foster for turning my manuscript into typewritten form.

CONTENTS

TABLE OF FIGURES

CHAPTER ONE

Introduction and Theoretical Background

1.0 General Introduction

Over the past four decades nuclear magnetic resonance (NMR) spectroscopy has proved to be of immense value in the investigation of the chemical and physical properties of solids, liquids and gases at the molecular level. This thesis is concerned with the structural and dynamic information that can be obtained from NMR studies of particular types of solids, namely those that contain more than one abundant resonant nucleus.

The inherent spin angular momentum (spin) that many atomic nuclei possess is the property on which the NMR technique relies. The presence of spin implies the presence of a nuclear magnetic moment. In solids containing spin-$\frac{1}{2}$ nuclei pairwise interaction (or coupling) of the nuclei (or spins) dominates the NMR experiment. It is the dipolar interaction which is of most interest in the present work.

Many NMR studies are concerned with essentially homonuclear spin systems (that is, as far as this work is concerned, groups of spin-bearing nuclei with the same atomic number) either because of the nature of the spin system or because of some external conditions imposed by the experiment (for example, double resonance techniques). In this thesis the main interest lies in heteronuclear spin systems (that is groups of spin-bearing nuclei with differing atomic numbers). Detailed discussion will be limited to systems with just two different types of spin-$\frac{1}{2}$ nucleus, such as systems containing ^{1}H and ^{19}F, or ^{1}H and ^{31}P nuclei. These two examples are the groupings of abundant spin-$\frac{1}{2}$ nuclei that occur most commonly, for example in:

(i) models of biological systems where ^{19}F acts as a 'spin-label';

(ii) the head groups of phospholipid molecules;

(iii) polymers, in particular partially fluorinated polymers;

(iv) glassy, aqueous electrolytes such as CsF,H_2O;

(v) ionic crystallites and crystalline hydrates, and

(vi) liquid crystalline systems.

The dipolar interaction is a short range interaction so the observed NMR behaviour is often dominated by the response of small, localised groups of spins. A major part of this thesis is an attempt to understand the interactions within small groups of spins and determine the manner in which they affect the observed NMR response. The general aim is to provide a background against which the local molecular structure and dynamics in more complex systems such as those listed above, can be studied. To summarise, the present work is aimed at understanding the NMR behaviour of small (up to four spins) heteronuclear, spin systems. As such it represents a contribution to an important, but as will become apparent later, not an 'over studied' area.

The thesis is divided into six chapters, of which a brief description follows. In Chapter One much of the notation to be used in the subsequent chapters is introduced. It is written in the current fashion, that is in terms of irreducible spherical tensor operators. The properties of rotational transformations, crucial to this notation, are also included in the chapter, as is an explanation of the relationship between spherical and Cartesian tensors. The Hamiltonians (namely the Zeeman, rf, dipolar and shielding) required for subsequent theoretical investigations are

introduced, they are written both in irreducible spherical tensor form and, for the dipolar Hamiltonian, in terms of the more familiar 'dipolar alphabet'. Also introduced is the density matrix operator and the rotating frame transformation. The second chapter deals with the derivation, using the density matrix formulism, of closed expressions to describe the NMR response, to one strong rf pulse, for isolated two, three and four spin heteronuclear systems (IS, IS_2 and I_2S_2, where I represents one type of spin and S another). A review of an approximate way of achieving the same result (the moment expansion) is also included in the chapter; the results of this method are compared with those of the closed calculations. Chapter Three describes the results of experimental measurements of the NMR response, to one strong rf pulse, for three compounds containing relatively isolated three spin systems: potassium hydrogen difluoride, caesium hydrogen difluoride and sodium fluoroethanoate. The relationship between these results and the theoretical responses is discussed in some detail. Theoretical results for the response of 4-methylphenylamine hydrogen difluoride (a compound which, it has been suggested, contains a hydrogen difluoride ion in which the hydrogen atom is not central) and also a four spin system are given and discussed. It is necessary, for the calculations presented in this chapter, to take polycrystalline averages: the procedure and computational details for achieving this are discussed in a separate section.

The analytic development of the NMR response to one pulse is extended in Chapter Four to include, in detail, two pulse and, more briefly, three pulse sequences. Again, an approximate

method of obtaining the two pulse results is reviewed. In Chapter Five the closed theoretical expressions developed in Chapter Four are discussed more fully. The responses are written in a more convenient, and general, form and then analysed in greater detail. In particular, the information available from the spin echoes, which, under certain circumstances, can be produced by the two pulse sequence, are discussed at some length. Background information concerning spin echoes in heteronuclear spin systems is included in the form of a literature review. At the end of the chapter the results of an experimental study of the two pulse responses for polycrystalline potassium hydrogen difluoride are reported.

In the final chapter (Six) attention is focussed on nuclear spin relaxation in heteronuclear spin systems and theoretical expressions are developed for several types of motional model. Two of these are used to model the spin-lattice relaxation for an assembly of hydrogen difluoride ions undergoing 180° rotational jumps at lattice sites. The results of this theoretical study together with experimental measurements of the spin-lattice relaxation behaviour of potassium and caesium hydrogen difluorides, as a function of temperature, are discussed in the final section of the chapter.

1.1 Spin Interaction in Solids: an Introduction

Many atomic nuclei possess spin angular momentum $\mathbf{I}\hbar$ (where $\hbar$ is Planck's constant divided by two pi) and have a magnetic moment $\boldsymbol{\mu}$ such that $\boldsymbol{\mu} = \gamma\hbar\mathbf{I}$, γ is the magnetogyric ratio of the nucleus. Such nuclei interact with magnetic fields, which may originate either from an 'internal' source (such as other nuclei or the motion of electrons), or from some external, applied source. In pulsed NMR it is usual to work under conditions where the 'size' of the externally applied magnetic field is much larger than the 'size' of any internal field.

Each nucleus has associated with it a nuclear spin quantum number, I, which can take integral or half-integral values (a nucleus with I = 0 does not possess spin angular momentum). The interaction between a nuclear spin and an applied, static magnetic field is called the Zeeman interaction, it results in 2I + 1 energy levels. The energies associated with these energy levels are given by the 2I + 1 eigenvalues of the Zeeman Hamiltonian, $\mathcal{H}^{Z}$. In a macroscopic sample, containing a large number of spins, there is, at equilibrium, a Boltzmann type distribution of the spins amongst these energy levels. Transitions between the Zeeman energy levels can be induced by an external time dependent interaction, of frequency ω, such that $\hbar\omega = \Delta E$ where ΔE is the energy difference between the initial and final energy levels. This interaction is described by a radio-frequency Hamiltonian, $\mathcal{H}^{RF}$.

Of course in a macroscopic sample the nuclear spins are never isolated. Local, internal interactions, between different nuclear spins and between nuclear spins and electrons, perturb the Zeeman energy levels. It is the detection and

identification of these perturbations which provides information on the environment (structural and electronic) of the spin. The two internal interactions which are of most concern in this thesis are the dipolar and shielding interactions.

The dipolar interaction is the direct pairwise interaction of two nuclear magnetic moments. Its magnitude depends on the relative positions of the nuclei, so it provides a useful way of probing molecular structure and characterising motional processes. In solids the dipolar interaction usually dominates any shielding interaction, whereas in liquids it is averaged to zero by isotropic motion. The dipolar Hamiltonian is labelled $\mathcal{H}^D$.

The electrons surrounding each nuclear spin create local magnetic fields which perturb the main magnetic field 'seen' by the spin: this, in essence, is the shielding interaction, it provides information about the electronic environment of the spin. The shielding, or, as it is more usually called, the chemical shift Hamiltonian is represented by $\mathcal{H}^{CS}$.

It is worthwhile noting that other spin interactions can be important in NMR studies. For example, for spins with $I \geq 1$ quadrupole interactions must be taken into account and in liquids and some high resolution solid studies an indirect dipolar interaction, called J-coupling, becomes important.

For the work described in this thesis the total Hamiltonian, $\mathcal{H}$, can be written:

$$\mathcal{H} = \mathcal{H}^Z + \mathcal{H}^{RF} + \mathcal{H}^D + \mathcal{H}^{CS}. \qquad 1.01$$

(Strictly speaking $\mathcal{H}^L$ the Hamiltonian which describes spin-lattice interactions should also be included in this

expression, but discussion of this is left until Chapter Six.) Full descriptions of these Hamiltonians are given in various texts (Spiess (1), Mehring (2), Abragam (3), Haeberlen (4)). A general description of the Hamiltonians, in their various forms, to be used in this thesis is given below.

Each of the component Hamiltonians, $\mathcal{H}^{\lambda}$, expresses the coupling of the nuclear spin vector with a second vector, which is either an applied field or another spin. Information about this coupling is contained in a second rank, Cartesian coupling tensor, $\mathbf{A}^{\lambda}$. The component Hamiltonian can be written very generally as:

$$\mathcal{H}^{\lambda} = \mathbf{I}.\mathbf{A}^{\lambda}.\mathbf{V} . \qquad 1.02$$

$\mathbf{I}$ is an operator representing the nuclear spin vector and $\mathbf{V}$ is an operator representing the vector to which it couples. Written in this way the Hamiltonian gives a straightforward picture of the physical relationship of $\mathbf{I}$ and $\mathbf{V}$, however, it can be written in another form which is particularly useful when rotations are needed

$$\mathcal{H}^{\lambda} = C^{\lambda} \sum_{L=0}^{2} \sum_{M=-L}^{L} (-1)^{M} R_{M}^{(L),\lambda} T_{-M}^{(L),\lambda}(\mathbf{I}\mathbf{V}) . \qquad 1.03$$

The $R_{M}^{(L),\lambda}$ contain spatial information only and are related to the coupling tensor $\mathbf{A}^{\lambda}$, whereas, $T_{M}^{(L),\lambda}(\mathbf{I}\mathbf{V})$ refers only to the spin variables. An explanation of these terms is given in the next section.

1.2 Operators, Axes and Tensors

1.2.1 Spin Operators

The wavefunctions associated with each spin state are characterised by the quantum number I and by a second quantum number m which describes quantisation along the applied magnetic

field, $I_z = m$ and, $m = -I, -I + 1, \ldots I - 1, I$. These wavefunctions are written $|Im\rangle$, no spatial information is included in the label because, at least for the purposes of this thesis, only spin operators will be considered. Using wavefunctions written in this way the component spin operators can be defined:

$$I_z|Im\rangle = m|Im\rangle \qquad 1.04$$

$$\left.\begin{aligned} I_x &= \tfrac{1}{2}(I_+ + I_-) \\ I_y &= \tfrac{1}{2i}(I_+ - I_-) \end{aligned}\right\} \qquad 1.05$$

where I_+ and I_- are the so-called raising and lowering operators:

$$I_\pm|Im\rangle = [I(I+1) - m(m \pm 1)]^{\frac{1}{2}}|I,m \pm 1\rangle . \qquad 1.06$$

The components of the spin operator in spherical form (these are the irreducible components of the spin vector operator) are:

$$I_0 \equiv I_z \qquad 1.07$$

and

$$I_{\pm 1} \equiv \mp \frac{1}{\sqrt{2}} I_\pm = \mp \frac{1}{\sqrt{2}}(I_x \pm iI_y) . \qquad 1.08$$

1.2.2 Coordinate Systems and the Rotation of Axes

The spin operators, as in common practice, are referred to a laboratory (LAB) based coordinate system (x,y,z) in which the z-axis lies along the axis of the applied magnetic field. (It is often convenient to introduce a rotating coordinate system in which this system rotates about its z-axis with an angular frequency ω_R (Section 1.4)).

The spatial part of the Hamiltonians (equation 1.03) can usefully be defined in three other coordinate systems. These are:

(i) A crystal based system (CRY) where the coordinate axes are based on some convenient feature of the crystal structure.

(ii) A molecule based system (MOL) in which the positions of the atoms in the molecule are described. This is necessary for intramolecular interactions.

(iii) A principal axes system (PAS) which is a system in which the second rank irreducible component of the coupling tensor is diagonal (Section 1.2.3).

All the coordinate systems are orthogonal. The advantages of these coordinate systems will become apparent later.

The next step is to consider how to specify an arbitrary rotation from one coordinate system to another. This is important because it is necessary to be able to express an operator such as $R^{(L),\lambda}_{M}$ in these different coordinate systems. A very general approach uses the Euler angles ($\alpha\beta\gamma$) as described below (Brink and Satchler (5), Rose (6)).

If a set of orthogonal axes (x,y,z) are rotated to new positions (x′,y′,z′), then the Euler angles are defined by carrying out the rotation in three steps.

First rotate the axes (x,y,z) through an angle α about the z-axis to new positions (x_1,y_1,z).

Then rotate the axes through an angle β about the y_1-axis to new positions (x'_1,y'_1,z′).

Finally rotate the axes through an angle γ about the z′-axis to final positions (x′,y′,z′).

The process is shown diagrammatically in Figure 1.1. All rotations are positive (that is a right-handed screw would travel away from the origin, when viewed from the origin, during a rotation).

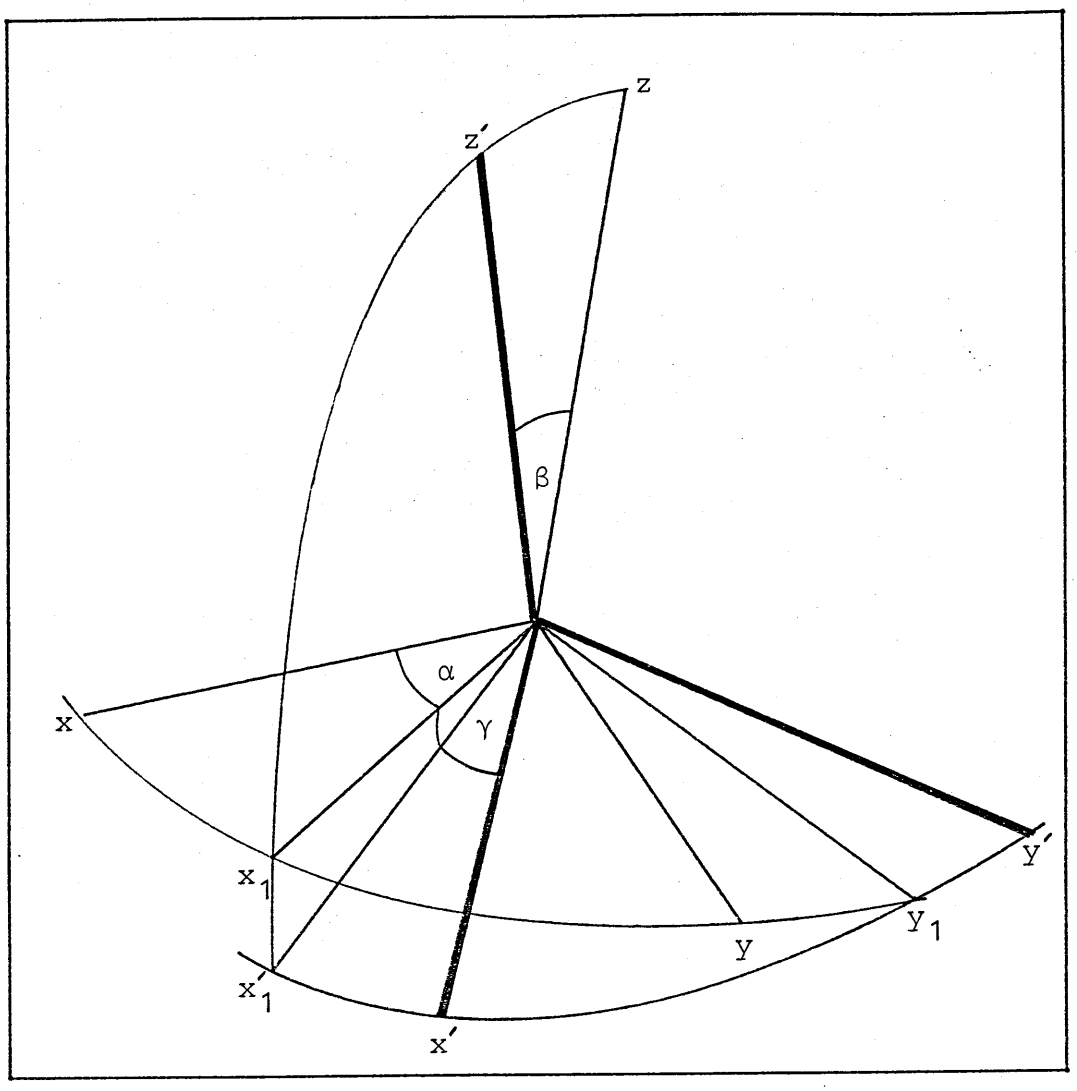

Figure 1.1 The rotations defined by the Euler angles $(\alpha\beta\gamma)$

The operator that performs this transformation is

$$D(\alpha\beta\gamma) = \exp(-i\gamma I_{z'}) \exp(-i\beta I_{y_1}) \exp(-i\alpha I_z) . \quad 1.09$$

Conveniently, the operator defined by equation 1.09 can be re-expressed in terms of rotations about the original z and y axes:

$$D(\alpha\beta\gamma) = \exp(-i\alpha I_z) \exp(-i\beta I_y) \exp(-i\gamma I_z) . \quad 1.10$$

Some properties of the rotation operator are given in Appendix A.

1.2.3 Tensors and Tensor Operators

The coupling tensor $\mathbf{A}^{\lambda}$ (equation 1.02) can be reduced, as can any general second rank, Cartesian tensor (so we shall drop the superscript λ for now), to three irreducible components - a scalar, an antisymmetric first rank tensor and a traceless, symmetric second rank tensor:

$$\mathbf{A}^{(2)} \rightarrow \mathbf{R}^{(0)} + \mathbf{R}^{(1)} + \mathbf{R}^{(2)} . \qquad 1.11$$

The superscript is the rank of the tensor. For dipolar coupling the antisymmetric component, $\mathbf{R}^{(1)}$, is zero and it has little effect on the shielding interaction in the systems of interest in this work (for a full discussion of this see Haeberlen (4), Chapter 3). The remaining irreducible components are defined as:

$$\mathbf{R}^{(0)} = \tfrac{1}{3}(A^{(2)}_{xx} + A^{(2)}_{yy} + A^{(2)}_{zz}) \qquad 1.12$$

$$\mathbf{R}^{(2)} = \begin{pmatrix} R^{(2)}_{xx} & R^{(2)}_{xy} & R^{(2)}_{xz} \\ R^{(2)}_{xy} & R^{(2)}_{yy} & R^{(2)}_{yz} \\ R^{(2)}_{xz} & R^{(2)}_{yz} & R^{(2)}_{zz} \end{pmatrix} \qquad 1.13$$

$$\text{where } R^{(2)}_{ab} = \tfrac{1}{2}(A^{(2)}_{ab} + A^{(2)}_{ba}) - \tfrac{1}{3}\sum_{c} A^{(2)}_{cc}\,\delta_{ab} . \qquad 1.14$$

The subscripts in this expression, a,b,c = x,y,z of the LAB system. For the irreducible component $\mathbf{R}^{(2)}$ there is an axes system in which its matrix is diagonal - this system is called the principal axes system, PAS. If the $\boldsymbol{\rho}^{(L)}$ are the irreducible components of the coupling tensor $\mathbf{A}^{\lambda}$ in the PAS, then:

$$\boldsymbol{\rho}^{(2)} = \begin{pmatrix} \rho_{XX}^{(2)} & 0 & 0 \\ 0 & \rho_{YY}^{(2)} & 0 \\ 0 & 0 & \rho_{ZZ}^{(2)} \end{pmatrix} \qquad 1.15$$

where $\rho_{aa}^{(2)} = A_{aa}^{(2)} - \frac{1}{3}\sum_{b} A_{bb}^{(2)}$ 1.16

(a,b = X,Y,Z of the PAS) and since the scalar part is the same in all coordinate systems:

$$\mathbf{R}^{(0)} = \boldsymbol{\rho}^{(0)}. \qquad 1.17$$

The $\mathbf{R}^{(2)}$ and $\boldsymbol{\rho}^{(2)}$ are related through the unitary transformation

$$\mathbf{R}^{(2)} = D(\alpha\beta\gamma)\, \boldsymbol{\rho}^{(2)} D^{-1}(\alpha\beta\gamma) \qquad 1.18$$

where, as explained in Appendix A, $D^{-1}(\alpha\beta\gamma)$ is the inverse of $D(\alpha\beta\gamma)$. The matrix $D(\alpha\beta\gamma)$ and the components $R_{xx}^{(2)}$ and $R_{yy}^{(2)}$ and $R_{zz}^{(2)}$ of $\mathbf{R}^{(2)}$ are also given in Appendix A. (Clearly, the full coupling tensor $\mathbf{A}^{\lambda,LAB}$ can also be related to $\mathbf{A}^{\lambda,PAS}$ through equation 1.18). The rotation matrix used here is that derived for the case when $(\alpha\beta\gamma)$ describe positive rotations of a function about a space fixed axes system - in this case the axes system (X,Y,Z) is the principal axes system. This convention is used throughout this thesis.

The (X,Y,Z) axes of the PAS are labelled according to the convention

$$|\rho_{ZZ}^{(2)}| \geq |\rho_{XX}^{(2)}| \geq |\rho_{YY}^{(2)}|.$$

It is convenient to define an asymmetry parameter

$$\eta = \frac{\rho_{YY}^{(2)} - \rho_{XX}^{(2)}}{\delta}, \quad 0 \leq \eta \leq 1 \qquad 1.19$$

where $\delta = \rho_{ZZ}^{(2)}$ is the principal value of the tensor, so that

$$\rho^{(2)} = \delta \begin{pmatrix} -\frac{1}{2}(1 + \eta) & 0 & 0 \\ 0 & -\frac{1}{2}(1 - \eta) & 0 \\ 0 & 0 & 1 \end{pmatrix} \qquad 1.20$$

In principle it is the three parameters $\rho^{(0)}$, δ and η which can be obtained from an experiment. In some cases (if the sample is polycrystalline) these three parameters are all that can be obtained from experiment in which case the orientation of the PAS with respect to the LAB system is not known. However, if the angles $(\alpha\beta\gamma)$ in equation 1.18 can be found (Haeberlen (4) Chapter 3 - B) then the position of the PAS with respect to the LAB system is known and then if the position of the MOL or CRY systems relative to the LAB system is known (which it can be for a single crystal study) it is possible to relate δ and η to the molecular or crystal structure of the sample. This process involves the use of equation 1.18 twice which can be a laborious process so it is more convenient to write the irreducible Cartesian components in the PAS as spherical components $\rho^{(L)}_M$ so that they transform according to

$$R^{(L)}_M = \sum_{M'} \rho^{(L)}_{M'} \mathcal{D}^{(L)}_{M'M}(\alpha\beta\gamma) \qquad 1.21$$

and the $R^{(L)}_M$ can be found in any axes system rotated with respect to the PAS. $\mathcal{D}^{(L)}_{M'M}(\alpha\beta\gamma)$ is an element of the Wigner rotation matrix, it can be re-expressed as

$$\mathcal{D}^{(L)}_{M'M}(\alpha\beta\gamma) = \exp(-i(M'\alpha + M\gamma))\ d^{(L)}_{M'M}(\beta).$$

The reduced Wigner rotation matrixes, $d^{(L)}(\beta)$, are real and can be calculated explicitly; the reduced matrixes for $L = \frac{1}{2}$ and $L = 2$ are given in Appendix A along with some of the important properties of the Wigner rotation matrices. Finally, the

relationship between the Cartesian and spherical components of $\boldsymbol{\rho}$ in the PAS are given below.

$$\rho_0^{(0)} = \boldsymbol{\rho}^{(0)} = \frac{1}{3}(A_{xx}^{(2)} + A_{yy}^{(2)} + A_{zz}^{(2)})$$

and

$$\rho_0^{(2)} = \sqrt{\tfrac{3}{2}}\delta,\ \rho_{+1}^{(2)} = \rho_{-1}^{(2)} = 0,\ \rho_{+2}^{(2)} = \rho_{-2}^{(2)} = -\tfrac{1}{2}\delta\eta. \quad 1.22$$

To summarise then, the $R_M^{(L),\lambda}$ in equation 1.03 are the irreducible spherical components of the coupling tensor $\mathbf{A}^{\lambda}$ in equation 1.02. The irreducible spherical components in a coodinate system (x,y,z) are related to the PAS components through equation 1.21.

The tensor operator $\mathbf{T}^{(L)}$ whose components appear in equation 1.03 is different in origin to the $R_M^{(L)}$ defined in equation 1.21. $\mathbf{T}^{(L)}$ is formed from the direct product of two irreducible spherical tensor operators $\mathbf{I}$ and $\mathbf{V}$ of rank L_1 and L_2 respectively such that $L = L_1 + L_2$. The irreducible spherical components of the new operator are

$$T_M^{(L)}(\mathbf{I}^{(L_1)}\mathbf{V}^{(L_2)}) = \sum_{m_1}\sum_{m_2}(I_{m_1}^{(L_1)}V_{m_2}^{(L_2)})\langle L_1L_2m_1m_2|LM\rangle. \quad 1.23$$

The left hand side of this equation indicates that the $T_M^{(L)}$ are formed from the product of $\mathbf{I}$ and $\mathbf{V}$, although the part in the bracket is usually omitted. The quantity $\langle L_1L_2m_1m_2|LM\rangle$ is a Clebsch-Gordan or vector coupling coefficient, it is defined by Brink and Satchler (5). L may take any value from $L_1 + L_2$ in integer steps to $|L_1 - L_2|$ and $M = m_1 + m_2$. Equation 1.23 is not used for the scalar product ($L_1 - L_2 = 0$) of two vectors ($L_1 = L_2 = 1$), instead:

$$T_0^{(0)} = \sum_{m=-1}^{1}(-1)^m I_m^{(1)} V_{-m}^{(1)}. \quad 1.24$$

The reason for writing the spin vector operator in its irreducible component form and a further reason for writing the spatial part of the Hamiltonian in the same way now becomes clear - equation 1.23 applies only when $\mathbf{I}$ and $\mathbf{V}$ are written in irreducible form. Equations 1.23 and 1.24 can be evaluated for the direct product of two vectors $\mathbf{I}$ and $\mathbf{V}$. The results are:

$$T_0^{(0)} = (I_o V_o - I_{+1} V_{-1} - I_{-1} V_{+1}) \qquad 1.25$$

$$\left.\begin{aligned} T_0^{(1)} &= \frac{1}{\sqrt{2}}(I_{+1} V_{-1} - I_{-1} V_{+1}) \\ T_{\pm 1}^{(1)} &= \frac{1}{\sqrt{2}}(\pm I_{\pm 1} V_o \mp I_o V_{\pm 1}) \end{aligned}\right\} \qquad 1.26$$

$$\left.\begin{aligned} T_0^{(2)} &= \frac{1}{\sqrt{6}}(I_{+1} V_{-1} + I_{-1} V_{+1} + 2 I_0 V_0) \\ T_{\pm 1}^{(2)} &= \frac{1}{\sqrt{2}}(I_{\pm 1} V_0 + I_0 V_{\pm 1}) \\ T_{\pm 2}^{(2)} &= I_{\pm 1} V_{\pm 1} . \end{aligned}\right\} \qquad 1.27$$

1.3 The Hamiltonians (in detail)

The Hamiltonian in irreducible spherical operator form is (equation 1.03)

$$\mathcal{H}^{\lambda} = C^{\lambda} \sum_{L=0}^{2} \sum_{M=-L}^{L} (-1)^M R_M^{(L),\lambda} T_{-M}^{(L),\lambda}(\mathbf{IV}) . \qquad 1.03$$

This Hamiltonian can be used either as it is or written in a more specific way. In this thesis both approaches are going to be used so, now that the background to equation 1.03 has been investigated, it can be expanded to give more explicit Hamiltonians.

1.3.1 The Zeeman Hamiltonian

This is the simplest of the Hamiltonians - the LAB system is the Zeeman PAS (the $R^{(L)}_M = \rho^{(L)}_M$ in equation 1.03) and the magnetic field is chosen to lie along the LAB z-axis and is taken to be homogeneous: $\mathbf{B} = (0,0,B_0)$. Using equations 1.25 - 1.27 in conjunction with equations 1.22 the Hamiltonian becomes

$$\mathcal{H}^Z = C^Z [R^{(0)}_0 T^{(0)}_0 + R^{(2)}_0 T^{(2)}_0]$$

since $B_{+1} = B_{-1} = 0$. From equation 1.22, and 1.16

$R^{(0)}_0 = \rho^{(0)}_0 = \frac{1}{3}(Z^{(2)}_{xx} + Z^{(2)}_{yy} + Z^{(2)}_{zz})$ and

$R^{(2)}_0 = \rho^{(2)}_0 = \sqrt{\frac{3}{2}}(Z^{(2)}_{zz} - \frac{1}{3}(Z^{(2)}_{xx} + Z^{(2)}_{yy} + Z^{(2)}_{zz}))$.

$\mathbf{Z}^{(2)}$ is the Zeeman coupling tensor which is just the unit matrix so $R^{(2)}_0 = 0$ and $R^{(0)}_0 = 1$. The coefficient C^Z is $-\gamma_i$ so, summed over all spins,

$$\mathcal{H}^Z = -\sum_i \gamma_i B_0 I_{0,i} = -\sum_i \omega_{0,i} I_{0,i} . \qquad 1.28$$

$\omega_{0,i}$ is the Larmor frequency of the ith nucleus, $\omega_{0,i} = \gamma_i B_0$. The sum is over all nuclei with non-zero spin.

1.3.2 The RF Hamiltonian

Following the procedure used for the Zeeman Hamiltonian but with $\mathbf{B}^{RF} = (0, B^{RF}_y \cdot \cos \omega t, 0)$ where ω is the radiation frequency (the coupling tensor is still the unit matrix) it can be shown that

$$\mathcal{H}^{RF} = B^{RF}_y \cos \omega t \sum_i \gamma_i I_{y,i} . \qquad 1.29$$

It is usual to think of the oscillating magnetic field associated with the radiation as two counter-rotating fields. The significance of this will become apparent shortly.

1.3.3 The Dipolar Hamiltonian

The dipolar coupling tensor is symmetric and traceless so there can be no terms in equation 1.03 with L = 0 or L = 1. Starting from

$$\mathcal{H}^D = \sum_{i<j} C^D_{ij} \sum_{M=-2}^{2} (-1)^M R^{(2)}_{M,ij} T^{(2)}_{-M,ij} (\mathbf{I}_i \mathbf{I}_j)$$

it is a straightforward matter to derive the familiar dipolar Hamiltonian (given in many standard texts, for example Abragam (3)

Using equation 1.21 $R^{(2)LAB}_{M,ij}$ can be related to the dipolar PAS:

$$\mathcal{H}^D = \sum_{i<j} C^D_{ij} \sum_{M=-2}^{2} (-1)^M \mathcal{D}^{(2)}_{0,M}(\alpha\beta\gamma)\, \rho^{(2)}_0 T^{(2)}_{-M}$$

only $\rho^{(2)}_0$ is non-zero ($\eta = 0$) so no additional sum is necessary. r_{ij} is the distance between spin i and spin j, $\rho^{(2)}_0 = \sqrt{\frac{3}{2}} r_{ij}^{-3}$. The $T^{(2)}_{-M}$ are given by equation 1.27 and the $\mathcal{D}^{(2)}_{0,M}(\alpha\beta\gamma)$ come from Appendix A:

$$\mathcal{H}^D = \sum_{i<j} C^D_{ij}\, r_{ij}^{-3} \{ [\tfrac{3}{4}\sin^2\beta\, e^{+2i\gamma}\, I_{+1,i}\, I_{+1,j} + \text{complex conjugate}]$$

$$+ [-\frac{3}{2\sqrt{2}} \sin\beta \cos\beta\, e^{+i\gamma} (I_{+1,i}\, I_{0,j} + I_{0,i}\, I_{+1,j}) + \text{complex conjugate}]$$

$$+ \tfrac{1}{4}(3\cos^2\beta - 1)(2I_{0,i}\, I_{0,j} + I_{+1,i}\, I_{-1,j} + I_{-1,i}\, I_{+1,j}) \}.$$

Replacing I_0 with I_z and $I_{\pm 1}$ with $\mp \frac{1}{\sqrt{2}} I_{\pm}$, with $C^D_{ij} = -2\gamma_i\gamma_j\hbar \cdot \frac{\mu_0}{4\pi}$ this becomes:

$$\mathcal{H}^D = -\frac{\mu_0}{4\pi} \sum_{i<j} \frac{\gamma_i\gamma_j\hbar}{r^3_{ij}} \cdot [A + B + C + D + E + F] \qquad 1.30$$

where $A = (3\cos^2\beta - 1)\, I_{z,i}\, I_{z,j}$

$B = -\frac{1}{4}(3\cos^2\beta - 1)(I_{+,i}\, I_{-,j} + I_{-,i}\, I_{+,j})$

$C = -\frac{3}{2}\sin\beta\cos\beta\, e^{+i\gamma}(I_{+,i}\, I_{z,j} + I_{z,i}\, I_{+,j})$

$D = C^*$

$E = \frac{3}{4}\sin^2\beta\, e^{+2i\gamma}\, I_{+,i}\, I_{+,j}$

$F = E^*$

and the symbol * stands for complex conjugate, μ_0 is the permeability of free space.

The Eulerian angles β and γ describe the laboratory system, with the z-axis parallel to the applied magnetic field, in the PAS of the dipolar interaction between spins i and j, that is r_{ij} is parallel to Z. In terms of the conventional polar coordinates (θ,ϕ) which describe the direction of the inter-nuclear vector in the LAB system (Abragam (3)) $\beta = \theta$ and the x-axis is fixed so that $\gamma = \pi - \phi$. The expressions for the individual letters of the dipolar alphabet are then as given in standard texts. It is worth noting that for a large number of spins the sum over $i < j$ can, alternatively, be written as $\frac{1}{2}\sum_i \sum_j$

1.3.4 The Shielding Hamiltonian

This is more complicated than the dipolar Hamiltonian because the shielding tensor need not be symmetric and traceless. A procedure similar to that used for the dipolar Hamiltonian can be used to develop the shielding Hamiltonian. Instead of repeating the process here it is included in Appendix B. The result for the truncated (Section 1.4) Hamiltonian is:

$$\mathcal{H}^{CS} = \sum_i \omega_{0,i}\, I_{0,i}\, \sigma_{zz,i} \qquad 1.31$$

where $\sigma_{zz,i}$ is the zz-component of the shielding tensor in the LAB system. The sum is over all spins.

Table 1.1 summarises the C, $R_M^{(L)}$ and $T_M^{(L)}$ for each Hamiltonian.

1.4 The Rotating Frame

There are two practical advantages in transforming the Hamiltonians from a static to a rotating coordinate system:

(a) It becomes easier to visualise and to describe the effect of an RF pulse on a spin system.

(b) When phase sensitive detection is used in an experiment the magnetisation is effectively measured in the rotating frame.

The static and rotating frame Hamiltonians are related through:

$$\mathcal{H}^{\lambda}_{R} = \exp(i\sum_i I_{0,i}\ \omega_{R,i}\ t)\ \mathcal{H}^{\lambda}\ \exp(-i\sum_i I_{0,i}\ \omega_{R,i}\ t). \qquad 1.32$$

(The subscript R indicates a quantity in the rotating frame.) This expression allows any number of rotating frames to be introduced. The transformation can introduce a time dependence into the spin part of a Hamiltonian since:

$$e^{i(\omega_{R,i}\ I_{0,i})t}\ I_{m,i}\ e^{-i(\omega_{R,i}\ I_{0,i})t} = I_{m,i}\ e^{i(m\omega_{R,i})t} \qquad 1.33$$

and, for the dipolar Hamiltonian:

$$e^{i(\omega_{R,i}\ I_{0,i} + \omega_{R,j}\ I_{0,j})t}\ I_{m,i}\ I_{m',j}\ e^{-i(\omega_{R,i}\ I_{0,i} + \omega_{R,j}\ I_{0,j})t}$$

$$= I_{m,i}\ I_{m',j}\ e^{i(m\omega_{R,i} + m'\omega_{R,j})t}. \qquad 1.34$$

When a Hamiltonian is truncated all those terms which have a zero time average in the rotating frame (those containing

Table 1.1 The spin and spatial components of the Hamiltonians

Interaction	λ	$T_0^{(0)}$	$T_0^{(2)}$	$T_{\pm1}^{(2)}$	$T_{\pm2}^{(2)}$
Zeeman	Z	$I_0 B_0$	-	0	0
RF	RF	$-I_{+1}B_{-1}^{RF} - I_{-1}B_{+1}^{RF}$	-	-	-
Dipolar	D	-	$\frac{1}{\sqrt{6}}(2I_{0,i}\ I_{0,j} + I_{+1,i}\ I_{-1,j} + I_{-1,i}\ I_{+1,j})$	$\frac{1}{\sqrt{2}}(I_{\pm1,i}\ I_{0,j} + I_{0,i}\ I_{\pm1,j})$	$I_{\pm1,i}\ I_{\pm1,j}$
Shielding	CS	$I_0 B_0$	$\sqrt{\frac{2}{3}} I_0 B_0$	$\frac{1}{\sqrt{2}}(I_{\pm1} B_0)$	0

Interaction	λ	c^λ	$\rho_0^{(0)}$	$\rho_0^{(2)}$	$\rho_{\pm1}^{(2)}$	$\rho_{\pm2}^{(2)}$
Zeeman	Z	$-\gamma_i$	1	0	-	-
RF	RF	$-\gamma_i$	1	0	0	0
Dipolar	D	$-2\gamma_i\gamma_j\hbar\frac{\mu_0}{4\pi}$	0	$\sqrt{\frac{3}{2}} r_{ij}^{-3}$	0	0
Shielding	CS	γ_i	$\frac{1}{3}(\sigma_{xx} + \sigma_{yy} + \sigma_{zz})$	$\sqrt{\frac{3}{2}}\delta$	0	$-\frac{1}{2}\delta\eta$

All the symbols are as defined in the text.

$e^{\pm i\omega t}$) are dropped. This has important consequences for the dipolar Hamiltonian; if $\omega_{R,i} = \omega_{R,j}$ only those terms with $m = -m'$ are not rejected by the truncation (these are the A and B terms in equation 1.30). When $\omega_{R,i} \neq \omega_{R,j}$ only the terms with $m = m' = 0$ are retained - the A term in equation 1.30. The terms not rejected by the truncation, the so called secular terms, are those which commute with $\mathcal{H}^Z$. Haeberlen (4) discusses this truncation and points out that it is equivalent to first order perturbation theory. Table 1.2 summarises the time independent spin components of the Hamiltonians in the rotating frame.

1.5 The Density Matrix

The formal definition of the density matrix is given in many standard texts - Slichter (7), Chapter 5, for example - so only a few key equations will be given here. The expectation value of an observable Q over an ensemble is

$$\langle Q \rangle = \mathrm{Tr}\{\sigma Q\} . \qquad 1.35$$

Tr stands for trace (diagonal sum), σ is the density matrix (whenever we use the density matrix we expect to take an average over a statistical ensemble).

In the rotating frame

$$\langle Q \rangle_R = \mathrm{Tr}\{\sigma_R Q\} . \qquad 1.36$$

At thermal equilibrium

$$\sigma \rightarrow \sigma(0) = \frac{\exp(-\hbar\mathcal{H}/kT)}{\mathrm{Tr}\{\exp(-\hbar\mathcal{H}/kT)\}} . \qquad 1.37$$

k is the Boltzmann constant and T the temperature. In the high temperature approximation ($\hbar\mathcal{H} << kT$) which always applies in this work, the exponentials in equation 1.37 may be expanded. Retaining the first two terms

Table 1.2 The time independent spin components of the Hamiltonians in the rotating frame.

Interaction	$T_0^{(0)}$	$T_0^{(2)}$	$T_{\pm1}^{(2)}$	$T_{\pm2}^{(2)}$
Zeeman	$I_0 B_0$	-	0	0
RF[1]	$\frac{1}{2} I_y B_y^{RF}$	-	-	-
Shielding	$I_0 B_0$	$\sqrt{\frac{2}{3}} I_0 B_0$	0	0
Dipolar[2]	-	$\frac{1}{\sqrt{6}}(2I_{0,i} I_{0,j} + I_{+1,i} I_{-1,j} + I_{-1,i} I_{+1,j})$	0	0
Dipolar[3]	-	$\sqrt{\frac{2}{3}} I_{0,i} I_{0,j}$	0	0

[1] $\omega_R = \omega$ (the rotating frame rotates at the frequency of the RF radiation). Under these conditions the RF field is stationary, this leads to the concept of a pulse angle (Chapter 2). The factor of $\frac{1}{2}$ appears because only one component of the counter-rotating fields (Section 1.3.2) is time independent in the rotating frame.

[2] $\omega_{R,i} = \omega_{R,j}$

[3] $\omega_{R,i} \neq \omega_{R,j}$

$$\sigma(0) \cong \frac{1-\hbar\mathcal{H}/kT}{Tr\{1-\hbar\mathcal{H}/kT\}} .$$

The dominant part of $\mathcal{H}$ is $\mathcal{H}^Z = -\omega_0 I_0$ and in any basis set $Tr\{I_0\} = 0$ so

$$\sigma(0) \cong \frac{1 + \omega_0 I_0/kT}{Tr\{1\}} . \qquad 1.38$$

$Tr\{1\}$ is the trace of the unit matrix with the same dimension as the density matrix, that is with the dimension of the spin space. At thermal equilibrium, then

$$\langle Q \rangle = \frac{Tr\{1 + \omega_0 I_0/kT\}}{Tr\{1\}}$$

Providing $Tr\{Q\} = 0$, which it is if Q is I_x, I_y or I_z, the first term in equation 1.38 can be omitted. Hence

$$\sigma(0) = \frac{\omega_0 I_0}{Tr\{1\}kT} \equiv cI_0 . \qquad 1.39$$

Even if the spin system is perturbed from equilibrium in some way the unity term in equation 1.38 would be unchanged so it could still be omitted. The equation of motion of the density matrix subjected to a perturbation is the Liouville-Von Neumann equation:

$$\frac{d}{dt}\sigma(t) = -i[\mathcal{H},\sigma(t)] \qquad 1.40$$

which has the solution

$$\sigma(t) = \exp(-i\mathcal{H}t)\ \sigma(0)\ \exp(i\mathcal{H}t) \qquad 1.41$$

where $\mathcal{H}$ is the time independent perturbing Hamiltonian.

1.6 Appendices

1.6.1 Appendix A

The rotation operator

$$D(\alpha\beta\gamma) = \exp(-i\alpha I_z)\ \exp(-i\beta I_y)\ \exp(-i\gamma I_z)$$

where $(\alpha\beta\gamma)$ are the Euler angles defined in Section 1.2.2, has the following properties, which arise since D is a unitary operator:

$$D^{\dagger}(\alpha\beta\gamma) = D^{-1}(\alpha\beta\gamma) = D(-\gamma,-\beta,-\alpha)\ . \qquad \text{A1}$$

$D^{\dagger}$ is the adjoint of D, $D^{\dagger}D = DD^{\dagger} = 1$. A2

The transformation of the tensor $\mathbf{P}^{(2)} = \delta \begin{pmatrix} -\frac{1}{2}(1+\eta) & 0 & 0 \\ 0 & -\frac{1}{2}(1-\eta) & 0 \\ 0 & 0 & 1 \end{pmatrix}$

for example, using

$$\mathbf{R}^{(2)} = D(\alpha\beta\gamma)\ \mathbf{P}^{(2)}\ D^{-1}(\alpha\beta\gamma)$$

is achieved with the matrix

$$D(\alpha\beta\gamma) = \begin{pmatrix} \cos\alpha\cos\beta\cos\gamma - \sin\alpha\sin\gamma & \sin\alpha\cos\beta\cos\gamma + \cos\alpha\sin\gamma & -\sin\beta\cos\gamma \\ -\cos\alpha\cos\beta\sin\gamma - \sin\alpha\cos\gamma & -\sin\alpha\cos\beta\sin\gamma + \cos\alpha\cos\gamma & \sin\beta\sin\gamma \\ \cos\alpha\sin\beta & \sin\alpha\sin\beta & \cos\beta \end{pmatrix} \qquad \text{A3}$$

and its inverse. The elements $R^{(2)}_{xx}$, $R^{(2)}_{yy}$ and $R^{(2)}_{zz}$ of the transformed tensor are

$$R^{(2)}_{xx} = \frac{\delta}{2}(-1 + 3\sin^2\beta\cos^2\gamma - \eta[\cos2\alpha(\cos^2\beta\cos^2\gamma - \sin^2\gamma) - \sin2\alpha\sin2\gamma\cos\beta]) \qquad \text{A4}$$

$$R^{(2)}_{yy} = \frac{\delta}{2}(-1 + 3\sin^2\beta\sin^2\gamma - \eta[\cos2\alpha(\cos^2\beta\sin^2\gamma - \cos^2\gamma) + \sin2\alpha\sin2\gamma\cos\beta]) \qquad \text{A5}$$

$$R_{zz}^{(2)} = \frac{\delta}{2}(3\cos^2\beta - 1 - \eta\sin^2\beta\cos 2\alpha) . \qquad A6$$

If the irreducible components of $\rho^{(2)}$ are known (equation 1.22) the transformation of the tensor can be alternatively expressed as

$$R_M^{(2)} = \sum_{M'} \rho_{M'}^{(2)} \mathcal{D}_{M'M}^{(2)}(\alpha\beta\gamma) .$$

The irreducible rotation matrices - the Wigner rotation matrices $\mathcal{D}^{(L)}(\alpha\beta\gamma)$ can be written (see also Table 1.3)

$$\mathcal{D}_{M'M}^{(L)}(\alpha\beta\gamma) = \exp(-i(M'\alpha + M\gamma))\ d_{M'M}^{(L)}(\beta) . \qquad A7$$

The Wigner rotation matrices have some important properties.

$$\mathcal{D}_{M'M}^{(L)}(\alpha\beta\gamma)^* = (-1)^{M'-M}\mathcal{D}_{-M',-M}^{(L)}(\alpha\beta\gamma) = \mathcal{D}_{MM'}^{(L)}(-\gamma,-\beta,-\alpha) \qquad A8$$

where * stands for complex conjugate. Also:

$$\int \mathcal{D}_{M'M}^{(L)}(\alpha\beta\gamma)^* \mathcal{D}_{N'N}^{(L')}(\alpha\beta\gamma)\ d(\alpha\beta\gamma) = \frac{8\pi^2}{2L+1}\delta_{LL'}\delta_{MN}\delta_{M'N'} \qquad A9$$

where

$$\int d(\alpha\beta\gamma) = \int_0^{2\pi} d\alpha \int_0^{\pi} \sin\beta\, d\beta \int_0^{2\pi} d\gamma . \qquad A10$$

1.6.2 Appendix B

From equation 1.03, ignoring the L = 1 terms, the shielding Hamiltonian is

$$\mathcal{H}^{CS} = C^{CS}(R_0^{(0)}\ T_0^{(0)} + \sum_{M=-2}^{2}(-1)^M\ R_M^{(2)}\ T_{-M}^{(2)}) .$$

Following the procedure used previously for the dipolar Hamiltonian:

$$\mathcal{H}^{CS} = C^{CS}(\rho_0^{(0)} T_0^{(0)} + \sum_{M=-2}^{2}\sum_{M'=-2}^{2}(-1)^M\ \rho_{M'}^{(2)}\mathcal{D}_{M'M}^{(2)}(\alpha\beta\gamma)\ T_{-M}^{(2)})$$

($\mathcal{D}_0^{(0)} = 1$). After truncation (Section 1.4) and using equation 1.27 this becomes

$$\mathcal{H}_R^{CS} = C^{CS}(\rho_0^{(0)} + \sum_{M'=-2}^{2}\sqrt{\tfrac{2}{3}}\rho_{M'}^{(2)}\mathcal{D}_{M'0}^{(2)}(\alpha\beta\gamma))\, I_0 B_0 .$$

Table 1.3

The reduced Wigner rotation matrix elements (the $d^{(L)}_{M'M}(\beta)$) for $L = \frac{1}{2}$ and $L = 2$.

$d^{(\frac{1}{2})}_{M'M}(\beta)$	$M = \frac{1}{2}$	$M = -\frac{1}{2}$
$M' = \frac{1}{2}$	$\cos(\beta/2)$	$-\sin(\beta/2)$
$M' = -\frac{1}{2}$	$\sin(\beta/2)$	$\cos(\beta/2)$

$d^{(2)}_{M'M}(\beta)$	2	1	M 0	-1	-2
2	$\cos^4(\beta/2)$	$-\frac{1}{2}\sin\beta(\cos\beta + 1)$	$\sqrt{\frac{3}{8}}\sin^2\beta$	$\frac{1}{2}\sin\beta(\cos\beta - 1)$	$\sin^4(\beta/2)$
1	$\frac{1}{2}\sin\beta(\cos\beta + 1)$	$\frac{1}{2}(2\cos\beta - 1)$ $(1 + \cos\beta)$	$-\sqrt{\frac{3}{2}}\sin\beta\cos\beta$	$\frac{1}{2}(2\cos\beta + 1)$ $(1 - \cos\beta)$	$\frac{1}{2}\sin\beta(\cos\beta - 1)$
M' 0	$\sqrt{\frac{3}{8}}\sin^2\beta$	$\sqrt{\frac{3}{2}}\sin\beta\cos\beta$	$\frac{1}{2}(3\cos^2\beta - 1)$	$-\sqrt{\frac{3}{2}}\sin\beta\cos\beta$	$\sqrt{\frac{3}{8}}\sin^2\beta$
-1	$-\frac{1}{2}\sin\beta(\cos\beta - 1)$	$\frac{1}{2}(2\cos\beta + 1)$ $(1 - \cos\beta)$	$\sqrt{\frac{3}{2}}\sin\beta\cos\beta$	$\frac{1}{2}(2\cos\beta - 1)$ $(1 + \cos\beta)$	$-\frac{1}{2}\sin\beta(\cos\beta + 1)$
-2	$\sin^4(\beta/2)$	$-\frac{1}{2}\sin\beta(\cos\beta - 1)$	$\sqrt{\frac{3}{8}}\sin^2\beta$	$\frac{1}{2}\sin\beta(\cos\beta + 1)$	$\cos^4(\beta/2)$

Equation 1.22 gives $\rho_{\pm 1}^{(2)} = 0$ so, using Appendix A:

$$\mathcal{L}_R^{CS} = C^{CS}(\rho_0^{(0)} + \frac{1}{\sqrt{6}}\rho_0^{(2)}(3\cos^2\beta - 1) + \tfrac{1}{2}\rho_2^{(2)} \sin^2\beta(e^{2i\alpha} + e^{-2i\alpha}))I_0B_0 .$$

From equation 1.22 and with $C^{CS} = \gamma$ it follows that

$$\mathcal{L}_R^{CS} = \omega_0 I_0[\tfrac{1}{3}(\sigma_{XX} + \sigma_{YY} + \sigma_{ZZ}) + \frac{\delta}{2}(3\cos^2\beta - 1 - \eta\sin^2\beta \cos 2\alpha)] . \qquad B1$$

The last part of this equation is just $R_{zz}^{(2)}$ (Appendix A, equation A6) and from equation 1.14 equation B1 simplifies to

$$\mathcal{L}_R^{CS} = \omega_0 I_0 \sigma_{zz} \qquad B2$$

where σ_{zz} is the zz-component of the shielding tensor in the LAB system. The Euler angles β and α in equation B1 are the polar angles of the applied field in the PAS of the shielding tensor.

1.7 References

(1) H.W. Spiess, 'Rotation of Molecules and Nuclear Spin Relaxation', NMR - Basic Principles and Progress, Volume 15, Springer-Verlag, Berlin 1978.

(2) M. Mehring, 'High Resolution NMR Spectroscopy in Solids', NMR - Basic Principles and Progress, Volume 11, Springer-Verlag, Berlin 1976.

(3) A. Abragam, ' The Principles of Nuclear Magnetism', Oxford University Press, Oxford 1961.

(4) U. Haeberlen, 'High Resolution NMR in Solids, Selective Averaging', Supplement 1, Advances in Magnetic Resonance, Academic Press, New York 1976.

(5) D.M. Brink and G.R. Satchler, 'Angular Momentum', Oxford University Press, Oxford 1971 (2nd edition).

(6) M.E. Rose, 'Elementary Theory of Angular Momentum', John Wiley and Sons Inc., New York 1957.

(7) C.P. Slichter, 'Principles of Magnetic Resonance', Harper and Row, New York 1963.

CHAPTER TWO

The NMR Response to a Single Pulse: Calculations

The time-dependent NMR signal following a single rf pulse, or a series of such pulses, can be calculated using the density matrix formulism (Lowe and Norberg(1)). Closed expressions can be obtained if the calculations are carried out for small groups of spins as, for example, recently shown by Boden and Kahol(2) in a study of a homonuclear four spin-$\frac{1}{2}$ system with rectangular geometry. For larger spin systems some form of time expansion is necessary to make the calculations practicable. The most straightforward approach is to use the so-called moment expansion (Powles and Strange(3), Mansfield(4)) although evaluation of all but the leading terms is difficult. Other expansion theorems have been suggested (Parker(5), Evans and Powles(6), Smith(7)), their advantages being that they converge more rapidly than the moment expansion, but again they tend to be very difficult to evaluate as shown, for example, by the recent study by Whitaker(8) of a cubic spin-$\frac{1}{2}$ lattice.

The aim of this chapter is to briefly review the density matrix formulism and demonstrate how it can be used to determine explicit expressions for the NMR signal following a 90^{o} rf pulse applied to heteronuclear, dipolar coupled spin-$\frac{1}{2}$ systems. Calculations are presented for isolated systems containing two, three and four nuclei. The two spin system is analysed in some detail in order to illustrate the technique used in the calculations, whereas only essential details are given for the three and four spin systems since these calculations follow along the same lines but involve more complex expressions. For completeness, and comparison, the treatment of a general multi-spin system using a moment expansion is outlined at the end of the chapter.

In the next chapter the relationship between these theoretical calculations and experimental studies is investigated. It should also be emphasised that the techniques illustrated in this chapter provide the background material for the more demanding analysis of NMR double and triple pulse responses for heteronuclear spin systems to be described in Chapter Four.

2.1 Calculating the NMR Signal: The Density Matrix Formulism

The signal, in an NMR experiment, is detected in the rotating xy plane. We shall assume in that which follows that it is the x-component of the signal that is measured. This component is proportional to the x-component of the magnetisation in the sample, which in turn is proportional to the x-component of the nuclear spin vector ($M_x = \gamma\hbar I_x$). The aim here is to produce an expression for the time-dependence of the expectation value of I_x, that is $\langle I_x \rangle_R$, starting from:

$$\langle I_x(t) \rangle_R = Tr\{\sigma_R(t)\ I_x\}.$$

The equation of motion of the density matrix (equation 1.40) subject to a time independent perturbation has the solution (from equation 1.41) in the rotating frame

$$\sigma_R(t) = \exp(-i\mathcal{H}_R t)\ \sigma_R(0)\ \exp(i\mathcal{H}_R t) \qquad 2.01$$

where $\sigma_R(0) = \sigma(0) = cI_z$.

One approach to evaluating this equation would be to write the perturbing Hamiltonian in the form of equation 1.03 and then work with the tensor components (see, for example, Sanctuary(9) and Pyper(10)). However, this approach is rather general and in view of the relative simplicity of the systems to be studied here it is easier to use the Hamiltonians in their more explicit form - Section 1.3.

The total Hamiltonian in the rotating frame is

$$\mathcal{H}_R = \mathcal{H}_R^Z + \mathcal{H}_R^{RF} + \mathcal{H}_R^D + \mathcal{H}_R^{CS}.$$

For simplicity the rotating frame subscript, R, will be dropped from now on. The effective Zeeman Hamiltonian in the rotating frame is

$$\mathcal{H}^Z = -\sum_i (\omega_{0,i} - \omega_{R,i}) I_{z,i}. \qquad 2.02$$

This can be combined with the shielding Hamiltonian (equation 1.31) to give an 'offset' Hamiltonian, $\mathcal{H}^{OFF}$.

$$\mathcal{H}^{OFF} = \mathcal{H}^Z + \mathcal{H}^{CS} = \sum_i \Delta\omega_i \, I_{z,i} \qquad 2.03$$

where

$$\Delta\omega_i = \omega_{R,i} - \omega_{0,i}(1 - \sigma_{zz,i}). \qquad 2.04$$

After an rf pulse, if it is assumed that $\omega_R (= \omega = \gamma\beta^{RF})$ is chosen carefully such that $\mathcal{H}^{RF} >> \mathcal{H}^{OFF}$, and further that $\mathcal{H}^{RF} >> \mathcal{H}^D$, equation 2.01 becomes

$$\begin{aligned} \sigma(\tau_p) &= \exp(-i\mathcal{H}^{RF}\tau_p)\ \sigma(0)\ \exp(i\mathcal{H}^{RF}\tau_p) \\ &= \exp(-i\omega\tau_p I_y)\ cI_z\ \exp(i\omega\tau_p I_y) \end{aligned} \qquad 2.05$$

where τ_p is the length of the pulse. Under these conditions the pulse has the same effect as a rotation about a single axis (compare equation 2.05 with equations 1.18 and 1.10). If $\omega\tau_p = \theta$ then for a rotation about such an axis (Appendix C)

$$\exp(-i\theta I_y)\ cI_z\ \exp(i\theta I_y) = c(I_z\cos\theta + I_x\sin\theta).$$

If τ_p is chosen so that $\theta = 90^o$ the pulse is called a 90^o pulse, θ is called the pulse angle. At the end of a 90^o pulse the density matrix is

$$\sigma(t = \tau_p) = cI_x$$

it follows that

$$\langle I_x(t = \tau_p)\rangle = cTr\{I_x^2\} \qquad 2.06$$

which is in contrast to its initial value:

$$\langle I_x(t = 0)\rangle = cTr\{I_z I_x\} = 0 . \qquad 2.07$$

From the end of the pulse the system evolves in time under the influence of $\mathcal{H}^D + \mathcal{H}^{OFF}$. (From the point of view of this evolution the pulse is considered to be infinitely short - a δ-pulse). At time t after the pulse

$$\sigma(t) = c\, e^{-i(\mathcal{H}^D + \mathcal{H}^{OFF})t}\, I_x\, e^{i(\mathcal{H}^D + \mathcal{H}^{OFF})t} . \qquad 2.08$$

The time development of the NMR signal after a pulse is usually called the free induction decay, or FID for short. Experimentally the signal decays to zero, but when the theoretical signal is calculated for a small, isolated system this is not so (Section 2.2), nevertheless the theoretical signal will still be referred to as an FID.

Providing $\mathcal{H}^D$ and $\mathcal{H}^{OFF}$ commute (which they do only if specific assumptions about the form of $\mathcal{H}^{CS}$ are made - these are discussed for individual spin systems in Section 2.2)

$$e^{i(\mathcal{H}^D + \mathcal{H}^{OFF})t} = e^{i\mathcal{H}^D t}\, e^{i\mathcal{H}^{OFF} t} = e^{i\mathcal{H}^{OFF} t}\, e^{i\mathcal{H}^D t} \qquad 2.09$$

consequently, the normalised 'signal' at time t after a 90^o pulse is

$$\langle I_x(t)\rangle = Tr\{e^{-i\mathcal{H}^{OFF} t}\, e^{-i\mathcal{H}^D t}\, I_x\, e^{i\mathcal{H}^D t}\, e^{i\mathcal{H}^{OFF} t}\, I_x\}/Tr\{I_x^2\}. \qquad 2.10$$

Two properties of the trace can be used to simplify this expression. Firstly, the trace is invarient to a cyclic

permutation of the terms within the bracket so the first and last two terms can be combined as

$$e^{i\mathcal{H}^{OFF}t}\, I_x\, e^{-i\mathcal{H}^{OFF}t} = e^{i(\Delta\omega I_z)t}\, I_x\, e^{-i(\Delta\omega I_z)t}$$

$$= I_x\cos\Delta\omega t - I_y\sin\Delta\omega t \qquad 2.11$$

(where Appendix C has been used), equation 2.10 becomes

$$\langle I_x(t)\rangle = [\mathrm{Tr}\{e^{-i\mathcal{H}^{D}t}\, I_x\, e^{i\mathcal{H}^{D}t}\, I_x\}\cos\Delta\omega t - \mathrm{Tr}\{e^{-\mathcal{H}^{D}t}\, I_x\, e^{i\mathcal{H}^{D}t}\, I_y\}\sin\Delta\omega t]/\mathrm{Tr}\{I_x^2\}. \qquad 2.12$$

Secondly, if under a rotation of 180^{o} about one of the coordinate system axes $\mathrm{Tr}\{\Phi\} \rightarrow \mathrm{Tr}\{-\Phi\}$ then $\mathrm{Tr}\{\Phi\} = 0$. Thus for such a rotation, about the x-axis, say, $\mathcal{H}^{D}$ and I_x are unchanged but $I_y \rightarrow -I_y$ so the second term in equation 2.12 is zero and

$$\langle I_x(t)\rangle = \frac{\cos\Delta\omega t}{\mathrm{Tr}\{I_x^2\}}\,\mathrm{Tr}\{e^{-i\mathcal{H}^{D}t}\, I_x\, e^{i\mathcal{H}^{D}t}\, I_x\}. \qquad 2.13$$

Equation 2.13 is a general expression for the form of an FID following a 90^{o} pulse. The evaluation of this expression for both small isolated spin systems and large collections of spins is considered in the following two sections.

2.2 Calculation of the Free Induction Decay for Isolated Spin Systems

The free induction decays will be calculated for two, three and four spin systems. To illustrate the technique of the calculation the two spin system will be discussed in some detail. The calculations for the three and four spin systems can be done in the same way but since they are considerably extended only the major points and the results will be given. As the title indicates the calculations are for isolated spin systems, furthermore, no relaxation processes are taken into account.

2.2.1 Two Spin Systems

For two different spins, I and S, ($\gamma_I \neq \gamma_S$) the rotating frame (truncated) Hamiltonians are

$$\mathcal{H}^D = [\tfrac{1}{2}C^D(3\cos^2\beta - 1)r^{-3}]I_zS_z = aI_zS_z \qquad 2.14$$

and

$$\mathcal{H}^{OFF} = \Delta\omega_I I_z + \Delta\omega_S S_z. \qquad 2.15$$

β is the angle between the internuclear vector and the applied magnetic field. To be able to use equation 2.13 condition 2.16 must hold:

$$[\mathcal{H}^D, \mathcal{H}^{OFF}] = 0. \qquad 2.16$$

$$[\mathcal{H}^D, \mathcal{H}^{OFF}] = a(\Delta\omega_I[I_zS_z, I_z] + \Delta\omega_S[I_zS_z, S_z]),$$

the commutators can be written:

$$[XY,Z] = X[Y,Z] + [X,Z]Y \qquad 2.17$$

and since $[I_z,I_z] = [I_z,S_z] = 0$, condition 2.16 is fulfilled. The basis states on which the Hamiltonians operate are the direct product, orthonormal basis states defined as $|\alpha\alpha\rangle$, $|\alpha\beta\rangle$, $|\beta\alpha\rangle$ and $|\beta\beta\rangle$ where α represents $m = \frac{1}{2}$ and β represents $m = -\frac{1}{2}$, the first term refers to the I spin and the second to the S.

If $|1\rangle$, $|2\rangle$, ... $|n\rangle$ are general states then the effect of an operator, Q, operating on them is

$$Q|n'\rangle = \sum_n C_n|n\rangle$$

where C_n is a coefficient (which can be zero) and there are n states. A matrix element

$$\langle n'' |Q| n' \rangle = \sum_n C_n \langle n'' | n \rangle = \sum_n C_n \delta_{n''n} \qquad 2.18$$

can be defined, $\delta_{n''n}$ is the Dirac delta function.

Using this equation the matrix elements of the Hamiltonian in equation 2.14 can be written:

$\mathcal{H}^D$	$\lvert\alpha\alpha\rangle$	$\lvert\alpha\beta\rangle$	$\lvert\beta\alpha\rangle$	$\lvert\beta\beta\rangle$
$\langle\alpha\alpha\rvert$	$\frac{1}{4}a$	0	0	0
$\langle\alpha\beta\rvert$	0	$-\frac{1}{4}a$	0	0
$\langle\beta\alpha\rvert$	0	0	$-\frac{1}{4}a$	0
$\langle\beta\beta\rvert$	0	0	0	$\frac{1}{4}a$

The matrix is diagonal because the basis states are eigenfunctions of the Hamiltonian, if they were not then the $\mathcal{H}^D$ matrix would not be diagonal and an additional step in the calculation would be required (as explained below). The matrix elements of $e^{\pm i\mathcal{H}^D t}$ are

$e^{\pm i\mathcal{H}^D t}$	$\lvert\alpha\alpha\rangle$	$\lvert\alpha\beta\rangle$	$\lvert\beta\alpha\rangle$	$\lvert\beta\beta\rangle$
$\langle\alpha\alpha\rvert$	$e^{\pm\frac{i}{4}at}$	0	0	0
$\langle\alpha\beta\rvert$	0	$e^{\mp\frac{i}{4}at}$	0	0
$\langle\beta\alpha\rvert$	0	0	$e^{\mp\frac{i}{4}at}$	0
$\langle\beta\beta\rvert$	0	0	0	$e^{\pm\frac{i}{4}at}$

2.19

Equation 2.18 applies to any operator so a matrix for I_x can also be constructed. It is assumed that the Zeeman energies of the I and S spins (that is to say $\omega_{0,I}$ and $\omega_{0,S}$) are sufficiently different for the rf radiation to interact with one (the I, $\omega \cong \omega_{0,I}$) but not the other. The matrix elements can be found using equations 1.05 and 1.06.

I_x	$\|\alpha\alpha\rangle$	$\|\alpha\beta\rangle$	$\|\beta\alpha\rangle$	$\|\beta\beta\rangle$
$\langle\alpha\alpha\|$	0	0	$\frac{1}{2}$	0
$\langle\alpha\beta\|$	0	0	0	$\frac{1}{2}$
$\langle\beta\alpha\|$	$\frac{1}{2}$	0	0	0
$\langle\beta\beta\|$	0	$\frac{1}{2}$	0	0

2.20

The form of the FID can now be calculated using equation 2.13, noting that $Tr\{I_x^2\} = 1$, the result is

$$\langle I_x(t)\rangle = \cos\Delta\omega_I t \cos\tfrac{1}{2}at \ . \qquad 2.21$$

There is an equivalent expression for $\langle S_x(t)\rangle$ when the pulse is applied to the S spin ($\omega \cong \omega_{0,S}$).

As already noted, if the direct product basis states are not eigenfunctions of $\mathcal{H}^D$ an extra step in the calculation is needed. This is most easily illustrated for a two like ($\gamma_i = \gamma_j$) spin calculation. The truncated dipolar Hamiltonian is now

$$\mathcal{H}^D = a(I_{z,i}\, I_{z,j} - \tfrac{1}{4}(I_{+,i}\, I_{-,j} + I_{-,i}\, I_{+,j}))$$

and

$$[\mathcal{H}^D, \mathcal{H}^{OFF}] = (I_{-,i}\, I_{+,j} - I_{+,i}\, I_{-,j})(\Delta\omega_i - \Delta\omega_j)$$

so condition 2.16 can only be met if $\Delta\omega_i = \Delta\omega_j$, that is if both spins are chemically and crystallographically equivalent (Boden and Kahol(11)). If this is the case then the matrix for $\mathcal{H}^D$ is

$\mathcal{H}^D$	$\|\alpha\alpha\rangle$	$\|\alpha\beta\rangle$	$\|\beta\alpha\rangle$	$\|\beta\beta\rangle$
$\langle\alpha\alpha\|$	$\frac{1}{4}a$	0	0	0
$\langle\alpha\beta\|$	0	$-\frac{1}{4}a$	$-\frac{1}{4}a$	0
$\langle\beta\alpha\|$	0	$-\frac{1}{4}a$	$-\frac{1}{4}a$	0
$\langle\beta\beta\|$	0	0	0	$\frac{1}{4}a$

The eigenfunctions of $\mathcal{H}^D$ are found by diagonalising the matrix using the following procedure.

Let $|a\rangle$ and $|b\rangle$ be the eigenfunctions of $\mathcal{H}^D$ so that

$$\mathcal{H}^D|a\rangle = E|a\rangle, \quad \mathcal{H}^D|b\rangle = E|b\rangle . \tag{2.22}$$

$$\left.\begin{aligned} \text{Let} \quad |a\rangle &= C_1|\alpha\beta\rangle + C_2|\beta\alpha\rangle \\ \text{and} \quad |b\rangle &= C_3|\alpha\beta\rangle + C_4|\beta\alpha\rangle . \end{aligned}\right\} \tag{2.23}$$

From the orthonormality of the direct product basis states it follows that

$$C_1^2 + C_2^2 = C_3^2 + C_4^2 = 1 \quad \text{and} \quad C_1C_3 + C_2C_4 = 0 . \tag{2.24}$$

From equations 2.22 and 2.23

$$\left.\begin{aligned} \langle\alpha\beta|\mathcal{H}^D|a\rangle &= C_1H_{11} + C_2H_{12} = E\langle\alpha\beta|a\rangle = EC_1 \\ \langle\beta\alpha|\mathcal{H}^D|b\rangle &= C_3H_{21} + C_4H_{22} = E\langle\beta\alpha|b\rangle = EC_4 \end{aligned}\right\} \tag{2.25}$$

where $H_{11} = \langle\alpha\beta|\mathcal{H}^D|\alpha\beta\rangle$, $H_{12} = \langle\alpha\beta|\mathcal{H}^D|\beta\alpha\rangle$ and so on.

For equations 2.25 to have a non-trivial solution the determinant

$$\begin{vmatrix} H_{11} - E & H_{12} \\ H_{21} & H_{22} - E \end{vmatrix}$$

must be equal to zero, then

$$(H_{11} - E)(H_{22} - E) - H_{12}H_{21} = 0 .$$

In conjunction with the matrix for $\mathcal{H}^D$ the solution of this equation gives

$$E = 0 \quad \text{or} \quad E = -\tfrac{1}{2}a$$

and by substituting these back into equation 2.25 and using equations 2.24

$$C_1 = -C_2 = C_3 = C_4 = \frac{1}{\sqrt{2}}$$

so the basis state eigenfunctions are

$$|\alpha\alpha\rangle,\ \frac{1}{\sqrt{2}}(|\alpha\beta\rangle + |\beta\alpha\rangle),\ \frac{1}{\sqrt{2}}(|\alpha\beta\rangle - |\beta\alpha\rangle) \text{ and } |\beta\beta\rangle \qquad 2.26$$

which are $|1\rangle$, $|2\rangle$, $|3\rangle$ and $|4\rangle$, respectively, for brevity. The new $\mathcal{H}^D$ matrix is

$\mathcal{H}^D$	$\|1\rangle$	$\|2\rangle$	$\|3\rangle$	$\|4\rangle$
$\langle 1\|$	$\frac{1}{4}a$	0	0	0
$\langle 2\|$	0	$-\frac{1}{2}a$	0	0
$\langle 3\|$	0	0	0	0
$\langle 4\|$	0	0	0	$\frac{1}{4}a$

and that for $e^{\pm i\mathcal{H}^D t}$ is

$e^{\pm i\mathcal{H}^D t}$	$\|1\rangle$	$\|2\rangle$	$\|3\rangle$	$\|4\rangle$
$\langle 1\|$	$e^{\pm\frac{i}{4}at}$	0	0	0
$\langle 2\|$	0	$e^{\mp\frac{i}{2}at}$		0
$\langle 3\|$	0	0	1	0
$\langle 4\|$	0	0	0	$e^{\pm\frac{i}{4}at}$

The matrix for $I_x = I_{x,i} + I_{x,j}$ is

I_x	$\|1\rangle$	$\|2\rangle$	$\|3\rangle$	$\|4\rangle$
$\langle 1\|$	0	$\sqrt{2}$	0	0
$\langle 2\|$	$\sqrt{2}$	0	0	$\sqrt{2}$
$\langle 3\|$	$\sqrt{2}$	0	0	$\sqrt{2}$
$\langle 4\|$	0	$\sqrt{2}$	0	0

Multiplying out according to equation 2.13 and with $\mathrm{Tr}\{I_x^2\} = 8$ the final result is

$$\langle I_x(t)\rangle = \cos\Delta\omega t \cos\tfrac{3}{4}at\ . \qquad 2.27$$

2.2.2 Three Spin Systems

The signal can be calculated in the same way as for the two spin systems, the increase in the number of basis states, however, makes the calculation, although still straightforward, more tedious. The eight direct product basis states are:

$|\alpha\alpha\alpha\rangle$, $|\alpha\alpha\beta\rangle$, $|\alpha\beta\alpha\rangle$, $|\beta\alpha\alpha\rangle$, $|\beta\beta\alpha\rangle$, $|\beta\alpha\beta\rangle$, $|\alpha\beta\beta\rangle$ and $|\beta\beta\beta\rangle$.

Three different types of system are possible:

(i) the spins can all be the same (an I_3 system), $\gamma_1 = \gamma_2 = \gamma_3$. This system has been treated by Moskvich, Sergeev and Dotsenko(12) and will not be considered further;

(ii) the spins can all be different, $\gamma_1 \neq \gamma_2 \neq \gamma_3$. In this case the calculation proceeds as it did for the IS spin system; the dipolar Hamiltonian takes the form

$$\mathcal{H}^D = aI_{z,1}I_{z,2} + cI_{z,1}I_{z,3} + bI_{z,2}I_{z,3} \qquad 2.28$$

where the numerical subscripts refer to the order in the $|--\rangle$, a, b and c are the coupling constants for the 1-2, 2-3 and 1-3 interactions respectively. The condition that $[\mathcal{H}^D, \mathcal{H}^{OFF}] = 0$ is met. Without repeating the details of the calculation:

$$\langle I_x(t)\rangle = \tfrac{1}{2}\cos\Delta\omega_I t[\cos\tfrac{1}{2}(a+c)t + \cos\tfrac{1}{2}(a-c)t]\,. \qquad 2.29$$

(iii) One spin is different from the others (an IS_2 spin system), for example, this includes chemical groupings such as CH_2F, CF_2H or PH_2.

For the IS_2 spin system spins 2 and 3 are the S spins, the dipolar Hamiltonian is:

$$\mathcal{H}^D = a(I_{z,1}\, S_{z,2}) + c(I_{z,1}\, S_{z,3}) + b(S_{z,2}\, S_{z,3} - \tfrac{1}{4}(S_{+,2}\, S_{-,3} + S_{-,2}\, S_{+,3})). \quad 2.30$$

If it is assumed that $\Delta\omega_2 = \Delta\omega_3$, $\mathcal{H}^D$ commutes with $\mathcal{H}^{OFF}$. The direct product basis states are not eigenfunctions of $\mathcal{H}^D$, but diagonalisation of two 2x2 submatrices within the $\mathcal{H}^D$ matrix, in the same way as for the I_2 system, produces the eigenfunctions shown in Table 2.1.

Table 2.1 The basis states and their energies for the IS_2 spin system

	Basis state	Energy
|1>	|ααα>	$\frac{1}{4}(a+b+c)$
|2>	N(|αβα> - R|ααβ>)	$\frac{1}{4}(-b+T)$
|3>	N(R|αβα> + |ααβ>)	$\frac{1}{4}(-b-T)$
|4>	|βαα>	$\frac{1}{4}(-a+b-c)$
|5>	|αββ>	$\frac{1}{4}(-a+b-c)$
|6>	N(|βαβ> - R|ββα>)	$\frac{1}{4}(-b+T)$
|7>	N(R|βαβ> + |ββα>)	$\frac{1}{4}(-b-T)$
|8>	|βββ>	$\frac{1}{4}(a+b+c)$

where: $T = [b^2 + (a-c)^2]^{\frac{1}{2}}$, $R = \frac{(a-c+T)}{b}$ and $N = (1+R^2)^{-\frac{1}{2}}$

For this system there are two results, one for the signal following a pulse applied to the I spin alone:

$$\langle I_x(t)\rangle = \tfrac{1}{2}\cos\Delta\omega t[\cos\tfrac{1}{2}(a+c)t + \frac{b^2}{T^2} + \frac{(a-c)^2}{T^2}\cos\tfrac{1}{2}Tt] \quad 2.31$$

and one for the signal following a pulse applied to the S spins alone:

$$\langle S_x(t)\rangle = \tfrac{1}{2}\cos\Delta\omega_S t\left[\cos\tfrac{1}{4}(a+c)t\left(\frac{T-b}{T}\cos\tfrac{1}{4}(2b-T)t + \frac{T+b}{T}\cos\tfrac{1}{4}(2b+T)t\right)\right]. \quad 2.32$$

2.2.3 Four Spin Systems

The main difficulty in the calculations for these spin systems lies in diagonalising the Hamiltonian matrix in order to produce the eigenfunctions, and their energies, of the dipolar Hamiltonian. Manual solution of 3x3 and 4x4 determinants and of the resulting cubic and quartic equations is only really viable under simplifying conditions. The I_2S_2 system can be tackled under the assumption that the heteronuclear coupling is the same for each spin:

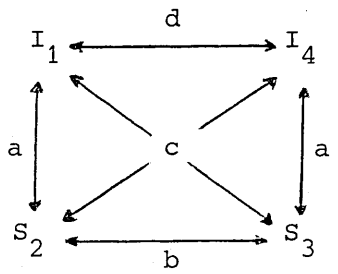

Under these conditions the dipolar Hamiltonian is

$$\mathcal{H}^D = a(I_{z,1}\,S_{z,2} + S_{z,3}\,I_{z,4}) + c(I_{z,1}\,S_{z,3} + S_{z,2}\,I_{z,4}) + b(S_{z,2}\,S_{z,3} - \tfrac{1}{4}(S_{+,2}\,S_{-,3} + S_{-,2}\,S_{+,3})) + d(I_{z,1}\,I_{z,4} - \tfrac{1}{4}(I_{+,1}\,I_{-,4} + I_{-,1}\,I_{+,4}))$$

and with $\Delta\omega_1 = \Delta\omega_4$ and $\Delta\omega_2 = \Delta\omega_3$, $\mathcal{H}^D$ and $\mathcal{H}^{OFF}$ commute. The diagonalisation of the Hamiltonian matrix involves the solution of a 4x4 determinant, as well as four 2x2 ones. The solution of a 4x4 determinant is included in Appendix D. The eigenfunctions of $\mathcal{H}^D$ and their energies are given in Table 2.2.

Table 2.2 The basis states and their energies for the I_2S_2 spin system

	Basis State	Energy
$\|1\rangle$	$\|\alpha\alpha\alpha\alpha\rangle$	$\frac{1}{4}(2a+2c+b+d)$
$\|2\rangle$	$\frac{1}{\sqrt{2}}\|\alpha\alpha\alpha\beta\rangle + \frac{1}{\sqrt{2}}\|\beta\alpha\alpha\alpha\rangle$	$\frac{1}{4}(b-2d)$
$\|3\rangle$	$\frac{1}{\sqrt{2}}\|\alpha\alpha\alpha\beta\rangle - \frac{1}{\sqrt{2}}\|\beta\alpha\alpha\alpha\rangle$	$\frac{1}{4}b$
$\|4\rangle$	$\frac{1}{\sqrt{2}}\|\alpha\alpha\beta\alpha\rangle + \frac{1}{\sqrt{2}}\|\alpha\beta\alpha\alpha\rangle$	$\frac{1}{4}(-2b+d)$
$\|5\rangle$	$\frac{1}{\sqrt{2}}\|\alpha\alpha\beta\alpha\rangle - \frac{1}{\sqrt{2}}\|\alpha\beta\alpha\alpha\rangle$	$\frac{1}{4}d$
$\|6\rangle$	$\|\alpha\beta\beta\alpha\rangle$	$\frac{1}{4}(-2a-2c+b+d)$
$\|7\rangle$	$P\|\alpha\alpha\beta\beta\rangle + A\|\beta\alpha\beta\alpha\rangle + A\|\alpha\beta\alpha\beta\rangle + P\|\beta\beta\alpha\alpha\rangle$	$-\frac{1}{4}(b+d-U)$
$\|8\rangle$	$B\|\alpha\alpha\beta\beta\rangle + Q\|\beta\alpha\beta\alpha\rangle - Q\|\alpha\beta\alpha\beta\rangle - B\|\beta\beta\alpha\alpha\rangle$	$-\frac{1}{4}(b+d-V)$
$\|9\rangle$	$A\|\alpha\alpha\beta\beta\rangle - P\|\beta\alpha\beta\alpha\rangle - P\|\alpha\beta\alpha\beta\rangle + A\|\beta\beta\alpha\alpha\rangle$	$-\frac{1}{4}(b+d+U)$
$\|10\rangle$	$Q\|\alpha\alpha\beta\beta\rangle - B\|\beta\alpha\beta\alpha\rangle + B\|\alpha\beta\alpha\beta\rangle - Q\|\beta\beta\alpha\alpha\rangle$	$-\frac{1}{4}(b+d+V)$
$\|11\rangle$	$\|\beta\alpha\alpha\beta\rangle$	$\frac{1}{4}(-2a-2c+b+d)$
$\|12\rangle$	$\frac{1}{\sqrt{2}}\|\beta\beta\alpha\beta\rangle + \frac{1}{\sqrt{2}}\|\beta\alpha\beta\beta\rangle$	$\frac{1}{4}(-2b+d)$
$\|13\rangle$	$\frac{1}{\sqrt{2}}\|\beta\beta\alpha\beta\rangle - \frac{1}{\sqrt{2}}\|\beta\alpha\beta\beta\rangle$	$\frac{1}{4}d$
$\|14\rangle$	$\frac{1}{\sqrt{2}}\|\beta\beta\beta\alpha\rangle + \frac{1}{\sqrt{2}}\|\alpha\beta\beta\beta\rangle$	$\frac{1}{4}(b-2d)$
$\|15\rangle$	$\frac{1}{\sqrt{2}}\|\beta\beta\beta\alpha\rangle - \frac{1}{\sqrt{2}}\|\alpha\beta\beta\beta\rangle$	$\frac{1}{4}b$
$\|16\rangle$	$\|\beta\beta\beta\beta\rangle$	$\frac{1}{4}(2a+2c+b+d)$

where $U = [4(a-c)^2 + (b+d)^2]^{\frac{1}{2}}$, $V = [4(a-c)^2 + (b-d)^2]^{\frac{1}{2}}$,

$\alpha = \frac{1}{2}(a-c) - \frac{1}{4}U$, $\beta = \frac{1}{2}(a-c) + \frac{1}{4}V$,

$$A = \left[\frac{8\alpha^2}{(b+d)^2 + 16\alpha^2}\right]^{\frac{1}{2}}, \quad B = \left[\frac{8\beta^2}{(b-d)^2 + 16\beta^2}\right]^{\frac{1}{2}}$$

$$P = \frac{(b+d)A}{4\alpha}, \quad Q = \frac{(b-d)B}{4\beta}$$

The calculation of the FID is straightforward, if a little tedious. The result for the I spins is

$$\langle I_x(t)\rangle = \tfrac{1}{4}\cos\Delta\omega_I t[(A+P)^2\cos\tfrac{1}{4}(b-2d+U)t + (A-P)^2\cos\tfrac{1}{4}(b-2d-U)t + (B+Q)^2\cos\tfrac{1}{4}(b+2d-V)t + (B-Q)^2\cos\tfrac{1}{4}(b+2d+V)t + 2\cos\tfrac{1}{2}(a+c)t\cos\tfrac{3}{4}dt]. \quad 2.33$$

The FID for the S spins is this expression but with the b and d interchanged.

2.3 Multi-Spin Systems: The Moment Expansion

The exponential operators in equations such as 2.13 can be expanded as a power series in time, with the result:

$$e^{-iAt}\,B\,e^{iAt} = B - i[A,B]t + i^2[A,[A,B]]\frac{t^2}{2!} - i^3[A,[A[A,B]]]\frac{t^3}{3!} + \ldots\ldots\ldots . \quad 2.34$$

It is then possible to rewrite equation 2.13 as

$$\langle I_x(t)\rangle = \cos\Delta\omega t[1 - M_2\frac{t^2}{2!} + M_4\frac{t^4}{4!} - M_6\frac{t^6}{6!} + \ldots\ldots] \quad 2.35$$

M_n is called the n^{th} moment

$$M_n = \mathrm{Tr}\{[\mathcal{H}^D,[\ldots,[\mathcal{H}^D,I_x]]\ldots]_{n\text{ times }} I_x\}/\mathrm{Tr}\{I_x^2\}. \quad 2.36$$

It is often only practicable to calculate the second moment, that is

$$M_2 = \mathrm{Tr}\{[\mathcal{H}^D,[\mathcal{H}^D,I_x]]I_x\}/\mathrm{Tr}\{I_x^2\} \equiv -\mathrm{Tr}\{[\mathcal{H}^D,I_x]^2\}/\mathrm{Tr}\{I_x^2\}. \quad 2.37$$

With the definition of $\mathcal{H}^D$ from equation 1.30 the evaluation of the commutator is straightforward, it turns out that

$$M_2 \propto \mathrm{Tr}\{I_{y,i}^2\, I_{z,j}^2\}.$$

Because the trace is invariant to the choice of basis states (which potentially makes the 'method of moments' a very powerful tool) the following trace relationships can be used:

$$Tr\{I^2_{x,i}\} = Tr\{I^2_{y,i}\} = Tr\{I^2_{z,i}\} = \tfrac{1}{3}I(I+1)(2I+1)^N \qquad 2.38$$

N is the number of spins. Using these relationships it can be shown (Abragam(13)) that for a system of spins-$\frac{1}{2}$ containing both homonuclear and heteronuclear interactions such that

$$M_2 = M_2^{II} + M_2^{IS} \qquad 2.39$$

$$M_2^{II} = \frac{9}{64}\sum_j (C^D_{ij}(3\cos^2\beta-1)_{ij}r^{-3}_{ij})^2 \qquad 2.40$$

and

$$M_2^{IS} = \frac{1}{16}\sum_k (C^D_{ij}(3\cos^2\beta-1)_{ik}r^{-3}_{ik})^2 . \qquad 2.41$$

The sum over j is over all the I spins surrounding the i^{th} I spin, the sum over k is over all the S spins surrounding it.

The question now arises as to how useful is the expansion to second order in time. For the full signal all the expressions calculated so far (2.21, 2.27, 2.29, 2.31, 2.32 and 2.33) contain terms which oscillate, an expansion to second order in time cannot mimic this. However, the expansion might be valid for part of the signal. As an example consider an isolated two spin system such as HF: Figure 2.1 shows the signal calculated from equation 2.21 (solid line) as a function of the HF separation at three different times. The signal calculated from the first two terms of Equation 2.35 is also shown (broken line), limiting the sum to just two spins precludes the inclusion of the higher order moments. Clearly the moment expansion (to second order) can be used at short

times and when the internuclear separation is large, where the expansion and the full expression are in close agreement, at long times or short internuclear distances there is a very marked difference between the two.

One advantage of the moment expansion is that it is possible to include any number of spins in a calculation. The second moment can, then, be used to include all the inter-system interactions left out of the exact calculation for an isolated spin system, in other words, it can provide a basis for finding a decay function f(t) if the sum over the spins is taken only over those spins not included in the isolated system calculation.

The expansion 2.35 can be written approximately as:

$$\langle I_x(t)\rangle \simeq \cos\Delta\omega t\left[1-M_2\frac{t^2}{2!}+3M_2^2\frac{t^4}{4!}-15M_2^3\frac{t^6}{6!}+\ldots\ldots\right]. \qquad 2.42$$

The coefficients of t^4 and t^6 are contained within, but are not exactly equal to, the fourth and sixth moments. This expansion is that of the Gaussian function

$$\langle I_x(t)\rangle \simeq e^{-\frac{1}{2}M_2t^2}. \qquad 2.43$$

The signal, then, should decay in the same way as a Gaussian function; there is, of course, a departure from the real decay but "this departure is not so important as to make a Gaussian model, which has the merit of simplicity, grossly incorrect" (Abragam (13)).

As a first approximation this Gaussian decay can be used as the function f(t) needed to make the theoretical expressions comparable with experiment - as will be discussed further in the next chapter.

2.4 Appendices

2.4.1 Appendix C

The effect of a rotation, about a coordinate axis, on the spin operators is given by Mehring(14), for convenience it is reproduced here:

$$e^{-i\theta I_x} \begin{Bmatrix} I_x \\ I_y \\ I_z \end{Bmatrix} e^{i\theta I_x} = \begin{Bmatrix} I_x \\ I_y\cos\theta + I_z\sin\theta \\ I_z\cos\theta - I_y\sin\theta \end{Bmatrix}$$

$$e^{-i\theta I_y} \begin{Bmatrix} I_x \\ I_y \\ I_z \end{Bmatrix} e^{i\theta I_y} = \begin{Bmatrix} I_x\cos\theta - I_z\sin\theta \\ I_y \\ I_z\cos\theta + I_x\sin\theta \end{Bmatrix}$$

$$e^{-i\theta I_z} \begin{Bmatrix} I_x \\ I_y \\ I_z \end{Bmatrix} e^{i\theta I_z} = \begin{Bmatrix} I_x\cos\theta + I_y\sin\theta \\ I_y\cos\theta - I_x\sin\theta \\ I_z \end{Bmatrix}$$

2.4.2 Appendix D

The solution of a 4x4 determinant is needed in Section 2.2.3.

$$D = \begin{vmatrix} H_{11} - E & H_{12} & H_{13} & H_{14} \\ H_{21} & H_{22} - E & H_{23} & H_{24} \\ H_{31} & H_{32} & H_{33} - E & H_{34} \\ H_{41} & H_{42} & H_{43} & H_{44} - E \end{vmatrix} = 0$$

This can be rewritten as (Stephenson (15))

$$D = (H_{11} - E)\, D_1 - H_{21}D_2 + H_{31}D_3 - H_{41}D_4 = 0$$

where

$$D_1 = (H_{22} - E)\begin{vmatrix} H_{33} - E & H_{34} \\ H_{43} & H_{44} - E \end{vmatrix} - H_{32}\begin{vmatrix} H_{23} & H_{24} \\ H_{43} & H_{44} - E \end{vmatrix} + H_{42}\begin{vmatrix} H_{23} & H_{24} \\ H_{33} - E & H_{34} \end{vmatrix}$$

$$D_2 = H_{12}\begin{vmatrix} H_{33} - E & H_{34} \\ H_{43} & H_{44} - E \end{vmatrix} - H_{32}\begin{vmatrix} H_{13} & H_{14} \\ H_{43} & H_{44} - E \end{vmatrix} + H_{42}\begin{vmatrix} H_{13} & H_{14} \\ H_{33} - E & H_{34} \end{vmatrix}$$

$$D_3 = H_{12}\begin{vmatrix} H_{23} & H_{24} \\ H_{43} & H_{44} - E \end{vmatrix} - (H_{22} - E)\begin{vmatrix} H_{13} & H_{14} \\ H_{43} & H_{44} - E \end{vmatrix} + H_{42}\begin{vmatrix} H_{13} & H_{14} \\ H_{23} & H_{24} \end{vmatrix}$$

$$D_4 = H_{12}\begin{vmatrix} H_{23} & H_{24} \\ H_{33} - E & H_{34} \end{vmatrix} - (H_{22} - E)\begin{vmatrix} H_{13} & H_{14} \\ H_{33} - E & H_{34} \end{vmatrix} + H_{32}\begin{vmatrix} H_{13} & H_{14} \\ H_{23} & H_{24} \end{vmatrix}.$$

The 2x2 determinants can be solved in the usual way:

$$\begin{vmatrix} a & b \\ c & d \end{vmatrix} = 0 = ad - cb = 0 .$$

The determinant needed in Section 2.2.3 has the elements H_{41}, H_{23}, H_{32} and H_{41} all equal to zero which reduces the number of terms, the resulting expression for the energy, E, is a quadratic in E^2 which can be solved in the normal way.

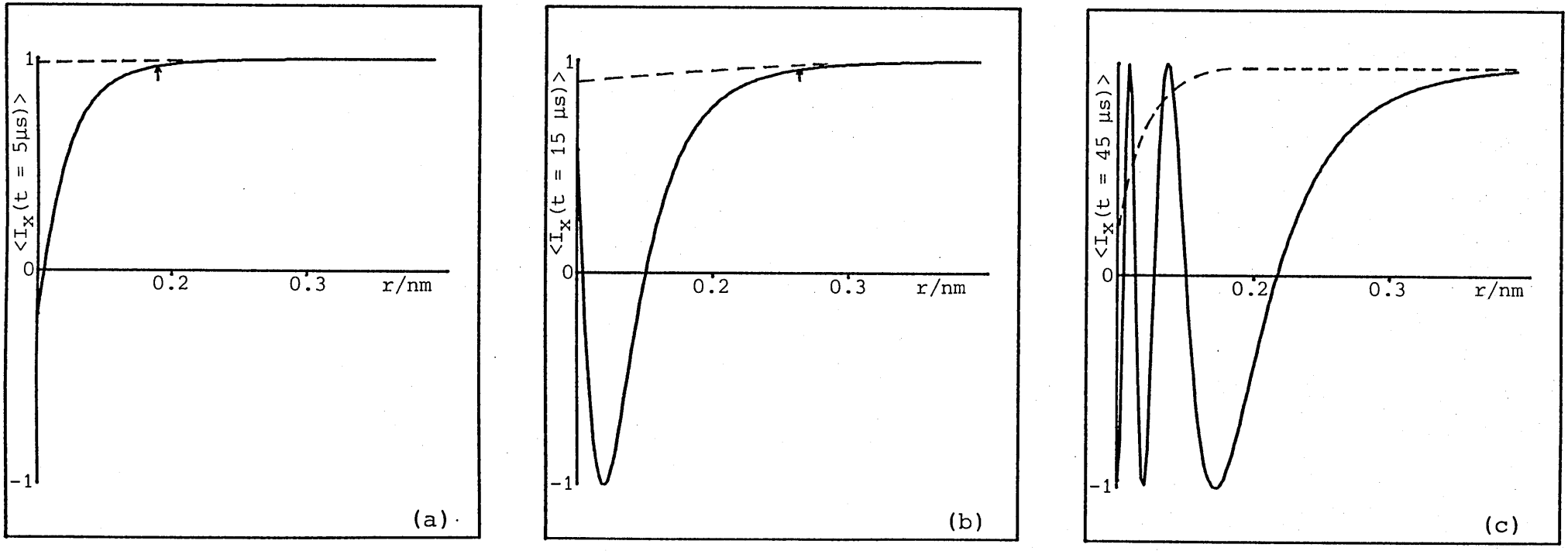

Figure 2.1 Normalised signal, for an HF system, versus H-F separation (with $\Delta\omega_I = 0$) calculated from equaton 2.21 (——) and its second order expansion, equation 2.35 (----). The second order expansion is within 95% of the full expression only to the right of the arrows.

2.5 References

(1) I.J. Lowe and R.E. Norberg, Phys. Rev., 107, 46-61 (1957).

(2) N. Boden and P.K. Kahol, Mol. Phys., 50(4), 645-665 (1983).

(3) J.G. Powles and J.H. Strange, Proc. Phys. Soc. (London), 82(1), 6-15 (1963).

(4) P. Mansfield, Progress in NMR Spectroscopy, 8(1), 41-101 (1971)

(5) G.W. Parker, Phys. Rev. B, 2(7), 2453-2459 (1970).

(6) W.A.B. Evans and J.G. Powles, Phys. Lett. A, 24(4), 218-219 (1967).

(7) T.B. Smith, J. Phys. C: Solid State Phys., 15, 5023-5032 (1982).

(8) M.A.B. Whitaker, Chem. Phys. Lett., 90(5), 351-354 (1982), and Mol. Phys., 53(1), 241-251 (1984).

(9) B.C. Sanctuary, J. Chem. Phys., 64(11), 4352-4361 (1976).

(10) N.C. Pyper, Mol. Phys., 21(1), 1-33 (1971) and Mol. Phys., 22(3), 433-458 (1971).

(11) N. Boden and P.K. Kahol, J. Mag. Res., 54, 419-426 (1983).

(12) Yu.N. Moskvich, N.A. Sergeev and G.I. Dotsenko, Phys. Stat. Sol. (a), 30, 409-418 (1975).

(13) A. Abragam, 'The Principles of Nuclear Magnetism', Clarendon Press, Oxford (1961).

(14) M. Mehring, 'High Resolution NMR Spectroscopy in Solids', NMR Basic Principles and Progress Volume 11, Springer-Verlag, Heidelberg (1976).

(15) G. Stephenson, 'Mathematical Methods for Science Students', Longman, London, second edition (1973).

CHAPTER THREE

The NMR Response to a Single Pulse: Experimental Studies

In principle, the analysis of a solid state NMR spectrum which is dominated by dipolar interactions should yield information on the structure of the solid since such interactions depend only on the relative position of the dipoles. In practice, though, the direct analysis of solid state NMR spectra has not developed into a generally useful tool for probing structure. This is, perhaps, because the spectrum of most solids is influenced by interactions between large numbers of spins and so lacks the well defined structure necessary for a detailed analysis. Modern NMR methods, in particular separated local field (SLF) spectroscopy, have to some extent overcome this problem but this technique can be applied only to relatively dilute spin species (^{13}C for example) interacting predominantly with abundant spin species (^{1}H for example) - Waugh(1). It should be remembered (Section 1.3.3), however, that the strength of the dipolar interaction between two spins falls off rapidly as the distance between them increases, in fact as $1/r^3$, so for solids in which the resonant nuclei occur in small and relatively isolated groups, it should be possible to obtain structural information from the spectrum. Indeed, that this is the case was first demonstrated by Pake(2) in his classic study of the water of crystallisation in calcium sulphate. There have been many subsequent structural studies of water molecules in crystalline hydrates using the NMR technique - Reeves(3). In this chapter we investigate the information content of the free induction decay of solids containing relatively isolated heteronuclear spin groupings. (The FID is related to the spectrum through a Fourier transformation so the information obtainable from the spectrum must, in principle, also be obtainable from the FID.) Admittedly, while of limited application, the results turn out to be of both general NMR and chemical interest.

In the last chapter we developed expressions for the FID's of various heteronuclear spin systems. The simplest of these was the IS spin system which served as a model to illustrate the main steps in the calculation. However, the IS_2 spin systems (with or without $D_{\infty h}$ symmetry) are of greater practical interest; it is this type of system on which we will concentrate, both experimentally and theoretically, in this chapter. More specifically, we have studied the following: potassium hydrogen difluoride, caesium hydrogen difluoride, 4-methylphenylamine hydrogen difluoride and sodium fluoroethanoate. We have also calculated the FID for a series of I_2S_2 spin systems, although these have not been compared with experiment.

Also in the previous chapter we introduced a decay function, f(t), to take into account inter-group interactions. This is necessary because in reality there is some uncertainty in the energy levels of an isolated system caused by spins not included in the calculation, this allows transitions between levels to occur over a range of frequencies. The upshot of this is that the observed signal is not a 'single' signal composed of a few well defined oscillating terms, but is instead a superposition of many such individual signals which, eventually, destructively interfere with one another to give zero signal. We shall find that f(t) can be a single Gaussian function.

As written the FID expressions in Chapter Two refer to single crystal samples at some general orientation with respect to the applied field. If the sample is polycrystalline, a suitable average has to be taken if the theory is to be compared with experiment. The procedure that we have used to carry out this averaging is outlined in Section 3.1. For completeness we have also included a brief description of the experimental apparatus.

3.1 The Polycrystalline Average

For each equivalent pair of resonant nuclei in a single crystal sample the polar angle θ - the angle between the applied, static magnetic field and the internuclear vector - is single-valued. In a polycrystalline sample there are, it is assumed, an infinite number of crystallites, each equivalent pair of nuclei in each crystallite having a different value of θ. If it is assumed that every crystallite orientation, with respect to the applied static magnetic field, occurs and occurs with equal probability then the total signal is the sum of the signals from each crystallite, which is just the integral over θ. Haeberlen(4) and Spiess(5) give general discussions of the polycrystalline average.

There are some systems for which this integration is analytic, these are ones in which the single crystal signal depends on a single dipolar coupling constant, such signals are of the form

$$\langle I_x(t)\rangle \alpha \cos(r^{-3} C^D(3\cos^2\theta - 1)t).$$

The polycrystalline average signal is

$$\langle I_x(t)\rangle \alpha \tfrac{1}{2}\int_0^{\pi} \cos(r^{-3} C^D(3\cos^2\theta - 1)t)\sin\theta \, d\theta \qquad 3.01$$

(the factor of $\frac{1}{2}$ is a normalisation constant) from which it can be shown (Appendix E) that

$$\langle I_x(t)\rangle \alpha y^{-1}\left(\cos\left(\frac{\pi y^2}{6}\right) C(y) + \sin\left(\frac{\pi y^2}{6}\right) S(y)\right) \qquad 3.02$$

where $y = (6r^{-3} C^D t/\pi)^{\frac{1}{2}}$ and $C(y)$ and $S(y)$ are the Fresnel integrals, values of which are tabulated in Abramowitz and Stegun(6). A function of the form of equation 3.02 is shown in Figure 3.1(a). The function is zero when $y = 2.03, 3.28, 4.04$ ..... so that if the times at which the signal is zero are

known then the internuclear separation can be found directly. If the signal contains a constant component (as it does for the IS_2 spin system - equation 2.31) the analysis is more difficult because the zeroes in equation 3.02 are not zeroes in the signal (Figure 3.1(b)) and it becomes necessary either to find the decay function or to fit the experiment to theory by computer. The oscillatory nature of the signal, because of the decay of the signal, tends to be well defined only when the oscillation is fast, that is when the pairwise interaction is large.

If the signal depends on more than one coupling constant the situation is more complicated, it is then necessary to relate the direction of one internuclear vector to another. This is done by defining the general polar angles (θ,ϕ) - Figure 3.2(a) and then defining system dependent angles (which are constant for a given system whatever its orientation with respect to the field) as required - Figures 3.2(b-d). In this way all the cosine terms, $\cos\beta_{ij}$, can be written in terms of θ,ϕ and constants, the integration is then carried out over θ and ϕ: the component of the signal for the ijth pair is

$$\langle I_x(t)\rangle_{ij} \propto \frac{1}{4\pi}\int_0^{2\pi}\left(\int_0^{\pi} \cos\left(3\sin^2\theta\,\cos^2(\phi + \text{constant})\,C^D_{ij}\right.\right.$$
$$\left.\left. r_{ij}^{-3}\,t\right)\sin\theta\,d\theta\right)d\phi \qquad 3.03$$

where $\frac{1}{4\pi}$ is a normalisation constant.

It was not possible to evaluate expressions of the form of 3.03 analytically so a numerical method was used instead. The required program was written in FORTRAN 77 and implemented on a DEC-20 computer. The integration itself used NAG(7) sub-routines D01FBF and D01BBF. Subroutine D01FBF computed an estimate of, in this case, a two dimensional integral given the

analytical form of the signal and suitable Gaussian weights and abscissae which were both generated by routine D01BBF. The weights and abscissae used were appropriate to a Gauss-Legendre quadrature formula. The accuracy of the integration, which could be varied, was checked against the analytical solution of the simpler case discussed earlier, satisfactory agreement was obtained.

The second moments, equations 2.40 and 2.41, can be calculated for a polycrystalline sample, the angular part becomes

$$\tfrac{1}{2}\int_0^{\pi}(3\cos^2\beta - 1)^2\sin\beta\, d\beta \equiv \frac{1}{4\pi}\int_0^{2\pi}\int_0^{\pi}(3\sin^2\theta\, \cos^2(\phi + \text{constant}) - 1)^2 \sin\theta\, d\theta\, d\phi$$

$$= \frac{4}{5}$$

so

$$M_{2,p}^{II} = \frac{9}{80}\sum_j (C_{ij}^D\, r_{ij}^{-3})^2 \qquad 3.04$$

and

$$M_{2,p}^{IS} = \frac{1}{20}\sum_k (C_{ik}^D\, r_{ik}^{-3})^2 . \qquad 3.05$$

It is worthwhile, at this stage, to consider briefly, the form of the decay function f(t) for a polycrystalline system. If we represent the single crystal FID as G(t) then we can write either

$$\langle I_x(t)\rangle \alpha \left[\int_0^{2\pi}\int_0^{\pi} G(t)\, \sin\theta\, d\theta\, d\phi\right] \exp(-\tfrac{1}{2}M'_{2,p}t^2) \qquad 3.06$$

or

$$\langle I_x(t)\rangle \alpha \int_0^{2\pi}\int_0^{\pi} [G(t)\, \exp(-\tfrac{1}{2}M'_2 t^2)]\, \sin\theta\, d\theta\, d\phi \qquad 3.07$$

where M_2' is the intersystem contribution to M_2 defined in equation 2.39 and $M_{2,p}'$ is the intersystem contribution to $M_{2,p}^{II} + M_{2,p}^{IS}$. Functions equivalent to

$$f(t) = \exp(-\frac{2}{5}M_2't^2)$$

and

$$f(t) = \int_0^{2\pi}\int_0^{\pi} \exp(-\tfrac{1}{2}M_2't^2)\sin\theta \, d\theta \, d\phi$$

are illustrated in Figure 3.3. At long times there is a marked difference between the two curves but for long times the polycrystalline average signal is small (curve (c)) so the different functions may produce little observable effect. The real test of their applicability will come when we analyse the experimental signals.

3.2 The NMR Spectrometer and Experimental Technique

A Bruker CXP 100b spectrometer was used for this work. The spectrometer provided high power rf pulses under the control of a microprocessor controlled pulse programmer. Data from the spectrometer was collected with a Datalab DL905 transient recorder which was capable of collecting 1024 points per sweep, in these studies each sweep lasted 200μs. The transient recorder was interfaced to an Apple Europlus II computer (with 48K of memory and floppy disc storage) which allowed data to be accumulated and processed. Stored data could, subsequently, be transferred to a Digital Equipment Corporation MINC 11/3 computer for further processing and also for plotting by a Tektronix 4662 digital plotter.

Two permanent magnets were used giving ^1H resonance frequencies of 59.5 and 25.5 MHz. All ^{19}F signals were obtained at a resonance frequency of 55.9 MHz. The measurements reported in this chapter were all carried out at 294K.

The spectrometer was initially tuned up on a liquid sample, a 50% H_2O/D_2O mixture for ^1H and a concentrated solution of caesium fluoride for ^{19}F, followed by retuning and the setting of the 90^o pulses on a solid sample, calcium sulphate dihydrate for ^1H and calcium fluoride for ^{19}F. Because of the length of the spin-lattice relaxation times of our samples we found it impracticable to tune up on the samples themselves, any error that may have occurred in setting up the resonance frequency was taken into account by adjusting the offset term in the calculated FID. The effect that the offset has on the signal is discussed in Appendix F.

The measured FID's of our samples typically lasted for only 40-80μs so in order to make an accurate comparison with theory several important factors had to be taken into account. Firstly, the rf pulse is not a 'δ-pulse', instead, it has a finite width (typically 1.5μs for ^1H and 2.4μs for ^{19}F in these studies). We have followed the analysis by Barnaal and Lowe(8) and have assumed that the NMR signal starts midway along the pulse. Secondly, the full FID could not be measured because the signal occurring within the dead time of the spectrometer was lost. For the experiments presented here the dead time was 8-10μs, it could not be shortened by further damping of the rf coil without an unacceptable reduction in the signal to noise ratio. The possibility of using a spin echo experiment to record the FID is discussed in the next two chapters. Finally, the finite band width of the rf coil and spectrometer receiver circuit can cause distortion of the signal. Our experiments on KHF_2 indicated that any such distortion was small and so detailed corrections were not made.

All our samples were white polycrystalline solids, all were used as supplied, without further purification, and sealed

under vacuum in 10mm glass tubes. FID's of the hydrogen difluoride samples recorded immediately after they had been prepared and then again several days later showed that there was no deterioration of the sample through contact with the glass.

3.3 Results and Discussion

3.3.1 Results for Potassium Hydrogen Difluoride, KHF_2

Potassium hydrogen difluoride is in many ways an ideal model system for our present studies (its only drawback is that it has a long spin-lattice relaxation time at room temperature): each HF_2^- ion is relatively isolated (the shortest intersystem distances are approximately three times the HF intrasystem distances), the two fluorine atoms are equivalent so that we may separate the offset and dipolar Hamiltonians (Section 2.1 equation 2.09), the compound is a solid at room temperature (melting point 238 ^{o}C), its crystal structure is known (Petersen and Levy(9), Carrell and Donohue(10)), intramolecular rotational motion can be neglected (as we will see in Chapter Six the ion does in fact undergo 180^{o} jumps about one of its C_2 axes but the motion does not affect intrasystem dipolar coupling).

KHF_2 has a tetragonal crystal structure with space group I4/mcm (Petersen and Levy(9)), the unit cell dimensions are (Carrell and Donohue(10)) a = 0.5672 nm and c = 0.6801 nm, the c-axis is the fourfold symmetry axis and there are four KHF_2 units in the unit cell, arranged as shown in Figure 3.4. Using the crystal data together with the neutron diffraction bond lengths the intersystem contribution to the rigid lattice second moments of KHF_2 was calculated from equations 2.40, 2.41, 3.04 and 3.05, the results are given in Table 3.1.

Table 3.1 Intersystem contributions to KHF_2 rigid lattice second moments

$M_2/rad^2\ s^{-2}$	Field along crystal 110 direction		Field along crystal c-axis	Powder
	Ion C_∞ axis $\parallel B_0$	Ion C_∞ axis $\perp B_0$		
M_2^{HH}	1.30×10^9	1.30×10^9	2.06×10^9	7.473×10^8
M_2^{FF}	2.11×10^9	2.40×10^9	2.44×10^9	1.650×10^9
M_2^{HF}	1.07×10^9	2.19×10^9	1.36×10^9	8.038×10^8
$M_2^{HK\ 1}$	1.22×10^5	1.22×10^5	2.06×10^5	1.603×10^6
Total M_2^H	2.37×10^9	3.49×10^9	3.42×10^9	1.553×10^9
Total M_2^F	3.18×10^9	4.59×10^9	3.81×10^9	2.454×10^9

[1] ^{39}K has spin $I = \frac{3}{2}$, natural abundance 93.2 % and $\gamma = 1.250 \times 10^7$ rad s^{-1} T^{-1}

Equation 2.31 provided the starting point for modelling the ^1H FID, it can be simplified, for an ion with $D_{\infty h}$ symmetry, to

$$\langle I_x(t)\rangle = \tfrac{1}{2}\cos\Delta\omega_H t\ (\cos(at) + 1) \qquad 3.08$$

where $a = \gamma_H\gamma_F\hbar\frac{\mu_0}{4\pi}r_{HF}^{-3}(3\cos^2\beta_{HF} - 1)$. Section 3.1 was used to find the powdered form of equation 3.08. Figure 3.5 shows the best computed signal (solid line) and the experimental signal (for clarity not all the experimental points are shown). The internuclear distances used in the calculation were r_{HF} = 0.1160 nm and r_{FF} = 0.2320 nm, the fitting procedure was sensitive to changes in these distances of approximately 0.001 nm. These distances are uncorrected for vibrational motion. The correction for the vibrational motion has been considered in some detail by Pratt and Smith(11). They calculated an overall correction of -0.0030 nm to the r_{HF} distance, the calculation was based on that of Ibers and Stevenson(12) using known vibrational data (Coté and Thompson (13), Boutin, Safford and Brajovic(14)). With this correction our HF_2^- bond lengths become r_{HF} = 0.1130 nm and r_{FF} = 0.2260 nm. These values are compared with those obtained by other authors in Table 3.2.

Table 3.2 The HF distance[1] in KHF_2

Study	r_{HF}/nm
Carrell and Donohue(10) - neutron diffraction	0.1147
Haeberlen and Spiess(15) - NMR	0.1153
Pratt and Smith(11) - NMR	0.1138
Present study	0.1130

[1]Corrected for vibrational motion except for reference (15).

A Gaussian decay function was used in calculating the theoretical signal:

$$f(t) = \exp(-6.0 \times 10^8 \, t^2) \, .$$

It was found that a sufficiently good fit was obtained by applying the decay after the polycrystalline average had been taken (as in equation 3.06). The time coefficient for the decay is less than that of the calculated rigid lattice value ($\frac{1}{2}M'_{2,p} = 7.75 \times 10^8$ rad^2 s^{-2}): the decays corresponding to these coefficients are compared in Figure 3.6. The most likely explanation of this is that the decay coefficient is motionally averaged by the 180° rotational jumps of the HF_2^- ion. The calculation of the reduction factor for this type of motion is complex and has not been attempted. Also, we have not taken into account the vibrational correction between the corrected neutron diffraction data used to calculate $M'_{2,p}$ and the effective crystal structure seen by the NMR experiment (the effect of lattice vibration on the intermolecular part of the NMR second moment is discussed by Polak, Sheinblatt and Shmueli(16)) although we would not expect this correction to be large. To take into account any error in tuning the spectrometer to the resonance frequency of KHF_2 an offset of 2 kHz was found to be necessary in calculating the FID.

The fluorine FID was calculated in the same way as the ^1H but from equation 2.32:

$$\langle S_x(t) \rangle = \tfrac{1}{2}\cos\Delta\omega_F t(\cos\tfrac{1}{2}at \cos\tfrac{3}{4}bt) \qquad 3.09$$

where a is the same as for the ^1H FID and

$$b = \gamma_F^2 \hbar \frac{\mu_0}{4\pi} r_{FF}^{-3} (3\cos^2\beta_{FF} - 1) .$$

The internuclear distances used in the calculation of the ^1H FID were used again to calculate the ^{19}F FID. The decay function was a Gaussian applied after the polycrystalline average had been taken:

$$f(t) = \exp(-1.0 \times 10^9 \, t^2) .$$

As for the ^1H FID this decay is slower than that expected from

$$f(t) = \exp(-\tfrac{1}{2} M_{2,p}^{F'} \, t^2)$$

the same reasoning applies ($\frac{1}{2}M_{2,p}^{F'} = 1.22 \times 10^9$ rad^2 s^{-2}). An offset of 3.7 kHz was used in the calculation. The experimental and calculated FID's are shown in Figure 3.7. It is interesting to note that the ratio $M'_{2,p}$(observed)/$M'_{2,p}$ (theoretical) for the ^{19}F decay (0.82) is approximately the same as that for the ^1H decay (0.77).

3.3.2 Results for Caesium Hydrogen Difluoride, $CsHF_2$

The ^1H and ^{19}F free induction decays for caesium hydrogen difluoride have been obtained and the theoretical FID's, calculated from equations 3.08 and 3.09 respectively, have been fitted to them. The results are shown in Figures 3.8 and 3.9. At room temperature $CsHF_2$ is isomorphous with KHF_2 (also at room temperature), only the unit cell dimensions are greater: a = 0.681 nm and c = 0.784 nm (Kruh, Fuwa and McEver(17)).

The internuclear separations used to calculate the KHF_2 FID's did not produce a good fit when used to calculate those for $CsHF_2$ so new values were found. The FID's shown in Figures 3.8 and 3.9 were obtained using r_{HF} = 0.1178 nm and r_{FF} =

$2r_{HF}$ (this is an increase of 0.0018 nm over that used for the KHF_2 calculation). We have not calculated the vibrational correction to this distance but the vibrational frequencies for $CsHF_2$ (Gilbert and Sheppard(18)) are not very different to those in KHF_2: the symmetric, antisymmetric stretching and bending wavenumbers (cm^{-1}, at 300 K) are 581, 1465 and 1241 for KHF_2 and 584, 1425 and 1227 for $CsHF_2$ so we did not expect the vibrational correction to account for all the difference in the H-F bond length. (We were unable to find any reported value for the frequency of the torsional motion, but, if the correction to the KHF_2 bond lengths (Pratt and Smith(11)) from this source (-0.0001 nm) is a guide then the correction would not be very big.)

Carrell and Donohue(10) obtained the H-F bond length in both $NaHF_2$ and KHF_2, the values they report show that the bond length in the potassium salt is slightly larger than that in the sodium, there is, however, a much greater difference in the vibrational frequencies of these two ions and they do comment that "apparently there is no significant difference among the distances". The sodium, potassium, rubidium and caesium hydrogen difluoride FID's have been studied by Ludman and Smith(19), they did not detect any difference in the HF bond lengths in the last three compounds but concluded that the sodium salt HF bond length was shorter than that in the others (by 0.0012 nm).

The evidence seems to indicate that the bond lengths in the alkali metal hydrogen difluoride ions tend to increase down the group. If this increase is significant it would seem likely that it cannot wholly be explained by vibrational motion, so the change may be the result of changes in the packing density of the ions or the characteristics of the cation.

Gaussian decays, applied after the polycrystalline averages had been taken, were found to be adequate: for the ^{1}H FID

$$f(t) = \exp(-4.4 \times 10^{8}\ t^{2})$$

and for the ^{19}F FID

$$f(t) = \exp(-4.0 \times 10^{8}\ t^{2}) \ .$$

The decay weights in these functions are less than the corresponding ones for KHF_2 but this probably reflects the increase in size of the unit cell in $CsHF_2$ and the consequent increase in the intersystem distances. It is worth noting that the fitting procedure for $CsHF_2$ was more sensitive to the decay weight than that for KHF_2 (for ^{1}H the weight being $(4.4 \pm 0.05) \times 10$ $rad^2\ s^{-2}$) but this might just be a consequence of the way in which the experimental signal was obtained - the KHF_2 FID's are the averages of 20 scans whereas those for $CsHF_2$ are the averages of 500 scans (the spin-lattice relaxation time of $CsHF_2$ is about 5 s at room temperature so scans could be repeated much more frequently without losing signal through saturation). The decays are calculated for an on resonance situation.

3.3.3 A Hydrogen Difluoride Ion with a Non-Central Hydrogen Atom

The structure of the HF_2^- ion has been the subject of conjecture for a number of years (Blinc(20)), the point of interest being the position of the hydrogen atom. An early ^{1}H NMR study of KHF_2 (Humphrey, Waugh and Yost(21)) showed that, to within experimental error, the hydrogen atom was in the centre of a linear ion (in other words the ion had $D_{\infty h}$ symmetry). Later NMR studies of KHF_2 (Haeberlen and Spiess(15),

Pratt and Smith(11) and the present one) came to the same conclusion. These NMR results are confirmed by a neutron diffraction study by Carrell and Donohue(10) .

The HF_2^- ion need not always have $D_{\infty h}$ symmetry, Williams and Schneemeyer(22) have reported a non-central hydrogen atom in 4-methylphenylamine hydrogen difluoride (MHD from now on), $C_7H_{11}NF_2$, (r_{HF} = 0.1025 and 0.1235 nm, r_{FF} = 0.2260 nm). They attribute this behaviour to the asymmetric crystal environment of the ion (in KHF_2 this environment is symmetric). Interestingly, Cousseau and Smith(23) have studied the ^{19}F FID of the same compound but concluded that the H atom was central, we shall return to this point shortly. The two types of ion have very different FID's. ^1H and ^{19}F FID's have been calculated for isolated ions of both types using the neutron diffraction bond lengths, the results are shown in Figures 3.10 (a) and (c) and 3.11(a) and (b) respectively (note the change of scale on the time axes). Strictly speaking we cannot calculate the ^{19}F FID for the ion in which the fluorine atoms are not equivalent, as we shall see shortly the calculation is somewhat artificial anyway, nevertheless the calculation serves to illustrate the point we are making. Equations 2.31 and 2.32 were used in the calculations, a Gaussian decay function was applied after a polycrystalline average had been performed and the calculation was done for the on resonance situation. As we have seen the experimental KHF_2 ^1H FID (Figure 3.10(d) is most like Figure 3.10(a) calculated for the ion with $D_{\infty h}$ symmetry. The sensitivity of the ^1H FID to the displacement of the hydrogen atom from the centre of the ion is illustrated in Figures 3.10(b) and (c), for MHD this displacement is about 5% of the total F-F distance, in Figure 3.10(b) the displacement is 2% of the F-F distance.

We have not measured the FID's of MHD but as mentioned above Cousseau and Smith(23) have obtained the ^{19}F FID (the ^{1}H FID of the HF_2^- ion is obscured by the signals from the other hydrogen atoms in the cation) this is reproduced in Figure 3.11(c). It is more like the theoretical signal for the hydrogen centred ion than that for the non-centred (this led the authors to assume that the ion had $D_{\infty h}$ symmetry, in marked contradiction to the neutron diffraction experiment). However in the MHD crystal the HF_2^- ion is not as isolated as it is in the KHF_2 crystal (where the nearest atoms to each H after the two F's at 0.1139 nm are two H's at 0.3401 nm) - Figure 3.12. The theoretical calculation should, then, contain at least five spins if it is to be used as a basis for determining the geometry of such a system. Unfortunately, the calculation of such a signal is complex and cannot easily be undertaken with the methods used so far. As an approximation we have calculated the signal for the closest three atoms, H(2), F(1) and H(1) in Figure 3.12, the result is shown in Figure 3.11(d). It is clear that structural observation for MHD using the ^{19}F FID must be treated with caution. There is insufficient evidence to suggest that the ^{19}F NMR result contradicts the neutron diffraction result.

3.3.4 Results for Sodium Fluoroethanoate, $CH_2FCOONa$

We include the FID's of sodium fluoroethanoate at this point to show that our theoretical expressions can be applied to more complex spin systems (equations 2.31 and 2.32 do not simplify to 3.08 and 3.09 for this compound).

The crystal structure of the sodium salt has been investigated by Vedavathi and Vijayan(24) but it was not possible to calculate the internuclear distances in the fluoromethyl group

from this reference. The crystal structure of fluoroethanoic acid, CH_2FCOOH, has been reported by Kanters and Kroon(25) and Roelofsen, Kanters and Brandts(26). We were able to calculate the CH_2F internuclear distances from these references and as we did not expect the internuclear distances in the acid to be very different from those in the sodium salt we used them as a starting point for the calculation of the FID's. (It was found that the H-H separation from references (25) and (26) were very different - 0.184 and 0.159 nm respectively. The calculation of the FID's based on the first figure bore a much greater resemblance to the experimental signal so we suspect that there is an error in the reported atomic coordinates in reference (26).)

The final calculation was based on the values r_{HF} = 0.184 nm, r_{HH} = 0.181 nm (to make the calculation valid we have had to assume that the hydrogen atoms are equivalent - that is we have made the two HF distances the same), the results are shown in Figures 3.13 and 3.14. The fits are not as good as they were for the hydrogen difluoride ions, this may be because we have assumed that the two HF distances are the same (the x-ray data shows them to be slightly different) or it could be because the signals were accumulated over a period of fourteen hours during which some drift in the tuning of the spectrometer was inevitable. Again, Gaussian decays (weights: 1.0×10^9 $rad^2\ s^{-2}$ for ^1H and 1.6×10^9 $rad^2\ s^{-2}$ for ^{19}F) were applied after averaging for the polycrystalline sample. The calculations were carried out under the assumption that the spectrometer was on resonance.

3.3.5 Theoretical Four Spin Systems

For the sake of completeness we have calculated the FID's for a series of hypothetical four spin systems. The calculations

were based on equation 2.33, they included a polycrystalline average, a Gaussian decay function and were for a spectrometer on resonance. The results are shown in Figures 3.15 and 3.16 these figures also include the geometries of the systems studied. Both Figures 3.15 and 3.16 illustrate the loss of detail in the signal as more spins are brought into the system. The decays in Figure 3.16 are all very similar, it is only when they are studied in greater detail that the differences become apparent.

3.4 Appendices

3.4.1 Appendix E

Polycrystalline averaged signals which depend on one dipolar coupling constant are of the form (equation 3.01)

$$\langle I_x(t)\rangle \alpha \tfrac{1}{2}\int_0^{\pi} \cos[r^{-3}\, C^D(3\cos^2\beta - 1)t]\, \sin\beta\, d\beta . \qquad 3.01$$

Let $a = \cos\beta$, so $da = -\sin\beta\, d\beta$ and the right-hand side of expression 3.01 becomes

$$-\tfrac{1}{2}\int_1^{-1} \cos[r^{-3}\, C^D(3a^2 - 1)t]da$$

$$\equiv \int_0^1 \cos[r^{-3}\, C^D(3a^2 - 1)t]da$$

with $\cos(A-B) = \cos A \cos B + \sin A \sin B$ this is

$$\int_0^1 \cos(r^{-3}\, C^D t)\, \cos(3r^{-3}\, C^D\, a^2\, t)da +$$

$$\int_0^1 \sin(r^{-3}\, C^D\, t)\, \sin(3r^{-3}\, C^D\, a^2\, t)da .$$

Now let $x = \left(\frac{6r^{-3}\, C^D\, t}{\pi}\right)^{\frac{1}{2}}.a$, then $x^2\frac{\pi}{2} = 3r^{-3}\, C^D\, t.a^2$

and $dx = \left(\frac{6r^{-3}\, C^D\, t}{\pi}\right)^{\frac{1}{2}}.da$

so that

$$\langle I_x(t)\rangle \alpha \left(\frac{\pi}{6r^{-3}\, C^D\, t}\right)^{\frac{1}{2}} \left[\cos(r^{-3}\, C^D\, t) \int_0^{(6r^{-3}\, C^D\, t/\pi)^{\frac{1}{2}}} \cos(\tfrac{\pi}{2}x^2)dx \; + \right.$$

$$\left. \sin(r^{-3}\, C^D\, t) \int_0^{(6r^{-3}\, C^D\, t/\pi)^{\frac{1}{2}}} \sin(\tfrac{\pi}{2}x^2)dx \right]$$

but $\int_0^{(6r^{-3}\, C^D\, t/\pi)^{\frac{1}{2}}} \cos(\tfrac{\pi}{2}x^2)dx = C((6r^{-3}\, C^D\, t/\pi)^{\frac{1}{2}})$

and $\int_0^{(6r^{-3}\, C^D\, t/\pi)^{\frac{1}{2}}} \sin(\tfrac{\pi}{2}x^2)dx = S((6r^{-3}\, C^D\, t/\pi)^{\frac{1}{2}})$,

with $y = (6r^{-3}\, C^D\, t/\pi)^{\frac{1}{2}}$

$$\langle I_x(t)\rangle \propto y^{-1}[\cos(\tfrac{\pi}{6}y^2)\ C(y) + \sin(\tfrac{\pi}{6}y^2)\ S(y)]\ . \qquad 3.02$$

3.4.2 Appendix F

As well as the polycrystalline average and the decay function real systems can be further complicated by a non-zero offset, $\Delta\omega$. From equations 2.04 and B1

$$\Delta\omega = \omega_R - \omega_0 + \omega_0\sigma_{zz}$$

$$= \omega_R - \omega_0 + \omega_0(\tfrac{1}{3}(\sigma_{xx} + \sigma_{yy} + \sigma_{zz}) + \tfrac{\delta}{2}(3\cos^2\beta - 1 - \eta\sin^2\beta\ \cos 2\alpha))\ . \qquad F1$$

The frequency term ω_R is a variable at the control of the experimenter so it is possible to choose ω_R so that $\Delta\omega = 0$, in practice, however, it is not always possible (if the shielding parameters, $\sigma^{(0)}$, δ and η, are not known) to be sure that this equality holds. The extent to which the shielding interaction affects the offset depends on the system being studied, for hydrogen nuclei the shielding is largely insignificant (the shielding anisotropy usually has a range up to about 30 ppm) when compared to the dipolar interaction. Other nuclei may have a significant shielding interaction, especially if the dipolar interaction is weak (fluorine shielding anisotropies are typically about 150 ppm, and for phosphorus they are several hundred ppm).

If the sample is polycrystalline the shielding term in equation 2.13 must be averaged as well as the dipolar terms. Because the angles β and α (the polar angles which relate the shielding PAS Z-axis to the LAB system), for different nuclei, are independent there is no need to re-express them in terms of some general angles, the integration, over β and α, can be done directly.

The effect the offset has on the signal essentially depends on the relative sizes of $\Delta\omega$ and the dipolar interactions. Figure 3.17 shows the effect of $\Delta\omega$ on the hypothetical signal:

$$\langle I_x(t)\rangle = \cos\Delta\omega t \cos at \exp(-8 \times 10^8 t^2). \qquad F2$$

Curve (a) is for $\Delta\omega = 0$, a curve with $\frac{a}{\Delta\omega} \cong 40$ is almost identical to (a), and is, therefore, not shown, the long time deviation is masked by the decay of the signal. Curves (b) and (c) are for $\frac{a}{\Delta\omega} \cong 10$ and 4 respectively, clearly a large offset can alter the character of the signal completely. The possibility of a non-zero offset distorting the signal must be borne in mind when a real signal is analysed.

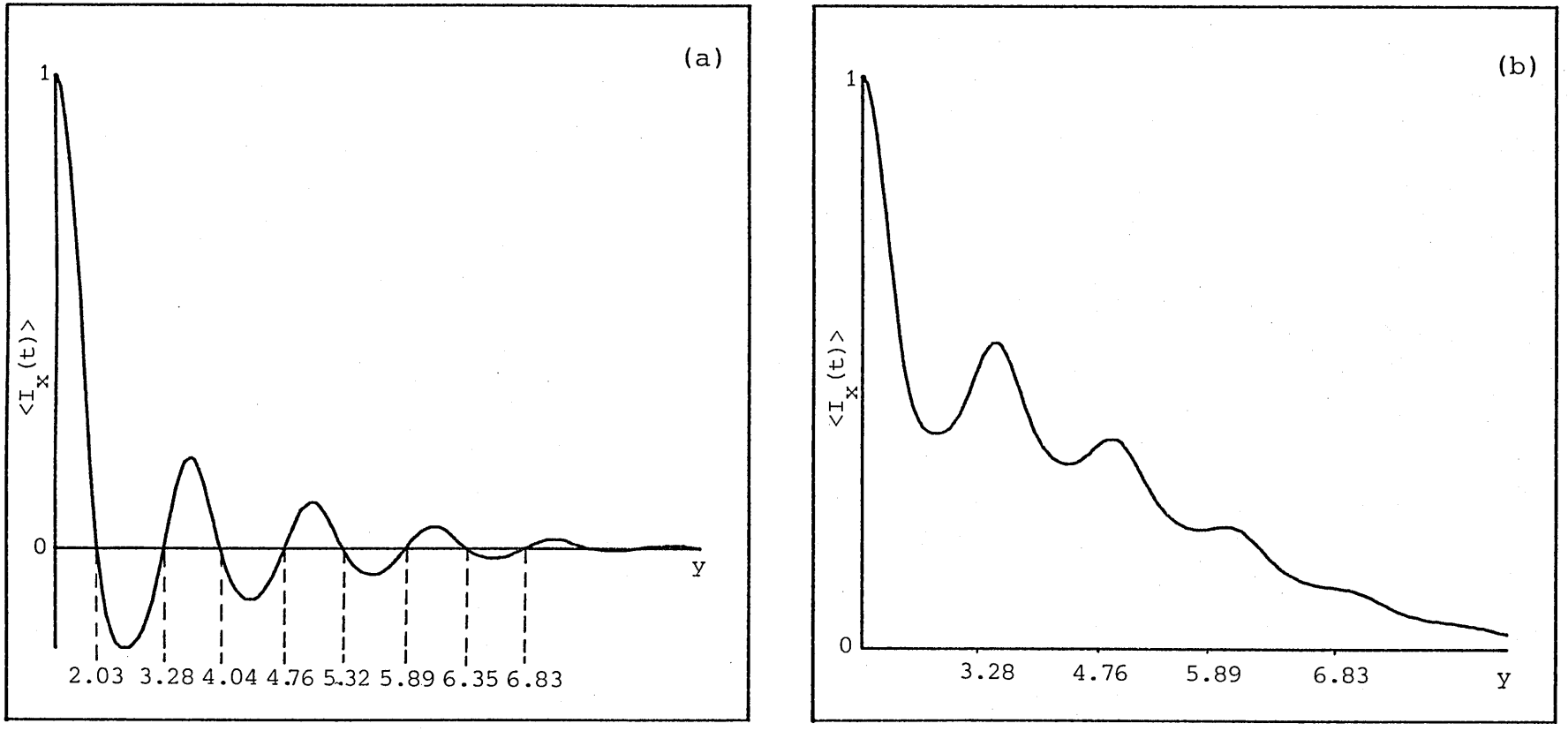

Figure 3.1 The signal for a polycrystalline sample calculated (a) from equation 3.02 and (b) from equation 2.31 which contains a constant component. Both signals include a Gaussian decay.

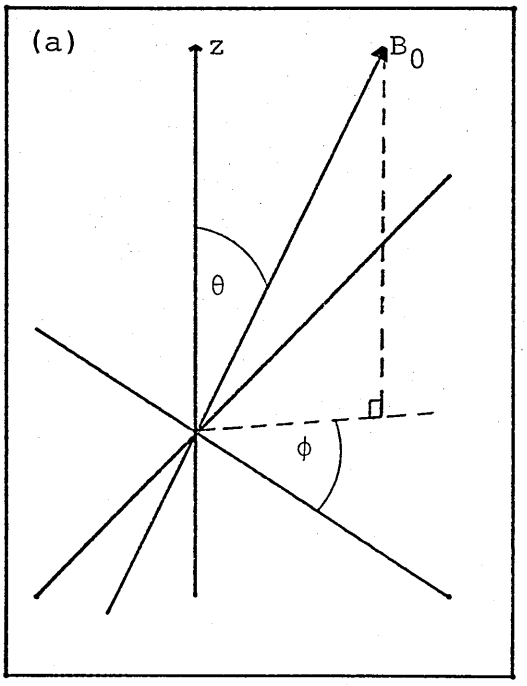

The polar angles

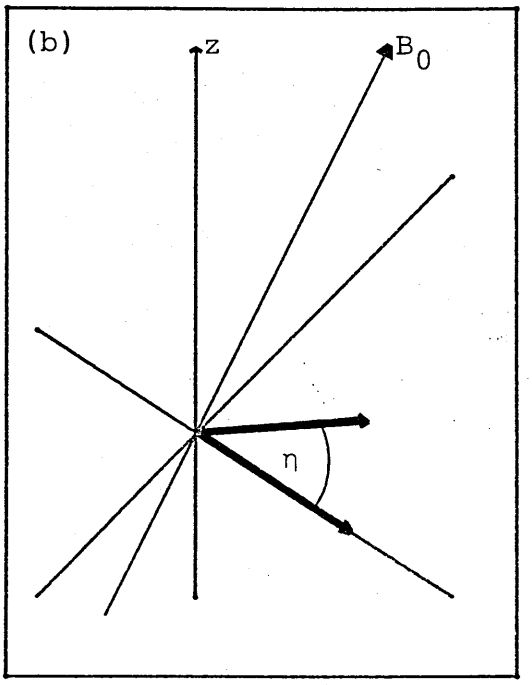

The ISS′ spin system

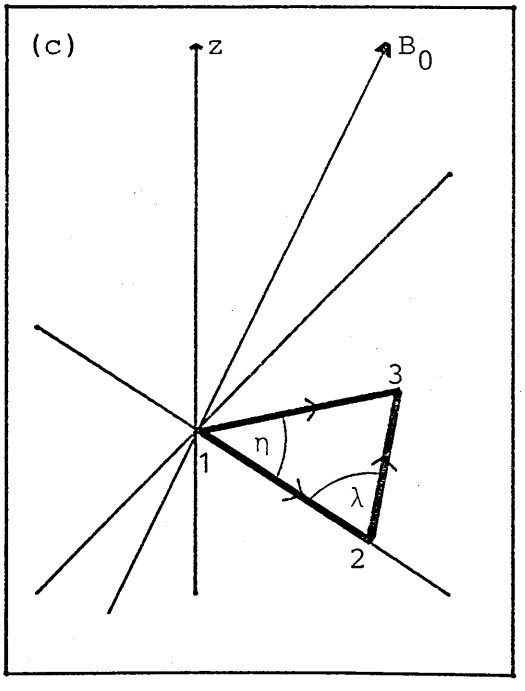

The IS_2 spin system

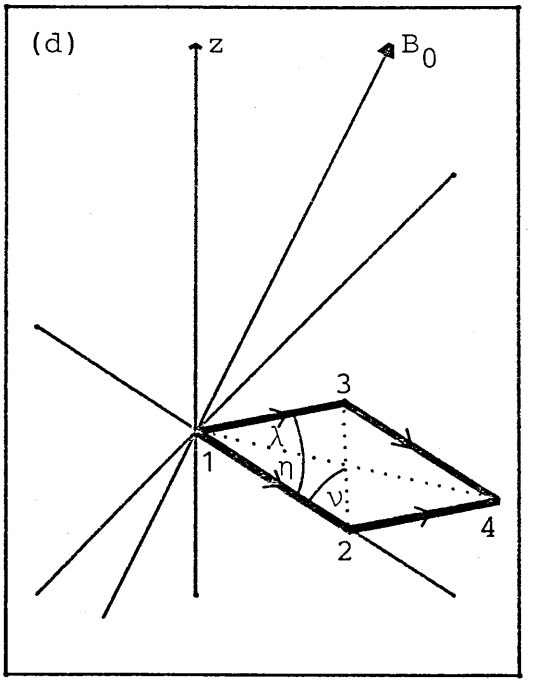

The I_2S_2 spin system

Figure 3.2 (a) the polar angles. (b), (c) and (d) the relationship between the direction cosines, $\cos\beta_{ij}$, and system dependent angles for various spin systems.

(b)

$\cos\beta_{12} = \sin\theta\cos\phi$

$\cos\beta_{13} = \sin\theta\cos(\phi-\eta)$

(c)

$\cos\beta_{12} = \sin\theta\cos\phi$

$\cos\beta_{13} = \sin\theta\cos(\phi-\eta)$

$\cos\beta_{23} = -\sin\theta\cos(\phi+\lambda)$

(d)

$\cos\beta_{12} = \sin\theta\cos\phi$

$\cos\beta_{13} = \sin\theta\cos(\phi-\lambda-\eta)$

$\cos\beta_{14} = \sin\theta\cos(\phi-\eta)$

$\cos\beta_{23} = -\sin\theta\cos(\phi+\nu)$

$\cos\beta_{34} = \cos\beta_{12}$

$\cos\beta_{24} = \cos\beta_{13}$

(by definition - Section 2.2.3)

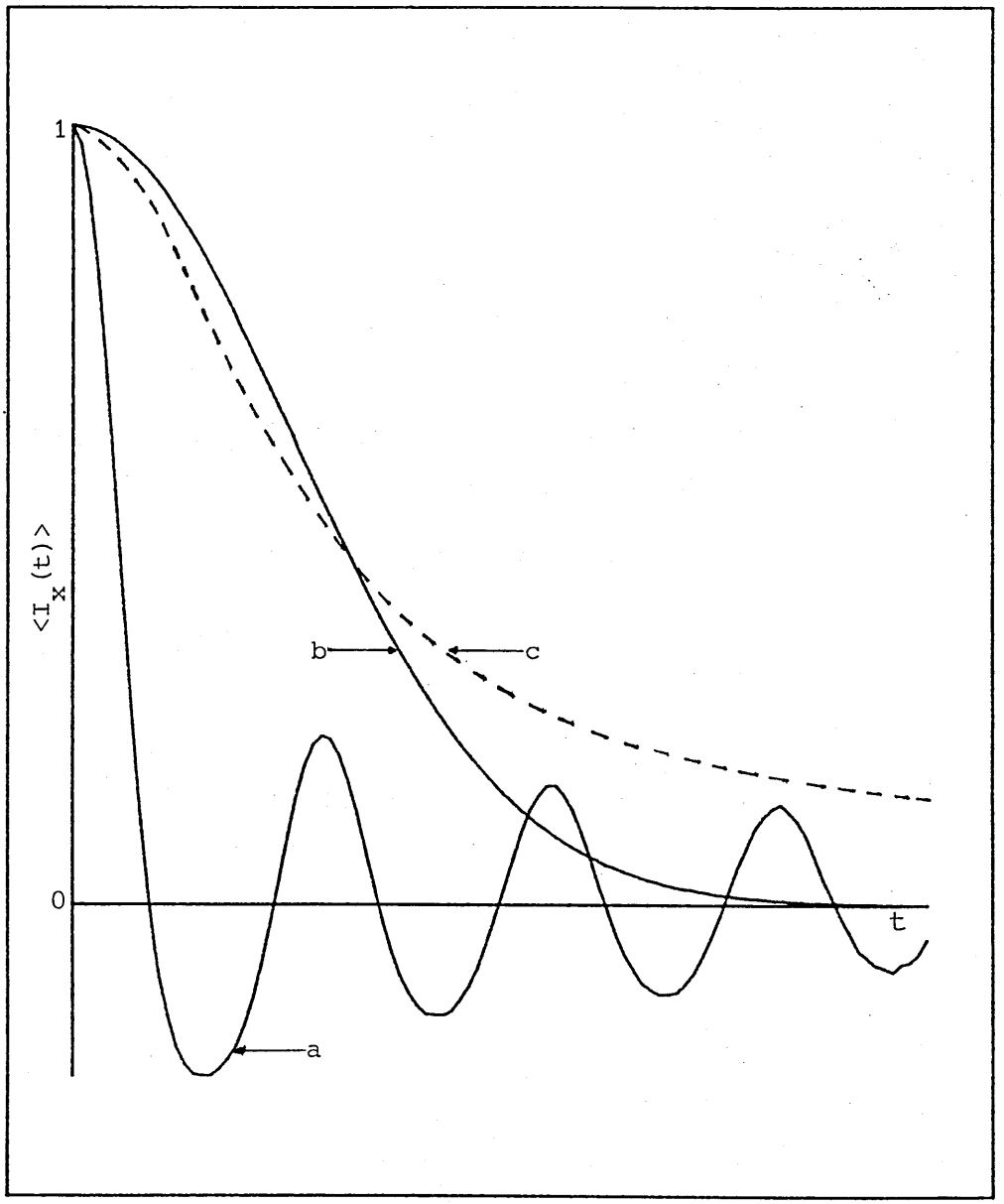

Figure 3.3 This illustrates the effect that the polycrystalline average has on the cosine function $\cos(3\cos^2\theta-1)at$: curve (a) is the integral $\langle I_x(t)\rangle = \frac{1}{2}\int_0^{\pi} \cos(3\cos^2\theta-1)at \sin\theta d\theta$. Curves (b) and (c) show the result of including a Gaussian decay function ($\sqrt{M_2'} = 1.12 \times 10^5$ rad $s^{-1} \cong \frac{1}{4}a$) inside the average.

Curve (b) is

$$\langle I_x(t)\rangle = \exp(-\tfrac{1}{2}\int_0^{\pi} \tfrac{1}{2}M_2' t^2 \sin\theta d\theta)$$

whereas curve (c) is

$$\langle I_x(t)\rangle = \tfrac{1}{2}\int_0^{\pi} \exp(-\tfrac{1}{2}M_2' t^2) \sin\theta d\theta.$$

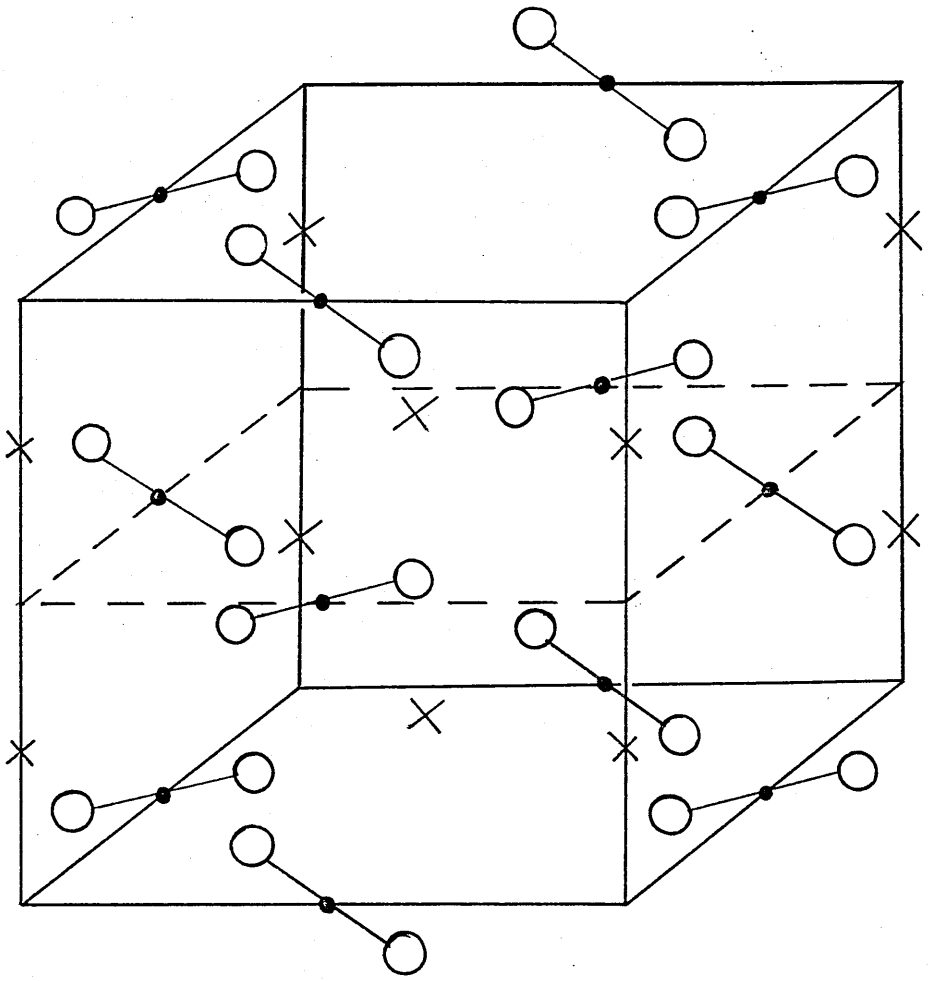

Figure 3.4 The KHF_2 unit cell (not to scale).
The cell dimensions are a = 0.5672 nm, c = 0.6801 nm.

• Hydrogen

○ Fluorine

× Potassium

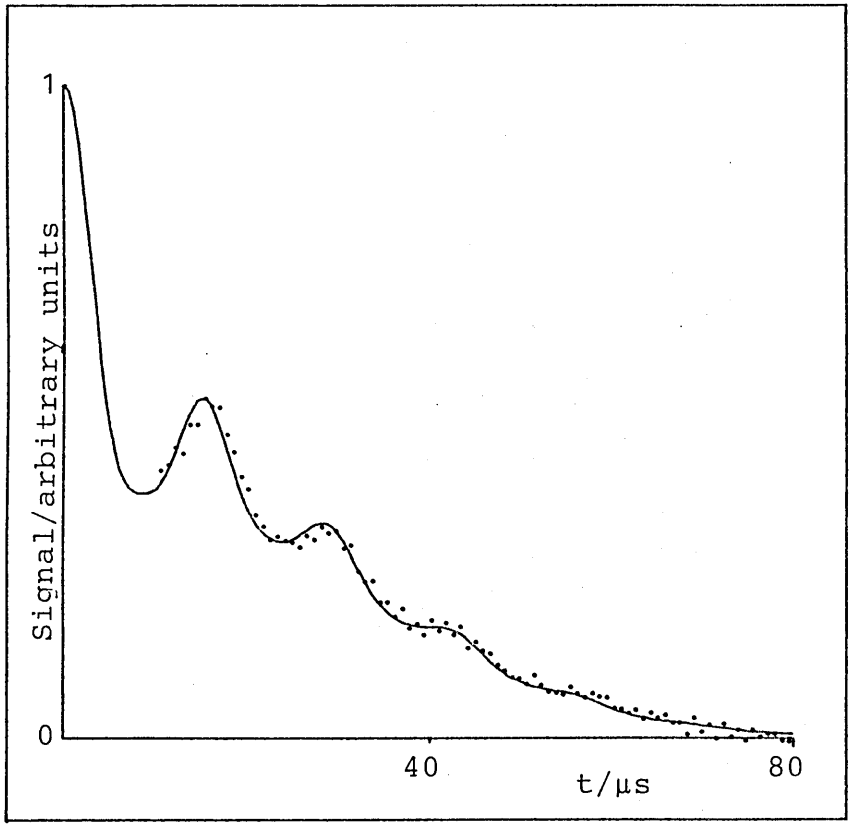

Figure 3.5 The experimental (.....) and calculated (——) ^{1}H FID for KHF_2 at 293 K.

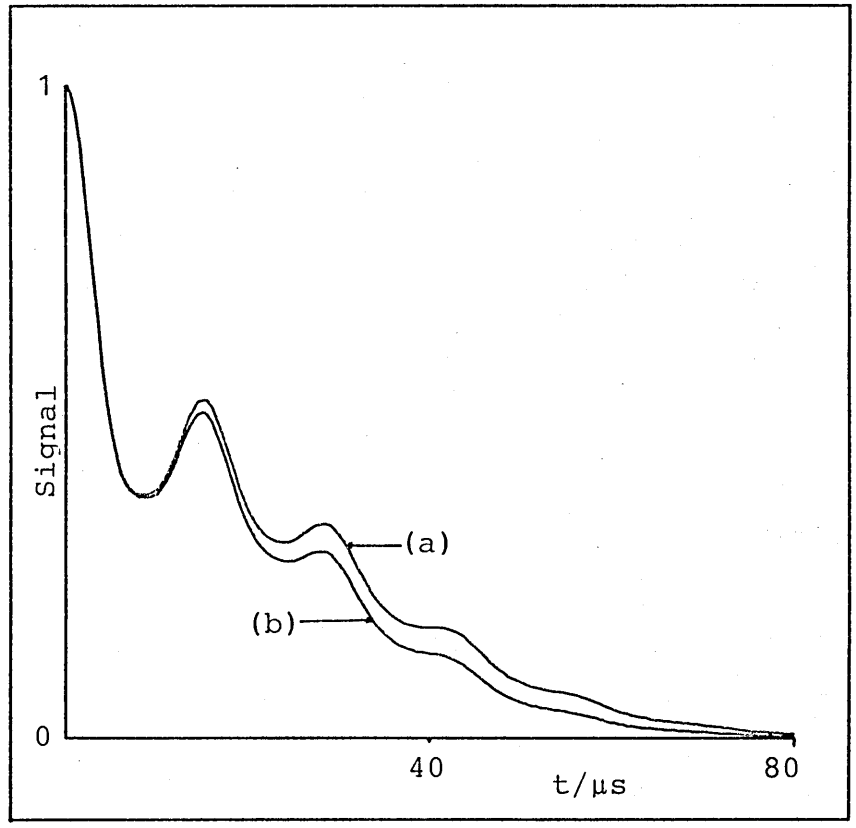

Figure 3.6 A comparison of the Gaussian decay functions $f(t) = \exp(-\alpha t^2)$ with (a) $\alpha = 6.00 \times 10^8$ rad^2 s^{-2} and (b) $\alpha = 7.75 \times 10^8$ rad^2 s^{-2}

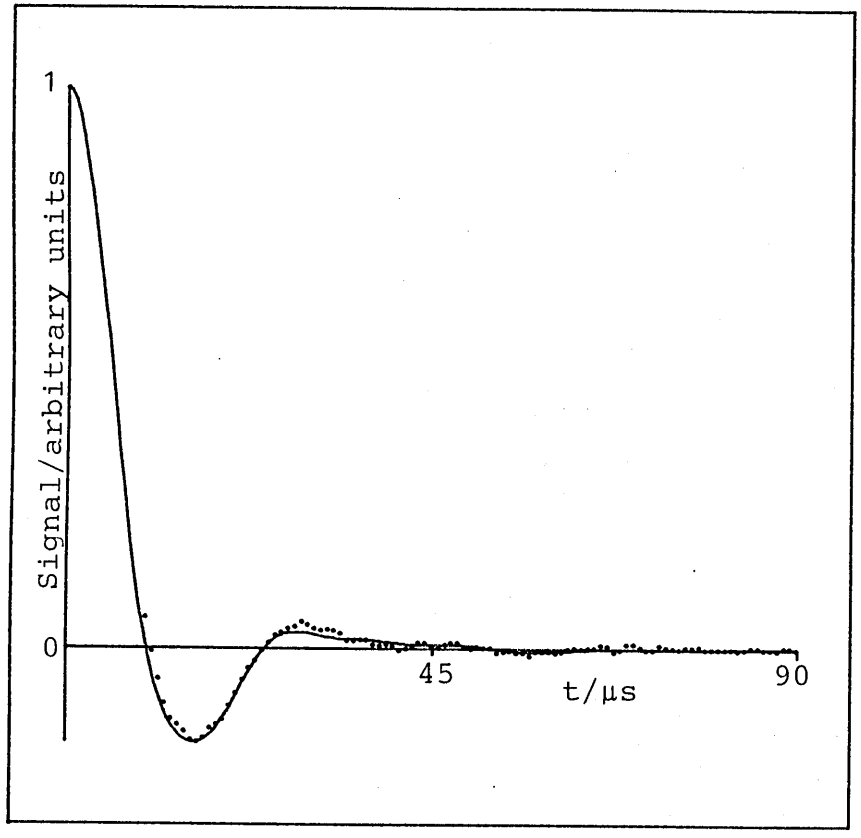

Figure 3.7 The experimental (.....) and calculated (——) ^{19}F FID for KHF_2 at 293 K.

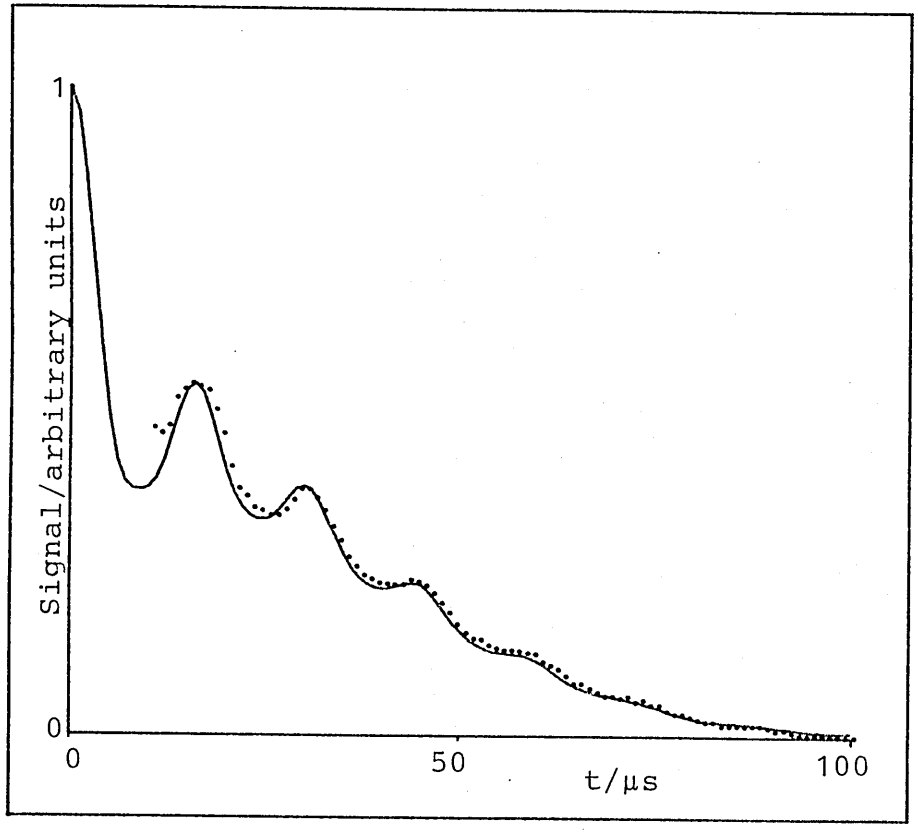

Figure 3.8 The experimental (.....) and calculated (——) ^{1}H FID for $CsHF_2$ at 293 K.

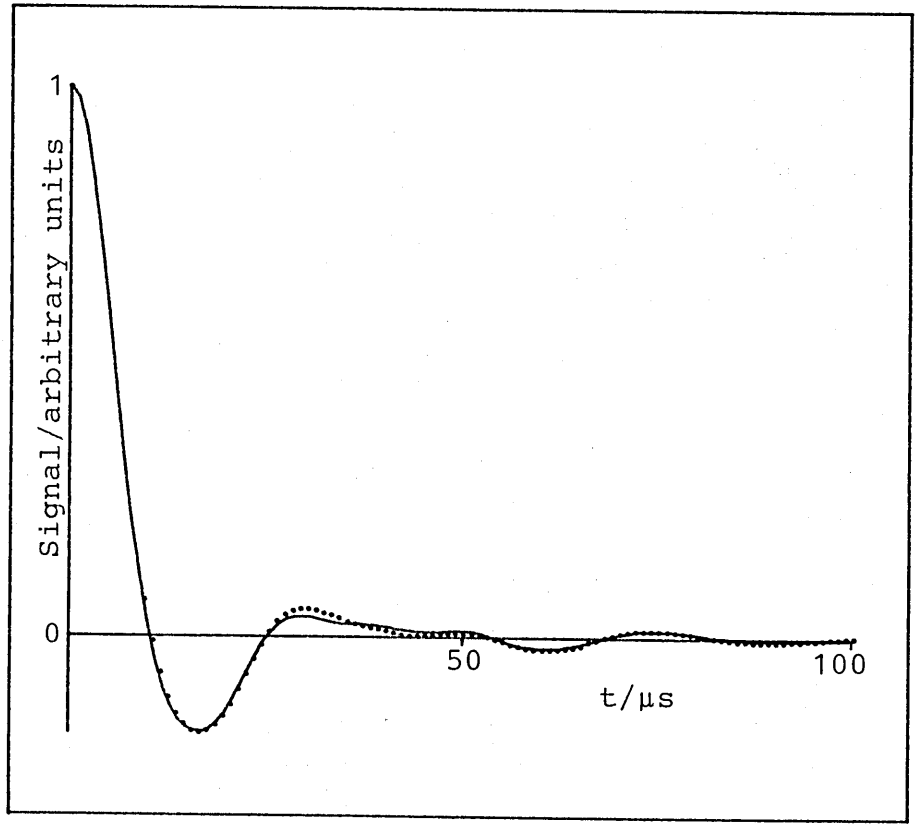

Figure 3.9 The experimental (.....) and calculated (——) ^{19}F FID for $CsHF_2$ at 293 K.

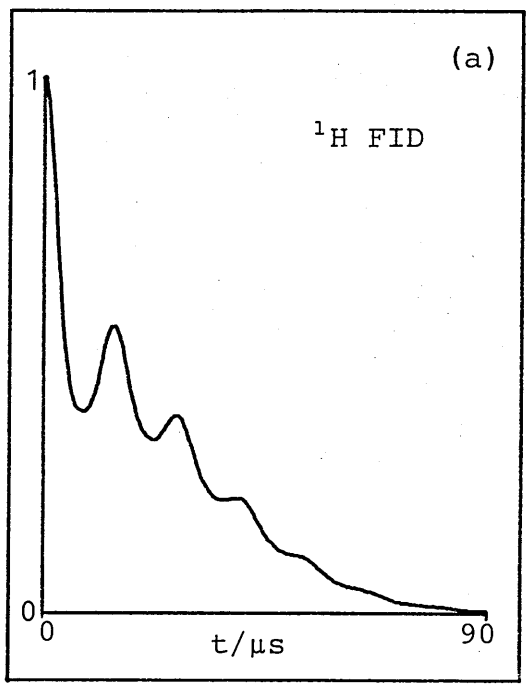

r_{HF} = 0.1139 nm

r_{FF} = 0.2278 nm

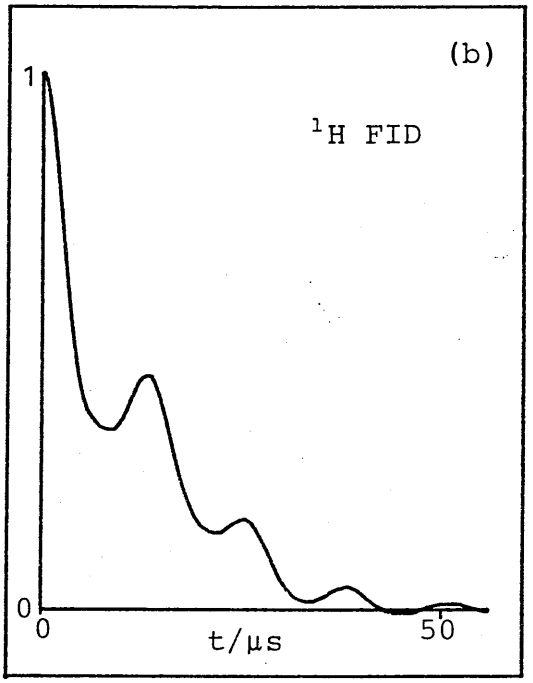

r_{HF} = 0.1085 and 0.1175 nm

r_{FF} = 0.2260 nm

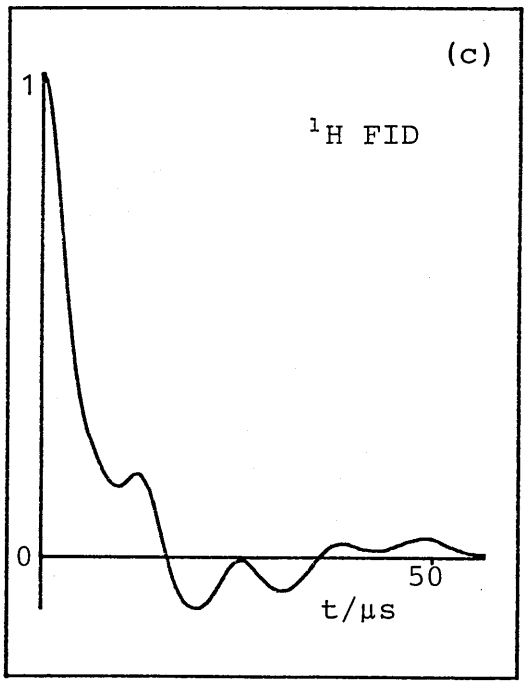

r_{HF} = 0.1025 and 0.1235 nm

r_{FF} = 0.2260 nm

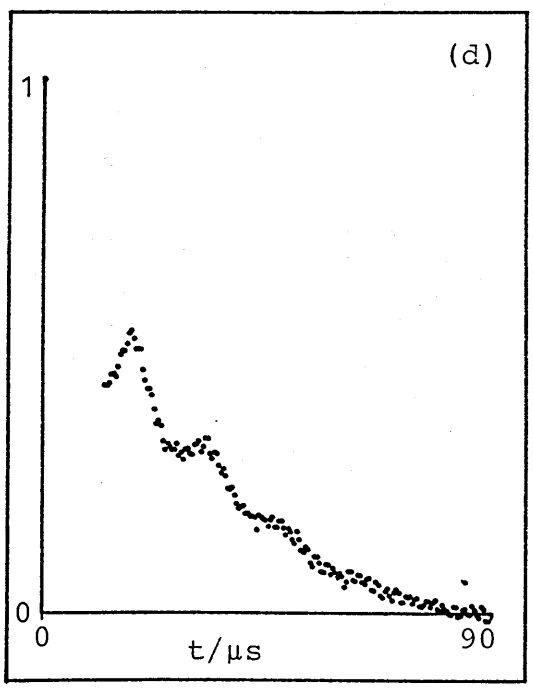

Experimental ^{1}H FID for KHF_2 at 293 K

Figure 3.10 ^{1}H FID's for different configurations of the HF_2^- ion. (All the theoretical FID's include a Gaussian decay function chosen so that the signal decays to zero in a time similar to that found experimentally.)

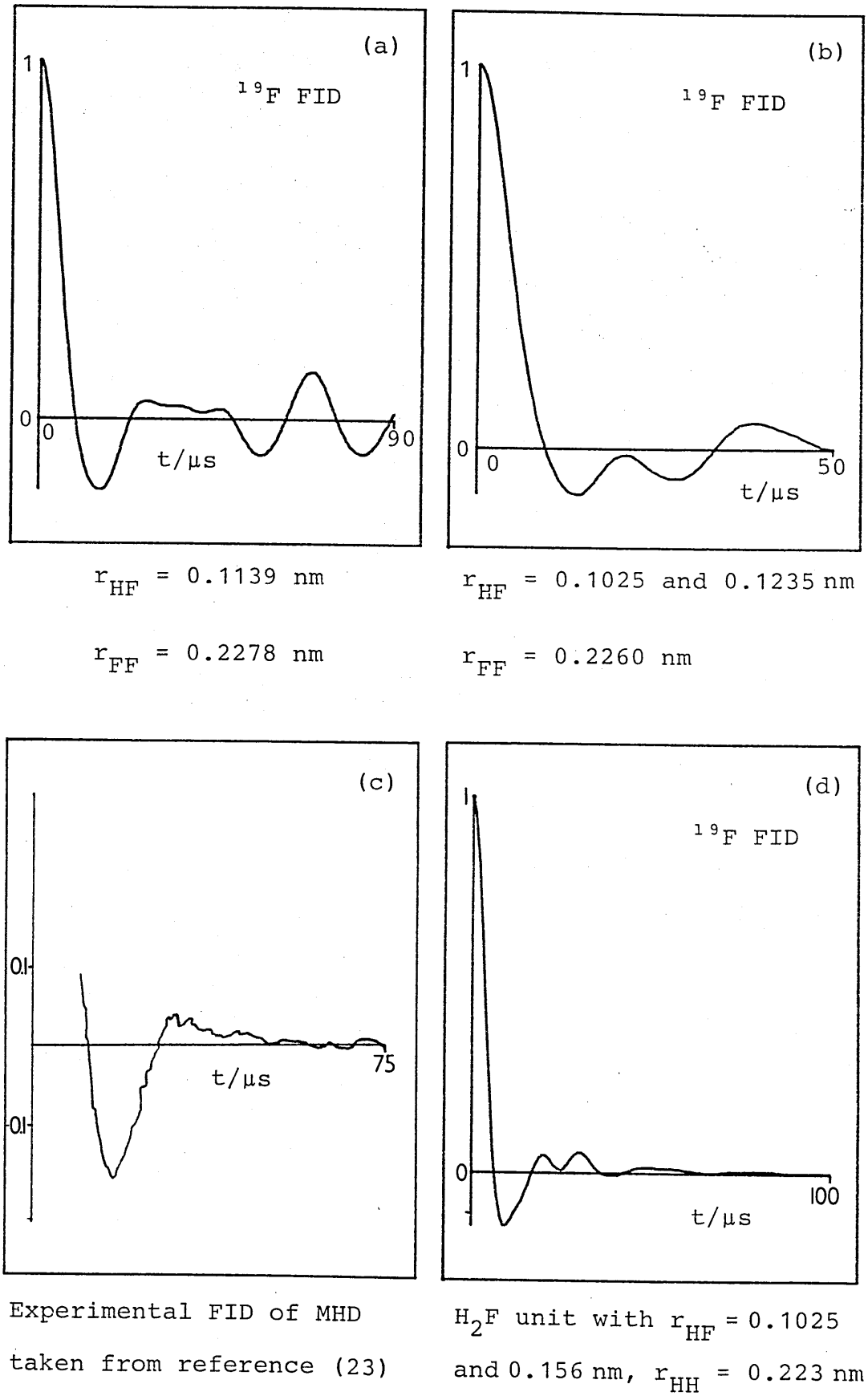

r_{HF} = 0.1139 nm

r_{FF} = 0.2278 nm

r_{HF} = 0.1025 and 0.1235 nm

r_{FF} = 0.2260 nm

Experimental FID of MHD taken from reference (23)

H_2F unit with r_{HF} = 0.1025 and 0.156 nm, r_{HH} = 0.223 nm

Figure 3.11 ^{19}F FID's for different configurations of the HF_2^- ion. (All the theoretical FID's include a Gaussian decay function as in Figure 3.10)

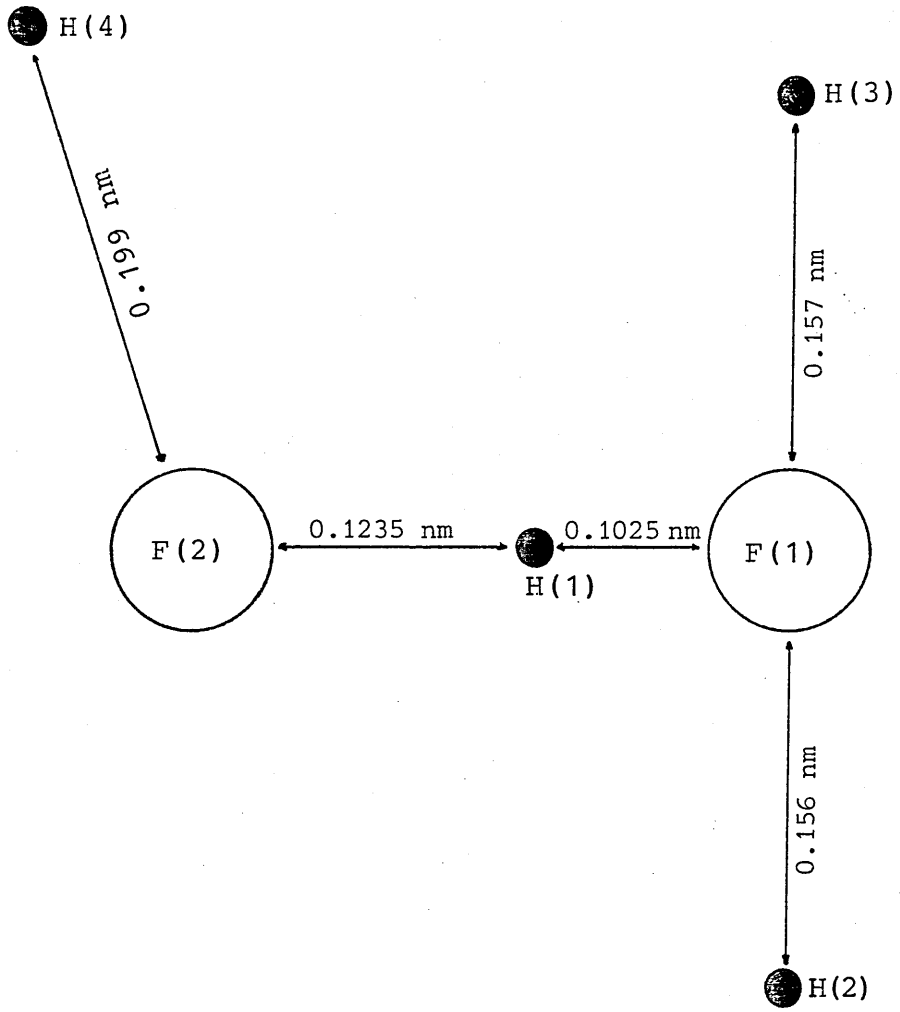

Figure 3.12 Schematic illustration of the short range (<0.2 nm) H-F internuclear distances around the ^{19}F atoms in the hydrogen difluoride ion in MHD (from reference (27)). The diagram is not to scale and the angles between the internuclear vectors are not representative of the true geometry.

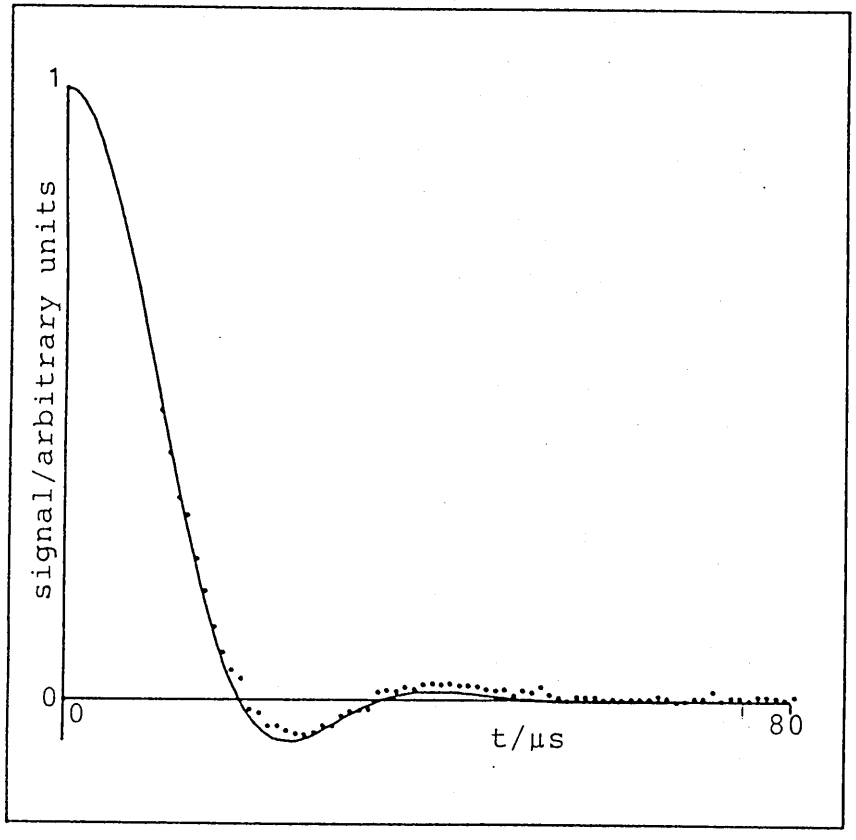

Figure 3.13 The experimental (.....) and calculated (——) ^{1}H FID for $CH_2FCOONa$ at 293 K.

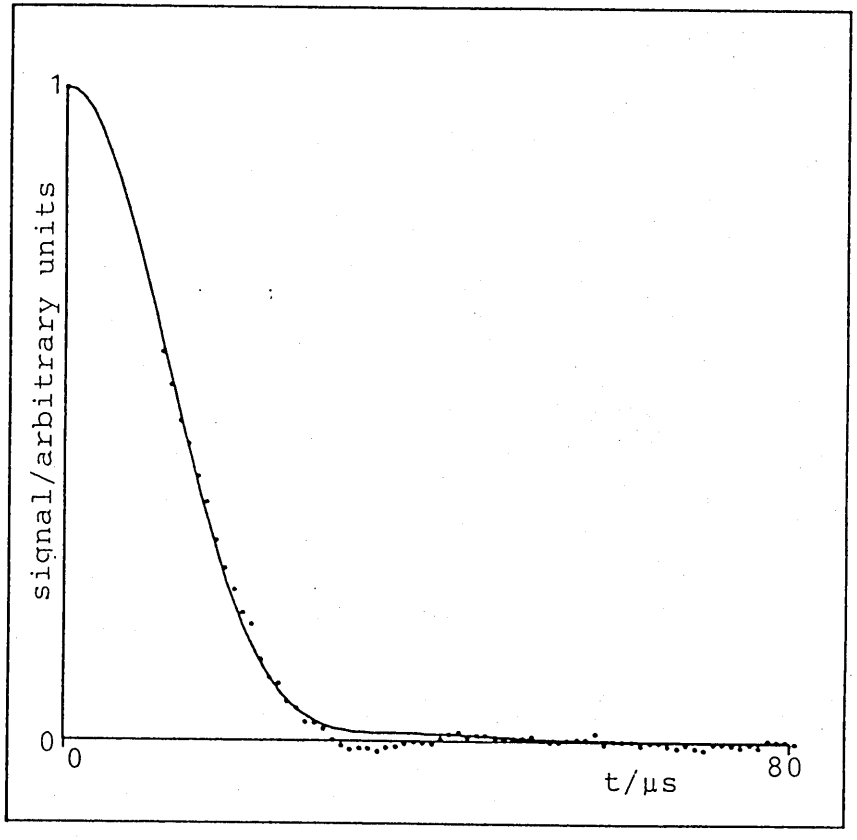

Figure 3.14 The experimental (.....) and calculated (——) ^{19}F FID for $CH_2FCOONa$ at 293 K.

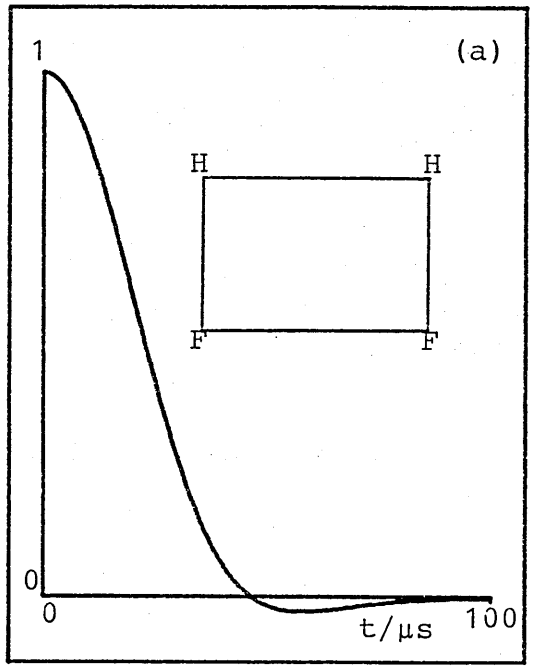

$r_{HH} = r_{FF} = 0.3$ nm

$r_{HF} = 0.2$ and 0.361 nm

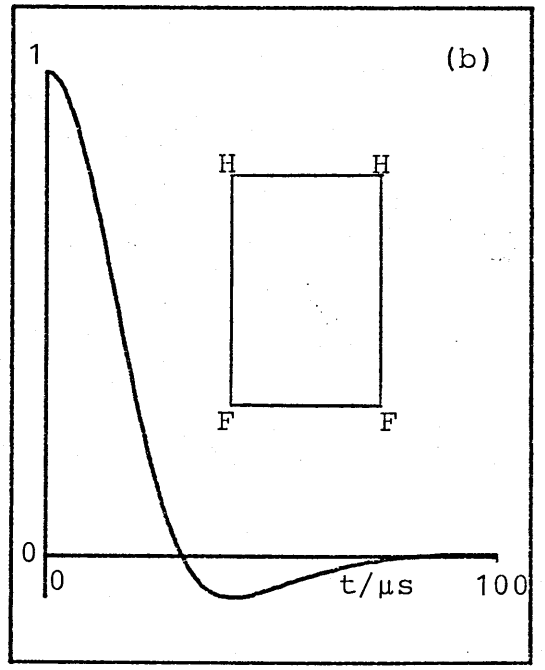

$r_{HH} = r_{FF} = 0.2$ nm

$r_{HF} = 0.3$ and 0.361 nm

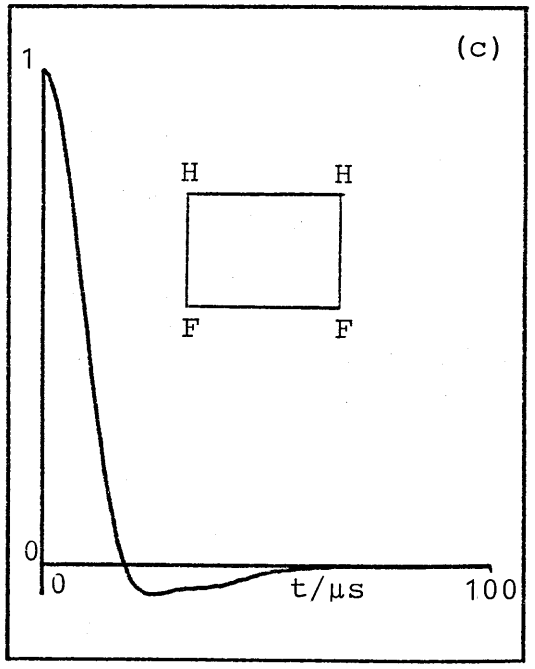

$r_{HH} = r_{FF} = 0.2$ nm

$r_{HF} = 0.15$ and 0.25 nm

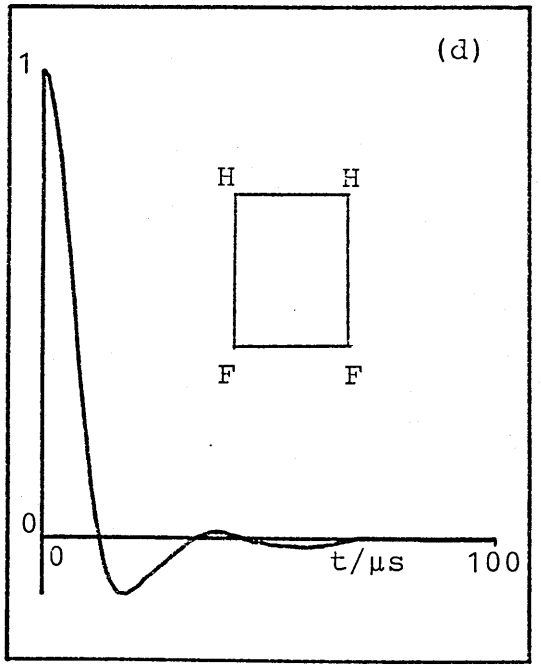

$r_{HH} = r_{FF} = 0.15$ nm

$r_{HF} = 0.2$ and 0.25 nm

Figure 3.15 FID's for hypothetical I_2S_2 spin systems. All those shown are for H_2F_2 systems and all include a Gaussian decay function (see Figure 3.10)

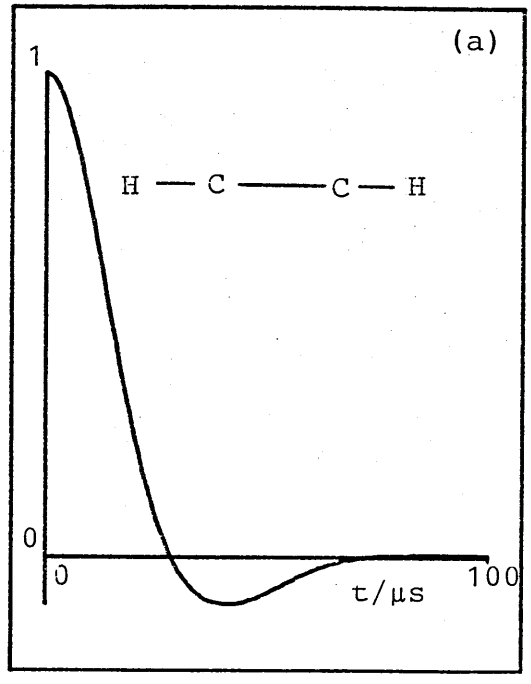

r_{HH} = 0.332 nm, r_{CC} = 0.120 nm
r_{CH} = 0.106 and 0.226 nm

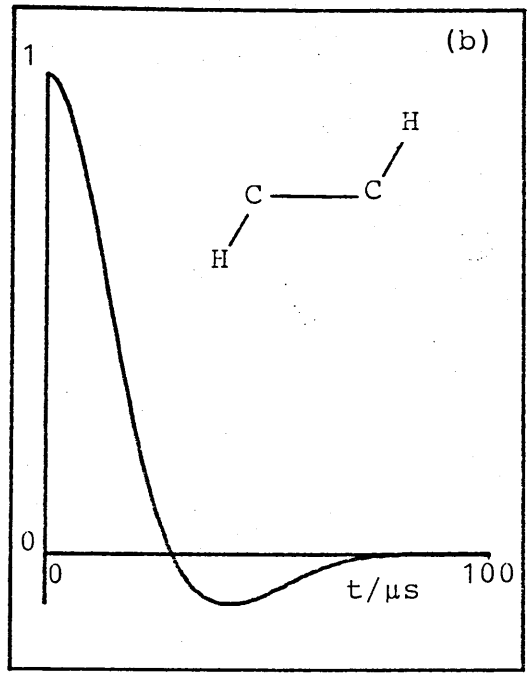

r_{HH} = 0.307 nm, r_{CC} = 0.133 n
r_{CH} = 0.108 and 0.211 nm

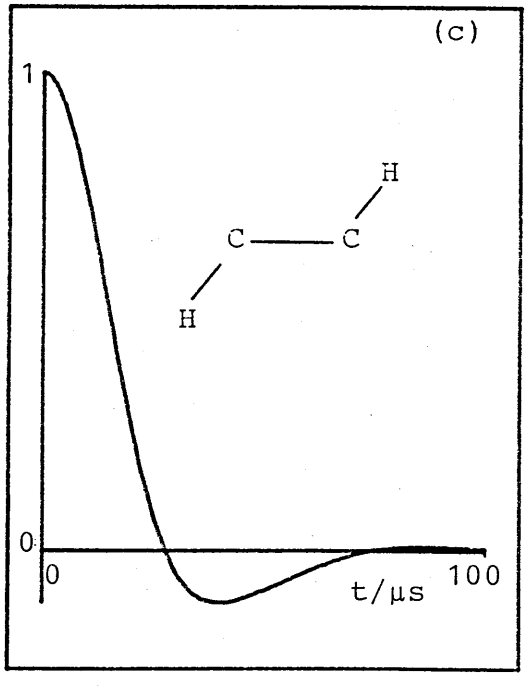

r_{HH} = 0.307 nm, r_{CC} = 0.133 nm
r_{CH} = 0.108 and 0.211 nm

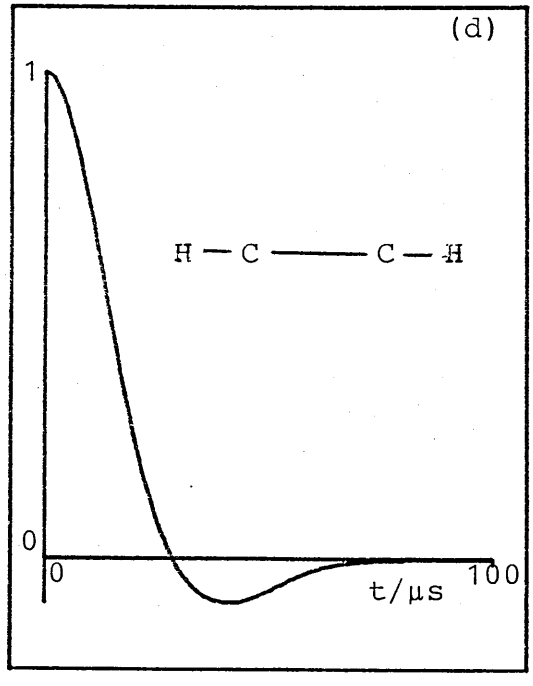

r_{HH} = 0.332 nm, r_{CC} = 0.120 nm
r_{CH} = 0.106 and 0.226 nm

Figure 3.16 FID's for an $^{1}H_{2}{}^{13}C_{2}$ spin system. (a) and (b) are ^{1}H resonances, (c) and (d) ^{13}C resonances. All the decays contain a Gaussian decay function (see Figure 3.10).

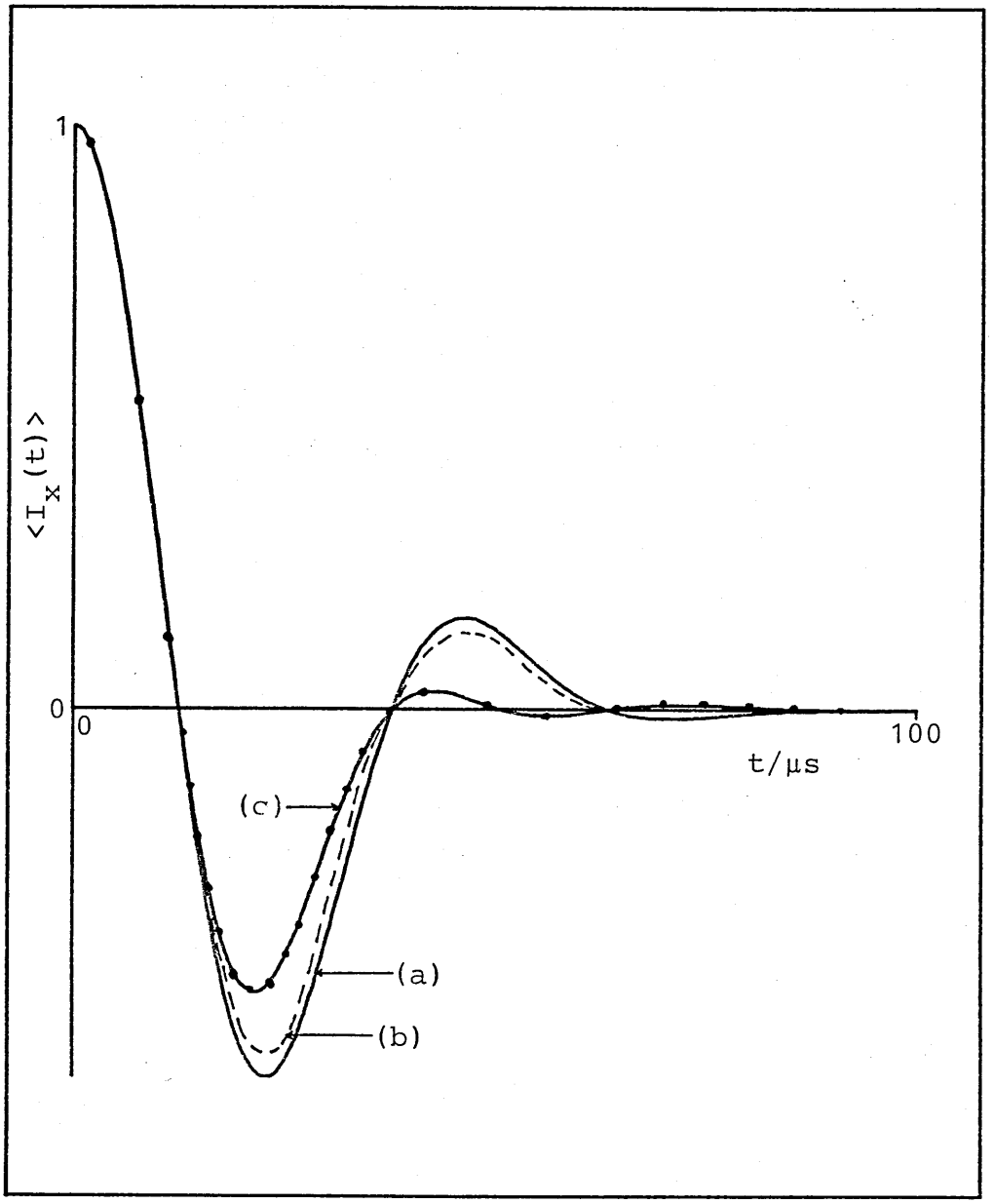

Figure 3.17 The effect of an offset on the signal $\langle I_x(t) \rangle = \cos\Delta\omega t \cos at \exp(-8.0 \times 10^8 t^2)$ with

(a) ——— $\Delta\omega = 0$

(b) – – – $\frac{a}{\Delta\omega} = 10$

(c) —●—●— $\frac{a}{\Delta\omega} = 4$

3.5 References

(1) J.S. Waugh, B.L. Neff, E.F. Rybaczewski and J.S. Sherfinski, J. Chem. Phys., 67(3), 1231-1236 (1977).

(2) G.E. Pake, J. Chem. Phys. 16, 327-336 (1948).

(3) L.W. Reeves, Progress in NMR Spectroscopy, 4, 193-236 (1969).

(4) U. Haeberlen, 'High Resolution NMR in Solids, Selective Averaging', Supplement 1, Advances in Magnetic Resonance, Academic Press, New York (1976).

(5) H.W. Spiess, 'Rotation of Molecules and Nuclear Spin Relaxation', NMR-Basic Principles and Progress - Volume 15, Springer-Verlag, Heidelberg (1978).

(6) M. Abramowitz and I.A. Stegun, 'Handbook of Mathematical Functions', Dover Publications Inc., New York (1965).

(7) FORTRAN NAG software library, mark 10.

(8) D.E. Barnaal and I.J. Lowe, Phys. Rev., 148(1), 328-331 (1966).

(9) S.W. Petersen and H.A. Levy, J. Chem. Phys., 20, 704-707 (1952).

(10) H.L. Carrell and J. Donohue, Israel J. Chem., 10, 195-200 (1972).

(11) J.C. Pratt and J.A.S. Smith, J. Chem. Soc., Faraday Trans., 71, 596-607 (1975).

(12) J.A. Ibers and D.P. Stevenson, J. Chem. Phys., 28, 929-938 (1958).

(13) G.L. Coté and H.W. Thompson, Proc. Roy. Soc., A210, 206-216 (1951).

(14) H. Boutin, G.F. Safford and V. Brajovic, J. Chem. Phys., 39(11), 3135-3140 (1963).

(15) P. van Hecke, H.W. Spiess and U. Haeberlen, J. Mag. Res., 22, 93-102 (1976).

(16) M. Polak, M. Sheinblatt and V. Shmueli, J. Mag. Res., 16, 252-264 (1974).

(17) R. Kruh, K. Fuwa and T.E. McEver, J. Am. Chem. Soc., 78, 4256-4258 (1956).

(18) A.S. Gilbert and N. Sheppard, Spectrochimica Acta, 32A, 923-930 (1976).

(19) C.J. Ludman, T.C. Waddington, E.K.C. Pang and J.A.S. Smith, J. Chem. Soc., Faraday Trans., 73, 1003-1014 (1977).

(20) R. Blinc, Nature, 182, 1016-1017 (1958).

(21) J.S. Waugh, F.B. Humphrey and D.M. Yost, J. Phys. Chem., 57, 486-490 (1953).

(22) J.M. Williams and L.F. Schneemeyer, J. Am. Chem. Soc., 95(17), 5780-5781 (1973).

(23) J. Cousseau, L. Gouin, E.K.C. Pang and J.A.S. Smith, J. Chem. Soc., Faraday Trans., 73, 1015-1019 (1977).

(24) B.M. Vedavathi and K. Vijayan, Acta. Cryst., B33, 946-948 (1977).

(25) J.A. Kanters and J. Kroon, Acta. Cryst., B28, 1946-1949 (1972).

(26) G. Roelofsen, J.A. Kanters and P. Brandts, Cryst. Struct. Comm., 7, 313-316 (1978).

(27) W.A. Denne and M.K. Mackay, J. Cryst. Mol. Struct., 1, 311-318 (1971).

CHAPTER FOUR

The NMR Response to Several Pulses: Calculations

In Chapter Two we discussed the calculation of the NMR signal following a single strong rf pulse for a series of isolated dipolar coupled heteronuclear spin systems. In this chapter the calculations are extended to include the response to two and three pulse sequences. The calculations are based on a closed density matrix treatment so much of the material developed in Chapter Two will be used without further comment. As a result of this, details of some of the important intermediate stages in the treatment of three and four spin systems can be given without overburdening the chapter with algebraic detail. Again, for completeness, and also as a self consistent check of the expressions that we will derive, the moment expansion is also discussed. The discussion of the results presented in this chapter and a brief review of the literature follows in the next chapter.

4.1 The Two Pulse Sequence and the Moment Expansion

The two pulse sequence can be written generally as

$$P_y(90^\circ) - \tau - P_\phi(\theta).$$

This notation implies that the first pulse is a 90° pulse (applied along the rotating frame y-axis so that it has the same effect as the pulse discussed in Chapter Two), it is followed after an interval τ by a second pulse, with pulse angle θ, applied along an axis at an angle ϕ (in the rotating xy plane) from the first. (If $\phi = 0^\circ$ the second pulse is said to be in phase with first and if $\phi = 90^\circ$ it is said to be 90° out of phase - which is a pulse applied along the x-axis.) The interval between the pulses is assumed to be greater than the spectrometer dead time (for a reason that will become clear shortly).

The signal at time τ after a 90^{o} pulse is given by equation 2.10:

$$\langle I_x(\tau)\rangle = Tr\{e^{-i\mathcal{H}^{OFF}\tau}\, e^{-i\mathcal{H}^{D}\tau}\, I_x\, e^{i\mathcal{H}^{D}\tau}\, e^{i\mathcal{H}^{OFF}\tau}\, I_x\}/Tr\{I_x^2\}.$$

If the assumptions that were made about the first pulse (Section 2.1) apply to the second then it too can be written as a rotation operator, D(R):

$$D(R) = D(-\phi,\ \theta,\ \phi) = e^{i\phi I_z}\, e^{-i\theta I_y}\, e^{-i\phi I_z} \qquad 4.01$$
$$D^{-1}(R) = D(-\phi,\ -\theta,\ \phi)$$

where θ and ϕ are the pulse and phase angles of the second pulse. After the second pulse the system again evolves under the influence of $\mathcal{H}^{D} + \mathcal{H}^{OFF}$ so that at a time t' after the second pulse (the time after the first pulse, assuming that both pulses are δ-pulses is $t = t' + \tau$) the signal is

$$\langle I_x(t)\rangle = Tr\{e^{-i\mathcal{H}^{OFF}t'}\, e^{-i\mathcal{H}^{D}t'}\, D(R)\, e^{-i\mathcal{H}^{OFF}\tau}\, e^{-i\mathcal{H}^{D}\tau}\, I_x\, e^{i\mathcal{H}^{OFF}\tau}\, e^{i\mathcal{H}^{D}\tau}\, D^{-1}(R)\, e^{i\mathcal{H}^{OFF}t'}\, e^{i\mathcal{H}^{D}t'}\, I_x\}/Tr\{I_x^2\}. \qquad 4.02$$

It is again emphasised that this expression can only be written if $[\mathcal{H}^{OFF}, \mathcal{H}^{D}] = 0$. The properties of the trace that were used before (to develop equations 2.12 and 2.13 can be used again to give

$$\langle I_x(t)\rangle = [Tr\{e^{-i\mathcal{H}^{D}t'}\, D(R)\, e^{-i\mathcal{H}^{D}\tau}\, I_x\, e^{i\mathcal{H}^{D}\tau}\, D^{-1}(R)\, e^{i\mathcal{H}^{D}t'}\, I_x\}\cos\Delta\omega\tau\, \cos\Delta\omega t' - Tr\{e^{-i\mathcal{H}^{D}t'}\, D(R)\, e^{-i\mathcal{H}^{D}\tau}\, I_y\, e^{i\mathcal{H}^{D}\tau}\, D^{-1}(R)\, e^{i\mathcal{H}^{D}t'}\, I_y\}\sin\Delta\omega\tau\, \sin\Delta\omega t']/Tr\{I_x^2\}.$$

The second of these traces gives the same result as the first so, using

$$\cos\Delta\omega\tau\, \cos\Delta\omega t' - \sin\Delta\omega\tau\, \sin\Delta\omega t' = \cos\Delta\omega(t' + \tau) = \cos\Delta\omega t$$

it follows that

$$\langle I_x(t)\rangle = \frac{\cos\Delta\omega t}{Tr\{I_x^2\}} Tr\{e^{-i\mathcal{H}^D t'} D(R)\, e^{-i\mathcal{H}^D \tau} I_x e^{i\mathcal{H}^D \tau} D^{-1}(R)\, e^{i\mathcal{H}^D t'} I_x\}. \quad 4.03$$

This expression can be evaluated analytically or it can be expanded as a power series in time, we will discuss the latter first.

The expansion has been carried out by Mansfield(1). Without repeating the working his results are given below. The result of the expansion is specific to the pulse sequence, it is most straightforward for a homonuclear spin system, for a $P_y(90^o)$ - τ - $P_{90o}(90^o)$ pulse sequence

$$\langle I_x(t)\rangle = \cos\Delta\omega t[1 - M_2\frac{(t-2\tau)^2}{2!} + M_4\frac{(t-2\tau)^4}{4!} + \tfrac{1}{4}M_{4\varepsilon}\tau^2(t-\tau)^2 + ...] \quad 4.04$$

$M_{4\varepsilon}$ is an error term, up to the fourth power in time it "is a measure of the irreversibility of the transverse decay" (Mansfield(1)).

The existence of the negative sign in front of the second term in equation 4.04 means that the signal will go through a maximum near $t = 2\tau$ (the extent to which it deviates from $t = 2\tau$ depends on the size of $M_{4\varepsilon}$ and higher order error terms, if these are zero the maximum occurs at $t = 2\tau$). This increase in signal up to a maximum and the subsequent decrease is called a spin echo. The extent to which the signal decay after the echo maximum resembles the FID is governed by the size of the error terms (compare equation 4.04 with 2.35), we will discuss this more fully in the next chapter. (To ensure that the echo falls outside the spectrometer dead time following the second pulse the spacing between the pulses must be longer

than the spectrometer dead time.) For a homonuclear spin system the signal following a $P_y(90^o) - \tau - P_{0o}(90^o)$ pulse sequence is zero for all τ because the second pulse takes all the magnetisation out of the rotating xy plane. The following expressions are for heteronuclear spin systems, the I spin is the resonant species. They are all given to second order in time.

The $P_y(90^o) - \tau - P_{90o}(90^o)$ pulse sequence

$$\langle I_x(t)\rangle \cong \cos\Delta\omega t\left[1 - (M_2^{II} + M_2^{IS})\frac{(t - 2\tau)^2}{2!} - M_2^{IS}(t - \tau)\tau\right] \qquad 4.05$$

This expression contains no contribution from interactions between non-resonant spins, they do, however, come into higher order terms. Equation 4.05 can be rewritten as:

$$\langle I_x(t)\rangle \cong \cos\Delta\omega t\left[1 - M_2^{II}\frac{(t - 2\tau)^2}{2!} - M_2^{IS}(t(t - 2\tau) + 2\tau^2)\right] \qquad 4.06$$

so that when $M_2^{II} >> M_2^{IS}$ the second term dominates and a definite echo, centred at $t = 2\tau$, should result. However, if $M_2^{II} << M_2^{IS}$ any maximum that occurs should not be centred on $t = 2\tau$.

The total second moment can be found from the second derivative of equation 4.05 at $t = 2\tau$:

$$\frac{d^2}{dt^2}\langle I_x(t)\rangle_{t = 2\tau} \alpha -M_2 = M_2^{IS} + M_2^{II}. \qquad 4.07$$

The accuracy with which M_2 can be determined in this way depends on the magnitude of M_2: the most accurate determinations will be possible when M_2 is small, the oscillation rate of the signal is then low (Section 2.3). M_2^{IS} can be found from a plot of echo height (that is signal at $t = 2\tau$) vs τ^2:

$$\langle I_x(t = 2\tau)\rangle \cong \cos\Delta\omega(2\tau)\left[1 - M_2^{IS}(2\tau^2)\right] \qquad 4.08$$

and then, by using equation 2.39, M_2^{II} can be found. The advantage of finding M_2^{II} in this way is that there is no need to decouple the S spins so the experimental conditions are easier to achieve. Both M_2^{IS} and M_2^{II} can be found using other pulse sequences.

The $P_y(90^o) - \tau - P_{0o}(90^o)$ pulse sequence

$$\langle I_x(t)\rangle = -[M_2^{IS}(t - \tau)\tau + \text{higher order terms}] \qquad 4.09$$

Immediately after the second pulse ($t = \tau$) the signal is zero (which in practice occurs within the spectrometer dead time) and for a short time the slope of the signal following the pulse should be M_2^{IS}:

$$\frac{d}{dt}\langle I_x(t)\rangle \alpha -M_2^{IS}\tau .$$

The degree of accuracy with which M_2^{IS} can be measured depends on the length of time for which the expansion holds.

The $P_y(90^o) - \tau - P_{90o}(180^o)$ pulse sequence

This is not discussed by Mansfield but it is by Engelsberg and Norberg(2):

$$\langle I_x(t)\rangle \cong \cos\Delta\omega t[1 - M_2^{IS}\frac{(t - 2\tau)^2}{2!} - M_2^{II}\frac{t^2}{2!}] . \qquad 4.10$$

This time the second term dominates, and an echo should be seen, when $M_2^{II} << M_2^{IS}$. At $t = 2\tau$

$$\langle I_x(t)\rangle \alpha 1 - M_2^{II}\frac{(2\tau)^2}{2!}$$

so a plot of echo height vs τ^2 should yield M_2^{II}.

As was seen in Chapter Two the second order expansion is only valid for short times or when M_2 is small, as the higher order terms become significant the position of the echo maximum

deviates from $t = 2\tau$. It is also apparent that the conditions for a well defined echo to result from 90° and 180° second pulses are mutually opposed. If echoes can be produced experimentally with both these sequences or if the position of the echo maximum is different from $t = 2\tau$, then the validity of the second order expansion should be questioned.

4.2 Calculating the Two Pulse Response for Small Isolated Spin Systems

4.2.1 Two Spin Systems

The calculations for the two spin systems will be discussed at some length, as they were for the FID's, so that the details of the calculation can be given, the three and four spin calculations will then be treated more briefly. Equation 4.03 is the starting point for the calculation, the Hamiltonians and basis states have been worked out already so the only new matrix that is needed is that for the rotation operator

$$D(R) = e^{i\phi I_z}\, e^{-i\theta I_y}\, e^{-i\phi I_z} .$$

For the general states $|m_1^I\ m_2^I \ldots m_p^I, m_1^S\ m_2^S \ldots m_q^S\rangle$ and $|m_1^{I'}\ m_2^{I'} \ldots m_p^{I'}, m_1^{S'}\ m_2^{S'} \ldots m_q^{S'}\rangle$ the matrix element of $e^{-i\theta I_y}$ is of the form

$$\langle m_1^{I'}\ m_2^{I'} \ldots m_p^{I'}, m_1^{S'}\ m_2^{S'} \ldots m_q^{S'} | e^{-i\theta(I_{y,1} + I_{y,2} + \ldots I_{y,p})} | m_1^I\ m_2^I \ldots m_p^I, m_1^S\ m_2^S \ldots m_q^S\rangle$$

$$= d^{(\frac{1}{2})}_{m_1^{I'} m_1^I}(\theta)\ d^{(\frac{1}{2})}_{m_2^{I'} m_2^I}(\theta) \ldots d^{(\frac{1}{2})}_{m_p^{I'} m_p^I}(\theta)\ \delta(m_1^{S'} m_1^S)\ \delta(m_2^{S'} m_2^S) \ldots \delta(m_q^{S'} m_q^S)$$

where the $d^{(\frac{1}{2})}(\theta)$ are defined in Appendix A. The matrix elements for $e^{\pm i\phi I_z}$ are

$$e^{\pm i\phi(m_1^I + m_2^I + \ldots m_p^I)} \prod_{m,m'}^{\text{all spins}} \delta(m' m) .$$

For the IS spin system the full, composite rotation matrix is

$D(R)$	$\|\alpha\alpha\rangle$	$\|\alpha\beta\rangle$	$\|\beta\alpha\rangle$	$\|\beta\beta\rangle$
$\langle\alpha\alpha\|$	$\cos(\theta/2)$	0	$-e^{i\phi}\sin(\theta/2)$	0
$\langle\alpha\beta\|$	0	$\cos(\theta/2)$	0	$-e^{i\phi}\sin(\theta/2)$
$\langle\beta\alpha\|$	$e^{-i\phi}\sin(\theta/2)$	0	$\cos(\theta/2)$	0
$\langle\beta\beta\|$	0	$e^{-i\phi}\sin(\theta/2)$	0	$\cos(\theta/2)$

with the inverse

$D^{-1}(R)$	$\|\alpha\alpha\rangle$	$\|\alpha\beta\rangle$	$\|\beta\alpha\rangle$	$\|\beta\beta\rangle$
$\langle\alpha\alpha\|$	$\cos(\theta/2)$	0	$e^{i\phi}\sin(\theta/2)$	0
$\langle\alpha\beta\|$	0	$\cos(\theta/2)$	0	$e^{i\phi}\sin(\theta/2)$
$\langle\beta\alpha\|$	$-e^{-i\phi}\sin(\theta/2)$	0	$\cos(\theta/2)$	0
$\langle\beta\beta\|$	0	$-e^{-i\phi}\sin(\theta/2)$	0	$\cos(\theta/2)$

The subsequent evaluation of equation 4.03 is straightforward, the result is:

$$\langle I_x(t)\rangle = \cos\Delta\omega t\{\cos^2(\theta/2)\ \cos\tfrac{1}{2}at - \sin^2(\theta/2)\ \cos2\phi\ \cos\tfrac{1}{2}a(t-2\tau)\}. \qquad 4.11$$

For a $P_y(90^o)$ - τ - $P_{90^o}(90^o)$ pulse sequence this becomes:

$$\langle I_x(t,\theta = 90^o,\phi = 90^o)\rangle = \tfrac{1}{2}\cos\Delta\omega t[\cos\tfrac{1}{2}at + \cos\tfrac{1}{2}a(t-2\tau)]. \qquad 4.12$$

Even after the second pulse there is a contribution to the signal from the initial FID (compare equation 4.12 with 2.21). Unless τ is chosen to coincide with a turning point in the FID this contribution will distort the shape of the echo relative to the shape of the FID. The position of the echo maximum also depends on the position of the second pulse. At $t = 2\tau$, which is not necessarily the echo maximum, the signal is

$$\langle I_x(t = 2\tau)\rangle \alpha \tfrac{1}{2}(\cos a\tau + 1) .$$

The signal for the $P_y(90^o) - \tau - P_{0o}(90^o)$ pulse sequence is

$$\langle I_x(t,\theta = 90^o,\phi = 0^o)\rangle = \tfrac{1}{2}\cos\Delta\omega t[\cos\tfrac{1}{2}at - \cos\tfrac{1}{2}a(t - 2\tau)]. \quad 4.13$$

Also

$$\langle I_x(t,\theta = 180^o,\phi = 90^o)\rangle = \cos\Delta\omega t\ \cos\tfrac{1}{2}a(t - 2\tau). \quad 4.14$$

For this last pulse sequence there is an echo maximum at $t = 2\tau$ for all τ, with the height of the maximum independent of τ, that is:

$$\langle I_x(t = 2\tau)\rangle = \cos\Delta\omega t.$$

There are no added complications in calculating the response to the $P_y(90^o) - \tau - P_\phi(\theta)$ pulse sequence for an I_2 spin system. Using the material that we have already derived the rotation matrix is easily found:

D(R)	|1>	|2>	|3>	|4>
<1|	$\cos^2(\theta/2)$	$-\frac{1}{\sqrt{2}}\sin\theta\ e^{i\phi}$	0	$\sin^2(\theta/2)\ e^{2i\phi}$
<2|	$\frac{1}{\sqrt{2}}\sin\theta\ e^{-i\phi}$	$\cos\theta$	0	$-\frac{1}{\sqrt{2}}\sin\theta\ e^{i\phi}$
<3|	0	0	1	0
<4|	$\sin^2(\theta/2)\ e^{-2i\phi}$	$\frac{1}{\sqrt{2}}\sin\theta\ e^{-i\phi}$	0	$\cos^2(\theta/2)$

The resulting signal is

$$\langle I_x(t)\rangle = \tfrac{1}{2}\cos\Delta\omega t\{\cos\tfrac{3}{4}at[\cos\theta(1 + \cos2\phi) + \cos^2\theta(1 - \cos2\phi)] + \cos\tfrac{3}{4}a(t - 2\tau)[\sin^2\theta(1 - \cos2\phi)]\}. \quad 4.15$$

The first point to note about this expression is that no echo can be formed if the pulses are in phase, under these conditions

$$\langle I_x(t,\phi = 0^o)\rangle = \cos\Delta\omega t[\cos\theta \cos\tfrac{3}{4}at] . \qquad 4.16$$

For a 90^o second pulse the signal is zero from the pulse onwards and for a 180^o pulse the signal is inverted. For an out of phase pulse sequence

$$\langle I_x(t,\phi = 90^o)\rangle = \cos\Delta\omega t[\cos^2\theta \cos\tfrac{3}{4}at + \sin^2\theta \cos\tfrac{3}{4}a(t - 2\tau)] . \qquad 4.17$$

The FID contribution to the signal (the first term in this equation) is lost for a 90^o second pulse, an echo is formed with maximum amplitude at $t = 2\tau$. The echo height is independent of τ. If the second pulse is a 180^o pulse then it has no effect on the signal (assuming that the pulse affects only the local dipolar interaction), no echo is formed. These points are consistent with observations made by Powles and Mansfield(3).

Equations 4.11 and 4.15, those that follow from them, and those that will be reported shortly are for normalised signals, that is at time zero they all reduce to $\langle I_x(t = 0)\rangle = 1$. This is one way of checking the accuracy of the equations, a second method relies on the moment expansion. We have already recorded the expansion to the second power in time of equation 4.03 for three specific pulse sequences - equations 4.04, 4.05, 4.09 and 4.10. Each of the corresponding equations 4.12, 4.13, 4.14, 4.16 and 4.17 can also be expanded as a power series in time ($\cos(xt) = 1 - x\frac{2t^2}{2!} + x\frac{4t^2}{4!} - x\frac{6t^6}{6!} + \ldots.$), for example, the expansion to the second power in time of equation 4.12 is

$$\langle I_x(t,\theta = 90^o,\phi = 90^o)\rangle \cong \cos\Delta\omega t[1 - \tfrac{1}{4}a^2\frac{(t - 2\tau)^2}{2!} - \tfrac{1}{4}a^2(t - \tau)\tau]$$

where we have used the relationship

$$t^2 + (t - 2\tau)^2 = 2(t - 2\tau)^2 + 4(t - \tau)\tau$$

But, according to equation 2.41, $M_2^{IS} = \frac{1}{4}a^2$ therefore

$$\langle I_x(t,\theta = 90^o,\phi = 90^o)\rangle \cong \cos\Delta\omega t[1 - M_2^{IS}\frac{(t - 2\tau)^2}{2!} - M_2^{IS}(t - \tau)\tau]$$

which is just equation 4.05 (with $M_2^{II} = 0$ which it must be for the isolated IS spin system). We can, then, check our analytic expressions against well established moment expansions, this will prove to be of particular value when the analytic expressions become more complex.

4.2.2 Three Spin Systems

There are no new problems associated with the calculations for the three spin systems. The evaluation of equation 4.03 for three unlike spins is straightforward, the result is

$$\begin{aligned}\langle I_x(t)\rangle = \tfrac{1}{2}\cos\Delta\omega t\{&\cos^2(\theta/2)[\cos\tfrac{1}{2}(a + c)t + \cos\tfrac{1}{2}(a - c)t] \\ &- \sin^2(\theta/2)\cos 2\phi[\cos\tfrac{1}{2}(a + c)(t - 2\tau) \\ &+ \cos\tfrac{1}{2}(a - c)(t - 2\tau)]\}. \qquad 4.18\end{aligned}$$

For the IS_2 spin system there are two results, one for the I spin and one for the S spins. As we did not include the $\mathcal{R}^D$, I_x and S_x matrices for this system in Chapter Two we have included them, together with the rotation matrices, in this chapter. The symbols used are defined in Chapter Two, Table 2.1.

$\mathcal{H}^D$	|1>	|2>	|3>	|4>	|5>	|6>	|7>	|8>
<1|	$\frac{1}{4}(a+b+c)$							
<2|		$\frac{1}{4}(-b+T)$						
<3|			$\frac{1}{4}(-b-T)$					
<4|				$\frac{1}{4}(-a+b-c)$				
<5|					$\frac{1}{4}(-a+b-c)$			
<6|						$\frac{1}{4}(-b+T)$		
<7|							$\frac{1}{4}(-b-T)$	
<8|								$\frac{1}{4}(a+b+c)$

D(R)	|1>	|2>	|3>	|4>	|5>	|6>	|7>	|8>
<1|	$\cos(\theta/2)$			$-e^{i\phi}\sin(\theta/2)$				
<2|		$\cos(\theta/2)$				$2RN^2e^{i\phi}\sin(\theta/2)$	$-N^2(1-R^2)e^{i\phi}\sin(\theta/2)$	
<3|			$\cos(\theta/2)$			$-N^2(1-R^2)e^{i\phi}\sin(\theta/2)$	$-2RN^2e^{i\phi}\sin(\theta/2)$	
<4|	$e^{-i\phi}\sin(\theta/2)$			$\cos(\theta/2)$				
<5|					$\cos(\theta/2)$			$-e^{i\phi}\sin(\theta/2)$
<6|		$-2RN^2e^{-i\phi}\sin(\theta/2)$	$N^2(1-R^2)e^{-i\phi}\sin(\theta/2)$			$\cos(\theta/2)$		
<7|		$N^2(1-R^2)e^{-i\phi}\sin(\theta/2)$	$2RN^2e^{-i\phi}\sin(\theta/2)$				$\cos(\theta/2)$	
<8|					$e^{-i\phi}\sin(\theta/2)$			$\cos(\theta/2)$

I_x	$\|1\rangle$	$\|2\rangle$	$\|3\rangle$	$\|4\rangle$	$\|5\rangle$	$\|6\rangle$	$\|7\rangle$	$\|8\rangle$
$\langle 1\|$				$\frac{1}{2}$				
$\langle 2\|$						$-RN^2$	$\frac{1}{2}N^2(1-R^2)$	
$\langle 3\|$						$\frac{1}{2}N^2(1-R^2)$	RN^2	
$\langle 4\|$	$\frac{1}{2}$							
$\langle 5\|$								$\frac{1}{2}$
$\langle 6\|$		$-RN^2$	$\frac{1}{2}N^2(1-R^2)$					
$\langle 7\|$		$\frac{1}{2}N^2(1-R^2)$	RN^2					
$\langle 8\|$					$\frac{1}{2}$			

Evaluating equation 4.03 for the I spin resonance we arrive at

$$\begin{aligned}\langle I_x(t)\rangle = \tfrac{1}{2}\cos\Delta\omega t\{&\cos^2(\theta/2)\left[\cos\tfrac{1}{2}(a+c)t + \left(\frac{a-c}{T}\right)^2\cos\tfrac{1}{2}Tt + \frac{b^2}{T^2}\right]\\ &- \sin^2(\theta/2)\cos 2\phi\left[\cos\tfrac{1}{2}(a+c)(t-2\tau)\right.\\ &+ \left(\frac{a-c}{T}\right)^4\cos\tfrac{1}{2}T(t-2\tau) + \frac{b^4}{T^4}\\ &\left.- \left(\frac{b(a-c)}{T^2}\right)^2(1 - 2\cos\tfrac{1}{2}T(t-\tau) - 2\cos\tfrac{1}{2}T\tau + \cos\tfrac{1}{2}Tt)\right]\}. \quad 4.19\end{aligned}$$

We can expand this equation, for a $P_y(90^o) - \tau - P_{90^o}(90^o)$ pulse sequence, to the second power in time, the result is

$$\langle I_x(t)\rangle \cong \cos\Delta\omega t\left[1 - \tfrac{1}{4}(a^2+c^2)\frac{(t-2\tau)^2}{2!} + \tfrac{1}{4}(a^2+c^2)(t-\tau)\tau\right]$$

which is what we would expect from equation 4.05 ($M_2^{II} = 0$ and $M_2^{IS} = \frac{1}{4}(a^2+c^2)$).

The matrices for the S spin resonance are more complicated:

D(R)	|1>	|2>	|3>	|4>	|5>	|6>	|7>	|8>
<1 |	$\cos^2(\theta/2)$	$-\frac{1}{2}N(1-R)e^{-i\phi}\sin\theta$	$-\frac{1}{2}N(1+R)e^{-i\phi}\sin\theta$		$e^{-2i\phi}\sin^2(\theta/2)$			
<2 |	$\frac{1}{2}N(1-R)e^{i\phi}\sin\theta$	$N^2(\cos^2(\theta/2)+R^2\cos^2(\theta/2)+2R\sin^2(\theta/2))$	$-N^2(1-R^2)\sin^2(\theta/2)$		$-\frac{1}{2}N(1-R)e^{-i\phi}\sin\theta$			
<3 |	$\frac{1}{2}N(1+R)e^{i\phi}\sin\theta$	$-N^2(1-R^2)\sin^2(\theta/2)$	$N^2(\cos^2(\theta/2)+R^2\cos^2(\theta/2)-2R\sin^2(\theta/2))$		$-\frac{1}{2}N(1+R)e^{-i\phi}\sin\theta$			
<4 |				$\cos^2(\theta/2)$		$-\frac{1}{2}N(1-R)e^{-i\phi}\sin\theta$	$-\frac{1}{2}N(1+R)e^{-i\phi}\sin\theta$	$e^{-2i\phi}\sin^2(\theta/2)$
<5 |	$e^{2i\phi}\sin^2(\theta/2)$	$\frac{1}{2}N(1-R)e^{i\phi}\sin\theta$	$\frac{1}{2}N(1+R)e^{i\phi}\sin\theta$		$\cos^2(\theta/2)$			
<6 |				$\frac{1}{2}N(1-R)e^{i\phi}\sin\theta$		$N^2(\cos^2(\theta/2)+R^2\cos^2(\theta/2)+2R\sin^2(\theta/2))$	$-N^2(1-R^2)\sin^2(\theta/2)$	$\frac{1}{2}N(1-R)e^{-i\phi}\sin\theta$
<7 |				$\frac{1}{2}N(1+R)e^{i\phi}\sin\theta$		$-N^2(1-R^2)\sin^2(\theta/2)$	$N^2(\cos^2(\theta/2)+R^2\cos^2(\theta/2)-2R\sin^2(\theta/2))$	$-\frac{1}{2}N(1+R)e^{-i\phi}\sin\theta$
<8 |				$e^{2i\phi}\sin^2(\theta/2)$		$\frac{1}{2}N(1-R)e^{i\phi}\sin\theta$	$\frac{1}{2}N(1+R)e^{i\phi}\sin\theta$	$\cos^2(\theta/2)$

	S_x	$\|1\rangle$	$\|2\rangle$	$\|3\rangle$	$\|4\rangle$	$\|5\rangle$	$\|6\rangle$	$\|7\rangle$	$\|8\rangle$
$\frac{1}{2}x$	$\langle 1\|$		N(1-R)	N(1+R)					
	$\langle 2\|$	N(1-R)				N(1-R)			
	$\langle 3\|$	N(1+R)				N(1+R)			
	$\langle 4\|$						N(1-R)	N(1+R)	
	$\langle 5\|$		N(1-R)	N(1+R)					
	$\langle 6\|$				N(1-R)				N(1-R)
	$\langle 7\|$				N(1+R)				N(1+R)
	$\langle 8\|$						N(1-R)	N(1+R)	

The evaluation of equation 4.03 and subsequent simplification eventually yields:

$$\begin{aligned}\langle S_x(t)\rangle = \tfrac{1}{8}\cos\Delta\omega t\{&[4(1-Y)\cos^4(\theta/2) + Y(1-Y)\sin^2\theta]\cos\tfrac{1}{4}(a+c)t\ \cos\tfrac{1}{4}(2b-t)t\\
&+ [4(1+Y)\cos^4(\theta/2) - Y(1+Y)\sin^2\theta]\cos\tfrac{1}{4}(a+c)t\ \cos\tfrac{1}{4}(2b+T)t\\
&+ [(1+Y)\sin^2\theta - 4Y(1+Y)\sin^4(\theta/2)]\cos2\phi\ \cos\tfrac{1}{4}(a+c)(t-2\tau)\ \cos\tfrac{1}{4}(2b+T)t\\
&+ [(1-Y)\sin^2\theta + 4Y(1-Y)\sin^4(\theta/2)]\cos2\phi\ \cos\tfrac{1}{4}(a+c)(t-2\tau)\ \cos\tfrac{1}{4}(2b-T)t\\
&- [(1-Y)^2\sin^2\theta]\cos2\phi\ \cos\tfrac{1}{4}(a+c)(t-2\tau)\ \cos\tfrac{1}{4}(2b-T)(t-2\tau)\\
&+ [(1-Y)^2\sin^2\theta]\cos\tfrac{1}{4}(a+c)t\ \cos\tfrac{1}{4}(2b-T)(t-2\tau)\\
&- [(1+Y)^2\sin^2\theta]\cos2\phi\ \cos\tfrac{1}{4}(a+c)(t-2\tau)\ \cos\tfrac{1}{4}(2b+T)(t-2\tau)\\
&+ [(1+Y)^2\sin^2\theta]\cos\tfrac{1}{4}(a+c)t\ \cos\tfrac{1}{4}(2b+T)(t-2\tau)\\
&- [2(1-Y^2)\sin^2\theta]\cos2\phi\ \cos\tfrac{1}{4}(a+c)(t-2\tau)\ \cos\tfrac{1}{2}b(t-2\tau)\ \cos\tfrac{1}{4}Tt\\
&- [2(1-Y^2)\sin^2\theta]\cos\tfrac{1}{4}(a+c)t(\cos\tfrac{1}{2}bt\ \cos\tfrac{1}{4}T(t-2\tau) - \cos\tfrac{1}{2}b(t-2\tau)\ \cos\tfrac{1}{4}Tt)\\
&- [8(1-Y^2)\sin^4(\theta/2)]\cos2\phi\ \cos\tfrac{1}{4}(a+c)(t-2\tau)\ \cos\tfrac{1}{2}bt\ \cos\tfrac{1}{4}T(t-2\tau)\}\end{aligned} \qquad 4.20$$

where $Y = \frac{b}{T}$.

Again, we can expand this equation to the second power in time, for the $P_y(90^o) - \tau - P_{90^o}(90^o)$ pulse sequence, we arrive at

$$\langle S_x(t)\rangle = \cos\Delta\omega t[1 - (\tfrac{1}{8}(a^2+c^2) + \tfrac{9}{16}b^2)\frac{(t-2\tau)^2}{2!} + \tfrac{1}{8}(a^2+c^2)(t-\tau)\tau]$$

which is consistent with equation 4.05 ($M_2^{II} = \frac{9}{16}b^2$, $M_2^{IS} = \frac{1}{8}(a^2+c^2)$). The response, to the general pulse sequence, of three like spins has been calculated by Moskvich, Sergeev and Dotsenko(4).

4.2.3 Four Spin Systems

We have calculated the response of the I_2S_2 spin system to the general pulse sequence $P_y(90^o) - \tau - P_\phi(\theta)$. Again we have included the matrices that were used in the calculation. The symbols are as defined in Chapter Two, Table 2.2, with, additionally, in the D(R) matrix, $c = \cos^2(\theta/2)$, $s = \sin^2(\theta/2)$.

$\frac{1}{4} \times$

$\mathcal{H}^D$	|1>	|2>	|3>	|4>	|5>	|6>	|7>	|8>	|9>	|10>	|11>	|12>	|13>	|14>	|15>	|16>
<1|	2a+2c+ b+d															
<2|		b-2d														
<3|			b													
<4|				-2b+d												
<5|					d											
<6|						-2a-2c +b+d										
<7|							-b-d+U									
<8|								-b-d+V								
<9|									-b-d-U							
<10|										-b-d-V						
<11|											-2a-2c +b+d					
<12|												-2b+d				
<13|													d			
<14|														b-2d		
<15|															b	
<16|																2a+2c +b+d

D(R)	|1>	|2>	|3>	|4>	|5>	|6>	|7>	|8>	|9>	|10>	|11>	|12>	|13>	|14>	|15>	|16>
<1|	C	$-\frac{1}{\sqrt{2}}e^{i\phi}\sin\theta$									$e^{2i\phi}s$					
<2|	$\frac{1}{\sqrt{2}}e^{-i\phi}\sin\theta$	$\cos\theta$									$-\frac{1}{\sqrt{2}}e^{i\phi}\sin\theta$					
<3|			1													
<4|				C			$-\frac{1}{\sqrt{2}}e^{i\phi}\sin\theta$ $(A+P)$		$-\frac{1}{\sqrt{2}}e^{i\phi}\sin\theta$ $(A-P)$			$e^{2i\phi}s$				
<5|					C			$-\frac{1}{\sqrt{2}}e^{-i\phi}\sin\theta$ $(B-Q)$					$-e^{-2i\phi}s$			
<6|						C								$-\frac{1}{\sqrt{2}}e^{i\phi}\sin\theta$		$e^{2i\phi}s$
<7|				$\frac{1}{\sqrt{2}}e^{-i\phi}\sin\theta$ $(A+P)$			$C-4APs$		$\frac{-2s}{(A^2-P^2)}$			$-\frac{1}{\sqrt{2}}e^{i\phi}\sin\theta$ $(A+P)$				
<8|					$\frac{1}{\sqrt{2}}e^{i\phi}\sin\theta$ $(B+Q)$			$C-4BQs$		$\frac{2s}{(B^2-Q^2)}$			$\frac{1}{\sqrt{2}}e^{-i\phi}\sin\theta$ $(B+Q)$			
<9|				$\frac{1}{\sqrt{2}}e^{-i\phi}\sin\theta$ $(A-P)$			$\frac{-2s}{(A^2-P^2)}$		$C+4APs$			$-\frac{1}{\sqrt{2}}e^{i\phi}\sin\theta$ $(A-P)$				
<10|					$\frac{1}{\sqrt{2}}e^{i\phi}\sin\theta$ $(B-Q)$			$\frac{2s}{(B^2-Q^2)}$		$C+4BQs$			$-\frac{1}{\sqrt{2}}e^{-i\phi}\sin\theta$ $(B-Q)$			
<11|	$e^{-2i\phi}s$	$\frac{1}{\sqrt{2}}e^{-i\phi}\sin\theta$									C					
<12|				$e^{-2i\phi}s$			$\frac{1}{\sqrt{2}}e^{-i\phi}\sin\theta$ $(A+P)$		$\frac{1}{\sqrt{2}}e^{-i\phi}\sin\theta$ $(A-P)$			C				
<13|					$-e^{2i\phi}s$			$-\frac{1}{\sqrt{2}}e^{i\phi}\sin\theta$ $(B+Q)$		$\frac{1}{\sqrt{2}}e^{i\phi}\sin\theta$ $(B-Q)$			C			
<14|						$\frac{1}{\sqrt{2}}e^{-i\phi}\sin\theta$							-	$\cos\theta$		$-\frac{1}{\sqrt{2}}e^{i\phi}\sin\theta$
<15|															1	
<16|						$e^{-2i\phi}s$								$\frac{1}{\sqrt{2}}e^{-i\phi}\sin\theta$		C

$\frac{1}{\sqrt{2}} \times$

I_x	|1>	|2>	|3>	|4>	|5>	|6>	|7>	|8>	|9>	|10>	|11>	|12>	|13>	|14>	|15>	|16>
<1|		1														
<2|	1										1					
<3|																
<4|							A+P		A-P							
<5|								B+Q		-B+Q						
<6|														1		
<7|				A+P								A+P				
<8|					B+Q								-B-Q			
<9|				A-P								A-P				
<10|					-B+Q								B-Q			
<11|		1														
<12|							A+P		A-P							
<13|								-B-Q		B-Q						
<14|						1										1
<15|																
<16|														1		

4 North End,
Brandon,
Durham.
DH7 8UN

15th February 1987

Ms A Redgewell,
Higher Degrees Office,
The Open University,
PO Box 49,
Milton Keynes.
MK7 6AD

Dear Ms Redgewell,

In reply to your letter (ref. HDL 5474) concerning the missing page 111 from my thesis, the omission is a pagination error.

Yours sincerely

D C Apperley

The resulting expression for the signal is:

$$\begin{aligned}
\langle I_x(t)\rangle = \cos\Delta\omega t\{ & [\tfrac{1}{2}\cos^4(\theta/2) - \tfrac{1}{8}\sin^2\theta]\cos\tfrac{1}{2}(a+c)t\ \cos\tfrac{3}{4}dt \\
& + (A+P)^2[\tfrac{1}{4}\cos^4(\theta/2) + \tfrac{1}{16}\sin^2\theta\cos2\phi - AP(\tfrac{1}{4}\sin^2\theta + \sin^4(\theta/2)\cos2\phi)] \\
& \qquad \cos\tfrac{1}{4}(b-2d+U)t \\
& + (A-P)^2[\tfrac{1}{4}\cos^4(\theta/2) + \tfrac{1}{16}\sin^2\theta\cos2\phi + AP(\tfrac{1}{4}\sin^2\theta + \sin^4(\theta/2)\cos2\phi)] \\
& \qquad \cos\tfrac{1}{4}(b-2d-U)t \\
& + (B+Q)^2[\tfrac{1}{4}\cos^4(\theta/2) + \tfrac{1}{16}\sin^2\theta\cos2\phi - BQ(\tfrac{1}{4}\sin^2\theta + \sin^4(\theta/2)\cos2\phi)] \\
& \qquad \cos\tfrac{1}{4}(b+2d-V)t \\
& + (B-Q)^2[\tfrac{1}{4}\cos^4(\theta/2) + \tfrac{1}{16}\sin^2\theta\cos2\phi + BQ(\tfrac{1}{4}\sin^2\theta + \sin^4(\theta/2)\cos2\phi)] \\
& \qquad \cos\tfrac{1}{4}(b+2d+V)t \\
& + [\tfrac{1}{8}\sin^2\theta(1-\cos2\phi)]((A+P)^4\cos\tfrac{1}{4}(b-2d+U)(t-2\tau) + (A-P)^4\cos\tfrac{1}{4}(b-2d-U)(t-2\tau) \\
& \qquad + (B+Q)^4\cos\tfrac{1}{4}(b+2d-V)(t-2\tau) + (B-Q)^4\cos\tfrac{1}{4}(b+2d+V)(t-2\tau)) \\
& + [\tfrac{1}{4}\sin^2\theta(1-\cos2\phi)]((A^2-P^2)^2\cos\tfrac{1}{4}(b-2d)(t-2\tau)\cos\tfrac{1}{4}Ut + (B^2-Q^2)^2\cos\tfrac{1}{4}Vt \\
& \qquad \cos\tfrac{1}{4}(b+2d)(t-2\tau)) \\
& - [\tfrac{1}{4}\sin^2\theta + \sin^4(\theta/2)\cos2\phi]((A^2-P^2)^2\cos\tfrac{1}{4}(b-2d)t\cos\tfrac{1}{4}U(t-2\tau) \\
& \qquad + (B^2-Q^2)^2\cos\tfrac{1}{4}(b+2d)t\cos\tfrac{1}{4}V(t-2\tau)) \\
& + [\tfrac{1}{8}\sin^2\theta\cos2\phi - \tfrac{1}{2}\sin^4(\theta/2)\cos2\phi]\cos\tfrac{1}{2}(a+c)(t-2\tau)\cos\tfrac{3}{4}dt \\
& + [\tfrac{1}{4}\sin^2\theta]\cos\tfrac{1}{2}(a+c)t\cos\tfrac{3}{4}d(t-2\tau) \\
& - [\tfrac{1}{4}\sin^2\theta\cos2\phi]\cos\tfrac{1}{2}(a+c)(t-2\tau)\cos\tfrac{3}{4}d(t-2\tau)\}\,. \qquad 4.21
\end{aligned}$$

The S spin response can be found simply by relabelling the spin system (so that the S spins become I spins and the I become S). The expansion of the FID (which comes from the first six cosine terms), after considerable algebra, is

$$\langle I_x(t)\rangle \cong \cos\Delta\omega t[1 - (\tfrac{9}{16}d^2 + \tfrac{1}{4}(a^2+c^2))\frac{t^2}{2!}].$$

This is consistent with equation 2.35 ($M_2 = M_2^{II} + M_2^{IS}$ with $M_2^{II} = \frac{9}{16}d^2$ and $M_2^{IS} = \frac{1}{4}(a^2+c^2)$). Similar expansions for specific pulse sequences are also consistent with the moment expansion.

4.3 The Three Pulse Sequence

The signals that we have calculated so far arise because we have induced transitions between states with different energies, more specifically between states that have $M(= m_1 + m_2 + ...)$ values different by unity - single quantum transitions (the m_n are the quantum numbers, $m_n = I_{z,n}$). For a general I_aS_b system of spin-$\frac{1}{2}$ nuclei there are $4(a+b)$ of these transitions, the total signal, for each resonance, has $4a$ or $4b$ transitions contributing to it. It is also possible to induce zero and multiple quantum transitions, that is transitions with $\Delta M = 0,2,3.....$, indeed by applying a two pulse sequence to our spin systems we have already caused zero and double quantum transitions, although they have no effect on the signal after the second pulse and can only be observed with a three (or more) pulse sequence. (The principles and techniques of multiple quantum NMR are reviewed by Bodenhausen(5).) Fewer of the energy levels can be linked by multiple quantum transitions so there are fewer contributions to the signal. If the individual zero or multiple quantum signals can be observed they are often much simpler than the single quantum signal (Warren and Pines(6)), this simplification is specially useful in large spin systems. In this short section we will investigate the zero and double quantum signals in the IS_2 spin system and see if any simplification is forthcoming.

The density matrix for the S spins in the IS_2 spin system after two pulses is shown in Table 4.1. Only those elements superscripted (1) contribute to the S spin signal after the two pulse sequence but there are other elements, those with (0) and (2) superscripts, present corresponding to zero and double quantum transitions. If a third, non-selective, pulse is

applied to the system it has the effect of mixing all these elements so that the final signal contains not only contributions from single but also from zero and double quantum transitions.

Table 4.1 The IS_2, S spin density matrix after two pulses

$\sigma_{11}^{(0)}$	$\sigma_{12}^{(1)}$	$\sigma_{13}^{(1)}$		$\sigma_{15}^{(2)}$			
$\sigma_{21}^{(1)}$	$\sigma_{22}^{(0)}$	$\sigma_{23}^{(0)}$		$\sigma_{25}^{(1)}$			
$\sigma_{31}^{(1)}$	$\sigma_{32}^{(0)}$	$\sigma_{33}^{(0)}$		$\sigma_{35}^{(1)}$			
			$\sigma_{44}^{(0)}$		$\sigma_{46}^{(1)}$	$\sigma_{47}^{(1)}$	$\sigma_{48}^{(2)}$
$\sigma_{51}^{(2)}$	$\sigma_{52}^{(1)}$	$\sigma_{53}^{(1)}$		$\sigma_{55}^{(0)}$			
			$\sigma_{64}^{(1)}$		$\sigma_{66}^{(0)}$	$\sigma_{67}^{(0)}$	$\sigma_{68}^{(1)}$
			$\sigma_{74}^{(1)}$		$\sigma_{76}^{(0)}$	$\sigma_{77}^{(0)}$	$\sigma_{78}^{(1)}$
			$\sigma_{84}^{(2)}$		$\sigma_{86}^{(1)}$	$\sigma_{87}^{(1)}$	$\sigma_{88}^{(0)}$

The signal after three pulses can be found by extending the two pulse calculation in the same way that the signal after two pulses was found by extending the single pulse calculation:

$$\langle I_x(t)\rangle = \frac{\cos\Delta\omega t}{\mathrm{Tr}\{I_x^2\}} \mathrm{Tr}\{e^{-i\mathcal{H}^D t'} D(R_3)\, e^{-i\mathcal{H}^D \tau_2} D(R_2)\, e^{-i\mathcal{H}^D \tau_1} I_x \; e^{i\mathcal{H}^D \tau_1} D^{-1}(R_2)\, e^{i\mathcal{H}^D \tau_2} D^{-1}(R_3)\, e^{i\mathcal{H}^D t'} I_x\} \quad 4.22$$

$D(R_2)$ is the rotation matrix for the second pulse and $D(R_3)$ that for the third.

We have evaluated expression 4.22 for the S spin resonance for an IS_2 spin system with $D_{\infty h}$ symmetry and for the specific pulse sequence

$$P_y(90^o) - \tau_1 - P_y(90^o) - \tau_2 - P_y(90^o)$$

(we have imposed these restrictions to keep the algebra within reasonable limits), the full result, for an on resonance ($\Delta\omega = 0$) system, is

$$\langle S_x(t) \rangle = A + B + C \qquad 4.23$$

where

$$A = -\cos\tfrac{3}{4}b\tau_1 \cos\tfrac{3}{4}bt' \cos\tfrac{1}{2}at' \cos\tfrac{1}{2}a\tau_1$$
$$B = \sin\tfrac{3}{4}b\tau_1 \sin\tfrac{3}{4}bt' \cos\tfrac{1}{2}a\tau_1 \cos\tfrac{1}{2}at' \cos a\tau_2$$
$$C = -\sin\tfrac{1}{2}at' \sin\tfrac{1}{2}a\tau_1 \cos\tfrac{1}{2}a\tau_2 \cos\tfrac{3}{4}b(t' + \tau_1 - \tau_2),$$

a, b and c are the dipolar coupling constants previously used for this spin system. The A term in this expression is the zero quantum contribution to the signal, B is the double quantum contribution and C the single quantum contribution. If τ_1 and τ_2 are chosen carefully it is possible to eliminate any two of the terms in expression 4.23 and so each separate contribution to the signal can be observed. For example if

$$\tau_1 = 2n\pi/a \qquad (n = 0,1,2....)$$

then the single quantum contribution (C) is lost and if

$$\tau_2 = n'\pi/2a \qquad (n' = 1,3,5....)$$

the double quantum contribution (B) is also lost, only the zero quantum term (A) is left; for n = 1

$$A = \cos\frac{3\pi}{2}\frac{b}{a} \cos\frac{3\pi}{2}\frac{b}{a}t' \cos\tfrac{1}{2}at$$

This expression is no simpler than those obtained after a one or two pulse sequence.

The corresponding calculation for the I spin resonance in the IS_2 spin system has also been carried out, here only zero and single quantum transitions are allowed (there are insufficient energy levels to allow double and higher quantum transitions). The result, for an on resonance system with an in phase second pulse with arbitrary pulse angle (θ), is

$$\langle I_x(t) \rangle = -\tfrac{1}{2}\sin\theta(1 + \cos at' \cos a\tau_1)$$

Interestingly, if the second pulse is a 180° pulse there should be no observable signal after the third pulse. Once again, though, there is no obvious simplification over the one and two pulse signals.

There appears to be little advantage in deriving these closed expressions for the multiple quantum signal for such a simple spin system. This is not to say that multiple quantum techniques are of no use in studying small spin systems. For example, Wang, Slichter and Sinfelt (7) have used multiple quantum techniques, purely as an analytical tool, to determine the relative concentrations of fragments of C_2H_2 adsorbed on a platinum surface. The real power of multiple quantum NMR, however, does seem to lie in dealing with systems of very many spins, where a closed calculation is impossible (because of a lack of detailed knowledge of the spin system and also because of a lack of computing power), as, for example, recently demonstrated by Pines(8).

4.4 References

(1) P. Mansfield, Phys. Rev., 137(3A), A961-A974 (1965).

(2) M. Engelsberg and R.E. Norberg, Phys. Rev. B, 5(9), 3395-3406 (1972).

(3) J.G. Powles and P. Mansfield, Phys. Lett., 2(2), 58-59 (1962).

(4) Yu. N. Moskvich, N.A. Sergeev and G.I. Dotsenko, Phys. Stat. Sol.(a), 30, 409-418 (1975).

(5) G. Bodenhausen, Progress in NMR Spectroscopy, 14, 137-173 (1981).

(6) W.S. Warren and A. Pines, J. Chem. Phys., 74(5), 2808-2818 (1981).

(7) P.K. Wang, C.P. Slichter and J.H. Sinfelt, Phys. Rev. Lett., 53(1), 82-85 (1984).

(8) J. Baum, M. Munowitz, A.N. Garroway and A. Pines, J. Chem. Phys., 83(5), 2015-2025 (1985).

CHAPTER FIVE

The NMR Response to Two Pulses: Discussion and Experiment

Analytic expressions for the NMR response of two, three and four spin heteronuclear, dipolar coupled systems to a two pulse sequence were developed in the last chapter. In this chapter the forms of these expressions, in relation to spin echo studies, are discussed. Background information on spin echo studies in heteronuclear spin systems is included in the form of a brief review of the literature. A preliminary experimental study of a model system (potassium hydrogen difluoride) is also included at the end of the chapter.

In reviewing the literature two features became apparent. Firstly, the number of spin echo studies in heteronuclear systems is relatively small and, secondly, very few of the studies involved purely spin-$\frac{1}{2}$ nuclei. Most of the studies that have been carried out have involved simple inorganic compounds although 1,3,5-trifluorobenzene (Boden and Gibb(1) and (2)) and potassium 4,4-difluoromyristate in lyotropic liquid crystalline phases (Post(3)) have also been studied.

In general the formation and properties of heteronuclear spin echoes depend on both I,I and I,S interactions. These interactions can, depending on the pulse sequence, to some extent be separated. Studies of echo phenomena in heteronuclear systems should then, in principle, provide information about the relative spatial arrangement and motional properties of specific groups of nuclei. There are a number of potential applications for such studies, for example, polymeric materials, liquid crystalline samples and glassy solutions of aqueous electrolytes, particularly those containing fluorine nuclei (Charlson(4)), could all be studied. The present work is not intended to become involved in detailed applications but is,

instead, intended to investigate, in a more general manner, the theoretical echo responses.

It is important to emphasise the relationship between the present work and other studies of echo phenomena in solids. During the last decade there have been a number of studies of the properties of proton 'solid' echo responses in homonuclear systems (these are reviewed by Boden and Kahol(5)) and applications have included, for example, thermotropic liquid crystals (Boden(6)). Dipolar coupled spin-1 systems have also been the subject of extensive calculations (Boden and Kahol(7), Moore and Mortimer(8)), the main aim here being the study of molecular crystals (Boden(9)). A key element in the discussion of the analytic responses for such systems has been their separation into an 'echo' component (those parts that are in phase at or around $t = 2\tau$) and a 'transient' component (those remaining terms which originate at $t = 0$). This separation is important experimentally because, for polycrystalline samples (including unaligned liquid crystalline phases), it is the echo component that dominates the experimental behaviour. In the present work the heteronuclear spin system responses are separated into three, rather than two, components. These are, a pure FID component, an echo component and what will be called a 'cross-term'. It is suggested that this approach may well be quite general for an I_nS_m spin system.

5.1 Spin Echo Studies in Heteronuclear Spin Systems: a Review of the Literature

Before starting the review a more compact way of writing the various pulse sequences will be established. The notation is as follows:

$P_x(90^o)$ represents $P_y(90^o)-\tau-P_{90^o}(90^o)$,

$P_y(90^o)$ represents $P_y(90^o)-\tau-P_{0^o}(90^o)$,

$P_x(180^o)$ represents $P_y(90^o)-\tau-P_{90^o}(180^o)$,

$P_y(180^o)$ represents $P_y(90^o)-\tau-P_{0^o}(180^o)$.

The response to a $P_x(180^o)$ sequence is the same as that for a $P_y(180^o)$ sequence except for a change of sign - the $P_y(180^o)$ gives a negative signal.

The first detailed theoretical treatment of spin echo phenomena in heteronuclear spin systems was given by Mansfield(10). The main results of his treatment have already been discussed in Chapter Four. Equations 4.05, 4.06 and 4.09 representing his expansions are valid to second order in time. Most of the subsequent experimental work is based on these equations. The $P_x(180^o)$ (or $P_y(180^o)$) pulse sequence was not explicitly considered by Mansfield, the expansion was reported at a later date by Engelsberg and Norberg(11), their result, discussed in Chapter Four, is given by equation 4.10.

The results of Mansfield's operator formulism were first used experimentally by Warren and Norberg(12) in a study of solid xenon at 4.2 K (^{129}Xe has spin I = $\frac{1}{2}$ and a relative abundance of 26.44%, ^{131}Xe has spin S = $\frac{3}{2}$ and a relative abundance of 21.18%). The internuclear distances are relatively large and calculations show that $M_2^{II}/M_2^{IS} = 6.54$ and $M_2^{II}/M_2^{SS} = 40.5$. The results for the ^{129}Xe resonance are most relevant to this review. The FID was found to be "very nearly" Gaussian with a second moment, M_2, in close agreement with theory. A solid echo was observed at $t = 2\tau$ for a $P_x(90^o)$ sequence, the half-echo shape closely resembled that for the FID for small pulse spacings. The response to a $P_y(90^o)$ sequence was in

qualitative agreement with theory but a quantitative analysis was not possible because the signal was found to be extremely sensitive to the width of the pulses. An echo was also observed for a $P_y(180^o)$ pulse sequence (even though $M_2^{II} > M_2^{IS}$), the envelope of the signal at $t = 2\tau$ measured as a function of τ was found to be approximately Gaussian. This decay was interpreted as being influenced solely by ^{129}Xe-^{129}Xe dipolar interactions, the measured decay constant was about one half of that expected from van Vleck theory, full details of the equations used by the authors were not, however, given. For the ^{131}Xe resonance only the response to the $P_y(180^o)$ sequence was unaffected by the quadrupole interaction (essentially, only the central, $m = \pm\frac{1}{2}$, transition was observed in the experiment). A well defined echo was observed ($M_2^{IS} > M_2^{SS}$), again, the signal amplitude at $t = 2\tau$ as a function of τ was found to be a Gaussian with a decay constant of about one half of the theoretical M_2^{SS}. No attempt was made to explain the differences between theory and experiment.

Hutchins and Day(13) have studied a single crystal of caesium fluoride, CsF, (^{133}Cs has spin $\frac{7}{2}$) with the major aim of examining the form of the FID. They also used the $P_y(90^o)$ sequence (^{19}F resonance) in an attempt to extract M_2^{FCs} from the initial slope of the signal. The signal was found to depend, critically, on the experimental conditions and only a qualitative agreement with theory was obtained.

Polycrystalline indium phosphide, InP, was investigated by Engelsberg and Norberg(11) (^{113}In and ^{115}In have spin $S = \frac{9}{2}$ but the former is only 4.23% abundant). The total phosphorus second moment is unaffected by quadupole affects (^{31}P has spin

$I = \frac{1}{2}$), calculation shows that $M_2^{II}/M_2^{IS} = 0.04$. Again, the results for the resonance of the spin-$\frac{1}{2}$ nucleus are most relevant here. The ^{31}P FID at 78 K was found to deviate from a Gaussian only after it had decayed to about 40% of its initial value. The measured value of M_2 was, however, only about half the theoretical value. This difference was attributed to interference between ^{31}P-$^{113,115}In$ electron coupled dipolar interactions and dipolar interactions of similar magnitude but opposite sign. A well resolved echo resulted from the $P_x(90^o)$ sequence ($M_2^{IS} > M_2^{II}$), the half-echo shape did not deviate significantly from that of the FID except for relatively large pulse separations. The decay of the maximum echo amplitude as a function of pulse spacing was initially a Gaussian with a decay constant equal to approximately one half M_2^{IS} which was not surprising in view of the behaviour of the FID. The $P_y(180^o)$ sequence also produced an echo from which a value of M_2^{II}, within 10% of the theoretical value, was extracted.

All three experimental studies summarised above deviate in some way from the behaviour predicted by the operator formulism. It is difficult to ascertain the extent to which these deviations can be attributed to the complexity of the spin systems involved (they each contain a quadrupolar nucleus), the experimental conditions or the limitations inherent in the second order time expansion.

A study of systems containing dipolar coupled hydrogen (spin I) and fluorine (spin S) nuclei was carried out by Boden and Gibb(1) and (2). For both solid $C_6H_6 + C_6F_6$, at 200 K, and solid 1,3,5-trifluorobenzene, at 255 and 170 K, the ^1H and ^{19}F FID's were found to be Gaussian functions for at least 70% of

their decays. There were no noticeable shielding affects (which was a little surprising for the ^{19}F resonance). It was also found that for a $P_x(90^o)$ sequence the decay of the echo amplitude, $E(\tau)$ could be represented by the expansion

$$E(\tau) = 1 - M_{2\varepsilon}^{IS} \frac{\tau^2}{2!} + M_{4\varepsilon}^{IS} \frac{\tau^4}{4!} - M_{6\varepsilon}^{IS} \frac{\tau^6}{6!} + ... \qquad 5.01$$

where

$$M_{2n\varepsilon}^{IS} = 1.3.5....(2n-1)(M_{2\varepsilon}^{IS})^n \text{ and } M_{2\varepsilon} = 2M_2^{IS}.$$

The decay of the echo amplitude was thus well represented by a Gaussian function with a decay constant dependent only on the I,S dipolar interactions. Equation 5.01 was found to be valid, experimentally, for $1 >> M_2^{IS}/M_2^{II} >> 1$. Homonuclear I,I interactions do not contribute to the decay of $E(\tau)$ even though the operator formulism predicts a contribution to fourth, and higher, order terms in the time expansion. For a $P_x(180^o)$ (and $P_y(180^o)$) sequence the experimental results indicated that the decay of the maximum echo emplitude was represented by a Gaussian function of the form

$$E(\tau) = 1 - M_2^{II} \frac{(2\tau)^2}{2!} + M_4^{II} \frac{(2\tau)^4}{4!} - M_6^{II} \frac{(2\tau)^6}{6!} + ... \qquad 5.02$$

provided that $M_2^{IS} > M_2^{II}$. In other words the decay of $E(\tau)$ depends, for this sequence, only on the I,I interactions. Overall the experimental results were shown to be internally consistent: the value of M_2 determined from the ^1H FID was found to be given by $M_2^{II} + M_2^{IS}$ derived from the echo studies.

Albert and Ripmeester(14) have studied spin-lattice relaxation in 1,3,5-trifluorobenzene, their results provide an external check of the spin echo results. The authors used known crystal data for 1,3,5-$C_6H_3F_3$ to estimate the values of the various

contributions to the ^{1}H and ^{19}F second moments. They found that their estimates were consistent with the observed spin-lattice relaxation behaviour. For the ^{1}H resonance the rigid lattice values of M_2^{HH} and M_2^{HF} were estimated to be 1.71×10^{-8} and 1.52×10^{-8} T^2, respectively. These values compare with $M_2^{HH} = 0.7 \times 10^{-8}$ T^2 and $M_2^{HF} = 3.36 \times 10^{-8}$ T^2 derived from equations 5.01 and 5.02 for the spin echo studies. It is interesting to note that the discrepancy for the $P_x(180^o)$ sequence is comparable to that observed by Warren and Norberg(12) in their study of solid xenon. Again, it is difficult to find a simple explanation for the differences in these studies: they could be experimental in origin or could be associated with limitations in the semi-empirical equations (5.01 and 5.02). In the spin echo studies of 1,3,5-$C_6H_3F_3$ the echo maxima did not fall at $t = 2\tau$, except for short pulse intervals, which suggests that higher order terms were influencing the formation of the echoes.

Finally a brief mention of a study of the liquid crystalline phases of the potassium 4,4-difluoromyristate/water system (Post(3)) will be made. An important interaction in the system is the dipolar coupling between the fluorine nuclei and the neighbouring protons. The interaction is characterised by the heteronuclear second moment, M_2^{FH}. The mobility in that part of the chain to which the fluorine atoms are attached is reflected in the size of M_2^{FH}. It was found experimentally that the $P_x(90^o)$ echo decay consisted of two components, of roughly equal magnitude: this is not compatible with the operator expansion. A detailed calculation for a model system consisting of a resonant pair of spin-$\frac{1}{2}$ nuclei coupled to a number of non-resonant nuclei (represented by a distribution

of local fields) produced an analytic expression which accounted for the observed behaviour.

To conclude this review we shall make the comment that there seems to be inconsistencies in most of the studies that have been carried out. One possible reason for this is the limited applicability of the second order time expansion. As with studies of homonuclear and dipolar coupled spin-1 systems it seems important to explore in some detail the behaviour of analytic expressions derived for simple model systems so as to obtain a greater understanding of the behaviour of heteronuclear systems.

5.2 The Analytic Forms of the Two Pulse Responses

In the following sections a general form for the analytic responses of two, three and four spin heteronuclear systems to two pulse sequences will be developed.

5.2.1 Two Spin Systems

Equation 4.11 for the IS spin system response to the general pulse sequence $P_y(90^o)-\tau-P_\phi(\theta)$ can be expressed as:

$$\langle I_x(t)\rangle = \cos^2(\theta/2)\ G(t) - \sin^2(\theta/2)\ \cos 2\phi\ G(t-2\tau) \qquad 5.03$$

where G(t) represents the FID following a 90^o pulse (equation 2.21)

$$G(t) = \cos\Delta\omega t\ \cos\tfrac{1}{2}at$$

and $G(t-2\tau)$ is a component with the same functional form as the FID but which depends on time as $(t-2\tau)$: we shall call this the echo component

$$G(t-2\tau) = \cos\Delta\omega t\ \cos\tfrac{1}{2}a(t-2\tau).$$

As we noted in Chapter Four the FID component contributes to the signal unless the second pulse is a 180^{o} pulse. If the pulse interval is chosen so that the second pulse occurs 'halfway', or further, along the FID then the resulting echo falls outside the original FID. The shape of the echo is then determined solely by the second term in equation 5.03.

For the I_2 spin system the response to the general pulse sequence (equation 4.15) can be expressed as:

$$\langle I_x(t)\rangle = \tfrac{1}{2}[\cos\theta(1+\cos2\phi) + \cos^2\theta(1-\cos2\phi)]G(t) + \tfrac{1}{2}\sin^2\theta(1-\cos2\phi)G(t-2\tau) \qquad 5.04$$

where $G(t)$ is the FID component - equation 2.27:

$$G(t) = \cos\Delta\omega t \cos\tfrac{3}{4}at$$

and $G(t-2\tau)$ is the echo component

$$G(t-2\tau) = \cos\Delta\omega t \cos\tfrac{3}{4}a(t-2\tau).$$

For this system, in contrast to the IS system above, the FID does not contribute to the signal for $P_x(90^{o})$ or $P_y(90^{o})$ pulse sequences. The echo component does not contribute for a $P_x(180^{o})$ or $P_y(180^{o})$ sequence. The argument concerning the choice of τ that we gave for the IS spin system applies again here.

5.2.2 Three Spin Systems

We can extend the process developed for the two spin systems to three spin systems. For three unlike spins we find:

$$\langle I_x(t)\rangle = \cos^2(\theta/2)\ G(t) - \sin^2(\theta/2)\ \cos2\phi\ G(t-2\tau). \qquad 5.05$$

Again, $G(t)$ is the FID (Equation 2.29) and $G(t-2\tau)$ is the echo component. The discussion of the IS spin system applies equally well to this expression. We can now turn

to more practical systems; it is at this point that deviations from the simple pattern established above become apparent. For an IS_2 spin system both the I and S spin responses have an additional component, which we shall call the 'cross-term' (it can be written so as to include terms which are the product of a term originating at t = 0 with a term originating at t = 2τ)). For the I spin responses:

$$\langle I_x(t)\rangle = \cos^2(\theta/2)\ G(t) - \sin^2(\theta/2)\ \cos2\phi\ G'(t-2\tau) + \sin^2(\theta/2)\ \cos2\phi\ A(t,\tau) \quad 5.06$$

where G(t) is the FID component (Equation 2.31):

$$G(t) = \tfrac{1}{2}\cos\Delta\omega t\left[\cos\tfrac{1}{2}(a+c)t + \left(\frac{a-c}{T}\right)^2 \cos\tfrac{1}{2}Tt + \left(\frac{b}{T}\right)^2\right].$$

and $G'(t-2\tau)$ is the echo component

$$G'(t-2\tau) = \tfrac{1}{2}\cos\Delta\omega t\left[\cos\tfrac{1}{2}(a+c)(t-2\tau) + \left(\frac{a-c}{T}\right)^4 \cos\tfrac{1}{2}T(t-2\tau) + \left(\frac{b}{T}\right)^4\right.$$

Interestingly, the cosine terms in the echo component have the same frequency as those in the FID but the coefficients, with the exception of the $\frac{1}{2}\cos\Delta\omega t$, are the square of those in the FID. As will be seen shortly this pattern is maintained through the S spin and the I_2S_2 spin system expressions The cross-term in equation 5.06 is

$$A(t,\tau) = \tfrac{1}{2}\cos\Delta\omega t\left[\frac{b^2(T^2-b^2)}{T^4}\right][1-2\cos\tfrac{1}{2}T\tau + \cos\tfrac{1}{2}Tt - 2\cos\tfrac{1}{2}T(t-\tau)].$$

In this and subsequent discussions we will assume that the phase angle is either 0° or 90° (if it were 45° the echo terms in the expressions that we have so far discussed would be zero for all pulse angles). The FID contributes to the I spin signal unless the second pulse is a 180° pulse (as it did for the IS spin system). Under these conditions and with t = 2τ:

$$\langle I_x(t = 2\tau, \theta = 180^o, \phi = 90^o)\rangle = \tfrac{1}{2}\cos\Delta\omega t\left[1 + \left(\frac{a-c}{T}\right)^4 + \left(\frac{b}{T}\right)^4 - \frac{b^2(T^2-b^2)}{T^4}\,(1 - 4\cos\tfrac{1}{2}T\tau + \cos T\tau)\right].$$

The cross-term in Equation 5.06 is lost only for spin systems where a = c, then T = b and

$$G'(t-2\tau) = G(t-2\tau)$$

so that

$$\langle I_x(t)\rangle = \cos^2(\theta/2)\; G(t) - \sin^2(\theta/2)\; \cos2\phi G(t-2\tau) \quad 5.07$$

where

$$G(t) = \tfrac{1}{2}\cos\Delta\omega t(\cos at+1).$$

It is important to realise that the condition a=c applies only to linear IS_2 spin systems with equal I,S bond lengths or to IS_2 'triangular' systems which have a particular geometry and orientation with respect to the field. For example a=c in a triangular system if the I,S bond lengths are equal and if the magnetic field is perpendicular to the plane of the triangle. We can rewrite Equation 5.07 as

$$\langle I_x(t)\rangle = \tfrac{1}{2}\cos\Delta\omega t[\cos^2(\theta/2)\;\cos(at) - \sin^2(\theta/2)\;\cos2\phi + \cos(a(t-2\tau)) + \cos^2(\theta/2) - \sin^2(\theta/2)\;\cos2\phi]$$

which is just the response of an IS spin system (compare this with equation 5.03) plus a constant and with twice the coupling constant (there are two identical IS interactions in the system). For such a system

$$\langle I_x(t = 2\tau,\ \theta = 180^o,\ \phi = 90^o)\rangle = \cos\Delta\omega t$$

as it was for the IS spin system.

The influence that the $A(t,\tau)$ term in Equation 5.06 has on the signal is discussed in Section 5.3. The S spin response is surprisingly complex and is less easy to write in a general form:

$$\langle S_x(t)\rangle = \cos^4(\theta/2)[G_1(t) + G_2(t)] - \sin^2\theta\cos2\phi[G'_1(t-2\tau) + G'_2(t-2\tau)] + B(t,\tau) \qquad 5.08$$

where $G_1(t) = \frac{1}{4}\cos\Delta\omega t\ (1-Y)(\cos(\omega_1+\omega_2)t + \cos(\omega_1-\omega_2)t)$

and $G_2(t) = \frac{1}{4}\cos\Delta\omega t\ (1+Y)(\cos(\omega_1+\omega_3)t + \cos(\omega_1-\omega_3)t)$.

These two contributions add to give the FID component:

$$G(t) = G_1(t) + G_2(t).$$

The echo components are

$$G'_1(t-2\tau) = \frac{1}{16}\cos\Delta\omega t(1-Y)^2(\cos(\omega_1+\omega_2)(t-2\tau) + \cos(\omega_1-\omega_2)(t-2\tau))$$

$$G'_2(t-2\tau) = \frac{1}{16}\cos\Delta\omega t(1+Y)^2(\cos(\omega_1+\omega_3)(t-2\tau) + \cos(\omega_1-\omega_3)(t-2\tau))$$

with

$$\omega_1 = \tfrac{1}{4}(a+c),\ \omega_2 = \tfrac{1}{4}(2b-T) \text{ and } \omega_3 = \tfrac{1}{4}(2b+T).$$

The cross-term is

$$B(t,\tau) = \tfrac{1}{4}Y\sin^2\theta(G_1(t) - G_2(t)) + C(t,\tau)$$

where $C(t,\tau)$ includes the terms from equation 4.20 not given above, rather than simply repeating those terms here we, instead, write them as the sum of individual cosines:

$$C(t,\tau) = \tfrac{1}{16}\cos\Delta\omega t\{$$

$$\sin^2\theta\cos2\phi[(1+Y)(\cos[(\omega_1+\omega_3)t-2\omega_1\tau] + \cos[(\omega_1-\omega_3)t-2\omega_1\tau])$$

$$+ (1-Y)(\cos(\omega_1+\omega_2)t-2\omega_1\tau] + \cos[(\omega_1-\omega_2)t-2\omega_1\tau])$$

$$- (1-Y^2)(\cos[(\omega_1+\omega_3)t - (2\omega_1+b)\tau] + \cos[(\omega_1-\omega_3)t - (2\omega_1-b)\tau]$$

$$+ \cos[(\omega_1+\omega_2)t - (2\omega_1+b)\tau] + \cos[(\omega_1-\omega_2)t - (2\omega_1-b)\tau])]$$

$$+ \sin^2\theta[(1-Y)^2(\cos[(\omega_1+\omega_2)t - 2\omega_2\tau] + \cos[(\omega_1-\omega_2)t + 2\omega_2\tau])$$

$$+ (1+Y)^2(\cos[(\omega_1+\omega_3)t - 2\omega_3\tau] + \cos[(\omega_1-\omega_3)t + 2\omega_3\tau])$$

$$- (1-Y^2)(\cos[(\omega_1+\omega_3)t - \tfrac{1}{2}T\tau] - \cos[(\omega_1+\omega_3)t - b\tau]$$

$$+ \cos[(\omega_1+\omega_2)t + \tfrac{1}{2}T\tau] - \cos[(\omega_1+\omega_2)t - b\tau]$$

$$+ \cos[(\omega_1-\omega_2)t - \tfrac{1}{2}T\tau] - \cos[(\omega_1-\omega_2)t + b\tau]$$

$$+ \cos[(\omega_1-\omega_3)t + \tfrac{1}{2}T\tau] - \cos[(\omega_1-\omega_3)t + b\tau])]$$

$$+ 4\sin^4(\theta/2)\cos2\phi[Y(1-Y)(\cos[(\omega_1+\omega_2)t - 2\omega_1\tau] + \cos[(\omega_1-\omega_2)t - 2\omega_1\tau])$$

$$- Y(1+Y)(\cos[(\omega_1+\omega_3)t - 2\omega_1\tau] + \cos[(\omega_1-\omega_3)t - 2\omega_1\tau])$$

$$- (1-Y^2)(\cos[(\omega_1+\omega_3)t - (2\omega_1+\tfrac{1}{2}T)\tau] + \cos[(\omega_1-\omega_3)t - (2\omega_1-\tfrac{1}{2}T)\tau]$$

$$+ \cos[(\omega_1+\omega_2)t - (2\omega_1-\tfrac{1}{2}T)\tau] + \cos[(\omega_1-\omega_2)t - (2\omega_1+\tfrac{1}{2}T)\tau])]\}.$$

As we pointed out for the I spin response the cosine terms in the FID component have the same frequency as those in the echo component and the coefficients in the echo component, except for the $\cos\Delta\omega t$, are the square of those in the FID. Although complex, the S spin response has some of the general characteristics of the I spin response. The response is greatly simplified when specific pulse sequences are considered, as described below.

In contrast to the I_2 spin system there is a contribution to the signal from the FID for a 90^o second pulse but it is lost for a 180^o second pulse, as is the echo component. A 180^o second pulse also greatly reduces the number of terms in the $C(t,\tau)$ term. When $t = 2\tau$

$$\langle S_x(t = 2\tau, \theta = 180^o, \phi = 90^o)\rangle = \tfrac{1}{2}\cos\Delta\omega t[Y(1+Y)\cos2\omega_3\tau$$

$$- Y(1-Y)\cos2\omega_2\tau + (1-Y^2)(\cos(2\omega_3-\tfrac{1}{2}T)\tau$$

$$+ \cos(2\omega_2-\tfrac{1}{2}T)\tau].$$

By far the greatest simplification comes for the special case when a = c, then, $\omega_1 = \frac{1}{2}a$, $\omega_2 = \frac{1}{4}b$, $\omega_3 = \frac{3}{4}b$ and Y = 1, so that

$$\langle S_x(t)\rangle = (\cos^4(\theta/2) - \tfrac{1}{4}\sin^2\theta)G_2(t) - \tfrac{1}{2}\sin^2\theta\ \cos2\phi\ G_2(t-2\tau) + C(t,\tau)$$

where

$$G_2(t) = \tfrac{1}{2}\cos\Delta\omega t(\cos(\omega_1+\omega_3)t + \cos(\omega_1-\omega_3)t)$$
$$\equiv \cos\Delta\omega t\ \cos\tfrac{1}{2}at\ \cos\tfrac{3}{4}bt \qquad 5.09$$

and

$$C(t,\tau) = \tfrac{1}{4}(\cos\theta-\cos^2\theta)\cos2\phi\left[\cos[(\omega_1+\omega_3)t - 2\omega_1\tau] + \cos[(\omega_1-\omega_3)t - 2\omega_1\tau]\right] + \tfrac{1}{4}\sin^2\theta\left[\cos[(\omega_1+\omega_3)t - 2\omega_3\tau] + \cos[(\omega_1-\omega_3)t + 2\omega_3\tau]\right].$$

For a 90° second pulse there is no FID contribution to the signal, the echo height as a function of τ is

$$\langle S_x(t = 2\tau, \theta = 90^\circ, \phi = 90^\circ)\rangle = \tfrac{1}{2}\cos(2\Delta\omega\tau)(1 + \cos(a\tau))$$

which is the same as that for the I spin FID for the same system (if the offset is zero). For a 180° second pulse there is no FID and no echo contribution to the signal. Then

$$\langle S_x(t = 2\tau, \theta = 180^\circ, \phi = 90^\circ)\rangle = \cos\Delta\omega t\ \cos\tfrac{3}{2}b\tau\ .$$

Equation 5.09 for the FID component of the signal is simply the product of the FID of the I_2 and IS spin systems. This simplification arises because in the special case when a = c $[\mathcal{H}^{D,IS}, \mathcal{H}^{D,II}] = 0$. We note in passing that the three like spin calculation of Moskvich, Sergeev and Dotsenko(15) is also written in terms of FID, echo and cross-term components the result is similar to equation 5.04 but with an additional term.

$$\langle I_x(t)\rangle = \tfrac{1}{2}[(\cos\theta(1+\cos2\phi) + \cos^2\theta(1-\cos2\phi)G(t) + \sin^2\theta(1-\cos2\phi)G(t-2\tau) + D(t,\tau)].$$

The analytical form of the terms can be found in reference (15). For a 180^{o} second pulse only the FID component remains and for a 90^{o} second pulse the FID term is lost.

5.2.3 Four Spin Systems

The four spin response, equation 4.21, can also be written in terms of FID, echo and a cross-term components:

$$\langle I_x(t)\rangle = (\cos^4(\theta/2) - \tfrac{1}{4}\sin^2\theta)G_1(t) + (\cos^4(\theta/2) + \tfrac{1}{4}\sin^2\theta\ \cos2\phi)\ G_2(t) + 2\sin^2\theta(1-\cos2\phi)G_2'(t-2\tau) - \sin^2\theta\ \cos2\phi\ G_1'(t-2\tau) + E(t,\tau) \qquad 5.10$$

where $G_1(t) = \tfrac{1}{4}\cos\Delta\omega t[2\cos\tfrac{1}{2}(a+c)t\ \cos\tfrac{3}{4}dt]$

and

$$G_2(t) = \tfrac{1}{4}\cos\Delta\omega t[(A+P)^2\ \cos\tfrac{1}{4}(b-2d+U)t + (A-P)^2\ \cos\tfrac{1}{4}(b-2d-U)t + (B+Q)^2\ \cos\tfrac{1}{4}(b+2d-V)t + (B-Q)^2\ \cos\tfrac{1}{4}(b+2d+V)t].$$

The free induction decay (equation 2.33) is $G(t) = G_1(t) + G_2(t)$. The cosine terms in the FID and echo ($G_1'(t-2\tau)$ and $G_2'(t-2\tau)$) components have the same frequencies and the coefficients of of the echo components, apart from the $\cos\Delta\omega t$, are the square of those in the FID. The cross-term $E(t,\tau)$ does not easily simplify so we shall not reproduce it in full, however, for a $P_x(90^{o})$ sequence it becomes:

$$E(t,\tau,\theta = 90^{o},\phi = 90^{o}) = \tfrac{1}{4}\cos\Delta\omega t[2(A^2-P^2)^2\cos\tfrac{1}{4}(b-2d)(t-2\tau)\ \cos\tfrac{1}{4}Ut + 2(B^2-Q^2)^2\ \cos\tfrac{1}{4}(b+2d)(t-2\tau)\ \cos\tfrac{1}{4}Vt + \cos\tfrac{1}{2}(a+c)t\ \cos\tfrac{3}{4}d(t-2\tau)].$$

We have evaluated this expression for four different spin system geometries, the results are given in the next section. For this same pulse sequence the FID component is zero. For a $P_x(180^o)$ sequence both the FID component and the echo component are lost, the cross-term becomes:

$$E(t,\tau,\theta = 180^o,\phi = 90^o) = \cos\Delta\omega t[AP(A+P)^2 \cos\tfrac{1}{4}(b-2d+u)t$$
$$- AP(A-P)^2 \cos\tfrac{1}{4}(b-2d-u)t$$
$$+ BQ(B+Q)^2 \cos\tfrac{1}{4}(b+2d-v)t$$
$$- BQ(B-Q)^2 \cos\tfrac{1}{4}(b+2d+V)t$$
$$+(A^2-P^2)^2 \cos\tfrac{1}{4}(b-2d)t \cos\tfrac{1}{4}U(t-2\tau)$$
$$+ (B^2-Q^2)^2 \cos\tfrac{1}{4}(b+2d)t \cos\tfrac{1}{4}V(t-2\tau)$$
$$+\tfrac{1}{2}\cos\tfrac{1}{4}(a+c)(t-2\tau) \cos\tfrac{3}{4}dt].$$

The observations from this and the two preceding sections are discussed in the next section.

5.3 A Discussion of the Responses

There are three main areas for discussion: (i) the general behaviour of the spin systems in response to the two pulse sequence, (ii) the relationship between the half-echo shape and the FID and (iii) the behaviour of the echo amplitude as a function of pulse spacing for $P_x(90^o)$ and $P_x(180^o)$ pulse sequences.

5.3.1 The General Behaviour

Table 5.1 summarises the effects of $P_x(90^o)$ and $P_x(180^o)$ pulse sequences for the spin systems studied in the last three sections.

Table 5.1 The effects of two pulse sequences

System	$P_x(90^o)$	$P_x(180^o)$	Cross-term
IS		FID lost	none
I_2	FID lost	echo lost	none
I		FID lost	always contributes to signal
IS_2(general)			
S		FID and echo lost	always contributes to signal
I		FID lost	none
IS_2(special case, a=c)			
S	FID lost	FID and echo lost	
I_3	FID lost	echo lost	zero for a $P_x(180^o)$ sequence
I_2S_2	FID lost	FID and echo lost	always contributes to signal

If we write the response to the two pulse sequence in terms of FID, echo and cross-term components then either a $P_x(90^o)$ or a $P_x(180^o)$ sequence will remove the FID or the echo component, or both. The resulting signal will then depend on the remaining FID or echo component and the cross-term (except in special cases). The behaviour of the cross-term is, then, a key feature of a given echo response: if it turns out to be small then the interpretation of the response can be straightforward.

We have already noted (Section 4.1) that Mansfield's (10) second order time expansion for the operator formulism suggests that 'definite' echoes, centred at $t = 2\tau$, should result from a $P_x(90^o)$ sequence if $M_2^{II} >> M_2^{IS}$ and from a $P_x(180^o)$ sequence if $M_2^{II} << M_2^{IS}$. The analytic responses

give us a different view of these conditions. For all the systems studied an echo component results from a $P_x(90^o)$ sequence (Table 5.1). The distortion of the echo, relative to the pure echo component, is dependent on the other contribution to the response, in particular that for the cross-term. For a $P_x(180^o)$ sequence the response of an I_2S_2 system and the S resonance response of the IS_2 system depend solely on the nature of the cross-term. We shall comment further on these observations later.

To summarise, all the responses that we have investigated can be written in terms of an FID component, an echo component and, except in special circumstances, a cross-term component. If the spin system involves an I-I (or S-S) interaction then a $P_x(90^o)$ sequence always produces an echo component while the $P_x(180^o)$ sequence always removes the echo component. It is interesting to question whether the general operator treatment could be modified in such a way that these general observations could be predicted for a many spin system, that is an I_nS_m system.

5.3.2 The Relationship Between the Half-Echo Shape and the FID

We shall limit this discussion to the systems of most practical interest, namely the IS_2 and I_2S_2 systems. The special case of an IS_2 system with a=c is studied experimentally in Section 5.4. It is difficult to make general statements about the relationship between the half-echo shape (that is the shape of the signal from the maximum echo amplitude onwards) and the FID because, as we have already seen with the FID's (Chapter Three), the response of a spin system to a pulse sequence depends on the geometry of the spin system.

We have, consequently, chosen to carry out a theoretical study of four representative spin systems, two of which we have discussed in previous chapters:

(i) an IS_2 system (HF_2) with r_{HF} = 0.1025 and 0.1235 nm, r_{FF} = 0.2260 nm (MHD in Chapter Three)

(ii) an IS_2 system (H_2F) with r_{HF} = 0.184 nm and r_{HH} = 0.181 nm, (sodium fluoroethanoate),

(iii) an I_2S_2 system (H_2F_2) with r_{HF} = 0.24 and 0.30 nm, $r_{HH} = r_{FF}$ = 0.18 nm and M_2^{HH}/M_2^{HF} = 5.66 and

(iv) an I_2S_2 system (H_2F_2) with r_{HF} = 0.12 and 0.2163 nm, $r_{HH} = r_{FF}$ = 0.18 nm and M_2^{HH}/M_2^{HF} = 0.108.

The calculations that we have carried out are all for polycrystalline systems.

The theoretical responses, to $P_x(90^o)$ and $P_x(180^o)$ sequences, of the systems considered all contain a cross-term component, Table 5.1. As will be shown the properties of this component determine, to a large extent, the degree of distortion of the half-echo shape relative to the FID.

The $P_x(180^o)$ Sequence

For systems (i) and (ii) the signal for the S resonance depends only on the cross-term. Figure 5.1(a) shows the cross-terms calculated as a function of t for a pulse spacing of τ=15 μs. For these systems at least it is clear that the response to the $P_x(180^o)$ sequence bears no relation to the FID (Chapter Three). It is also important to note that the figure illustrates that, for this pulse sequence, an echo need not be observed. The I spin response for the same system depends on the cross-term and, additionally, on the echo component so, providing the cross-term is small, we

would expect to see a definite echo, its shape slightly distorted with respect to that of the FID (the coefficients inside the echo component are not those of the FID although the frequencies are - Sections 5.2.2 and 5.2.3). Figure 5.1(b) shows the cross-term for these systems, again as a function of t and with $\tau = 15$ μs, in both cases they account for less than 10% of the total signal; definite echoes, with half-echo shapes distorted relative to the FID only by the coefficients in the echo component, should, then, result.

For the I_2S_2 spin system the $P_x(180^o)$ sequence removes all but the cross-term component from the response. Calculations although not shown here, confirm that the comments made concerning the IS_2 S spin response are also applicable in this case.

The $P_x(90^o)$ Sequence

For the (i) and (ii) systems both the I and S spin responses contain FID, echo and cross-term components. If the cross-term components are small then the half-echo shapes will still be distorted by the FID components as well as by the differing coefficients in the echo component. Figures 5.2(a) and (b) show the cross-term components for these systems, the I spin components are indeed small so will have little effect on the signal but, in contrast, the S spin components will make a significant contribution to the response. (The I spin cross-terms showed no significant increase in size for $\tau = 10$ and 34 μs, so it is probably the case that for these systems the cross-term component is small for all τ.)

For the four spin systems the FID does not contribute to the signal so the distortion of the half-echo shape will depend

on the coefficients in the echo component and also on the size of the cross-term component. Figure 5.3(a-d) shows the I spin cross-term components for systems (iii) and (iv) ((a) and (c)) as well as for two other similar systems. The size of the cross-term contribution to the signal clearly depends on the geometry of the system. The components shown in Figure 5.3 are for one specific value of the pulse spacing. It is, however, possible to show that the size of the components depend on the pulse spacing as well as the geometry of the system. From the expression for the cross-term component, for this pulse sequence, it is evident (see Section 5.2.3) that it must have a maximum value at $t = \tau = 0$. We have established that for systems (iii) and (iv) the maximum values are 0.389 and 0.476 respectively, in other words, the cross-term components would be expected to contribute significantly to the half-echo shape for short pulse spacings.

To summarise, it seems likely that, for a general IS_2 or I_2S_2 spin system, the half-echo shape will not be the same as the shape of the FID for $P_x(90^o)$ and $P_x(180^o)$ sequences. Even when the FID and cross-term components do not significantly contribute to the signal the form of the coefficients in the echo component will ensure that there is some distortion in the half-echo shape relative to that of the FID. For a $P_x(180^o)$ sequence the I_2S_2 and IS_2 S spin responses depend only on the cross-term component so that the existence of an echo and (if it is observable) its half-shape will be markedly dependent on the geometry of the spin system.

5.3.3 The Effect of Pulse Spacing on Echo Amplitude

The behaviour of the echo amplitude (or more precisely the behaviour of the maximum signal amplitude in the vicinity of $t = 2\tau$) as a function of pulse spacing for $P_x(90^o)$ and $P_x(180^o)$ pulse sequences is discussed in this section. The discussion will be limited to the four systems (i) - (iv) described in Section 5.3.2; again only polycrystalline systems are considered.

The $P_x(180^o)$ Sequence

The S spin response for systems (i) and (ii) depends only on the cross-term component (Table 5.1): that is there is no 'true' echo contribution to the response. However, the cross-term component may pass through a maximum giving rise to an 'apparent' echo at, or near, $t = 2\tau$. Indeed for system (i) the response does show this behaviour, but only for $\tau < 20\mu s$ is the maximum at $t = 2\tau$, when $\tau = 40\mu s$ the maximum occurs at $t = 72\mu s$. The behaviour of the maximum signal amplitude as a function of pulse spacing is discussed in detail below.

Figure 5.4(a) shows the decay of the computed signal maximum (not that at $t = 2\tau$) for system (i) as a function of τ^2. Figure 5.4(b) shows the corresponding logarithmic plot. In a real system the existence of intersystem interactions would ensure that the signal amplitude would eventually decay to zero, rather than attain a constant value after approximately 70% of the signal decay. The plots show that the signal amplitude decays smoothly and in a non-Gaussian fashion. According to the operator expansion (Chapter Four, equation 4.10) the initial slope of the curve in Figure 5.4(a) is equal

to $-2M_2^{SS}$ where $M_2^{SS} = M_2^{FF} = 1.506 \times 10^9$ rad^2 s^{-2}. From a practical viewpoint, with a spectrometer dead time of about 10μs and allowing for experimental scatter, it is quite feasible that an experimental plot of ln (maximum signal amplitude) versus τ^2 would appear to be Gaussian for at least 50-60% of the signal decay, as in Figure 5.4(b). Indeed, if the data in the figure is analysed in this manner, and if it is assumed that the decay can be represented by the Gaussian function $\exp(-2M_{2,\varepsilon}^{SS}\tau^2)$, then it results in a value of $M_{2,\varepsilon}^{SS} \cong (7.9 \pm 0.4) \times 10^8$ rad^2 s^{-2}. In other words the value of $M_{2,\varepsilon}^{SS}$ extracted from a plot of the form of Figure 5.4(b) is approximately one half of that extracted from a plot of the form of Figure 5.4(a). This result is particularly interesting when it is recalled from the literature review in Section 5.1 that a discrepancy of this magnitude was found by Warren and Norberg (12) in their study of solid xenon and by Boden and Gibb (1) and (2)/Albert and Ripmeester (14) in their studies of 1,3,5 tri-fluorobenzene. The present result may well account for the observed differences between theory and experiment. However, irrespective of this, the result indicates that even for a simple system a Gaussian decay can be obtained with a time constant related to M_2^{SS}, although the relationship is not as predicted by the operator formulism.

For system (ii) the computer calculations show that the maximum S signal response decays rapidly and for practical pulse spacings, that is $10\mu s \leqslant \tau \ll 40\mu s$, there is no clear maximum. This behaviour is consistent with the larger value of $M_2^{SS} = M_2^{HH} = 7.287 \times 10^9$ rad^2 s^{-2} when compared to that of system (i).

The corresponding I spin responses for systems (i) and (ii) depend mainly on the echo component (in Section 5.3.2 the

cross-term components were shown to be small). Consequently, an echo maximum should be observed at, or near, $t = 2\tau$ for both systems. Calculations, although not shown here, confirm that this is the case; for system (i) the echo maximum occurs at $t = 2\tau$ for $10\mu s \leqslant \tau \leqslant 40\mu s$ and within $2\mu s$ of $t = 2\tau$ for system (ii) over the same range of τ values. Both echo envelopes show little decay and are slightly modulated. Any decay observed experimentally will, then, reflect inter rather than intra system interactions.

For the I_2S_2 systems only the cross-term components contribute to the signal. The size of $M_2^{II} = M_2^{HH}$ is similar to that in system (ii) so the maximum signal amplitude decays rapidly. For system (iii), for which $M_2^{HH} > M_2^{HF}$, the signal does not go through a maximum near $t = 2\tau$. For system (iv), for which $M_2^{HH} < M_2^{HF}$, an echo occurs only when $\tau < 12\mu s$. For both systems there is little signal amplitude when $\tau > 10\mu s$.

The $P_x(90^\circ)$ Sequence

The pure echo I and S responses for systems (i) and (ii) are complicated by contributions from the FID and cross-term components. The calculated behaviour of the signal for system (i) shows that echoes occur at $t = 2\tau$ for $10\mu s \leqslant \tau \leqslant 40\mu s$ for both I and S responses. The maximum signal amplitude decays slowly with increasing pulse spacing in both cases so a decay observed experimentally must reflect intersystem interactions. The behaviour of the signal for system (ii), for which the H-F dipolar interaction is weaker than in system (i), is more interesting. Figure 5.5(a) shows a plot of ln(maximum signal amplitude) versus τ^2 for the first 70-80% of the decay of the S response. The corresponding plot for the first 50-60% of the decay for the I response is shown in Figure 5.5(b). The

signal maximum for the S response is within 2μs of $t = 2\tau$ over the range $10\mu s \leqslant \tau \leqslant 40\mu s$ whereas for the I response the signal maximum occurs at $t = 2\tau$ for $16\mu s < \tau \leqslant 40\mu s$, below 16μs there is no clear echo. Both of the echo height envelopes can be represented by a modulated decay function added to a constant term. The resonant nucleus and the geometry of the spin system determine the size of this constant term. Neither decay is Gaussian in nature.

For systems (iii) and (iv) the behaviour of the signal is determined by the interplay of the echo and cross-term components, there is no FID contribution to the signal. The echo falls at $t = 2\tau$ for $10\mu s \leqslant \tau \leqslant 40\mu s$ for system (iv) but the echo height envelope does not significantly decay for this range of τ. The echo for system (iii) falls within 1μs of $t = 2\tau$ over the same range of τ, this time, though, the echo height envelope does decay slowly - for $\tau = 40\mu s$ the echo height is approximately 60% of its value at $\tau = 0$. The decay is non-Gaussian, as is illustrated in Figure 5.6.

For both the I and S responses in both the IS_2 and I_2S_2 spin systems the behaviour of the maximum signal amplitude is such that it decays to a constant value if intersystem interactions are ignored. In 'real' systems, therefore, where there are intersystem interactions a two component echo decay, as a function of pulse spacing, might be expected. Indeed such a decay has been reported by Post (3) in studies of the potassium 4,4-difluoromyristate/water system (Section 5.1). In contradiction to this type of decay, however, Boden and Gibb (1) and (2) found Gaussian type decays for both polycrystalline $C_6H_6 + C_6F_6$ and 1,3,5 - $C_6H_3F_3$ (Section 5.1).

It is apparent from Figures 5.5(a), 5.5(b) and 5.6 that the initial decay could be fitted, empirically, to a Gaussian function: this is especially true for the IS_2 S response. If such a procedure is followed the decay constants obtained do not relate simply to M_2^{IS} or M_2^{SI}. Qualitatively, though, the size of the decay constant increases with the increasing strength of the I,S dipolar interaction.

The discussion presented in this section gives an indication of the complexity of the response to both $P_x(180^o)$ and $P_x(90^o)$ sequences. It is clear that there is scope for further computational work, although it should be noted that the necessity to take a polycrystalline average for complicated responses makes this a very time consuming endeavour. Detailed experimental work with model systems with known crystal structure is also required. The present work shows that the separation of I,I and I,S dipolar interactions using echo techniques is not as straightforward as has been previously suggested. It also shows that the predictions of the operator formulism are of limited value.

5.4 Spin Echo Studies of a 'Simple' Heteronuclear Spin System: The Hydrogen Difluoride Ion in KHF_2

According to Table 5.1 and equations 5.07 and 5.09 the behaviour of the responses for a linear IS_2 spin system with $D_{\infty h}$ symmetry (a = c) is relatively simple. An experimental study of such a system - polycrystalline KHF_2 at 293 K has, therefore, been carried out with the aim of assessing whether the responses are, indeed, easily interpreted and also to provide a background for future experimental studies.

The experimental details are the same as those described in Chapter Three. There were, however, two additional features to the experimental technique used for these experiments. Firstly, in order to establish the correct position of the echo maxima we compensated for the finite width of the rf pulses. If, as before, the response effectively starts halfway along the pulse then the effective pulse spacing is as shown in Figure 5.7: the values of τ that we report are $\tau = \tau_s + \tau_p$. Secondly, because of the long spin-lattice relaxation time of KHF_2 ($T_1 \simeq 180$ s at 293 K - Chapter Six) signal averaging was not used for the experiments in which the maximum signal amplitude (echo height) was measured as a function of pulse spacing. As a consequence of this a large number of data points was needed. To reduce the time needed to collect this data the interval between successive measurements was reduced to substantially less than the prescribed $5 \times T_1$. The effect that such a procedure has on echo height measurements is discussed in Appendix G.

The theoretical responses reported in this section were calculated using the (vibrationally uncorrected) structure of the HF_2^- ion determined from the FID experiments of Chapter Three, that is $r_{FF} = 2r_{HF} = 0.2320$ nm.

5.4.1 The $P_x(90^o)$ Sequence

The experimental ^1H and ^{19}F responses to this pulse sequence for polycrystalline KHF_2 at 293 K are shown (as dotted lines, the dots represent every fourth point of the digitised data) in Figure 5.8 and 5.9 respectively. The pulse spacings were chosen to give well resolved echo maxima while keeping the time between pulses as short as possible. For both responses

well defined echoes were observed despite the fact that $M_2^{HF} >> M_2^{HH}$ ($M_2^{HF} = 8.36 \times 10^{10}$ rad^2 s^{-2}, $M_2^{HH} = 7.45 \times 10^8$ rad^2 s^{-2}) and $M_2^{FH} >> M_2^{FF}$ ($M_2^{FH} = 4.18 \times 10^{10}$ rad^2 s^{-2}, $M_2^{FF} = 2.94 \times 10^9$ rad^2 s^{-2}). According to the second order time expansion of the operator formulism definite echoes should not occur under these conditions. However, as Mansfield (10) points out, for relatively large pulse spacings, which is the case here, higher order terms will contribute and echoes may be observed. As will become clear soon the analytic expressions predict the existence of well resolved echoes for these large pulse spacings.

Even though the echo maxima are well resolved for both responses it is difficult to extract accurate values of the total second moments because the signal near the echo maximum changes rapidly with time. For tightly coupled spin systems such as the one studied here it is better to fit the response to the theoretical signal to obtain structural information rather than rely on the use of second moment data. The calculated ^{1}H and ^{19}F responses - the solid lines in Figures 5.8 and 5.9 - are based on equations 5.07 and 5.09:

$$\langle I_x(t,\theta = 90^\circ, \phi = 90^\circ)\rangle = \tfrac{1}{4}\cos\Delta\omega_H t(\cos(at) + \cos(a(t-2\tau)) + 2)$$

$$\langle S_x(t,\theta = 90^\circ, \phi = 90^\circ)\rangle = \tfrac{1}{2}\cos\Delta\omega_F t(\cos\tfrac{1}{2}a(t-2\tau)\ \cos\tfrac{3}{4}b(t-2\tau) + \cos\tfrac{1}{2}at\ \cos\tfrac{3}{4}b(t-2\tau))$$

To obtain the fits shown in the figures it was found necessary to multiply the final polycrystalline signal by a Gaussian decay function with a time origin at the mid-point of the second pulse. The time constants were 3.6×10^8 rad^2 s^{-2} and 1.0×10^9 rad^2 s^{-2} for the ^{1}H and ^{19}F responses respectively. The value for the ^{1}H signal is less than that for the FID and

illustrates that the second rf pulse, not surprisingly, affects the inter as well as the intra system interactions. It is clear from the figures that a reasonably good fit to the experimental data is achieved using calculations based on an isolated IS_2 spin system.

The decay of the maximum echo amplitude (expressed as an arbitrary amplitude) as a function of pulse spacing is shown, for the ^1H resonance, in Figure 5.10. For the range of pulse spacings studied the maximum echo amplitude always occurred within 2μs of $t = 2\tau$. The theoretical signal at $t = 2\tau$, from equation 5.07, is the sum of two components:

$$\langle I_x(t=2\tau)\rangle = \tfrac{1}{2}G(2\tau) + \tfrac{1}{2}G(t-2\tau).$$

Experimentally the FID component, $G(2\tau)$ is effectively 'over' when $2\tau > 60\mu s$ (that is it has little affect on the echo when $\tau > 30\mu s$) - see Figure 3.5. Even for the shortest pulse spacings the quantity $G(2\tau)$ is small (at $\tau = 10\mu s$ $G(2\tau)$ is approximately 35% of its value at $\tau = 0$). The experimental results should, then, be dominated by the $G(t-2\tau)$ component, especially for large pulse spacings. At $t = 2\tau$ $G(t-2\tau)$ is a constant so the intersystem interactions must be the chief cause of the observed decay of the echo height. The data in Figure 5.10 are plotted as ln(echo height) versus τ^2 in Figure 5.11. Overall the decay is not Gaussian, this is presumably because of the contribution to the signal from the FID component at small pulse spacings. If the data, at the larger pulse spacings, are fitted to the empirical Gaussian function $\exp(-\frac{1}{2}M_{2,\varepsilon}\tau^2)$ a value of $M_{2,\varepsilon} = (1.1\pm0.1) \times 10^9$ rad^2 s^{-2} is obtained. This value is not unreasonable when compared to the value for the total intersystem ^1H second moment given in Table 3.1 (1.553×10^9 rad^2 s^{-2}) which has not been corrected

for motion. It does, then, seem that the intersystem dipolar interaction is the cause of the decay of the maximum echo amplitude.

From equation 5.09 the S response at $t = 2\tau$ is

$$\langle S_x(t=2\tau)\rangle = \tfrac{1}{2}\cos a\tau + \tfrac{1}{2}$$

(assuming that $\Delta\omega = 0$). The investigation of the ^{19}F echo height as a function of pulse spacing should yield information about the H-F dipolar coupling constant, a. In this particular system, though, this coupling is very strong (because of the small H-F separation) and pulse spacings shorter than those feasible with the present equipment are necessary if this information is to be obtained from a time expansion to second order.

5.4.2 The $P_x(180^\circ)$ Sequence

The ^1H and ^{19}F experimental responses for polycrystalline KHF_2 at 293 K are shown as dotted lines (every fourth point in the digitised data is shown) in Figures 5.12 and 5.13 respectively. The corresponding theoretical responses, calculated from equations 5.07 and 5.09, are shown as solid lines. Again, the pulse spacings were selected so as to give well resolved echo maxima, the distances derived from the FID's were used in the calculations and Gaussian functions (discussed in more detail below) were used to make the calculated polycrystalline signals decay.

According to equation 5.07,

$$\langle I_x(t,\theta = 180^\circ,\phi = 90^\circ)\rangle = G(t-2\tau) \qquad 5.11$$

so the ^1H half-echo shape ($t \geqslant 2\tau$) should closely resemble that of the FID. The best fit to the experimental data was achieved using a Gaussian decay with a time origin at the echo maximum but the decay constant (1.1×10^9 rad^2 s^{-2}) was roughly twice the magnitude found for the FID. In other words, the half-echo shape is characterised by a faster overall decay. This again suggests, as would be expected, that the pulse sequence affects the intersystem dipolar interactions.

Only the cross-term component contributes to the observed ^{19}F response:

$$\langle S_x(t,\theta = 180^o,\phi = 90^o)\rangle = \tfrac{1}{2}(\cos[(\tfrac{1}{2}a + \tfrac{3}{4}b)t - a\tau] + \cos[(\tfrac{1}{2}a - \tfrac{3}{4}b)t - a\tau]) \qquad 5.12$$

(assuming that $\Delta\omega = 0$). In this case the best fit to the experimental data was achieved using a Gaussian decay with a time origin at the second pulse: even so the fit is not as good as that for the ^1H response. There is no resemblance to the ^{19}F FID (Figure 3.7) for this response.

It is evident from equation 5.11 that for an assembly of isolated IS_2 groups there will be no decay of the echo height with increasing pulse spacing (at $t = 2\tau$ $G(t-2\tau)$ is a constant). In real systems, though, intersystem interactions will cause the echo height to decay. This decay is shown in Figure 5.14 - a plot of the ^1H echo height versus pulse spacing. Figure 5.15 is the corresponding logarithmic plot as a function of τ^2. The latter figure shows that the initial 50% of the decay is approximately Gaussian. If the decay is represented by the empirical function $\exp(-\frac{1}{2}M_{2,\varepsilon}\tau^2)$ then $M_{2,\varepsilon} = (2.6\pm0.1) \times 10^9$ rad^2 s^{-2} which is greater than the total rigid lattice intersystem value for M_2^H (1.553×10^9 rad^2 s^{-2}).

From equation 5.12 the ^{19}F response at $t = 2\tau$ becomes:

$$\langle S_x(t = 2\tau) \rangle = \cos\tfrac{3}{2}b\tau \qquad 5.13$$

Figure 5.16 shows the echo height plotted against pulse spacing and Figure 5.17 is the corresponding logarithmic plot as a function of τ^2. The latter plot shows that the decay of the echo height is (perhaps surprisingly) Gaussian for at least 80% of its length. This behaviour must be the result of the interplay between the decay caused by the intra F-F dipolar interaction, described by the polycrystalline average of equation 5.13, and the decay caused by the irreversible dephasing of intersystem dipolar interactions. It is, however, not clear why a Gaussian decay should result. If this decay is analysed in the same way as the ^1H decay then a value of $M_{2,\varepsilon} = (3.9 \pm 0.1) \times 10^9$ rad^2 s^{-2} is obtained. This value is also greater than the total rigid lattice intersystem value for $M_2^F (2.454 \times 10^9$ rad^2 s$^{-2})$. Interestingly, though, $M_{2,\varepsilon}^H / M_2^H$ is approximately the same as $M_{2,\varepsilon}^F / M_2^F$.

In conclusion it can be said that the responses of polycrystalline KHF_2 to both $P_x(90^o)$ and $P_x(180^o)$ sequences are not as 'straightforward' as might have been anticipated. The observed echo behaviour depends markedly on the resonance (^1H or ^{19}F) studied and, depending on the pulse sequence, can reflect either intersystem dipolar interactions alone or a combination of inter and intra system interactions. While, admittedly, a simple model system, further study, particularly the calculation of motional averaging affects on the interion dipolar interactions, is required. It is also important that experimental studies for other well characterised systems are undertaken, with the aim of establishing a general experimental pattern of behaviour.

5.5 Appendix G

If successive pulse pairs ($P_x(90^o)$ and $P_x(180^o)$ sequences) are applied at intervals of less than $5 \times T_1$, but greater than $5 \times T_2$(effective), then there should be no loss of signal, through saturation, from the second pair repetition onwards providing the interval between repetitions is kept constant. The proof of this, which, for simplicity, we will assume is the same as that for a single pulse, is as follows.

The measurable components of the magnetisation at equilibrium are

$$\langle M_z \rangle = M_o \text{ and } \langle M_x \rangle = \langle M_y \rangle = 0.$$

Immediately after a 90^o pulse along the rotating frame y-axis

$$\langle M_z \rangle = 0, \langle M_x \rangle = M_o \text{ and } \langle M_y \rangle = 0.$$

At time t later (t is much greater than the length of the FID) the measurable components are (Abragam (16))

$$\langle M_z \rangle = M_o(1-\exp(-t/T_1)) \text{ and } \langle M_x \rangle = \langle M_y \rangle = 0.$$

Immediately after a second pulse

$$\langle M_z \rangle = 0, \langle M_x \rangle = M_o(1-\exp(-t/T_1)) \text{ and } \langle M_y \rangle = 0$$

and at an identical time t later:

$$\langle M_x \rangle = \langle M_y \rangle = 0,$$

$\langle M_z \rangle$ has two components, one from the decay of the magnetisation $\langle M_x \rangle$: $M_o(1-\exp(-t/T_1))^2$ and the second from the decay of the magnetisation which had not decayed before the second pulse: $M_o(1-\exp(t/T_1))\exp(-t/T_1)$. So, in total

$$\langle M_z \rangle = M_o[(1-\exp(t/T_1))^2 + (1-\exp(t/T_1))\exp(-t/T_1)]$$

$$= M_o[1-\exp(t/T_1)].$$

Thus, providing the repetition time, t, is kept constant, the magnetisation before the third, and subsequent, pulse is the same as that before the second.

To check that the above analysis can be applied to pulse pairs we carried out an experiment on a standard sample - gypsum, $CaSO_4.2H_2O$ - at 293 K. The following pulse sequence was used:

$$[P_y(90^o)-\tau_1-P_{90^o}(90^o)-t']_n-P_y(90^o)-\tau_2-P_{90^o}(90^o)$$

where instead of varying the pulse spacing for the first n measurements it was kept constant at τ_1 = 15μs; this did not affect the aim of the experiment. The echo height was then measured for t′ = 400ms, 1200ms and 4000ms. For the first two repetition rates the echo amplitude, except when n=1, was depressed when compared to that for the third repetition rate (which was greater than $5 \times T_1$; T_1 = 392ms being measured in a separate experiment). As predicted the loss of echo amplitude was given by the factor (1-exp(-t′/392)). It can be concluded that as long as the first measurement in a series of echo height measurements, as a function of pulse spacing, is ignored and the interval between pulse pairs is kept constant, then a repetition time of considerably less than $5 \times T_1$ can be used.

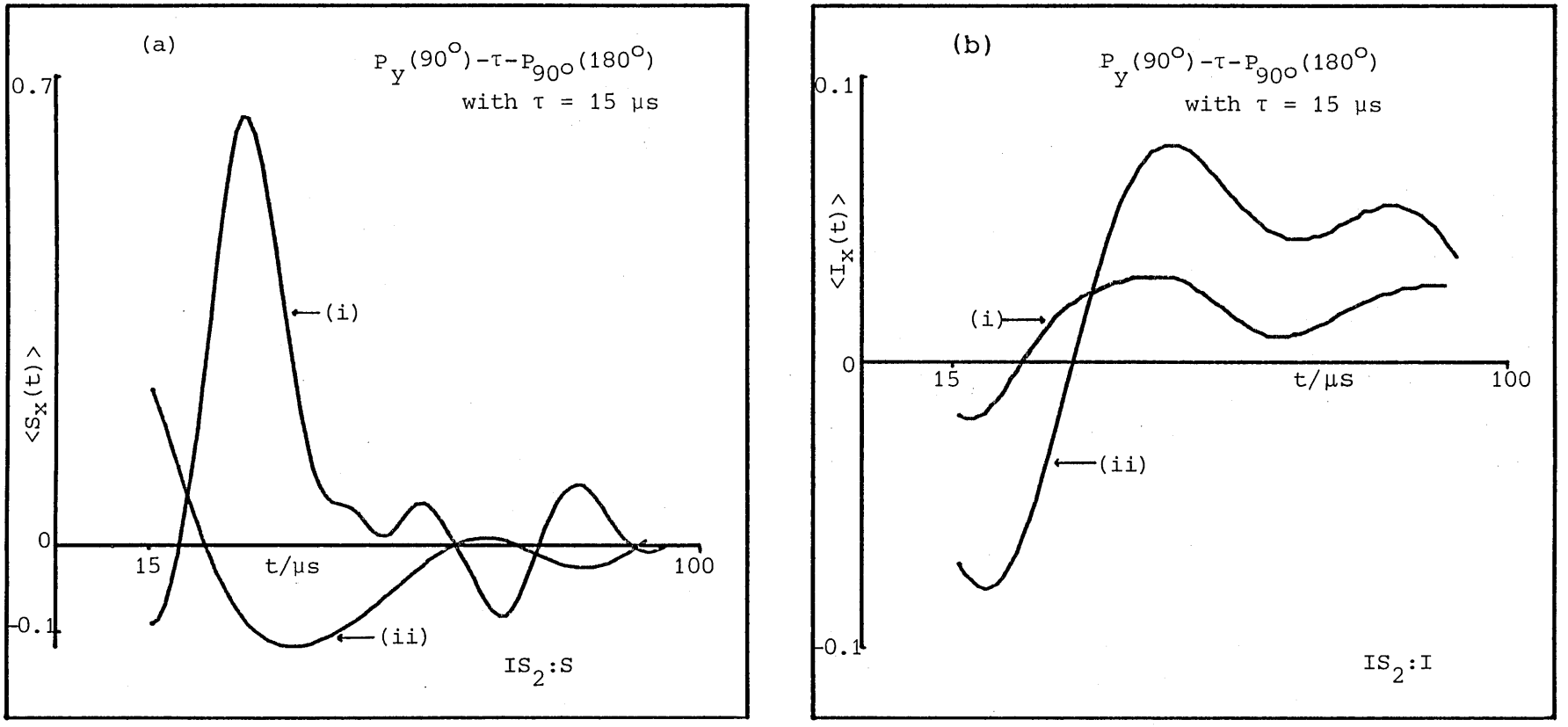

Figure 5.1 The magnitude of the cross-term components for the IS_2 spin system for the pulse sequence shown, (a) S spin response and (b) I spin response. The geometries of systems (i) and (ii) are given in the text.

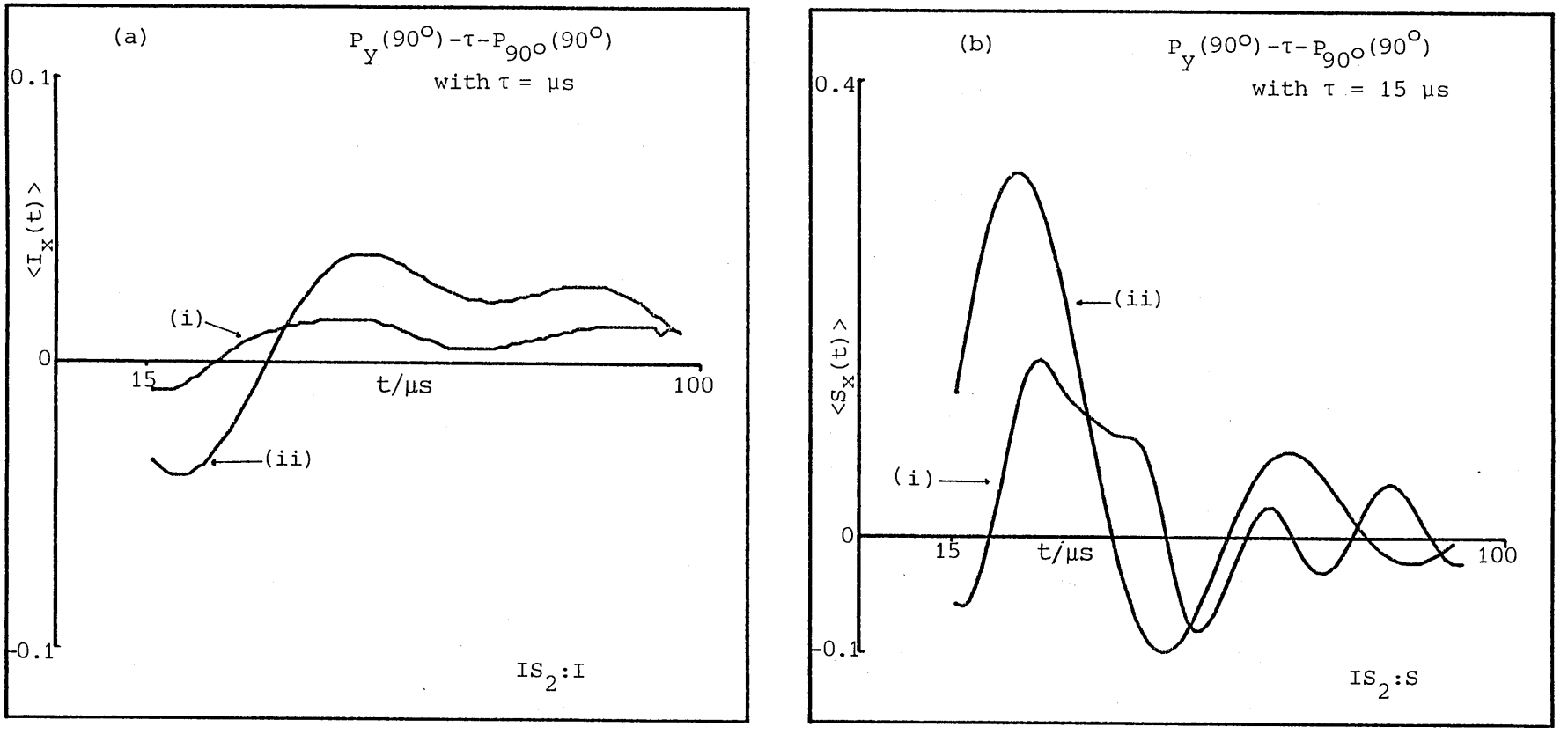

Figure 5.2 The magnitude of the cross-term components for the IS_2 spin system for the pulse sequence shown, (a) I spin response and (b) S spin response.

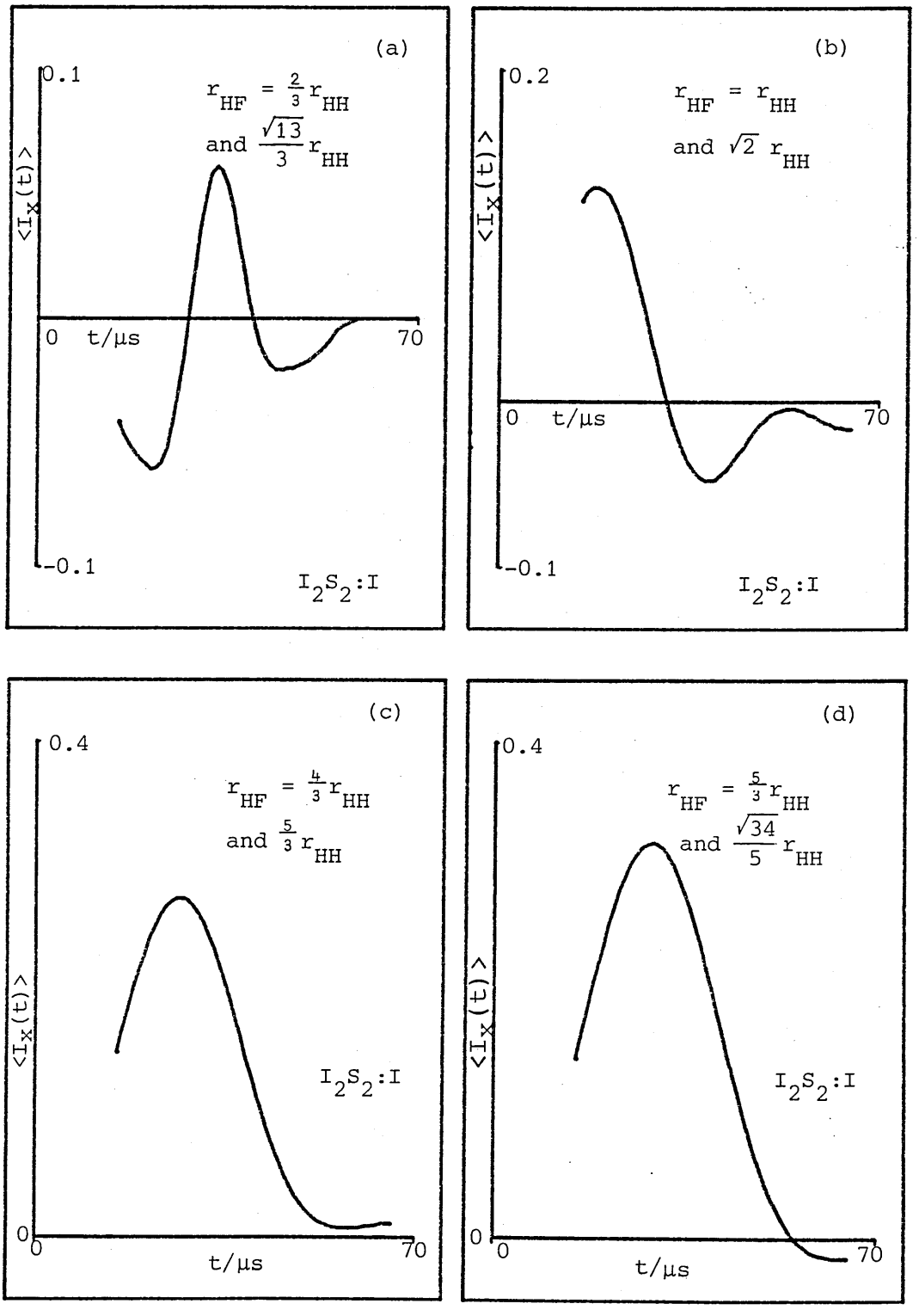

Figure 5.3 The magnitude of the cross-term component for the I spin in an H_2F_2 spin system for a $P_y(90^o)$-τ-$P_{90^o}(90^o)$ pulse sequence with τ = 15 μs. In each case the spin system geometry is such that $r_{HH} = r_{FF} = 0.18$ nm. The HF separations are expressed as fractions of r_{HH}.

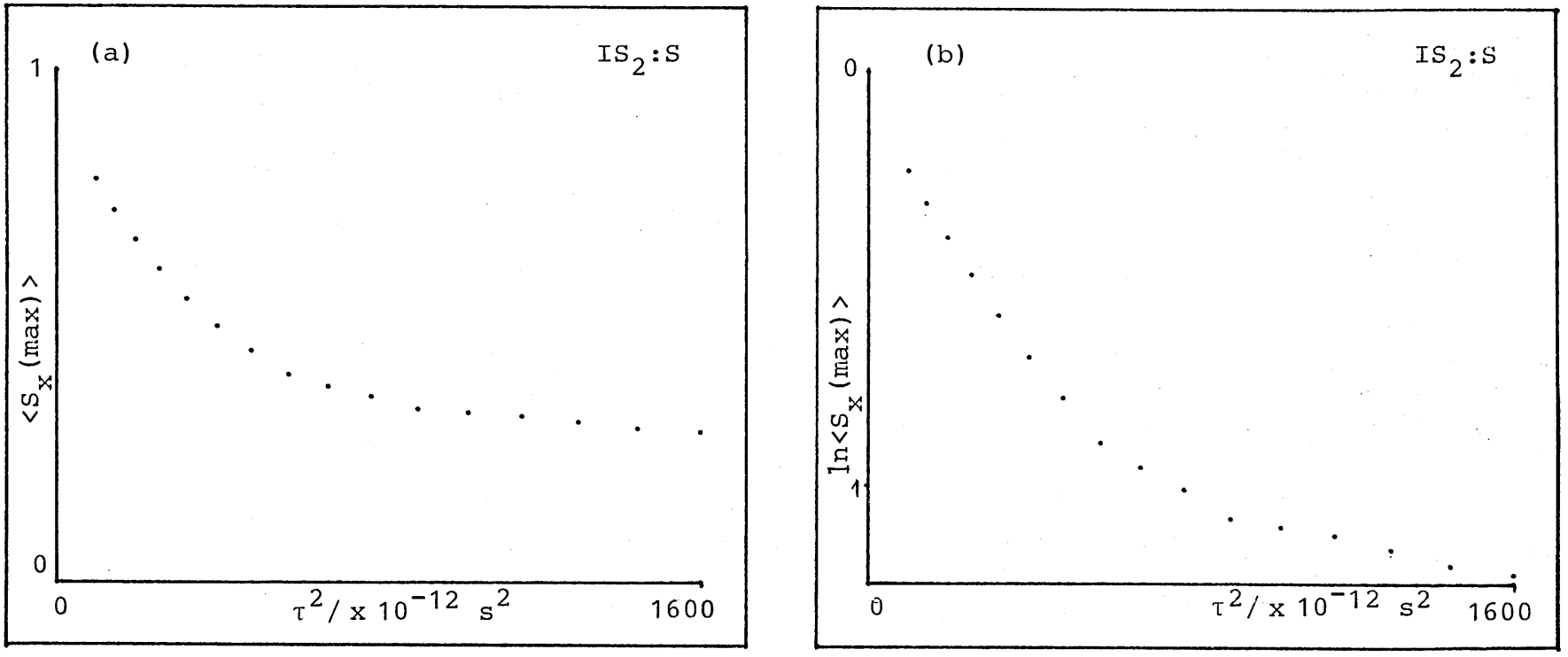

Figure 5.4 The maximum signal amplitude for the S spin response of system (i) to the the $P_y(90^o)$-τ-$P_x(180^o)$ pulse sequence.

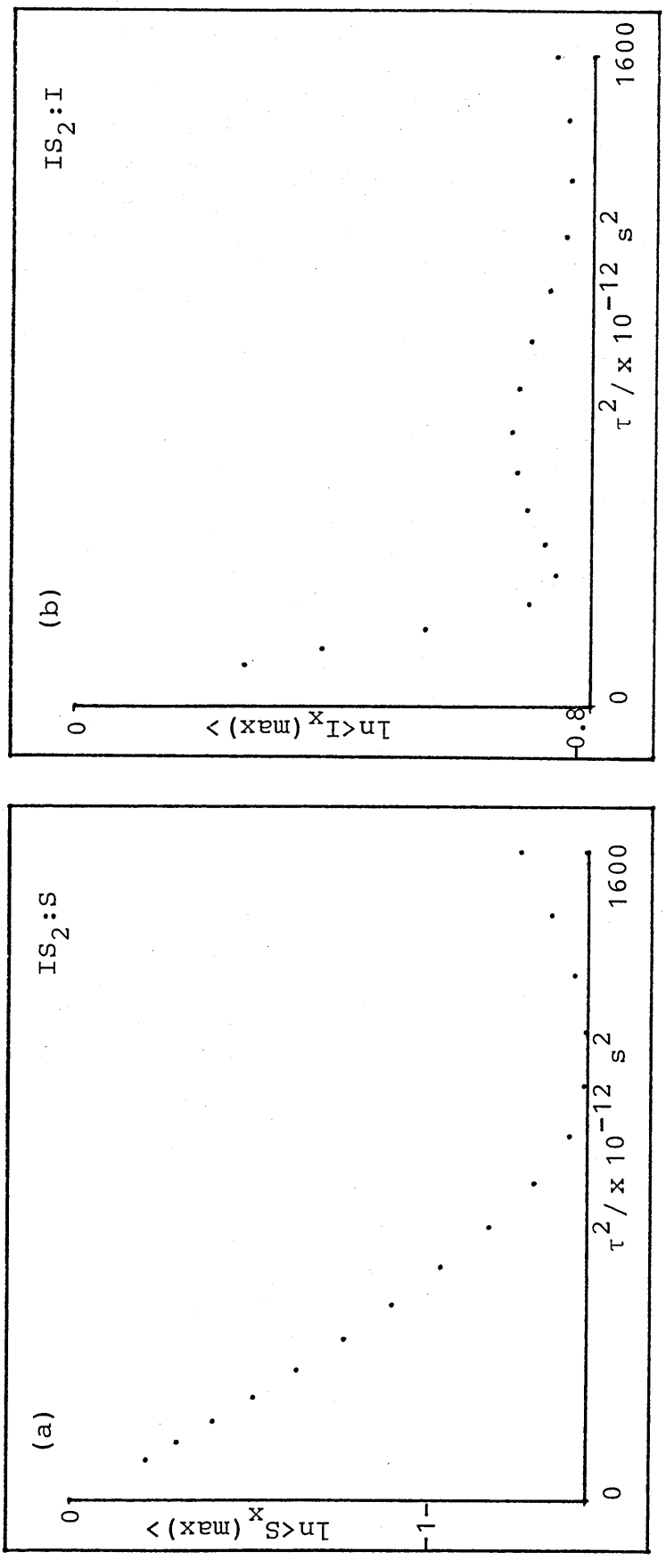

Figure 5.5 Plots of ln(maximum signal amplitude) versus τ^2 for the S and I responses of system (ii) to the $P_y(90^o)-\tau-P_x(90^o)$ pulse sequence.

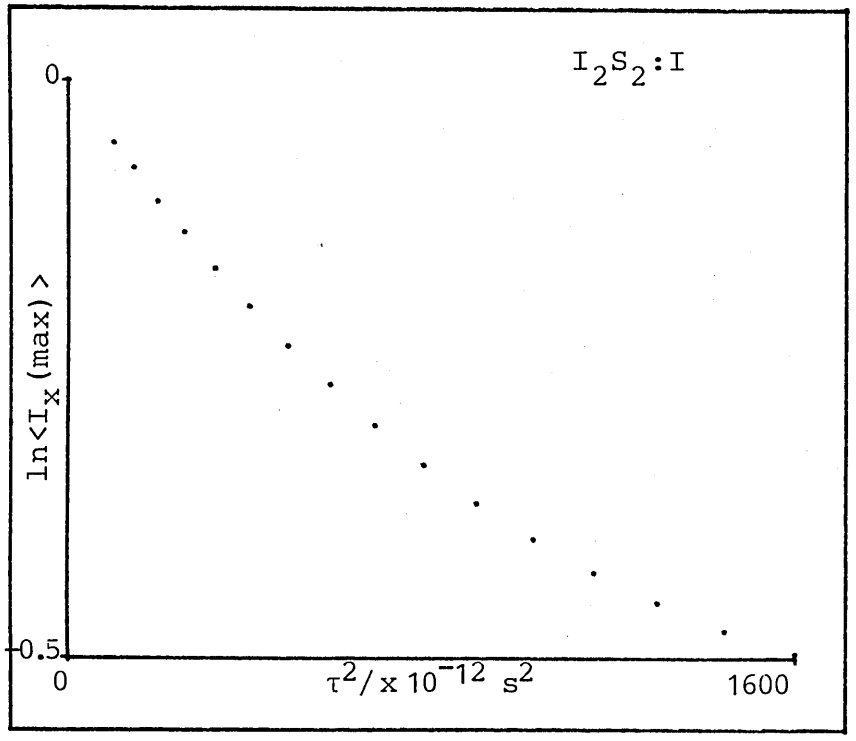

Figure 5.6 Plots of ln(maximum signal amplitude) versus τ^2 for the I spin response of system (iii) to the $P_y(90^o)$-τ-$P_x(90^o)$ pulse sequence

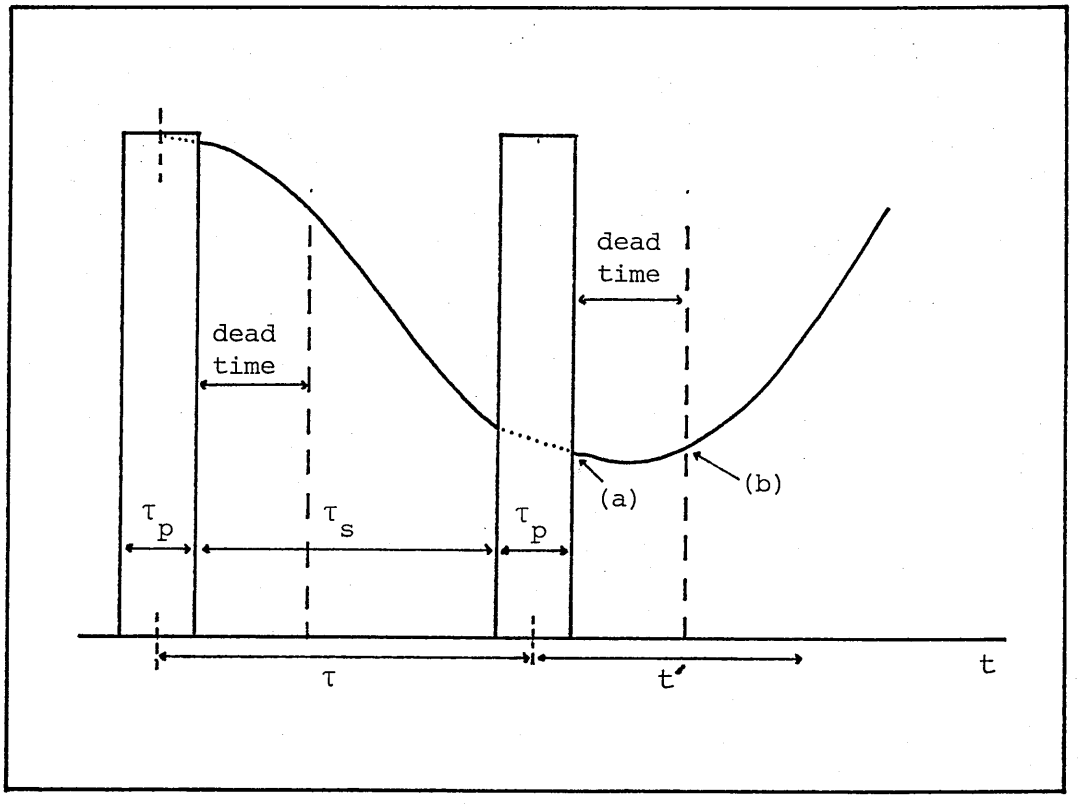

Figure 5.7 The effective pulse spacing when the pulses have a finite width is $\tau_s + \tau_p$, assuming that the signal starts in the middle of the pulse. (a) is the first point recorded by the spectrometer ($t' = \frac{1}{2}\tau_p$). (b) is the first point unaffected by the recovery of the spectrometer following the pulse.

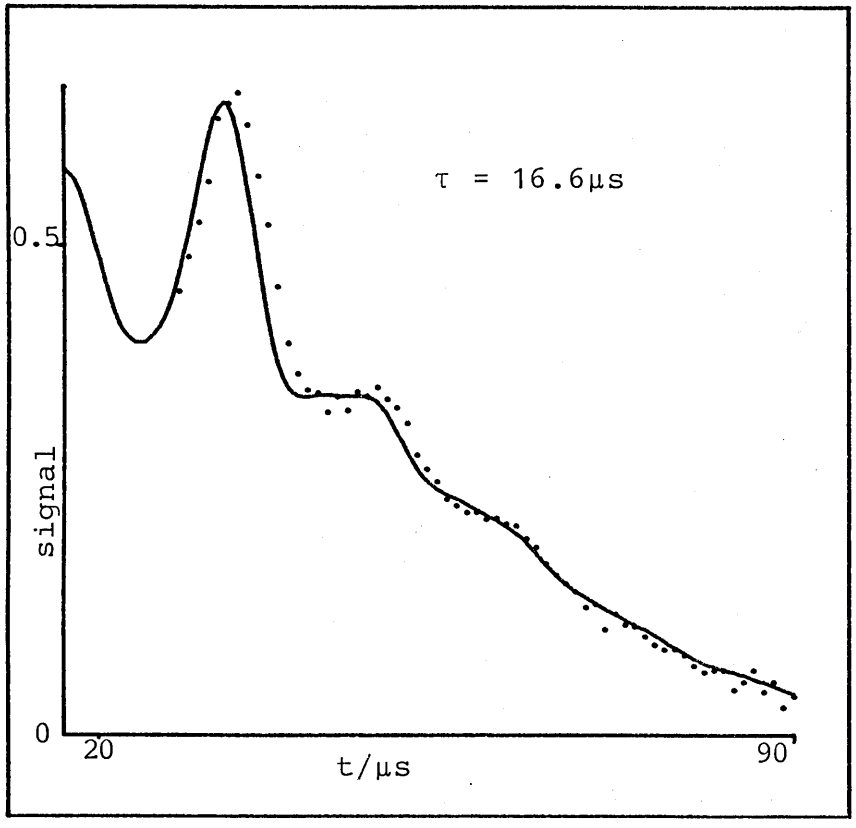

Figure 5.8 The experimental (....) and calculated (-) ^{1}H response to the $P_x(90^{o})$ sequence for polycrystalline KHF_2 at 293 K.

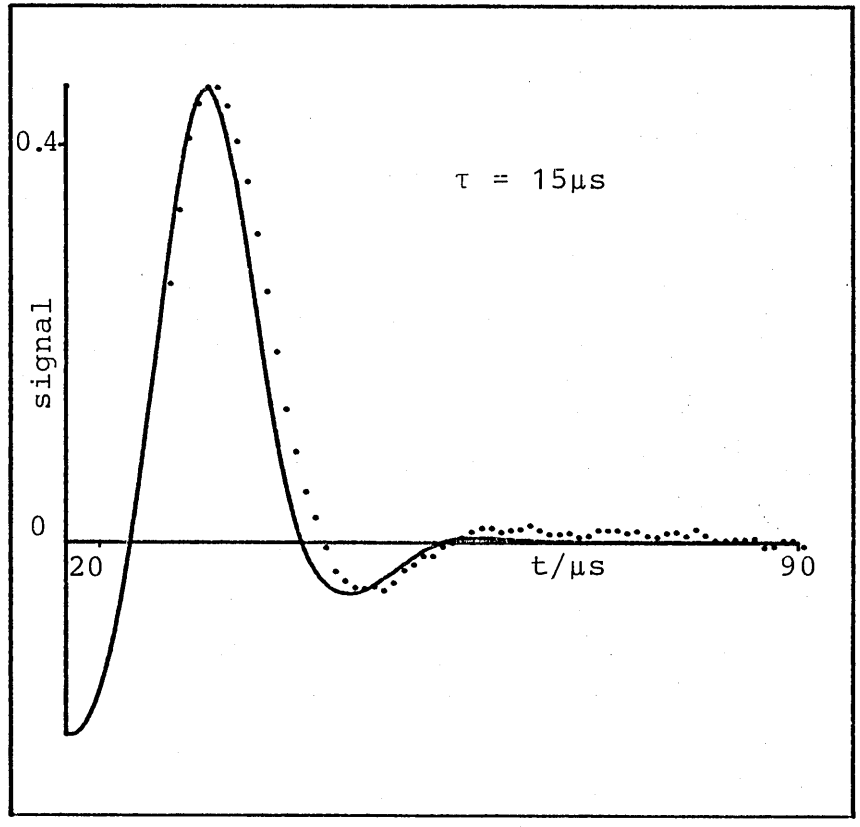

Figure 5.9 The experimental (....) and calculated (-) ^{19}F response to the $P_x(90^{o})$ sequence for polycrystalline KHF_2 at 293 K.

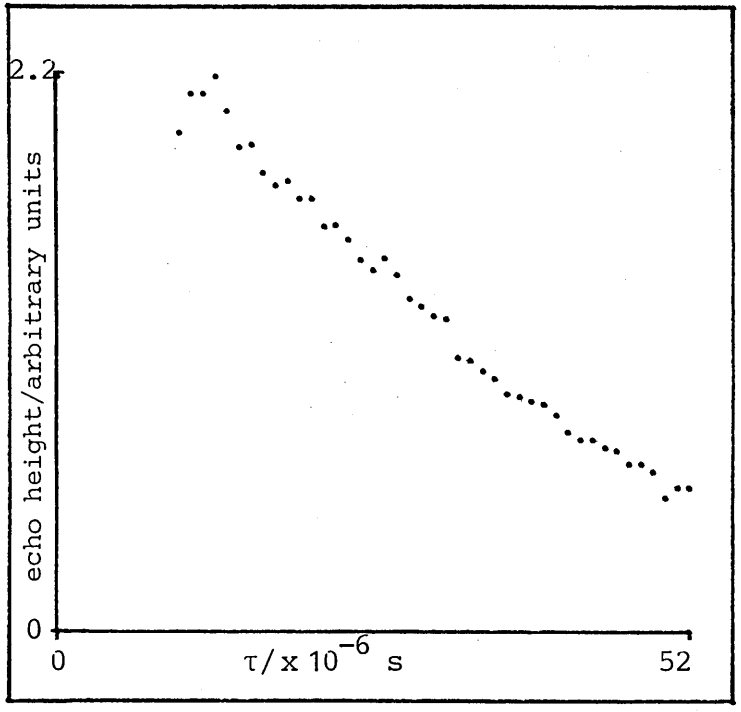

Figure 5.10 The ^1H echo height as a function of pulse spacing for a $P_x(90^o)$ sequence for polycrystalline KHF_2 at 293 K.

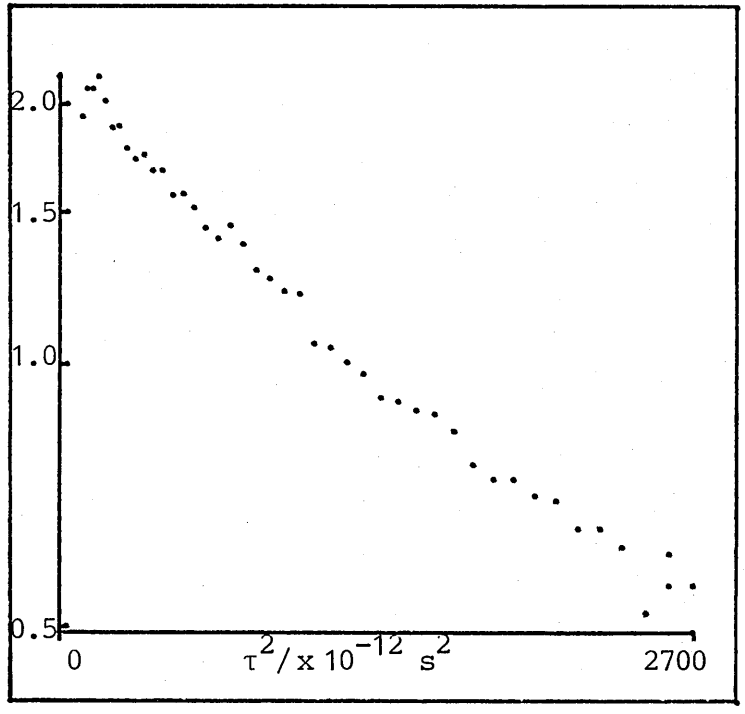

Figure 5.11 Log-normal plot of the ^1H echo height versus τ^2 for a $P_x(90^o)$ sequence for polycrystalline KHF_2 at 293 K.

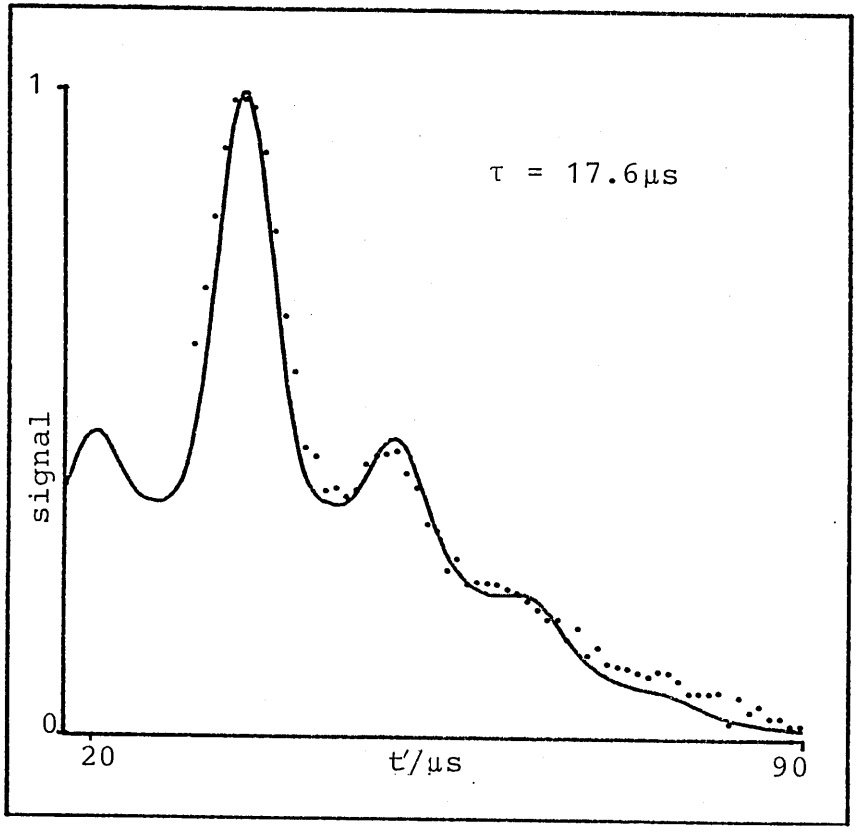

Figure 5.12 The experimental (....) and calculated (-) ^{1}H response to a $P_x(180^o)$ sequence for polycrystalline KHF_2 at 293 K.

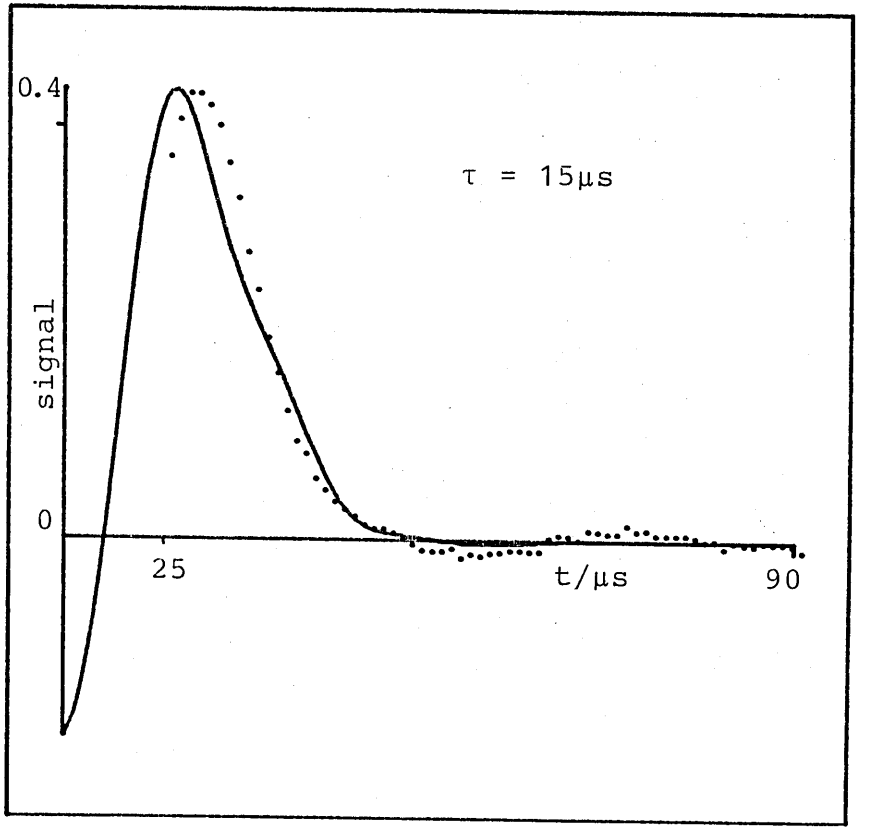

Figure 5.13 The experimental (....) and calculated (-) ^{19}F response to a $P_x(180^o)$ sequence for polycrystalline KHF_2 at 293 K.

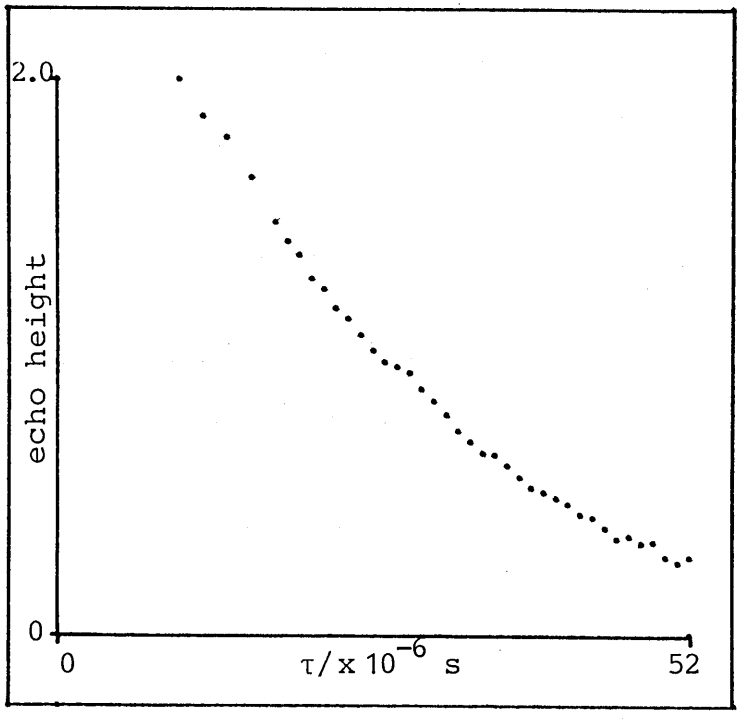

Figure 5.14 The ^1H echo height as a function of pulse spacing for a $P_x(180^o)$ sequence for polycrystalline KHF_2 at 293 K.

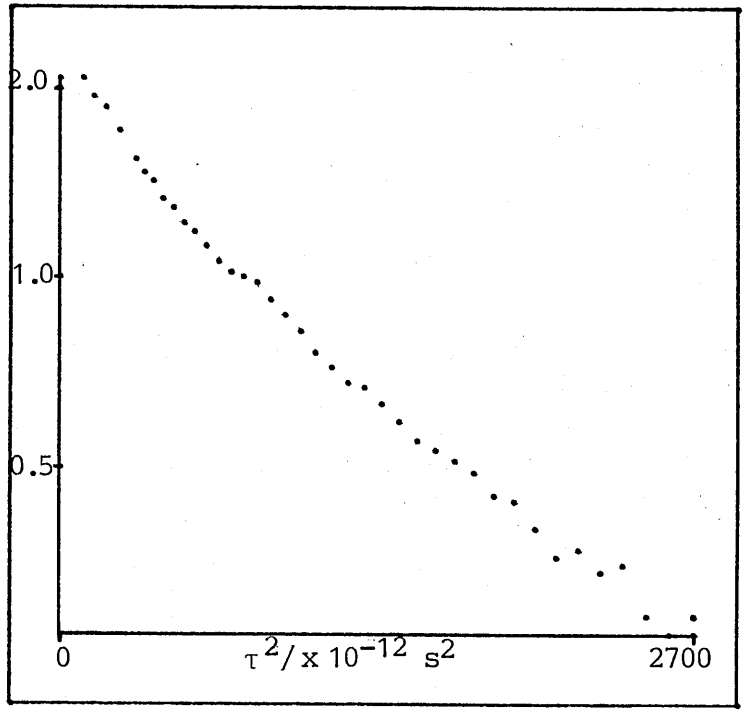

Figure 5.15 Log-normal plot of the ^1H echo height versus τ^2 for a $P_x(180^o)$ sequence for polycrystalline KHF_2 at 293 K.

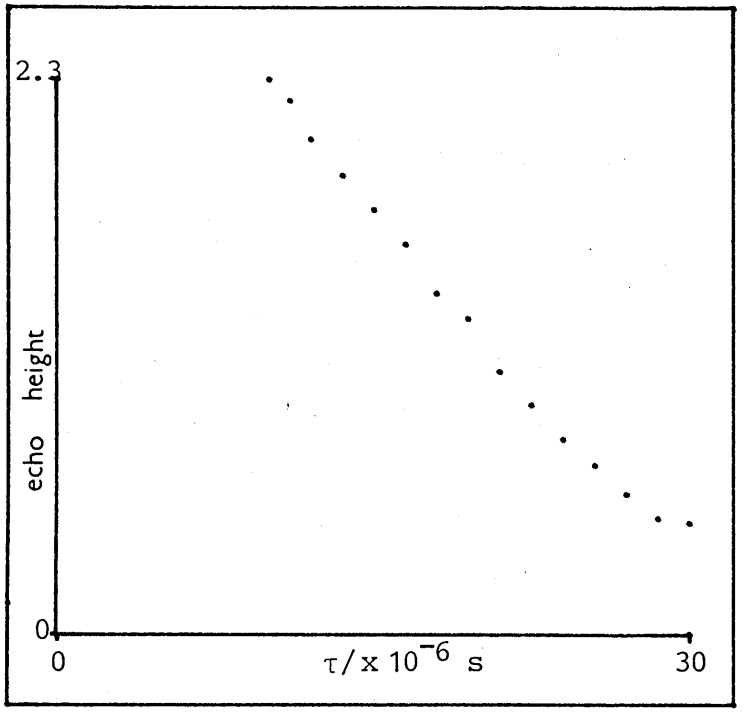

Figure 5.16 The ^{19}F echo height as a function of pulse spacing for a $P_x(180^o)$ sequence for polycrystalline KHF_2 at 293 K.

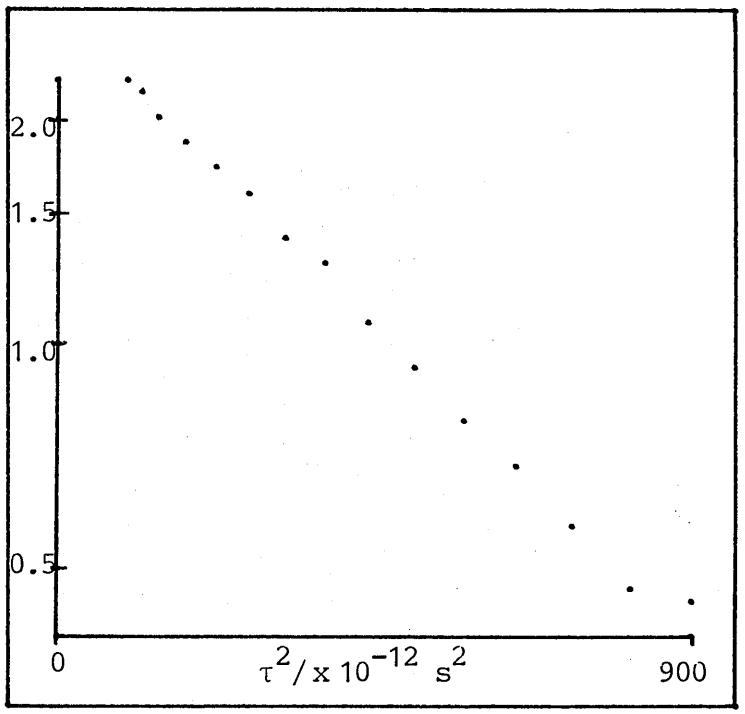

Figure 5.17 Log-normal plot of the ^{19}F echo height versus τ^2 for a $P_x(180^o)$ sequence for polycrystalline KHF_2 at 293 K.

5.6 References

(1) N. Boden and M. Gibb, Mol. Phys., 27(5), 1359-1371 (1974).

(2) N. Boden, M. Gibb, Y.K. Levine and M. Mortimer, J. Mag. Res., 16, 471-482 (1974).

(3) J.F.M. Post, R.L. Kamman and H.J.C. Berendsen, J. Mag. Res., 47, 264-281 (1982).

(4) C. Charlson, M. Mortimer and G. Oates, unpublished work.

(5) N. Boden and P.K. Kahol, Mol. Phys., 50(4), 645-665 (1983).

(6) N. Boden, L.D. Clark, C.G. Clarke and P.K. Kahol, Mol. Phys., 50(4), 667-698 (1983).

(7) N. Boden and P.K. Kahol, Mol. Phys., 40(5), 1117-1135 (1980).

(8) E.A. Moore and M. Mortimer, Phys. Letters, 80A(2,3) 195-198 (1980).

(9) N. Boden, L.D. Clark, S.M. Hanlon and M. Mortimer, Faraday Symp. Chem. Soc., 13, 109-123 (1979) (published 1978).

(10) P. Mansfield, Phys. Rev., 137(3A), A961-A974 (1965).

(11) M. Engelsberg and R.E. Norberg, Phys. Rev. B, 5(9), 3395-3406 (1972).

(12) W.W. Warren and R.E. Norberg, Phys. Rev. 154(2), 277-286 (1967).

(13) D.K. Hutchins and S.M. Day, Phys. Rev, 180(2), 432-438 (1969).

(14) S. Albert and J.A. Ripmeester, J. Chem. Phys., 70(3), 1352-1358 (1979).

(15) Yu. N. Moskvich, N.A. Sergeev and G.I. Dotsenko, Phys. Stat. Sol.(a), 30, 409-418 (1975).

(16) A Abragam, 'The Principles of Nuclear Magnetism', Clarendon Press, Oxford, 1961.

CHAPTER SIX

Nuclear Spin Relaxation in IS Spin Systems: Theory and Application to the Hydrogen Difluoride Ion in KHF_2 and $CsHF_2$

For a number of years the measurement of NMR spin relaxation times has proved to be a powerful technique for the characterisation, and determination of the rate, of molecular reorientation processes in solids (Abragam(1), Allen(2), Wolf(3), Torchia and Szabo(4)). Such measurements are also sensitive to the nature of any structural phase transition. In this final chapter theoretical and experimental spin relaxation in solids containing heteronuclear spin systems is investigated. In particular nuclear spin-lattice relaxation in polycrystalline potassium and caesium hydrogen difluorides is considered.

The theory for spin relaxation processes in a system of two spins was first presented by Solomon(5): for a pair of interacting unlike spins, I and S, the nuclear spin-lattice relaxation can become non-exponential depending on the rate of molecular motion. The complexity of coupled I,S nuclear spin relaxation has been demonstrated by O'Reilly(6) in a study of ammonium fluoroberyllate. There have, however, been relatively few studies of spin relaxation in heteronuclear spin systems; perhaps because of the lack of well characterised samples or because of the added complexity of the coupled relaxation between the I and S spins as well as their relaxation to the lattice. Nevertheless, as will be demonstrated here, this added complexity can be used to advantage to characterise motional processes.

In the theoretical part of this chapter the irreducible spherical tensor operator notation (introduced in Chapter One) will be used to describe a theory for spin-lattice relaxation, due to thermal reorientation processes, for heteronuclear spin systems in solids. The approach used allows expressions for

either single crystal or polycrystalline samples to be derived. So that the theory can be applied to real systems three specific motional models are described: (i) a three spin, two site model, (ii) a four spin, two site model and (iii) a multi-site intramolecular rotation model. Two of the models ((i) and (ii)) are used in the interpretation of experimental spin-lattice relaxation measurements for polycrystalline potassium and caesium hydrogen difluorides. The relaxation behaviour in these systems can be both double and (apparently) single exponential; as will be shown this occurs because the coefficients governing the relative proportions of the two exponential components are temperature dependent. The investigation of $CsHF_2$ is more detailed than that for KHF_2 since a comprehensive spin relaxation study of the latter has been reported by Furukawa and Kiriyama(7). The results for $CsHF_2$ differ substantially from those reported by Kriger, Gabuda and Moroz(8) in which non-exponential relaxation behaviour was apparently not observed. The behaviour of the ^1H and ^{19}F spin-lattice relaxation times for $CsHF_2$ in the vicinity of the structural phase transition at 334 K (Westrum(9)) is of particular interest.

6.1 The Derivation of Relaxation Rates

In this section we will investigate the influence of molecular motion, rotational motion in particular, on spin-lattice relaxation rates in heteronuclear spin systems. The general approach used here is based on that given by Abragam(1) and recently reviewed by Spiess(10).

The Hamiltonians that we used in calculating the time development of the NMR signal after a given pulse sequence

were time independent - the rigid lattice approximation. When there is motion in the system the Hamiltonians become time dependent and the equation of motion of the density matrix (equation 1.40) in the rotating frame becomes:

$$\frac{d\sigma_R}{dt} = -i[\mathcal{H}_R(t), \sigma_R] . \qquad 6.01$$

In this study the Hamiltonian $\mathcal{H}_R$ will be the dipolar Hamiltonian in the rotating frame. We shall ignore the shielding interaction and assume that $\omega_R = \omega = \omega_0$ so

$$\sigma_R = \exp(i\omega_0 I_0 t)\ \sigma\ \exp(-i\omega_0 I_0 t). \qquad 6.02$$

Abragam(1) shows that equation 6.01 can be written as

$$\frac{d\sigma_R}{dt} = -\int_0^\infty \langle [\mathcal{H}_R(t), [\mathcal{H}_R(t-\tau), \sigma_R(t)]] \rangle d\tau \qquad 6.03$$

where the brackets <> represent an average over a statistical ensemble, τ (which must not be confused with the pulse spacing of previous chapters) is a time interval which is much longer than the time it takes for a molecular reorientation to occur within the sample; it is assumed that the motion takes the form of discrete jumps. Equation 6.03 is only an approximation. Abragam discusses, in detail, the conditions that must hold if the approximation is to be accurate. We shall assume that these conditions apply in the work presented in this chapter. For simplicity we have used $\sigma_R(t)$ in equation 6.03 and will use it in subsequent equations but it is understood (Abragam(1)) to represent the departure of the density matrix from its equilibrium value: $\sigma_R(t) - \sigma_R(0)$.

Now that motion has been introduced it is easier, as will become clear, to adopt the irreducible spherical tensor notation described in Chapter One. The time dependence of the Hamiltonian in equation 6.03 can be expressed as follows:

$$\mathcal{H}_R^D(t) = \sum_{i<j} C_{ij} \sum_{M=-2}^{2} (-1)^M T^{(2)}_{M,ij}(t)\, R^{(2)}_{-M,ij}(t) \qquad 6.04$$

with, from equations 1.23 and 1.34

$$T^{(2)}_{M,ij}(t) = \sum_{m=-1}^{1} \langle 11m, M-m | 2M\rangle\, I_{m,i}\, I_{M-m,j}\, \exp(i\omega_{m,ij}t) \qquad 6.05$$

where

$$\omega_{m,ij} = m\omega_{0,i} + (M-m)\omega_{0,j}. \qquad 6.06$$

The substitution of equation 6.05 into 6.04 and the result into 6.03 produces

$$\frac{d\sigma_R}{dt} = -\sum_{i<j}\sum_{k<l} C_{ij}C_{kl} \int_0^\infty \sum_{M=-2}^{2}\sum_{M'=-2}^{2}\sum_{m=-1}^{1}\sum_{m'=-1}^{1} (-1)^{M+M'}$$
$$\langle 11m, M-m|2M\rangle\langle 11m', M'-m'|2M'\rangle \langle R^{(2)}_{-M,ij}(t)\, R^{(2)}_{-M',kl}(t-\tau)\rangle$$
$$\left[I_{m,i}\, I_{M-m,j}, [I_{m',k}\, I_{M'-m',l}, \sigma_R]\right] \exp(i\omega_{m,ij}t)$$
$$\exp(i\omega_{m,kl}(t-\tau))\, d\tau. \qquad 6.07$$

In this equation only those terms with $m' = -m$ and $M' = -M$ have a non-zero time average (the secular terms), it is also possible (Spiess(10)) to put $L' = L$. Then, with $\langle 11m, M-m|2M\rangle = \langle 11, -m, -M+m|2, -M\rangle$ and defining the spectral density $j^{(2)}_{M,ijkl}(\omega_{m,kl})$ and correlation function $g^{(2)}_{M,ijkl}(\tau)$ as

$$j^{(2)}_{M,ijkl}(\omega_{m,kl}) = (-1)^M \tfrac{1}{2}\int_{-\infty}^{\infty} g^{(2)}_{M,ijkl}(\tau)\, \exp(i\omega_{m,kl}\tau)\, d\tau$$
$$= (-1)^M \int_0^\infty \langle R^{(2)}_{-M,ij}(t)\, R^{(2)}_{M,kl}(t-\tau)\rangle \exp(i\omega_{m,kl}\tau)\, d\tau \qquad 6.08$$

equation 6.07 reduces to

$$\frac{d\sigma_R}{dt} = -\sum_{i<j}\sum_{k<l} C_{ij}C_{kl} \sum_{M=-2}^{2}\sum_{m=-1}^{1} (-1)^{-M} \langle 11m, M-m|2M\rangle^2 \left[I_{m,i}\right.$$
$$\left. I_{M-m,j}, [I_{-m,k}\, I_{-M+m,l}, \sigma_R]\right] \exp(i\omega_{m,ij}t - i\omega_{m,kl}t)$$
$$j^{(2)}_{M,ijkl}(\omega_{m,kl}). \qquad 6.09$$

Returning to the laboratory axes system (Abragam(1) and omitting the summation signs for convenience):

$$\frac{d\sigma}{dt} = -i[I_0,\sigma]\omega_0 + \exp(-i\omega_0 I_0 t)\,\frac{d\sigma_R}{dt}\exp(i\omega_0 I_0 t). \qquad 6.10$$

The last term in equation 6.10 will remove the various exponentials in t from equation 6.09. For spin-lattice relaxation equations 6.09 and 6.10 must be equivalent - the z-axis is unaffected by the rotating frame transformation - we shall see shortly that this is the case.

The spin-lattice relaxation rate is, phenomenologically, the rate at which the magnetisation returns to equilibrium in the z-direction:

$$\frac{d\langle I_0\rangle}{dt} = -\frac{1}{T_1}\langle I_0\rangle .$$

To calculate T_1, then, we need an expression for $d\langle I_0\rangle/dt$. Multiplying equation 6.10 by I_0 and taking the trace gives, using equation 1.35,

$$\frac{d}{dt}\langle I_0\rangle = \mathrm{Tr}\{-i[I_0,\sigma]I_0\omega_0\} + \mathrm{Tr}\{e^{-i\omega_0 I_0 t}\,\frac{d\sigma_R}{dt}\,e^{i\omega_0 I_0 t}\,I_0\}$$

the first term is equivalent to

$$\mathrm{Tr}\{i\sigma[I_0,I_0]\omega_0\} = 0$$

and the second depends on

$$\mathrm{Tr}\{\left[I_{m,i}\;I_{M-m,j},[I_{-m,k}\;I_{-M+m,l},\sigma_R\right]I_0\}$$

which can be rearranged to give the expectation value

$$\langle\left[I_{-m,k}\;I_{-M+m,l},[I_{m,i}\;I_{M-m,j},I_0\right]\rangle. \qquad 6.11$$

At this point it is necessary to decide on the form of I_0. For relaxation caused by interactions between like spins the sum

$$I_0 \equiv \sum_q I_{0,q} \qquad 6.12$$

can run over all spins and the commutators in equation 6.11 become

$$M[I_{m,i}\ I_{M-m,j}, I_{-m,k} I_{-M+m,l}].$$

For relaxation caused by interactions between unlike (IS) spins the sum in equation 6.12 is restricted to the I spins only, if spin i is assumed to be an I spin and spin j to be an S spin the commutators become

$$m[I_{m,i}\ S_{M-m,j}, I_{-m,k}\ I_{-M+m,l}]$$

It follows that, for homonuclear interactions

$$\frac{d}{dt}\langle \sum_{i<j} (I_{0,i} + I_{0,j})\rangle = -\sum_{i<j}\sum_{k<l} C_{ij}C_{kl} \sum_{M=-2}^{2} \sum_{m=-1}^{1} (-1)^{-M} \langle 11m, M-m | 2M\rangle^2 M\langle [I_{m,i}\ I_{M-m,j}, I_{-m,k}\ I_{-M+m,l}]\rangle$$

and, for heteronuclear interactions

$$\frac{d}{dt}\langle \sum_i I_{0,i}\rangle = -\sum_i \sum_j \sum_{k<l} C_{ij}C_{kl} \sum_{M=-2}^{2} \sum_{m=-1}^{1} (-1)^{-M} \langle 11m, M-m | 2M\rangle^2 m\langle [I_{m,i}\ S_{M-m,j}, I_{-m,k}\ I_{-M+m,l}]\rangle$$

where the sum over i is over I spins only and that over j is over S spins only.

A commutator of the form $[I_{m,i}\ I_{M-m,j}, I_{-m,k}\ I_{-M+m,l}]$ is zero if k and l are both different from i or j. There are two other possibilities:

i) when k or l is i or j:

$$[I_{m,i}\ I_{M-m,j}, I_{-m,i}\ I_{-M+m,l}] = -mI_{0,i}\ I_{M-m,j}\ I_{-M+m,l}$$

and

$$[I_{m,i}\ I_{M-m,j}, I_{-m,k}\ I_{-M+m,j}] = -(M-m) I_{m,i}\ I_{0,j}\ I_{-m,k},$$

any other combination of subscripts gives expressions analogous to these. (M-m) and m can take the values $0,\pm1$ so the expectation values of the commutators are of the form $\langle I_{0,i}\ I_{0,j}\ I_{0,l}\rangle$, $\langle I_{+1,i}\ I_{0,j}\ I_{-1,l}\rangle$ or permutations of these, their values depend on the density matrix. After a single 90° pulse ($\sigma \propto I_x$) it can be shown, using the properties of the trace, that these expectation values are both zero. This raises the possibility that, for a more complicated density matrix, say that after two or more pulses, the relaxation rate could be different from that after a single pulse.

ii) when k and l are i and j respectively:

$$[I_{m,i}\ I_{M-m,j}, I_{-m,i}\ I_{-M+m,j}] = -(M-m) I_{m,i}\ I_{-m,i}\ I_{0,j} - mI_{0,i}\ I_{-M+m,j}\ I_{M-m,j}.$$

The expectation values of this commutator are given in Table 6.1. In the table, for like spins $\langle I_{0,j}\rangle = \langle I_{0,i}\rangle$ and, from now on, we will drop the subscripts on the I_i, I_j so $I_j = I_i = I$. These expressions for the commutators also apply when spin j is an S spin ($I_{m,j} \rightarrow S_{m,j}$, $I_j \rightarrow S$). It is now clear that only those terms with k = i and l = j are non-zero for spin-lattice relaxation so it follows that the exponential in t in equation 6.09 can be dropped, then

$$\frac{d}{dt}\langle I_0\rangle_R = \frac{d}{dt}\langle I_0\rangle$$

as we predicted.

We are now in a position to write, for homonuclear interactions

$$\frac{d}{dt}\langle I_{0,i}\rangle = -\tfrac{1}{6}\sum_j c_{ij}^2\ I(I+1)\,[4j^{(2)}_{2,ijij}(2\omega_{0,I}) + j^{(2)}_{1,ijij}(\omega_{0,I})]\langle I_{0,i}\rangle \qquad 6.13$$

Table 6.1 The commutator $[I_{m,i}\ I_{M-m,j},\ I_{-m,i}\ I_{-M+m,j}]$

M	m	Commutator	Expectation Value[1]
±2	±1	$\pm\frac{1}{2}[(\mathbf{I}_i^2-I_{0,i}^2)I_{0,j} + (\mathbf{I}_j^2-I_{0,j}^2)I_{0,i}]$	$\pm\frac{1}{3}[I_i(I_i+1)\langle I_{0,j}\rangle + I_j(I_{j+1})\langle I_{0,i}\rangle]$
±1	±1	$\mp I_{0,i}\ I_{0,j}^2$	$\mp\frac{1}{3}I_j(I_{j+1})\langle I_{0,i}\rangle$
±1	0	$\mp I_{0,i}^2\ I_{0,j}$	$\mp\frac{1}{3}I_i(I_{i+1})\langle I_{0,j}\rangle$
0	±1	$\mp\frac{1}{2}[(\mathbf{I}_i^2-I_{0,i}^2)I_{0,j} - (\mathbf{I}_j^2-I_{0,j}^2)I_{0,i}]$	$\mp\frac{1}{3}[I_i(I_i+1)\langle I_{0,j}\rangle - I_j(I_{j+1})\langle I_{0,i}\rangle]$

[1] In the high temperature approximation (Section 1.5) $\mathbf{I}^2 = I(I+1)$ and $I_0^2 = \frac{1}{3}I(I+1)$

where the sum over j is over all the surrounding I spins. We used Brink and Satchler(11) to evaluate the Clebsch-Gordan coefficients and used the fact that $j^{(2)}_{M}(\omega_m) = j^{(2)}_{-M}(\omega_{-m})$ to write equation 6.13. Similarly, for heteronuclear interactions

$$\frac{d}{dt}\langle I_{0,i}\rangle = -\tfrac{1}{9}\sum_j C^2_{ij}[S(S+1)(6j^{(2)}_{2,ijij}(\omega_{0,I}+\omega_{0,S}) + 3j^{(2)}_{1,ijij}(\omega_{0,I}) + j^{(2)}_{0,ijij}(\omega_{0,I}-\omega_{0,S}))\langle I_{0,i}\rangle + I(I+1)(6j^{(2)}_{2,ijij}(\omega_{0,I}+\omega_{0,S}) - j^{(2)}_{0,ijij}(\omega_{0,I}-\omega_{0,S}))\langle S_{0,j}\rangle] \qquad 6.14$$

where the sum over j is over all the S spins surrounding the i^{th} spin, it is assumed that all the I spins are equivalent. The relaxation rate of a sample must be the same as that for an individual spin so it is possible to define a macroscopic relaxation rate such that

$$\frac{d}{dt}\langle I_{0,i}\rangle = -(\frac{1}{T^I_1} + \frac{1}{T^{II}_1})\langle I_{0,i}\rangle - \frac{1}{T^{IS}_1}\langle S_{0,j}\rangle \qquad 6.15$$

where

$$\frac{1}{T^I_1} = \frac{2I(I+1)}{3}(\gamma_I^2\hbar\mu_0/4\pi)^2\sum_j[4j^{(2)}_{2,ijij}(2\omega_{0,I}) + j^{(2)}_{1,ijij}(\omega_{0,I})], \qquad 6.16$$

$$\frac{1}{T^{II}_1} = \frac{4S(S+1)}{9}(\gamma_I\gamma_S\hbar\mu_0/4\pi)^2\sum_j[6j^{(2)}_{2,ijij}(\omega_{0,I}+\omega_{0,S}) + 3j^{(2)}_{1,ijij}(\omega_{0,I}) + j^{(2)}_{0,ijij}(\omega_{0,I}-\omega_{0,S})] \qquad 6.17$$

and

$$\frac{1}{T^{IS}_1} = \frac{4I(I+1)}{9}(\gamma_I\gamma_S\hbar\mu_0/4\pi)^2\sum_j[6j^{(2)}_{2,ijij}(\omega_{0,I}+\omega_{0,S}) - j^{(2)}_{0,ijij}(\omega_{0,I}-\omega_{0,S})]. \qquad 6.18$$

A way of evaluating the spectral densities, the $j^{(2)}_{M,ijij}(\omega_{m,ij})$, must now be found. The spectral density is the Fourier transform of the correlation function.

6.2 The Correlation Function

The correlation function, $g^{(2)}_{M,ijij}(\tau)$, is defined by equation 6.08

$$g^{(2)}_{M,ijij}(\tau) = \langle R^{(2)}_{-M,ij}(t)\ R^{(2)}_{M,ij}(t-\tau)\rangle,$$

it contains the details of the motional process causing relaxation. If it is assumed that the motion is random and stationary the time origin can be moved without affecting the average

$$g^{(2)}_{M,ijij}(\tau) = \langle R^{(2)}_{-M,ij}(t+\tau)\ R^{(2)}_{M,ij}(t)\rangle. \qquad 6.19$$

The $R^{(2)}_{M}$ are defined in the LAB coordinate system, they are related to the values in a crystal based system, CRY, through (equation 1.21)

$$R^{(2)}_{M,ij}(t) = \sum_{M'=-2}^{2} R^{(2),CRY}_{M',ij}(t)\,\mathcal{D}^{(2)}_{M'M}(\Phi)$$

and

$$R^{(2)}_{-M,ij}(t+\tau) = \sum_{N'=-2}^{2} R^{(2),CRY}_{N',ij}(t+\tau)\,\mathcal{D}^{(2)}_{N',-M}(\Phi)$$

where $\Phi = (\phi,\theta,\Psi)$ - the angles which rotate the CRY system into coincidence with the LAB system, these are independent of time (the crystal is stationary with respect to the laboratory). If the sample is polycrystalline every possible set of angles Φ can occur and a polycrystalline average (Section 3.1) must be taken: the angular part of the correlation function is independent of the angle Ψ so it can be written, for a powder, as

$$g^{(2)}_{M,ijij}(\tau)_p = \frac{1}{4\pi}\int_0^{2\pi}\int_0^{\pi} \sum_{M'=-2}^{2}\sum_{N'=-2}^{2} \mathcal{D}^{(2)}_{N',-M}(\Phi)\,\mathcal{D}^{(2)}_{M'M}(\Phi)\ \sin\theta d\theta d\phi$$
$$\langle R^{(2)}_{N',ij}(t+\tau)\ R^{(2),CRY}_{M',ij}(t)\rangle.$$

Using equations A8 and A9 it follows that $M' = -N'$ and then

$$g^{(2)}_{M,ijij}(\tau)_p = \sum_{M'=-2}^{2} \tfrac{1}{5}(-1)^{M'-M} \langle R^{(2),CRY}_{-M',ij}(t+\tau)\ R^{(2),CRY}_{M',ij}(t)\rangle .$$

The dipolar PAS and the CRY system are related through a further transformation:

$$R^{(2),CRY}_{M',ij}(t) = \rho^{(2)}_{0,ij}(t)\mathcal{D}^{(2)}_{0M'}(\Omega_{ij}(t))$$

and

$$R^{(2),CRY}_{-M',ij}(t+\tau) = \rho^{(2)}_{0,ij}(t+\tau)\mathcal{D}^{(2)}_{0,-M'}(\Omega_{ij}(t+\tau))$$

where $\Omega_{ij}(t) = (\alpha(t),\beta(t),\gamma(t))_{ij}$. Only $\rho^{(2)}_0$ is non-zero for the dipolar interaction ($\rho^{(2)}_0 = \sqrt{\tfrac{3}{2}} r^{-3}_{ij}$ - Table 1.1) so no additional summation is needed. The time dependence in the internuclear separation in these equations allows changes in the separation, caused by the relative motion of the spins, to be included in the calculation: if the separation were to remain fixed it would effectively restrict the calculation to relaxation, in rigid molecules, caused by intramolecular interactions. Now

$$g^{(2)}_{M,ijij}(\tau)_p = \tfrac{3}{10}\sum_{M'=-2}^{2}(-1)^{M'-M}\langle r^{-3}_{ij}(t+\tau)\ r^{-3}_{ij}(t)\,\mathcal{D}^{(2)}_{0,-M'}(\Omega_{ij}(t+\tau))\,\mathcal{D}^{(2)}_{0M'}(\Omega_{ij}(t))\rangle . \qquad 6.20$$

For a single crystal the first transformation (CRY → LAB) is not necessary and the angles Ω_{ij} can relate the PAS directly to the LAB system. With $\Phi = 0$

$$\mathcal{D}^{(2)}_{N',-M}(0)\mathcal{D}^{(2)}_{M'M}(0) = \delta_{N',-M}\,\delta_{M'M}$$

so, for a single crystal, the correlation function is

$$g^{(2)}_{M,ijij}(\tau) = \tfrac{3}{2}\langle r^{-3}_{ij}(t+\tau)\ r^{-3}_{ij}(t)\mathcal{D}^{(2)}_{0,-M}(\Omega_{ij}(t+\tau))\mathcal{D}^{(2)}_{0M}(\Omega_{ij}(t))\rangle . \qquad 6.21$$

However, although this equation is relatively simple it does make the calculation of the relaxation time difficult if the calculation is to be carried out over a range of crystal orientations (with respect to the field). This is because the $\mathcal{D}(\Omega_{ij})$ must be re-evaluated for each crystal orientation - a tedious process if the relaxation time is significantly affected by a large number of interactions. We can circumvent this problem by including the CRY → LAB transformation, as we did for the polycrystalline system, only this time we do not carry out the integration, instead:

$$g^{(2)}_{M,ijij}(\tau) = \sum_{M'=-2}^{2}\sum_{N'=-2}^{2} \mathcal{D}^{(2)}_{N',-M}(\Phi)\mathcal{D}^{(2)}_{M'M}(\Phi)\langle r_{ij}^{-3}(t)\mathcal{D}^{(2)}_{0M'}(\Omega_{ij}(t)) r_{ij}^{-3}(t+\tau)\mathcal{D}^{(2)}_{0N'}(\Omega_{ij}(t+\tau))\rangle. \quad 6.22$$

Now the angles Ω_{ij} (which relate the PAS and CRY system) need only be calculated once, any change in crystal orientation can be included in the angles Φ (which relate the CRY and LAB systems). The average in the last equation and that for the powder, equation 6.20, are of the same form so we need only one theory to evaluate them both. To carry out this evaluation, however, it is necessary to introduce a specific motional model.

6.3 The Evaluation of the Average

In this section we shall use the notation <> to represent the average in equation 6.20 or 6.22:

$$\langle\rangle = \langle r_{ij}^{-3}(t+\tau)\ r_{ij}^{-3}(t)\mathcal{D}^{(2)}_{0,-M}(\Omega_{ij}(t+\tau))\mathcal{D}^{(2)}_{0M}(\Omega_{ij}(t))\rangle.$$

This can be written as a probability:

$$\langle\rangle = \sum_{\Omega,r}(r_{ij}^{-3}\mathcal{D}^{(2)}_{0,-M}(\Omega_{ij})p(\Omega,r,\Omega^t,r^t,\tau) \sum_{\Omega^t,r^t}((r^t_{ij})^{-3}\mathcal{D}^{(2)}_{0M}(\Omega^t_{ij}))p(\Omega^t,r^t). \quad 6.23$$

The summations are over all possible values of Ω, r, Ω^t and r^t, $\Omega^t \equiv \Omega_{ij}(t)$, $\Omega \equiv \Omega_{ij}(t+\tau)$ and similarly for r^t and r. If there are many of these values and if the interval between them is small the summations can be replaced by integrals. $p(\Omega^t, r^t)$ is the probability of Ω^t and r^t occurring at time t and $p(\Omega, r, \Omega^t, r^t, \tau)$ is the probability that Ω and r occur at time τ after Ω^t and r^t occurred at time t. We will evaluate these probability functions for three different motional models (i) a three spin, two site model (Section 6.3.1), (ii) a four spin, two site model (Section 6.3.3) and (iii) a multisite, intramolecular rotation model (Section 6.3.4). Such models are relevant to heteronuclear relaxation in polycrystalline samples of metal hydrogen difluorides.

6.3.1 A Three Spin, Two Site Model

The three spin model can be used to calculate the I spin relaxation in IS_2 spin systems. The treatment is based on that given by Look and Lowe(12) who considered intermolecular relaxation for a pair of water molecules undergoing 180^o jumps. In the present work the relaxation of a stationary I spin (i), caused by two S spins exchanging sites (one of these spins is spin j), is studied. We assume that there is no cross-correlation between the two IS spin interactions so that we can treat each interaction separately (which effectively means that the problem is a two spin, two site model - apart from a factor of two). Because the S spins interchange sites there can be no relaxation of the S spins caused by intramolecular S,S spin interaction, providing the two sites are equivalent. Each S spin can occupy one of two sites, a or b.

Let $p_i(a)$ be the probability that spin i is at its a site, since this spin is stationary $p_i(a) = 1$. Similarly, let

$p_j(a,\tau)$ and $p_j(b,\tau)$ be the probability that spin j is at its a or b site, respectively, at time $t+\tau$. Let $p_j(a,b,\tau)$ be the probability that spin j is at its a site at time $t+\tau$ when it was at its b site at time t, there are analogous definitions for $p_j(b,a,\tau)$, $p_j(a,a,\tau)$ and $p_j(b,b,\tau)$. Then, from equation 6.23

$$\begin{aligned}<> = p_i(a)[&p_j(a,\tau=0)f^{(M')}(a,a)(p_j(a,a,\tau)f^{(-M')}(a,a) + \\ &p_j(b,a,\tau)f^{(-M')}(a,b)) + p_j(b,\tau=0)f^{(M')}(a,b) \\ &(p_j(b,b,\tau)f^{(-M')}(a,b) + p_j(a,b,\tau)f^{(-M')}(a,a))] \end{aligned} \quad 6.24$$

where $f^{(M')}(a,b)$ is $r_{ij}^{-3}\mathcal{D}^{(2)}_{0M'}(\Omega_{ij})$ evaluated with spin i at its a site and spin j at its b site.

If the probability, W, that spin j jumps from its a site to its b site is the same as the probability that it jumps from its b site to its a site and if the probability is the same for all the S spins then:

$$\frac{d}{d\tau}p_j(a,\tau) = -\frac{d}{d\tau}p_j(b,\tau) = -Wp_j(a,\tau) + Wp_j(b,\tau). \quad 6.25$$

Using $p_j(a,\tau) + p_j(b,\tau) = 1$ equation 6.25 can be solved to give

$$\ln(2p_j(a,\tau) - 1) = -2W\tau + c$$

and $$\ln(2p_j(b,\tau) - 1) = -2W\tau + c$$

where c is a constant of integration. Under initial conditions such that $p_j(a,\tau=0) = 1$ and $p_j(b,\tau=0) = 0$ it follows that

$$\left.\begin{aligned} p_j(a,\tau) = p_j(a,a,\tau) &= \tfrac{1}{2}(1 + e^{-\tau/\tau_c}) \equiv p_j(b,b,\tau) \\ \text{and} \\ p_j(b,\tau) = p_j(b,a,\tau) &= \tfrac{1}{2}(1 - e^{-\tau/\tau_c}) \equiv p_j(a,b,\tau) \end{aligned}\right\} \quad 6.26$$

where $\tau_c = \frac{1}{2W}$. Substituting these probabilities back into equation 6.24 the average, after a little algebra, simplifies to

$$\sum_{M'=-2}^{2} <> = \tfrac{1}{2} Z_{ij} \exp(-\tau/\tau_c) \qquad 6.27$$

where the time independent terms have been dropped (in anticipation of Section 6.4) and

$$Z_{ij} = Z_{ij}^{(2)} - Z_{ij}^{(1)} + \tfrac{1}{2} Z_{ij}^{(0)}$$

with

$$Z_{ij}^{(M')} = A_{aa,aa}^{(M')} + A_{ab,ab}^{(M')} - 2A_{aa,ab}^{(M')}$$

and

$$A_{aa,ab}^{(M')} = r_{ij}^{-3}(a,a)\ r_{ij}^{-3}(a,b)\ d_{0M'}^{(2)}(\beta(a,a))\ d_{0,-M'}^{(2)}(\beta(a,b)) \cos M'(\gamma(a,a) - \gamma(a,b)). \qquad 6.28$$

$r(a,b)$, $\beta(a,b)$ and $\gamma(a,b)$ are the values of r_{ij}, β_{ij} and γ_{ij} when the j spin is at its b site, the i spin is always at its a site. The other terms are defined in the same way.

6.3.2 Generalisation of the Three Spin Treatment

Our present model of a stationary I spin interacting with two S spins exchanging sites at random can be generalised to include cases where an S spin moves between N equivalent sites at random (or N S spins exchanging sites at random, although any S-S interaction must be ignored in such cases). The crux of the problem is in finding the probability that the S spin is at a particular site. To do this we extend the reasoning that we used before: the average (equation 6.23) that we wish to calculate depends upon the product of the probability that the I spin is at its site (which is one because it does not move) with the sum of the probabilities that the S spin (spin j) is at its various sites. So equation 6.24 can be written more generally as

$$<> = p_i(a)\left[\sum_{n=1}^{N} p_j(n,\tau = 0) f^{(M')}(a,n) \sum_{m=1}^{N} p_j(m,n,\tau) f^{(-M')}(a,m)\right] \qquad 6.29$$

where the symbols are those used in equation 6.24 and m and n represent additional sites. If the probability that the S spin at one site jumps to any other site is W then we can write down a set of differential equations (like equation 6.25) for the probability that the S spin is at any particular site, for the m^{th} site

$$\frac{d}{d\tau} p_j(m,\tau) = -(N-1)Wp_j(m,\tau) + \sum_{n \neq m} Wp_j(n,\tau). \qquad 6.30$$

The S spin must always be somewhere, so

$$\sum_{n=1}^{N} p_j(n,\tau) = 1$$

and equation 6.30 becomes

$$\frac{d}{d\tau} p_j(m,\tau) = -NWp_j(m,\tau) + W .$$

For the initial condition that the S spin is at its a site, say, this equation can be solved to give the generalised form of equation 6.26:

$$\left.\begin{aligned} p_j(a,\tau) &= \frac{1}{N}(1 + (N-1)\exp(-NW\tau)) \\ \text{and} \\ p_j(m \neq a,\tau) &= \frac{1}{N}(1 - \exp(-NW\tau)) . \end{aligned}\right\} \qquad 6.31$$

The probability that the S spin is at its a site at time $t+\tau$ after having been at site a at time t is then given by $p_j(a,a,\tau) = p_j(a,\tau)$ and the probability that it is at any other site, with the same initial condition, is $p_j(m,a,\tau) = p_j(m,\tau)$. Equivalent expressions can be written for any other site.

Equations 6.31 are especially useful for systems containing two or three S spins (or sites) because there is no problem in conceiving a motional process consisting of random jumps, of equal probability, between all the sites. We have already seen the outcome of putting N = 2 in equation 6.31, for N = 3

$$p_j(a,a,\tau) = p_j(b,b,\tau) = p_j(c,c,\tau) = \tfrac{1}{3}(1 + 2\exp(-2\tau/\tau_c))$$
$$p_j(a,b,\tau) = p_j(b,a,\tau) = p_j(a,c,\tau) = p_j(c,a,\tau) = p_j(b,c,\tau) =$$
$$p_j(c,b,\tau) = \tfrac{1}{3}(1 - \exp(-\tau/\tau_c) \quad \text{where } \tau_c = 1/3\ W.$$

When $N \geqslant 4$ the situation is complicated by the possibility of unequal jump probabilities, for example if there are 4 S spin sites arranged in a square:

a b

d c

it is unlikely that a jump from a to c (or c to a, b to d, d to b) will be as probable as a jump between adjacent sites along the edge of the square. We can, however, consider a motional model where the S spin cycles round the N sites, jumping only to nearest neighbour sites. The differential equation, corresponding to equation 6.30, for such a model is

$$\frac{d}{d\tau}p_j(m,\tau) = W(p_j(m+1,\tau) + p_j(m-1,\tau) - 2p_j(m,\tau)).$$

This equation has been solved by Torchia and Szabo(4). For four sites (spins), for example:

$$p_j(a,a,\tau) = p_j(b,b,\tau) = p_j(c,c,\tau) = p_j(d,d,\tau) =$$
$$\tfrac{1}{4}(1 + \exp(-\tau/\tau_c) + 2\exp(-\tau/2\tau_c))$$

$$p_j(a,b,\tau) = p_j(b,a,\tau) = p_j(a,d,\tau) = p_j(d,a,\tau) = p_j(b,c,\tau) =$$
$$p_j(c,b,\tau) = p_j(c,d,\tau) = p_j(d,c,\tau) = \tfrac{1}{4}(1 - \exp(-\tau/\tau_c))$$

$$p_j(a,c,\tau) = p_j(c,a,\tau) = p_j(b,d,\tau) = p_j(d,b,\tau) =$$
$$\tfrac{1}{4}(1 + \exp(-\tau/\tau_c) - 2\exp(-\tau/2\tau_c)) \quad \text{with } \tau_c = 1/4W.$$

6.3.3 A Four Spin, Two Site Model

This section is an extension of Section 6.3.1. It is necessary to account for S spin relaxation caused by the relative motion of different pairs of S spins. In the four spin model that we will adopt all the spins are mobile so the calculation is a little longer but the principles that were used before still apply. Without repeating details and using the notation of Section 6.3.1:

$$\sum_{M'=-2}^{2} \langle\rangle = \tfrac{1}{8}X_{ij} \exp(-2\tau/\tau_c) + \tfrac{1}{4}Y_{ij} \exp(-\tau/\tau_c) \qquad 6.32$$

where the time independent terms have again been ignored and

$$X_{ij} = X_{ij}^{(2)} - X_{ij}^{(1)} + \tfrac{1}{2}X_{ij}^{(0)}, \quad Y_{ij} = Y_{ij}^{(2)} - Y_{ij}^{(1)} + \tfrac{1}{2}Y_{ij}^{(0)}$$

with

$$X_{ij}^{(M')} = A_{aa,aa}^{(M')} + A_{ab,ab}^{(M')} + A_{ba,ba}^{(M')} + A_{bb,bb}^{(M')} + 2A_{aa,bb}^{(M')} +$$
$$2A_{ab,ba}^{(M')} - 2A_{aa,ba}^{(M')} - 2A_{aa,ab}^{(M')} - 2A_{ab,bb}^{(M')} - 2A_{ba,bb}^{(M')}$$

and

$$Y_{ij}^{(M')} = A_{aa,aa}^{(M')} + A_{ab,ab}^{(M')} + A_{ba,ba}^{(M')} + A_{bb,bb}^{(M')} - 2A_{aa,bb}^{(M')} - 2A_{ab,ba}^{(M')}.$$

6.3.4 A Multisite Intramolecular Rotation Model

This model represents a rigid spin system undergoing rotation in such a way that only intrasystem interactions cause relaxation, intersystem interactions are not taken into account. The model could apply to small molecules (containing a small spin system) rotating as a whole or to isolated parts of a larger molecule rotating as a unit as, for example, might a fluoromethyl (CH_2F) group.

The treatment given here is based on the rotational random walk model of Brownian motion given by Ivanov(13). In the two site models of the last sections the relative positions of the spins were automatically taken into account because the positions of the two sites were known. In the new model, where there are many sites, the exact positions of the spins, relative to the crystal, will not be known so that when the sum over all interactions is taken the positions of the spins relative to the molecule must be included in the calculation (otherwise the model would be of a system of non-related spin pairs). To do this a third transformation is introduced (this again emphasises the advantage of the spherical tensor notation). As before a polycrystalline average is taken over the angles relating the CRY and LAB systems, the additional transformation MOL → CRY is then included, the MOL system moves relative to the crystal so this transformation is time dependent, the average is calculated for this motion. The third transformation PAS → MOL enables information about specific spin system geometries to be included in the calculation, the spins remain fixed relative to the molecule so this transformation is time independent.

The additional transformation is carried out in the same way as the previous ones, the polycrystalline correlation function becomes

$$g^{(2)}_{M,ijij}(\tau)_p = \tfrac{3}{10}\sum_{M'}\sum_{M''}\sum_{N'}(-1)^{M'-M} r_{ij}^{-6} \mathcal{D}^{(2)}_{0M''}(\Omega_{ij})\mathcal{D}^{(2)}_{0N''}(\Omega_{ij})$$

$$\langle \mathcal{D}^{(2)}_{M'',-M'}(\Psi(t+\tau))\mathcal{D}^{(2)}_{N''M'}(\Psi(t))\rangle \qquad 6.33$$

where Ψ are the angles which take the MOL system into the CRY system. Because this model is multi-site (it is assumed that the intervals between sites are small) the summations in equation 6.23 can be replaced by integrals:

$$<> = \int \mathcal{D}^{(2)}_{M'',-M'}(\Psi)\ p(\Psi,\Psi^t,\tau)\ d\Psi \quad \int \mathcal{D}^{(2)}_{N''M'}(\Psi^t)\ p(\Psi^t)\ d\Psi^t$$

where $d\Psi$ and $d\Psi^t$ are expressions of the form of equation A10. The probability that angles Ψ occur at time $t+\tau$ can be written in terms of the probability, $p(\Psi,N)$, that they occur after N rotations, given that the probability that there are N rotations in the interval τ is $p_N(\tau)$:

$$p(\Psi,\Psi^t,\tau) = \sum_{N=0}^{\infty} p_N(\tau)\ p(\Psi,N). \qquad 6.34$$

$p_N(\tau)$ is given by a Poisson distribution:

$$p_N(\tau) = \frac{1}{N!}\left(\frac{\tau}{\tau_c}\right)^N \exp(-\tau/\tau_c) \qquad 6.35$$

τ_c is the time between successive jumps. The probability $p(\Psi,N)$ can be written in terms of the probability of an individual rotation, R, occurring:

$$p(\Psi,N) = \int p(\chi,N-1)\ p(R)\ dR.$$

χ is the orientation after N-1 rotations which becomes Ψ after the N^{th} rotation. The subsequent evaluation of this equation is included in Appendix H, the result is

$$p(\Psi,N) = \sum_n \sum_{n'} \sum_m \frac{5}{8\pi^2} \mathcal{D}^{(2)}_{mn'}(\Psi^t)^*\ (A^{(2)})^N_{nm}\ \mathcal{D}^{(2)}_{nn'}(\Psi) \qquad 6.36$$

with $A^{(2)} = \int \mathcal{D}^{(2)}(R)^* p(R)\, dR$.

From equation 6.35

$$\sum_{N=0}^{\infty} p_N(\tau)\ (A^{(2)})^N_{nm} = \exp(-(1-A^{(2)}_{nm})\frac{\tau}{\tau_c})$$

so from equations 6.36 and 6.34 and with $p(\Psi^t) = \frac{1}{8\pi^2}$ the average becomes, after a little algebra

$$<> = \sum_{n}\sum_{n'}\sum_{m}\frac{5}{64\pi^2}(-1)^{n-n'}\int\mathcal{D}^{(2)}_{M'',-M'}(\Psi)\,\mathcal{D}^{(2)}_{-n,-n'}(\Psi)^*\,d\Psi$$

$$\int\mathcal{D}^{(2)}_{N''M'}(\Psi^t)\,\mathcal{D}^{(2)}_{mn'}(\Psi^t)^*\,d\Psi^t\quad \exp\left(-(1-A^{(2)}_{nm})\frac{\tau}{\tau_c}\right)$$

where $A^{(2)}_{nm} = \int\mathcal{D}^{(2)}_{nm}(R)^*\,p(R)dR$. Using equation A9 it follows that $M''=-n$, $M'=n'$ and $N''=m$

$$<> = (-1)^{-M''-M'}\,\tfrac{1}{5}\left(\exp-(1-A^{(2)}_{-M''N''})\frac{\tau}{\tau_c}\right). \qquad 6.37$$

6.4 The Spectral Densities

The spectral densities are related to the correlation functions through the Fourier transform - equation 6.08

$$j^{(2)}_{M,ijij}(\omega_{m,ij}) = (-1)^{M}\tfrac{1}{2}\int_{-\infty}^{\infty} g^{(2)}_{M,ijij}(\tau)\; e^{i\omega_{m,ij}\tau}d\tau$$

The correlation functions, for polycrystalline systems, are found from equation 6.20 and the averages in equations 6.27 and 6.32 or from equation 6.37. The time independent parts of these averages have been omitted because they do not contribute to the observed relaxation. The remaining parts have a common form for the time dependence: $\exp(-u\tau/\tau_c)$, u is a constant, the Fourier transform of this is

$$\int_{-\infty}^{\infty} e^{-u\tau/\tau_c}\; e^{-i\omega_{m,ij}\tau}d\tau = \frac{2\left(\frac{\tau_c}{u}\right)}{1+\frac{\omega^2_{m,ij}\tau_c^2}{u^2}}\,.$$

Consequently, the spectral densities, for the two site models, are (for the three spin)

$$j^{(2)}_{M,ijij}(\omega_{m,ij})_p = \tfrac{3}{20}Z_{ij}\,\frac{\tau_c}{1+\omega^2_{m,ij}\tau_c^2} \qquad 6.38$$

and (for the four spin)

$$j^{(2)}_{M,ijij}(\omega_{m,ij})_p = \tfrac{3}{40}\left[\tfrac{1}{4}X_{ij}\,\frac{\tau_c}{1+\frac{1}{4}\omega^2_{m,ij}\tau_c^2} + Y_{ij}\,\frac{\tau_c}{1+\omega^2_{m,ij}\tau_c^2}\right].$$

6.39

The corresponding expression for the multi-site model is more complicated

$$j^{(2)}_{M,ijij}(\omega_{m,ij})_p = \tfrac{3}{50}\sum_{M''}\sum_{N''}(-1)^{-M''} r_{ij}^{-6}\, \mathcal{D}^{(2)}_{0M''}(\Omega_{ij})\,\mathcal{D}^{(2)}_{0N''}(\Omega_{ij})$$

$$\frac{(1-A^{(2)}_{-M''N''})\tau_c}{(1-A^{(2)}_{-M''N''}) + \omega^2_{m,ij}\tau_c^2} \cdot \qquad 6.40$$

This expression can be simplified if the motion is restricted to rotation about a single axis, the MOL z-axis say, then R = (μ,0,0) and only those terms with $-M'' = N'' \neq 0$ are non-zero. Using Appendix A to find the rotation matrix elements equation 6.40 becomes

$$j^{(2)}_{M,ijij}(\omega_{m,ij})_p = \tfrac{3}{50} r_{ij}^{-6}\Bigg\{\tfrac{3}{8}\sin^4\beta_{ij}\left[\frac{(1-A^{(2)}_{22})\tau_c}{(1-A^{(2)}_{22})^2 + \omega^2_{m,ij}\tau_c^2} + \frac{(1-A^{(2)}_{-2,-2})\tau_c}{(1-A^{(2)}_{-2,-2})^2 + \omega^2_{m,ij}\tau_c^2}\right] + \tfrac{3}{2}\sin^2\beta_{ij}\cos^2\beta_{ij}\left[\frac{(1-A^{(2)}_{11})\tau_c}{(1-A^{(2)}_{11})^2 + \omega^2_{m,ij}\tau_c^2} + \frac{(1-A^{(2)}_{-1,-1})\tau_c}{(1-A^{(2)}_{-1,-1})^2 + \omega^2_{m,ij}\tau_c^2}\right]\Bigg\}.$$

6.5 Experimental Relaxation Rates

For a heteronuclear spin system the experimental relaxation rate depends on $\langle I_z\rangle - I_e$, (I_e is the equilibrium value of $\langle I_z\rangle$) as it would for a homonuclear spin system, and additionally on $\langle S_z\rangle - S_e$ (equation 6.15) (Abragam(1), Solomon(5)). The relative dependence on these two quantities can be found by solving the two equations

$$\frac{d}{dt}\langle I_z\rangle = -\left(\frac{1}{T_1^I} + \frac{1}{T_1^{II}}\right)(\langle I_z\rangle - I_e) - \frac{1}{T_1^{IS}}(\langle S_z\rangle - S_e)$$

and

$$\frac{d}{dt}\langle S_z\rangle = -\left(\frac{1}{T_1^S} + \frac{1}{T_1^{SS}}\right)(\langle S_z\rangle - S_e) - \frac{1}{T_1^{SI}}(\langle I_z\rangle - I_e).$$

The details of this solution are given in Appendix I, the result is

$$\langle I_z\rangle - I_e = C' \exp(-t/T_1') + C'' \exp(-t/T_1'') \qquad 6.41$$

with

$$\frac{1}{T_1'}, \frac{1}{T_1''} = \tfrac{1}{2}\left[\left(\frac{1}{T_1^I} + \frac{1}{T_1^{II}} + \frac{1}{T_1^S} + \frac{1}{T_1^{SS}}\right) \pm \left(\left(\frac{1}{T_1^I} + \frac{1}{T_1^{II}} - \frac{1}{T_1^S} - \frac{1}{T_1^{SS}}\right)^2 + \frac{2}{T_1^{IS}}\frac{2}{T_1^{SI}}\right)^{\frac{1}{2}}\right] \qquad 6.42$$

($1/T_1'$ takes the positive sign) and

$$C' = \frac{(\langle I_z\rangle_0 - I_e)\left(\frac{1}{T_1^I} + \frac{1}{T_1^{II}} - \frac{1}{T_1''}\right) + (\langle S_z\rangle_0 - S_e)\frac{1}{T_1^{IS}}}{\left(\frac{1}{T_1'} - \frac{1}{T_1''}\right)}, \qquad 6.43$$

taking $(\langle I_z\rangle_0 - I_e) = 1$, then $C'' = 1 - C'$, $\langle I_z\rangle_0 \equiv \langle I_z(t = 0)\rangle$

There is a corresponding expression for $\langle S_z\rangle - S_e$. $\langle I_z\rangle - I_e$ can be determined from an experiment, its value, though, depends on the preparation pulse - in Section 6.1 it was assumed that a 90^o pulse was applied to the I spins, in which case $\langle I_z\rangle_0 = 0$ and $\langle S_z\rangle_0 = S_e$.

There are several interesting points that arise from equation 6.43 when the system is prepared so that $\langle I_z\rangle_0 = 0$ and $\langle S_z\rangle_0 = S_e$. Firstly, C'' can, potentially, become zero, when it does the relaxation can be described by a single exponential function. C'' is zero when $\frac{1}{T_I^{IS}}$ (or $\frac{1}{T_1^{SI}}$) is zero which (using equation 6.18 and an equation of the form of 6.38) occurs when

$$\tau_c^2 = \frac{-5}{5\omega_{0,I}^2 - 14\omega_{0,I}\omega_{0,S} + 5\omega_{0,S}^2}. \qquad 6.44$$

This condition is clearly independent of the spin system geometry. For example, for an H,F system ($\omega_{0,H} = 1.605 \times 10^8$ rad s^{-1}, $\omega_{0,F} = 1.510 \times 10^8$ rad s^{-1}) $\frac{1}{T_1^{IS}}$ is zero when $\tau_c = 7.20 \times 10^{-9}$ s. The relaxation function can also be approximately single exponential for a range of τ_c values on either side of τ_c given by equation 6.44. It is also evident from equation 6.44 that $\frac{1}{T_1^{IS}}$ cannot be zero (and so cannot change sign) if

$$5\omega_{0,I}^2 - 14\omega_{0,I}\omega_{0,S} + 5\omega_{0,S}^2 > 0$$

that is when

$$2.380 < \frac{\omega_{0,I}}{\omega_{0,S}} < 0.4202 .$$

Secondly, in the low temperature approximation ($\omega^2\tau_c^2 >> 1$)

$$\frac{1}{T_1^{II}} \cong -\frac{1}{T_1^{IS}}, \quad \frac{1}{T_1^{SS}} \cong -\frac{1}{T_1^{SI}} \quad \text{and} \quad \frac{1}{T_1^{I}} \cong \frac{1}{T_1^{S}} \cong 0$$

then

$$\frac{C'}{C''} \cong \frac{T_1^{SI}}{T_1^{IS}} = \frac{\text{number of I spins}}{\text{number of S spins}} . \qquad 6.45$$

For an IS_2 spin system, for example, in the low temperature approximation $\frac{C'}{C''} = \frac{1}{2}$ and the relaxation function is double exponential whatever the spin system geometry. In the high temperature approximation ($\omega^2\tau_c^2 << 1$) no such simplification is possible. Calculations show , however, that the ratio $\frac{C'}{C''}$ is constant but its value depends on the spin system under study. In some cases the relaxation function may appear (experimentally) to be a single exponential, such behaviour can be explained if one of the coefficients (C'' or C') becomes dominant over the other. We shall discuss these points, in relation to experimental data, in more detail shortly.

6.6 Nuclear Spin Relaxation in Polycrystalline KHF_2 and $CsHF_2$

Studies of the temperature dependence of the nuclear spin-lattice relaxation of both polycrystalline KHF_2 and $CsHF_2$ are reported in this section. The experimental results are interpreted using the theoretical models (of an assembly of IS_2 groups, each with $D_{\infty h}$ symmetry and undergoing 180° jumps about a C_2 axis) developed in Sections 6.3.1 and 6.3.3.

There have been a number of studies of nuclear spin-lattice relaxation in polycrystalline samples of ionic hydrogen difluorides: Furukawa and Kiriyama(7) and Kriger, Moroz and Gabuda(15) have studied KHF_2, Furukawa and Kiriyama(16) and Reynhardt, Watton and Petch(17) have studied NH_4HF_2 and Kriger, Gabuda and Moroz(8) have studied $CsHF_2$. Each investigation has concentrated on characterising the motion of the hydrogen difluoride ion, for KHF_2 and $CsHF_2$ the nature of the 'high temperature' structural phase transition has also been probed (NH_4HF_2 does not undergo such a transition). At room temperature KHF_2 and $CsHF_2$ are isostructural; at 469.8 K KHF_2 undergoes a transition into a NaCl type structure (Petersen and Levy(18), Davis and Westrum(19)), $CsHF_2$ undergoes a transition at 331.4 K into a CsCl type structure (Kruh, Fuwa and McEver(20), Westrum(9)).

The most comprehensive ^1H and ^{19}F spin relaxation study of polycrystalline KHF_2 is that of Furukawa and Kiriyama(7). These authors confirmed that in the low temperature phase the HF_2^- ion was indeed undergoing 180° jumps. Below 400 K they found that the magnetisation recovery, for both nuclei, was non-exponential. Such behaviour was not observed by Kriger, Moroz and Gabuda(15) even though their measurements were made

over a similar temperature range. Furukawa and Kiriyama also suggested that the spin relaxation above the phase transition was due to diffusional disorder superimposed on rapid isotropic reorientation of the HF_2^- ion.

The only ^1H and ^{19}F spin relaxation study of $CsHF_2$ is that of Kriger, Gabuda and Moroz(8). They found that the magnetisation recovery was exponential over the temperature range 200 K to 330 K and suggested that the observed relaxation could only be explained if the HF_2^- ion was undergoing 180^o jumps. They also suggested that the change in behaviour at the phase transition was a consequence of the isotropic reorientation of the HF_2^- ion.

In the present work we have not studied KHF_2 in detail because of the extensive work of Furukawa and Kiriyama(7). The few measurements that we did make were to test our theoretical expressions. In doing this we extended the number of spins included in the calculation compared to the work of Furukawa and Kiriyama. We paid particular attention to the temperature dependence of the coefficients governing the non-exponential magnetisation recovery. Apart from the work of Eguchi(21) on solid fluoroform we are unaware of any such study having been reported before.

The study of $CsHF_2$ is more detailed because preliminary experiments indicated that there were differences between the relaxation behaviour to be reported here and that reported by Kriger, Gabuda and Moroz(8). A full interpretation of the relaxation behaviour above the structural phase transition is not given here as further work is required.

6.6.1 The Experiment

The details of the spectrometer are given in Chapter Three, Section 3.2. The ^{1}H measurements were carried out at a frequency of 25.55 MHz and those for ^{19}F at 24.05 MHz. The temperature control system was of a conventional gas-flow type. Dry nitrogen gas was passed through a coolant bath (ice or liquid nitrogen depending on the temperature to be maintained) and then over a heater which was regulated by a control device (an Oxford Instruments DTC2 unit) according to the temperature sensed by a reference thermocouple situated close to the sample tube. The temperature of the sample was recorded, at the beginning and end of each experiment, by replacing the sample with a monitoring thermocouple. The temperatures at the beginning and end of each experiment were found to be within 1.5 K of each other.

The recovery of the magnetisation following a 90° pulse was determined using the following pulse sequence:

$$P_y(90^{\circ})-\tau_1-P_y(90^{\circ})-\tau_2-P_{90^{\circ}}(90^{\circ}).$$

The height of the echo produced by the last two pulses (τ_2 = 16μs) was measured as a function of τ_1. Signal averaging was used. When the recovery was non-exponential the following equation (equation 6.41) was used in the analysis of the data

$$\frac{M_z(\tau_1)-M(0)}{M(0)} \propto \langle I_z(\tau_1)\rangle - I_e = C'\exp(-\tau_1/T_1') + C''\exp(-\tau_1/T_1'').$$

Values for T_1', T_1'', C' and C'' were found by fitting the experimental results to this equation using a non-linear least squares fitting procedure. The value of $M(0)$ was measured with τ_1 greater than five times the longest T_1.

The fitting procedure used the NAG library routine E04FDF, "for finding the unconstrained minimum of a sum of squares of M non-linear functions in N variables". When the recovery was exponential equation 6.41 was used with $C''=0$. The results of all the experiments were fitted over the first 80% of the decay of the observed echo height. The relaxation measurements for $CsHF_2$ were carried out in collaboration with Mr. Gordon Oates of the Chemistry Department at the Open University.

6.6.2 The Theory

The nuclear spin-lattice relaxation behaviour of both KHF_2 and $CsHF_2$ in their low temperature (tetragonal) phases can be modelled on an assembly of IS_2 groups each undergoing 180° rotational jumps about a C_2 axis (Sections 6.3.1 and 6.3.3). As a consequence of this type of motion and the symmetry of the HF_2^- ion in these compounds there is no intramolecular contribution to either the ^1H or the ^{19}F relaxation. The relaxation of the ^1H nuclei is caused by the modulation of the interion H-F dipolar interactions. The ^{19}F relaxation is caused by the modulation of interion F-H and F-F dipolar interactions. The observed relaxation rates for the system are given by equation 6.42, the components of that equation are:

$$\frac{1}{T_1^{HH}} = \frac{1}{20}(\gamma_H\gamma_F\hbar\mu_0/4\pi)^2 \sum_j z_{ij}\left[\frac{6\tau_c}{1+(\omega_{0,H}+\omega_{0,F})^2\tau_c^2} + \frac{3\tau_c}{1+(\omega_{0,H})^2\tau_c^2} + \frac{\tau_c}{1+(\omega_{0,H}-\omega_{0,F})^2\tau_c^2}\right] \qquad 6.46$$

$$\frac{1}{T_1^{HH}} = \frac{1}{20}(\gamma_H\gamma_F\hbar\mu_0/4\pi)^2 \sum_j z_{ij}\left[\frac{6\tau_c}{1+(\omega_{0,F}+\omega_{0,H})^2\tau_c^2} + \frac{3\tau_c}{1+(\omega_{0,F})^2\tau_c^2} + \frac{\tau_c}{1+(\omega_{0,F}-\omega_{0,H})^2\tau_c^2}\right] \qquad 6.47$$

$$\frac{1}{T_1^{HF}} = \frac{2}{T_1^{FH}} = \frac{1}{20}(\gamma_H\gamma_F\hbar\mu_0/4\pi)^2 \sum_j Z_{ij}\left[\frac{6\tau_c}{1+(\omega_{0,H}+\omega_{0,F})^2\tau_c^2} - \frac{\tau_c}{1+(\omega_{0,H}-\omega_{0,F})^2\tau_c^2}\right] \qquad 6.48$$

where Z_{ij} is defined in Section 6.3.1,

$$\frac{1}{T_1^F} = \frac{3}{80}(\gamma_F^2\hbar\mu_0/4\pi)^2 \sum_j \left[(X_{ij}+Y_{ij})\frac{\tau_c}{1+\omega_{0,F}^2\tau_c^2} + (\tfrac{1}{4}X_{ij})\frac{\tau_c}{1+\frac{1}{4}\omega_{0,F}^2\tau_c^2} + (4Y_{ij})\frac{\tau_c}{1+4\omega_{0,F}^2\tau_c^2}\right] \qquad 6.49$$

and $\frac{1}{T_1^H} = 0$

where X_{ij} and Y_{ij} are defined in Section 6.3.3. These equations are derived from equations 6.16-6.18 in Section 6.1 and equations 6.38 and 6.39 in Section 6.4.

The evaluation of the expressions given above requires information on the geometry of the system under study. The crystal structure and unit cell dimensions of the tetragonal phases of KHF_2 and $CsHF_2$ are both known (Petersen and Levy (18) and Kruh, Fuwa and McEver (20), respectively). This evaluation was undertaken, for both systems, so as to include 44 HF_2^- ions surrounding a central HF_2^- ion (but note that there are only 11 unique positions). For comparison the evaluation was carried out using just 6 neighbouring ions - the number used by Furukawa and Kiriyama (7) in their calculation of the heteronuclear contribution to relaxation in KHF_2. The results of the evaluation of the geometrical terms (the X_{ij}, Y_{ij} and Z_{ij} in equations 6.46-6.49 are given in Table 6.2.

Table 6.2 The structural parameters for KHF_2 and $CsHF_2$

		$Z_{ij}/x10^{57}$ m^{-6}	$X_{ij}/x10^{57}$ m^{-6}	$Y_{ij}/x10^{57}$ m^{-6}
KHF_2	sum over 6 ions	1.92	2.70	5.13
KHF_2	sum over 44 ions	2.19	3.14	6.19
$CsHF_2$	sum over 6 ions	1.90	4.89	3.73
$CsHF_2$	sum over 44 ions	2.14	5.23	4.70

For an experiment in which the spin system is prepared with a 90^o pulse on the I (or S) resonance the return of the magnetisation to its equilibrium value is described by the two coupled differential equations given in Section 6.5. The solution of these equations is given as a double exponential function, equation 6.41, with variables T_1', T_1'', C' and C'' $(=1-C')$ which can be calculated, as a function of the rotational jump correlation time, τ_c, using equations 6.46-6.49 and Table 6.2.

At this point a brief review of the relaxation behaviour that would be expected for tetragonal KHF_2 and $CsHF_2$ is worthwhile. For both compounds, if $\omega_{0,H}\tau_c$ or $\omega_{0,F}\tau_c >> 1$ (large τ_c) then, for the ^1H resonance $C'/C'' = \frac{1}{2}$ while for the ^{19}F resonance $C'/C'' = 2$ (for the ^{19}F resonance the system can be thought of as an I_2S system). In these circumstances the magnetisation will return to its equilibrium value in a non-exponential manner. At the other extreme, $\omega_{0,H}\tau_c$ or $\omega_{0,F}\tau_c << 1$ (small τ_c) the ratio C'/C'' is constant but its magnitude depends on the arrangement of the HF_2^- ions: for KHF_2 calculation shows that for the ^1H resonance $C'/C'' = 22.9$ and for $CsHF_2$ calculation shows that for the ^1H resonance $C'/C'' = 16.9$. The corresponding ratio for the ^{19}F resonance in $CsHF_2$ is $C'/C'' = \frac{1}{16.9}$ (changing the resonant nucleus has the effect of 'reversing' the

coefficients, $C'(H) \equiv C''(F)$ and $C''(H) \equiv C'(F)$). In all cases, under these conditions, one coefficient is dominant; this means that experimentally the observed magnetisation recovery will be exponential.

For both compounds and for both resonances the point at which the magnetisation recovery is truly exponential, that is C' or $C'' = 0$, is calculated to fall between $\tau_c = 6.5 \times 10^{-9}$ s and 7.5×10^{-9} s (see Section 6.5 equation 6.44).

6.6.3 Results and Discussion for KHF_2

A series of ^1H spin-lattice relaxation measurements for polycrystalline KHF_2 were carried out in the temperature range 300-413 K. The latter temperature was the highest stable temperature that could be achieved with the present equipment. Figure 6.1(a) shows a log-normal plot of the recovery of the magnetisation as a function of pulse spacing at 413 K. Figure 6.1(b) is the corresponding plot at 315 K. At the higher temperature the magnetisation recovery is approaching exponential behaviour ($T_1' = 0.45$ s), although the value of the intercept indicates that there is still a contribution from a faster relaxation process. At 315 K the recovery of the magnetisation is non-exponential: the values of T_1' and T_1'' obtained by fitting the data to equation 6.41 are shown in the figure. These, and other measurements (not shown) are in reasonable agreement with those reported by Furukawa and Kiriyama (7) (provided the different ^1H resonance frequencies used in the two studies is taken into account).

In view of the extensive study of spin relaxation in KHF_2 by Furukawa and Kiriyama our study was not done in any detail.

However, it is interesting to consider how the coefficients governing the double exponential behaviour of the recovery of the magnetisation vary with temperature as this was not discussed by these authors. Figure 6.2(a) shows the measured coefficient C′, as a function of temperature. There is a distinct change in behaviour near temperature T = 370 K (10^3 K/T = 2.7). The coefficient calculated as a function of correlation time, τ_c, is shown in Figure 6.2(b) (the relationship between τ_c and temperature is discussed in the next section). Although the experimental data are limited there is clearly some relationship between theory and experiment. In general terms the measurement of the temperature dependence of the coefficients governing the recovery of the magnetisation for heteronuclear spin systems would seem to provide a useful check of a relaxation model. In the next section, where we have more experimental data, we shall demonstrate this more effectively.

6.6.4 Results and Discussion for $CsHF_2$

Both ^1H and ^{19}F spin-lattice relaxation measurements, for polycrystalline $CsHF_2$, have been carried out in the temperature range 175-390 K. The experimental results are summarised in Figure 6.3. At low temperatures, below approximately 200 K, the recovery of the magnetisation, for both resonances, shows double exponential behaviour, see, for example, Figure 6.4(a). Above 200 K the observed magnetisation recovery, for both resonances, tends towards single exponential behaviour, the time constant for the ^1H relaxation being greater than that for ^{19}F relaxation. The recovery of the magnetisation at a temperature at which the changeover from double to single exponential behaviour is almost complete is shown in Figure 6.4(b). At 331 ± 2 K there is a break in the relaxation

behaviour of both nuclei: this corresponds to the phase transition where the tetragonal structure changes to a cubic one (the I4/mcm structure becomes Pm3m (Westrum (9)). At temperatures above 331 K the magnetisation recovery for the ^{1}H resonance was found to be exponential but that for the ^{19}F resonance was found to be double exponential. This section will be primarily concerned with the relaxation behaviour at temperatures below 331 K, that is with relaxation in the tetragonal phase.

The general relaxation behaviour described above is different in several ways to that reported by Kriger, Gabuda and Moroz (8). These authors investigated the relaxation behaviour of polycrystalline $CsHF_2$ in the temperature range 200-400 K and consequently did not observe two component relaxation at low temperatures and failed to detect the second, low temperature, minimum in the ^{19}F relaxation time. Above the phase transition they observed only single component relaxation for both the ^{1}H and ^{19}F resonances. The magnitudes of their observed spin-lattice relaxation times are in qualitative agreement with those of the present study.

If it is assumed that the rotational motion of the hydrogen difluoride ion is a thermally activated process such that

$$\tau_c = \tau_0 \exp(E_a/RT) \qquad 6.50$$

then the value of the activation energy, E_a, can be derived from the temperature dependence of the T_1 data since $T_1 \propto \tau_c^{-1}$ on the high temperature side of the minima (τ_0 is a constant and R is the gas constant). Neglecting the ^{1}H relaxation times near the phase transition, the average activation energy (from the ^{1}H and ^{19}F results) between 250 and 300 K is

E_a = 23.1 ± 3.0 kJ mol^{-1}. This value is larger than the corresponding value of E_a = 14.7 ± 2.1 kJ mol^{-1} reported by Kriger, Gabuda and Moroz (8). Using the value of E_a derived from the data shown in Figure 6.3, equation 6.50 and taking into account the temperature at which the minima shown in Figure 6.3 occur, it was found that τ_0 = 2.4 ± 1.0 x 10^{-14} s.

The theoretical relaxation times, below the phase transition, calculated using equations 6.46-6.49, Table 6.2 and equation 6.50, are shown as solid lines in Figure 6.3. The agreement with the experimental measurements is reasonably good, indeed $CsHF_2$ provides a classic illustration of the details of heteronuclear spin relaxation. Figure 6.5 shows the experimentally observed and calculated values of the coefficient C′ for the recovery of the ^1H magnetisation: the relaxation model is confirmed by the reasonably good agreement between the two.

In Figure 6.3 three points require further comment. Firstly, the size of the activation energy, measured in the temperature range 250-300 K is smaller than that found for KHF_2 (Furukawa and Kiriyama (7)): 23.1 ± 3.0 kJ mol^{-1} compared with 50.5 ± 2.0 kJ mol^{-1}. Although isostructural, the unit cell dimensions for $CsHF_2$ are larger than those for KHF_2 (for KHF_2 a = 0.5672 nm, c = 0.6801 nm (Carrell and Donohue (22)) and for $CsHF_2$ a = 0.614 nm, c = 0784 nm (Kruh, Fuwa and McEver (20))) so the observed difference in activation energy is presumably associated with this structural difference. Secondly, at temperatures near to the temperature of the phase transition there appears to be a 'levelling-off' in the ^1H relaxation rate. This may be due to impurities present in the sample or could be associated with the

mechanism of the phase transition. Thirdly, at low temperatures (below 200 K) the activation energy was found to be 34.0 ± 2.6 kJ mol^{-1} which is greater than that found on the high temperature side of the minima. It seems likely, then, that the activation energy for the rotational motion of the hydrogen difluoride ion is temperature dependent. Such behaviour might be associated with a contraction in the unit cell as the temperature falls: crystallographic data to support this argument is unfortunately not available.

The activation energy for the motional process occurring above the phase transition is 19.6 ± 1.5 kJ mol^{-1}, a value which is not very different from that on the low temperature side of the transition. Above the phase transition (in the cubic phase) the form that the motion takes is uncertain. In the X-ray study by Kruh, Fuwa and McEver (20) it is suggested that in the cubic phase the HF_2^- ions are randomly oriented and also that free isotropic rotation is sterically prohibited. As in KHF_2 it is possible that ionic diffusion (Furukawa and Kiriyama (7)) will affect the relaxation behaviour. Without further calculations we are, at present, unable to shed further light on the motion in the cubic phase. These points may, however, go some way to explain the observed behaviour of the ^1H FID in the cubic phase. Figure 6.6(a) is the ^1H FID in the cubic phase. Figure 6.6(a) is the ^1H FID recorded just above the transition temperature (at 334 ± 2 K). The most striking feature of this FID is the loss of the modulation seen in the FID at 293 K. The length of both decays is, however, approximately equal. For temperatures up to about 365 K the length of the decay does not change significantly; above this temperature there is a gradual increase in the length of the FID. For comparison the part of the FID at

390 K which corresponds to Figure 6.6(a) is shown in Figure 6.6(b). In addition to more calculation measurements of $T_{1\rho}$ (the spin-lattice relaxation time in the rotating frame) and, perhaps, experiments on the deuterated ion might give a greater understanding of the mechanism of the phase transition and of the motion of the HF_2^- ion in the cubic phase.

6.7 Appendices

6.7.1 Appendix H

In Section 6.3.4 the probability of the orientation Ψ occurring after N jumps is given as:

$$p(\Psi,N) = \int p(\chi,N-1)\ p(R)\ dR.$$

Under a rotation R the orientation χ is transformed into orientation Ψ so:

$$p(\Psi,N-1) = D(R)\ p(\chi,N-1),$$

since $D(R)D(R^{-1}) = 1$

$$p(\Psi,N) = \int D(R^{-1})\ p(\Psi,N-1)\ p(R)\ dR.$$

Let

$$\sum_n \sum_{n'} C^{(2)}_{nn'}(N)\ \mathcal{D}^{(2)}_{nn'}(\psi) = p(\Psi,N) \qquad H1$$

so that

$$\sum_n \sum_{n'} C^{(2)}_{nn'}(N)\ \mathcal{D}^{(2)}_{nn'}(\Psi) = \int D(R^{-1}) \sum_m \sum_{m'} C^{(2)}_{mm'}(N-1)\ \mathcal{D}^{(2)}_{mm'}(\Psi)\ .p(R)dR \qquad H2$$

but

$$D(R^{-1})\mathcal{D}^{(2)}_{mm'}(\Psi) = \sum_{m''} \mathcal{D}^{(2)}_{mm''}(R^{-1})\mathcal{D}^{(2)}_{m''m'}(\Psi).$$

After substituting this into H1, multiplying both sides of the result by $\mathcal{D}^{(2)}_{nn'}(\Psi)^*$, integrating and applying equation A9 it follows that $m'' = n$ and $m' = n'$ and then

$$C^{(2)}_{nn'}(N) = \sum_m C^{(2)}_{mn'}(N-1)\ A^{(2)}_{nm} \qquad H3$$

where

$$A^{(2)}_{nm} = \int \mathcal{D}^{(2)}_{nm}(R)\ p(R)\ dR.$$

The recursive application of equation H3 gives

$$C^{(2)}_{nn'}(N) = \sum_m C^{(2)}_{mn'}(0)\ (A^{(2)})^N_{nm} \qquad H4$$

but at time t, before any jumps have occurred, from equation H1

$$C^{(2)}_{mn'}(0)\mathcal{D}^{(2)}_{mn'}(\Psi) = p(\Psi,0) = \delta(\Psi,\Psi^t)$$

multiplying this by $\mathcal{D}^{(2)}_{mn'}(\Psi)$, integrating and applying equation A9:

$$C^{(2)}_{mn'}(0) = \frac{5}{8\pi^2}\mathcal{D}^{(2)}_{mn'}(\Psi^t)^* \qquad H5$$

since $\int f(x)\,\delta x\,dx = f(0)$ by definition. Substituting equation H5 into H4 and the result into H1 gives equation 6.36:

$$p(\Psi,N) = \sum_n \sum_{n'} \sum_m \frac{5}{8\pi^2}\mathcal{D}^{(2)}_{mn'}(\Psi^t)^*\ (A^{(2)})^N_{nm}\ \mathcal{D}^{(2)}_{nn'}(\Psi). \qquad 6.36$$

6.7.2 Appendix I

Two coupled differential equations of the form

$$\left.\begin{aligned} \frac{dx}{dt} &= Dx = -a(x-x_0) - b(y-y_0) \\ \frac{dy}{dt} &= -c(y-y_0) - d(x-x_0) \end{aligned}\right\} \text{I1}$$

are solved as follows: rearranging I1

$$(D+a)x + by = ax_0 + by_0$$
$$dx + (D+c)y = cy_0 + dx_0$$

so

$$\begin{vmatrix} D+a & b \\ d & D+c \end{vmatrix} x = \begin{vmatrix} (ax_0 + by_0) & b \\ (cy_0 + dx_0) & D+c \end{vmatrix} 1$$

which, when expanded, gives

$$(D+a)(D+c)x - dbx = (ax_0+by_0)(D+c) - (cy_0+dx_0)b.$$

Since $\frac{d}{dt}(1) = 0$ this is

$$\frac{d^2x}{dt^2} + (a+c)\frac{dx}{dt} + (ac-db)x = (ax_0+by_0)c - (cy_0+dx_0)b. \quad I2$$

The general solution of this equation is (Stephenson (14))

$$x = A \exp(-m't) + B \exp(-m''t) + C \quad I3$$

m′ and m″ are found by putting $x = e^{-mt}$ and setting the right-hand side of equation I2 to zero, it follows that

$$m^2 - m(a+c) + (ac-db) = 0$$

with

$$m = \tfrac{1}{2}[(a+c) \pm ((a+c)^2 - 4(ac-db))^{\frac{1}{2}}], \quad I4$$

m′ takes the positive sign and m″ the negative. The constants A and B in equation I3 are found by substituting equation I3 into I1 and using the zero time condition ($\langle I_z \rangle - I_e = A+B$), C is found by putting $t \to \infty$ so that $x \to x_0 \to C$.

The results for the specific equations used in Section 6.5 are given in that section, they are obtained in the manner outlined above. There is, of course, an analogous expression for y.

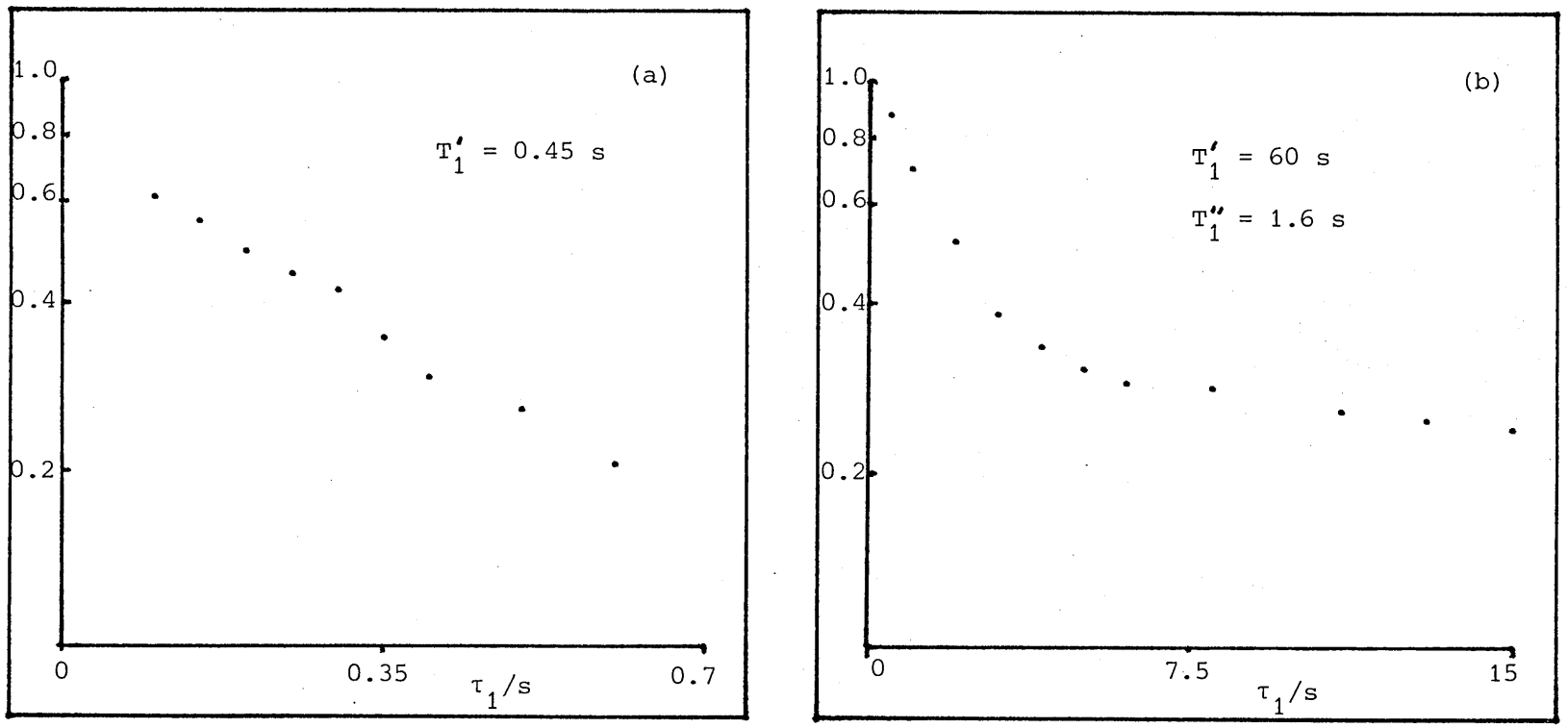

Figure 6.1 Log-normal plot of the ^1H magnetisation recovery as a function of τ_1, for polycrystalline KHF_2 at (a) 413 K and (b) 315 K.

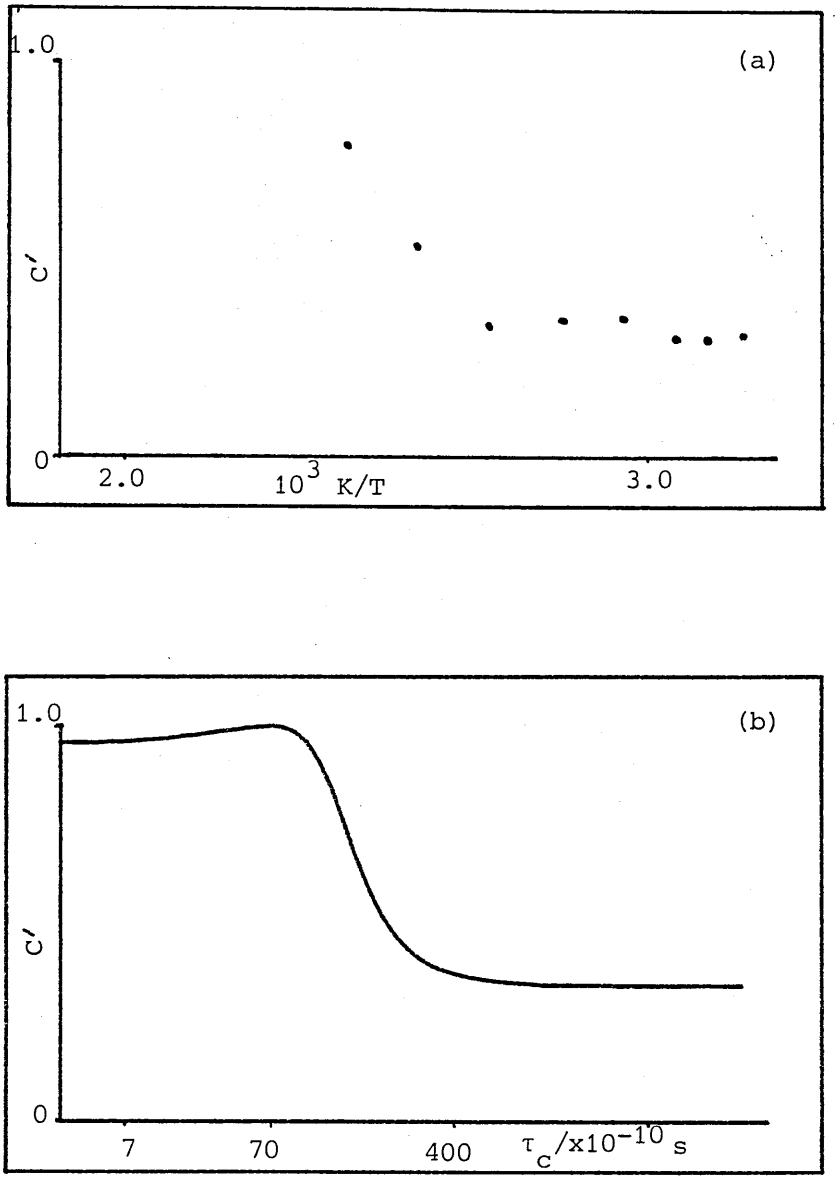

Figure 6.2 The (a) experimental and (b) calculated coefficient C′, corresponding to the longer time constant, for the double exponential recovery of the ^1H magnetisation in polycrystalline KHF_2.

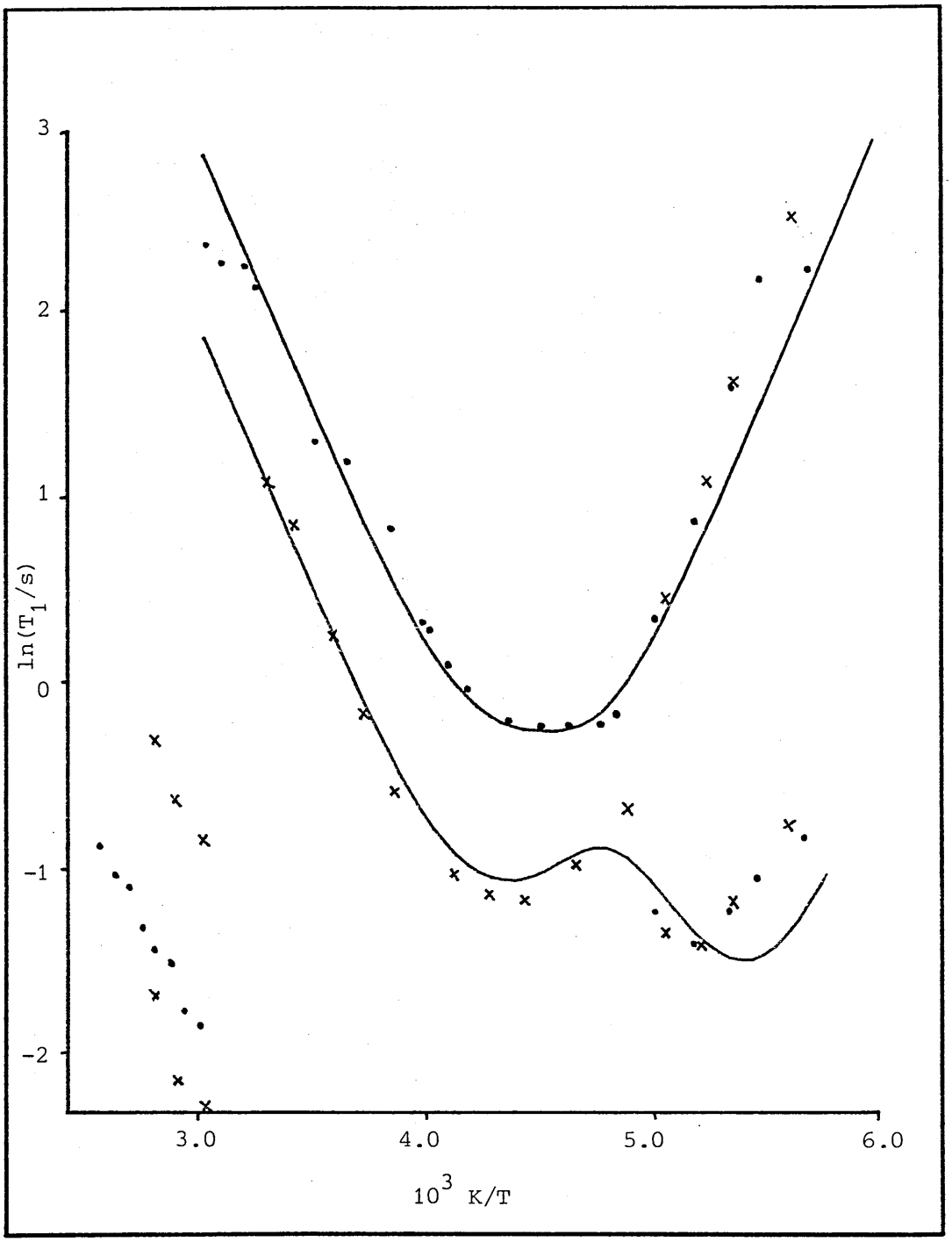

Figure 6.3 Experimental (•^{1}H, x ^{19}F) nuclear spin relaxation times for polycrystalline $CsHF_2$ as a function of temperature. The solid lines are calculated on the basis of a model in which the HF_2^- ion undergoes 180° rotational jumps.

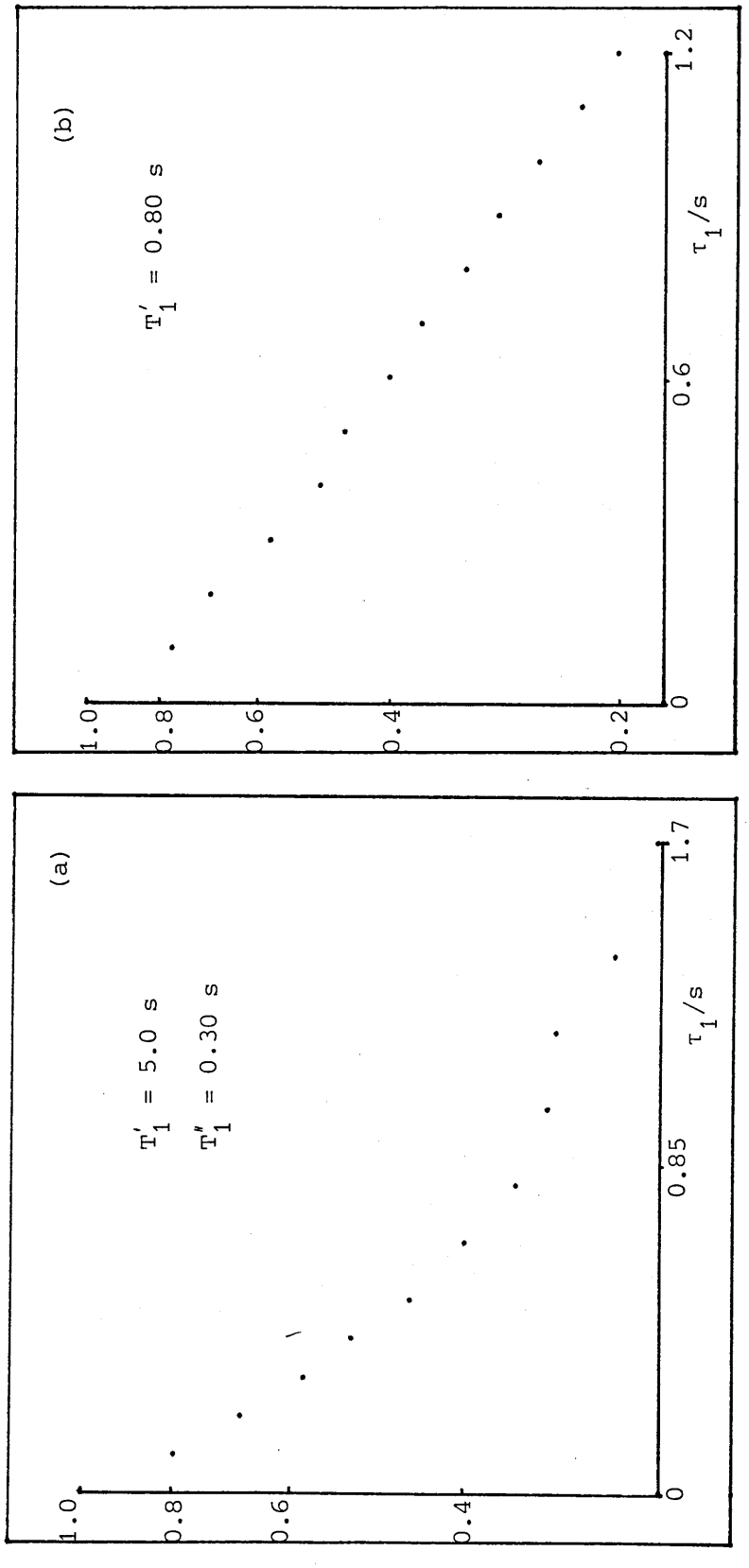

Figure 6.4 Log-normal plot of the ^1H magnetisation recovery as a function of τ_1 for polycrystalline $CsHF_2$ at (a) 188 K and (b) 210 K.

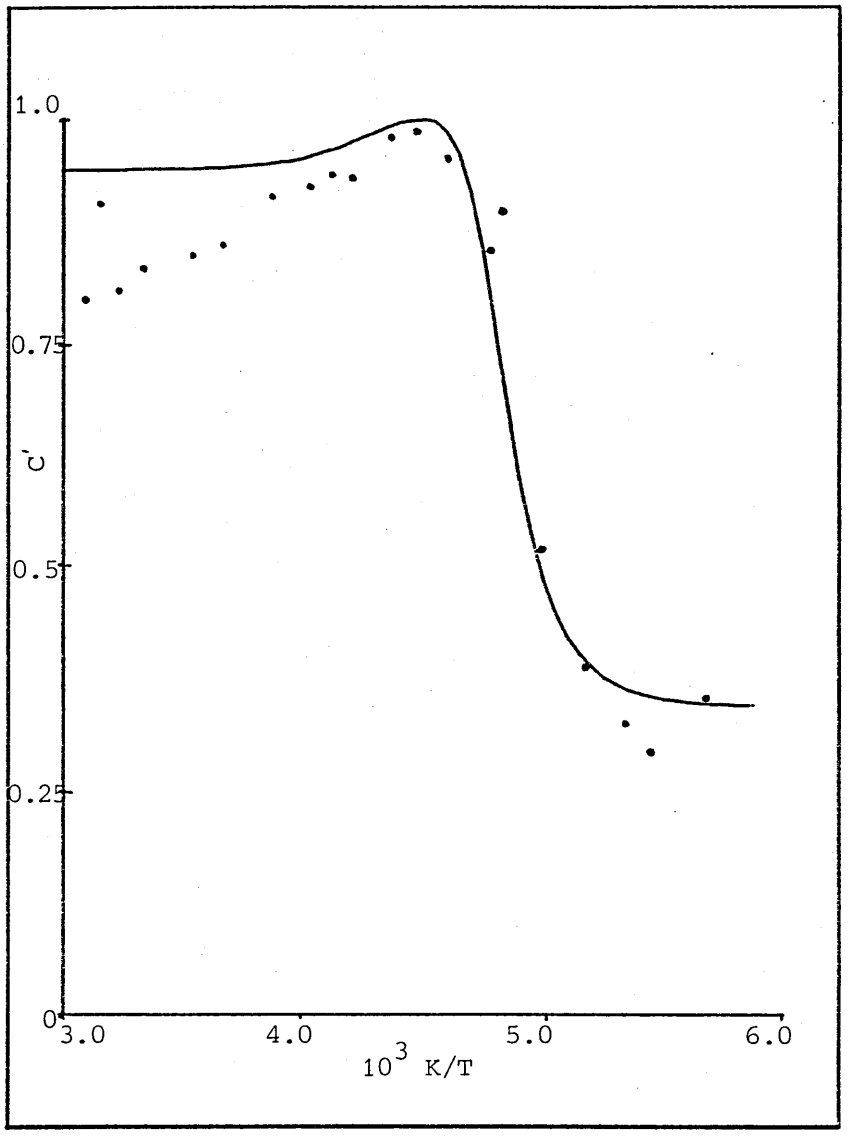

Figure 6.5 The experimental (....) and calculated coefficient C′, corresponding to the longer time constant, for the double exponential recovery of the ^1H magnetisation in polycrystalline $CsHF_2$ as a function of temperature.

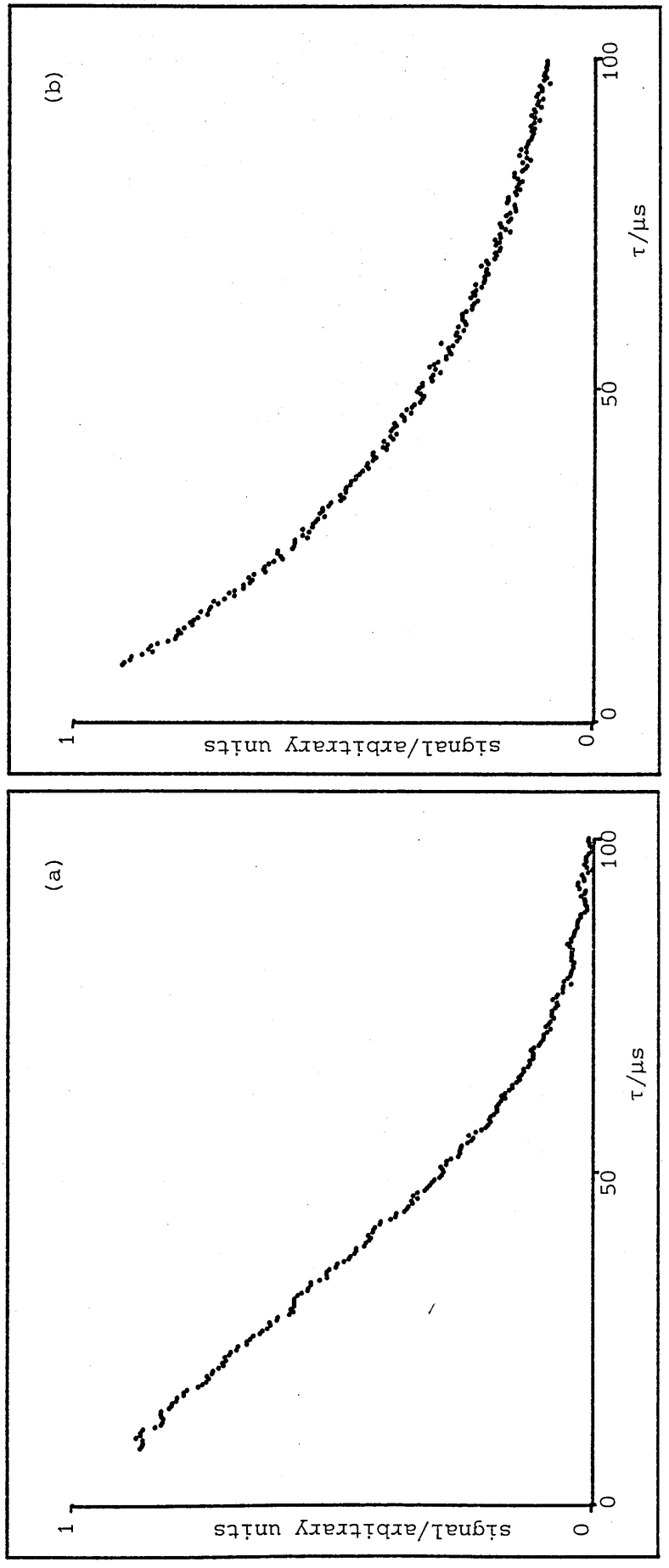

Figure 6.6 The experimental ^1H FID for polycrystalline $CsHF_2$ at (a) 334 K and (b) 390 K. Experimentally, the transition temperature was found to be 334 ± 2 K.

6.8 References

(1) A. Abragam, 'The Principles of Nuclear Magnetism', Clarendon Press, Oxford, 1961.

(2) P.S. Allen, J. Phys. C: Solid State Phys., 6, 3174-3186 (1973).

(3) D. Wolf, 'Spin Temperature and Nuclear Spin Relaxation in Matter: Basic Principles and Applications', Clarendon Press, Oxford, 1979.

(4) D.A. Torchia and A. Szabo, J. Mag. Res., 49, 107-121 (1982).

(5) I. Solomon, Phys. Rev., 99(2), 559-565 (1955).

(6) D.E. O'Reilly, E.M. Petersen and T. Tsang, Phys. Rev., 160(2), 333-342 (1967).

(7) Y. Furukawa and H. Kiriyama, Bull. Chem. Soc. Japan, 51(12), 3438-3442 (1978).

(8) Yu. G. Kriger, S.P. Gabuda and N.K. Moroz, Sov. Phys. Solid State, 17(11), 2239-2240 (1976).

(9) E.F. Westrum Jr., C.P. Landee, Y. Takahashi and M. Chavret, J. Chem. Thermodynamics, 10(9), 835-846 (1978).

(10) H.W. Spiess, 'Rotation of Molecules and Nuclear Spin Relaxation', NMR-Basic Principles and Progress, volume 15, Springer-Verlag, Berlin (1978).

(11) D.M. Brink and G.R. Satchler, 'Angular Momentum', Oxford University Press, Oxford (1968).

(12) D.C. Look and I.J. Lowe, J. Chem. Phys., 44 (8), 2995-3000 (1966).

(13) E.N. Ivanov, Soviet Physics JETP, 18(4), 1041-1045 (1964).

(14) G. Stephenson, 'Mathematical Methods for Science Students', Longman, London, second edition (1973).

(15) Yu. G. Kriger, N.K. Moroz and S.P. Gabuda, Sov. Phys. Solid State, 18(3), 514-515 (1976).

(16) Y. Furukawa and H. Kiriyama, Bull. Chem. Soc. Japan 52(2), 339-343 (1979).

(17) E.C. Reynhardt, A. Watton and H.E. Petch, J. Chem. Phys. 71(11), 4421-4429 (1979).

(18) S.W. Petersen and H.A. Levy, J. Chem. Phys., 20, 704-707 (1952).

(19) M.L. Davis and E.F. Westrum Jr., J. Phys. Chem. 65, 338-344 (1961).

(20) R. Kruh, K. Fuwa and T.E. McEver, J. Am. Chem. Soc., 78, 4256-4258 (1956).

(21) T. Eguchi, M. Kishita, H. Chihara and G. Soda, Bull. Chem. Soc. Japan, 55(3), 676-679 (1982).

(22) H.L. Carrell and J. Donohue, Israel J. Chem., 10, 195-200 (1972).